



UNIVERSITY OF LINCOLN

Understanding the role of connexin 43 hemichannel activity in
mediating tubulointerstitial inflammation and fibrosis in models
of diabetic nephropathy.

Chelsy Louise Cliff

A thesis submitted in partial fulfilment of the requirements of the
University of Lincoln for the degree of
Doctor of Medical and Biomedical Science

School of Life Sciences
University of Lincoln, UK

June, 2023

Abstract

Diabetic nephropathy is a severe secondary complication affecting approximately one third of people with diabetes, and it is the leading cause of end stage renal disease. Diabetic kidney disease is also an established risk factor for further secondary complications, including diabetic retinopathy and cardiovascular disease. Characterised by chronic inflammation, damage to the proximal tubule of the kidney correlates with disease severity and progression. However, with current therapy focusing on control of blood glucose and blood pressure, treatments targeting inflammation in established disease are lacking.

Targeting of the NOD-like receptor protein-3 (NLRP3) inflammasome is an area currently attracting a lot of attention. A driver of tubulointerstitial inflammation, the NLRP3 inflammasome is a major immune complex mediating caspase 1 cleavage of pro-inflammatory cytokines interleukin (IL1 β) and interleukin 18 (IL18). These cytokines are subsequently released into the intracellular space, where they contribute to local inflammation. Attempts have been made to target components of the inflammasome in sterile disease, but many approaches have resulted in off-target effects or been met with associated increased risk incurred by blocking the ability of the inflammasome to respond to pathogenic insult. Studies examining other chronic inflammatory conditions, including diabetic retinopathy, demonstrate a link between increased opening of transmembrane connexons or hemichannels and activation of the inflammasome. Connexin hemichannels open in response to injury and release large amounts of ATP into the extracellular environment. This local disease/injury associated signal activates purinergic P2X7 receptors (P2X7R) leading to inflammasome complex formation. Blocking connexin 43 (Cx43) hemichannel opening in models of diabetic retinopathy has effectively prevented inflammasome activation in response to sterile inflammation but left the complex available to respond to microbial challenge. As the major connexin isoform in the kidney, increased Cx43 hemichannel activity has also been implicated in the pathogenesis of diabetic nephropathy however, a link between Cx43 and the inflammasome in the kidney is yet to be established.

The aim of this project was to understand the role of Cx43 hemichannel activity in mediating tubulointerstitial inflammation and fibrosis in the diseased kidney and to determine the link between increased hemichannel activity and inflammasome activity. This project also assessed the ability of the hemichannel blocker Tonabersat to negate the

downstream effects of altered Cx43 hemichannel activity. Transcriptomic analysis of publicly available data sets (NephroSeq) demonstrated a correlation between Cx43 expression and a decline in function in human renal biopsies. Data in this thesis show an increase in Cx43 hemichannel activity in primary human renal proximal tubule epithelial cells (RPTECs) treated with inflammatory cytokines and high glucose, in addition to upregulation of markers associated with inflammation, partial epithelial-to-mesenchymal transition (pEMT) and fibrosis. Through collaboration and utilising a unilateral ureteral obstruction (UUO) mouse model of advanced tubulointerstitial injury with tubule specific Cx43^{-/-} genetic deletion, I identify a link between Cx43 expression and inflammasome activity followed by infiltration and activation of macrophages and fibroblasts. Findings were recapitulated *in vitro*, where use of Tonabersat determined these effects to be dependent on increased Cx43 hemichannel activity, which when blocked, protected against upregulation of markers associated inflammation and fibrosis. Already demonstrating promise in Phase 2b clinical trials for diabetic retinopathy, these findings highlight the potential therapeutic benefit of blocking Cx43-hemichannels as a viable future treatment of diabetic nephropathy.

Published material

Papers

1. Roger E., Chadjichristos C. E., Kavvadas P., Price G. W., **Cliff C. L.**, Hadjadj S., Renciot J., Squires P. E. and Hills C. E. (2023) 'Connexin-43 hemichannels orchestrate NOD-like receptor protein-3 (NLRP3) inflammasome activation and sterile inflammation in tubular injury'. *Cell Communication and Signalling*, 21(1):263. doi: 10.1186/s12964-023-01245-7.
2. Williams, B. M., **Cliff, C. L.**, Demirel, I., Squires, P. E. and Hills, C. E. (2022) 'Blocking connexin 43 hemichannel-mediated ATP release reduces communication within and between tubular epithelial cells and medullary fibroblasts in a model of diabetic nephropathy', *Diabetic Medicine*, 39(12):e14963. doi: 10.1111/DME.14963.
3. Williams, B. M. †, **Cliff, C. L.** †, Lee, K., Squires, P. E. and Hills, C. E. (2022) 'The Role of the NLRP3 Inflammasome in Mediating Glomerular and Tubular Injury in Diabetic Nephropathy', *Frontiers in Physiology (Renal & Epithelial Physiology)*, 2022, 13:907504. doi: 10.3389/fphys.2022.907504 . († joint 1st author)
4. **Cliff, C. L.** †, Williams, B. M. †, Chadjichristos, C. E., Mouritzen, U., Squires, P. E. and Hills, C. E. (2022) 'Connexin 43: A Target for the Treatment of Inflammation in Secondary Complications of the Kidney and Eye in Diabetes', *International Journal of Molecular Sciences* 2022, 23, 600. <https://doi.org/10.3390/ijms23020600>. († joint 1st author)
5. Potter, J. A., Price, G. W., **Cliff, C. L.**, Green, C. R., Squires, P. E. and Hills, C. E. (2021) 'Collagen I modifies connexin-43 hemichannel activity via integrin $\alpha 2\beta 1$ binding in TGF β 1-evoked renal tubular epithelial cells', *International Journal of Molecular Sciences*, 22(7):3644. doi: 10.3390/ijms22073644.
6. Potter, J., Price, G., **Cliff, C.**, Williams, B., Hills, C. and Squires, P. (2021) 'Carboxyfluorescein Dye Uptake to Measure Connexin-mediated Hemichannel Activity in Cultured Cells', *BIO-PROTOCOL*, 11(3):e3901. doi: 10.21769/bioprotoc.3901.
7. Price, G. W., Potter, J. A., Williams, B. M., **Cliff, C. L.**, Wall, M. J., Hills, C. E. and Squires, P. E. (2020) 'Examining Local Cell-to-Cell Signalling in the Kidney Using

- ATP Biosensing', in. *Methods in Molecular Biology*, 2346:135–149. doi: 10.1007/7651_2020_297.
8. Price, G. W., Potter, J. A., Williams, B. M., **Cliff, C. L.**, Squires, P. E. and Hills, C. E. (2020) 'Connexin-mediated cell communication in the kidney: A potential therapeutic target for future intervention of diabetic kidney disease?: Joan Mott Prize Lecture', *Experimental Physiology*, 105(2):219–229. doi: 10.1113/EP087770.

Conference Proceedings

1. **Cliff, C.**, Chadjichristos, C., Williams, B., Phillips, P., Roger, E., Kavvadas, P., Hadjadj, S., Renciot, J., Squires, P. and Hills, C. (2023) 'Blocking connexin-43 hemichannels dampens tubulointerstitial inflammation and fibrosis in models of diabetic nephropathy', *Diabetic Medicine*, 40(S1), p. e15047. doi: 10.1111/DME.15047.
2. **Cliff, C.**, Williams, B., Hills, C. and Squires, P. (2023) 'Tonabersat breaks the cycle of Cx43-hemichannel mediated activity and NLRP3 inflammasome activation in a model of diabetic nephropathy', *Diabetic Medicine*, 40(S1), p. e15048. doi: 10.1111/DME.15048.
3. Williams, B., **Cliff, C.**, Ward, J., Squires, P. and Hills, C. (2023) 'Blocking connexin-43 hemichannels reduces high glucose-evoked nod-like receptor protein-3 inflammasome activation in a model of diabetic nephropathy', *Diabetic Medicine*, 40(S1), p. e15048. doi: 10.1111/DME.15048.
4. **Cliff, C.**, Williams, B., Chadjichristos, C., Squires, P., & Hills, C. (2022). Evaluating a role for Connexin-43 hemichannel mediated ATP release in priming and activation of the NLRP3 inflammasome in a human model of diabetic kidney disease. *Diabetic Medicine*, 39(S1).
5. Williams, B., **Cliff, C. L.**, Demirel, I., Squires, P. and Hills, C. (2022) 'Connexin-43 hemichannel mediated ATP release stimulates fibroblast activation in an in vitro model of diabetic kidney disease', *Diabetic Medicine*, 39(1). doi: 10.13039/501100000361.
6. **Cliff, C.**, Squires, P., Williams, B., Potter, J., & Hills, C. (2021). Blocking connexin-43 (CX43) hemichannels negates glucose-associated inflammation in clonal proximal tubular epithelial cells. *Diabetic Medicine*, 38(S1). https://doi.org/10.1111/dme.9_14555

7. Potter, J., Price, G., **Cliff, C.**, Williams, B., Hills, C. and Squires, P. (2020) 'Inhibition of intern A2B1 negates collagen-1 induced changes in connexion-mediated hemichannel activity in an in vitro model of diabetic nephropathy', *Diabetic Medicine*, 37(S1), pp. 24–26. doi: 10.1111/DME.11_14244.
8. Price, G., Potter, J., Williams, B. M., **Cliff, C. L.**, Squires, P. and Hills, C. (2020) 'A role for connexin-43 hemichannel-mediated adenosine triphosphate triphosphate (ATP) release in inflammation of the diabetic proximal tubule', *Diabetic Medicine*, 37(1). doi: 10.13039/501100000361.

Acknowledgements

Firstly, I would like to thank my supervisors and lab parents Professor Claire Hills (Claire bear) and Professor Paul Squires (P Dizzle), for your endless support, guidance and wisdom over the last four years. Thank you for always believing in me and providing me with the skills and knowledge to grow into the scientist I am today. You have pushed me out of my comfort zone and driven me to be the very best I can. More than that, thank you for providing a wonderful environment to work, learn and eat cake. The yum-yums are always the best part of every lab meeting, as well as the belly ache from laughing. I have had the best four years and am looking forward to many more with our wonderful lab family.

I would like to thank our collaborators Dr Christos Chadjichristos and team at INSERM for all of their hard work and contributions to our Programme of research. Many thanks to Neil, the PCR king, for passing on your wisdom and Issam for your help collecting blood samples.

To my dissertation and master's supervisor Dr Mike Christie, thank you for being a wonderful supervisor and instilling me with the enthusiasm, confidence and knowledge to pursue a career in research. You are an inspiring mentor, and I don't know where I would be without your help setting me on this path.

I would like to thank previous UOL Renal group members Gareth and Beth for giving me a great start to my PhD journey. A special thanks goes to Joe Potter, for passing down all of your lab wisdom with endless kindness and patience. The way in which you mentored me whilst only being a few years more experienced was incredible. I wish you only the absolute best in the future, which I know will be full of success and happiness.

I have been incredibly fortunate to meet some wonderful friends in JBL over the years, Ahmed, Razan, Chutima, Laura, Will, Dania, Choaping, Forough, Mel, Kristian and Rhys who accepted me, weirdness and all. Because of you, my days were full of fun, laughter and encouragement, making me smile on even the hardest days. I cannot put into words how grateful I am for all of the wonderful memories we have made, but I can buy you all a drink so hit me up. I am looking forward to making many more memories together in the future. Biggest shoutout to Ahmed, for being here by my side from my very first day, you are the best G.

To Paige and Joanna, my little eggs. You are both incredibly talented, kind and supportive, and you have made the last year my happiest yet. Thank you for bringing non-stop sunshine and giggles to work every day and keeping me sane (mostly) through my write up. I am so excited to be continuing working with people I love through my post-doc, and watching you grow into the brilliant scientists I know you are.

Thank you to my lovely friends Sophie, Grace and Amy for always understanding when I had to dash to the lab in the middle of happy hour, for being so supportive no matter what time of night I messaged you and for coming to visit me for super fun sleepovers. I love you to the moon and back.

A huge thank you to my wonderful family, Mum, Nan, Grandad, James and Mark. Thank you for putting up with my utter chaos, sending me care packages when everything is going wrong, and for being proud of me even when you have no idea what I am nattering on about. I will always be grateful for everything you have and continue to do for me. I am super lucky to have you all.

Finally, to Alex, my Fiancé, I owe you the biggest thank you for putting up with my endless antics, cleaning the house when I am too busy 'in the zone', keeping me company through the late nights at work, taxiing me around at all sorts of times, keeping me fed and watered when I am too busy to do so myself, and always believing in me. I owe you big time. Now that this is finished, I cannot wait to marry you! I could continue but everyone has stopped reading at this point so hey ho. All my love xo

Contents

Abstract.....	II
Published material.....	IV
Papers	IV
Conference Proceedings	V
Acknowledgements	VII
Contents.....	1
List of Figures.....	7
List of Tables.....	13
Abbreviations	14
1.0. Introduction	0
1.1. Introduction to diabetes.....	0
1.1.1. Incidence.....	0
1.1.2. Role of insulin.....	0
1.1.3. Type 1 diabetes.....	3
1.1.4. Type 2 diabetes.....	7
1.1.5. Other types of diabetes	8
1.1.6. Diagnosis	9
1.1.7. Treatment.....	10
1.2. Complications of diabetes	11
1.2.1. Micro and macrovascular complications	11
1.2.2. Cardiovascular disease	11
1.2.3. Retinopathy	13
1.2.4. Neuropathy.....	16
1.2.5. Impaired Wound Healing	17
1.3. Diabetic nephropathy	19

1.3.1. Diagnosis	21
1.3.2. Clinical Stages.....	21
1.3.3. Glomerulonephritis	23
1.4. Tubulointerstitial injury	24
1.4.1. Proximal tubule inflammation.....	24
1.4.2. Monocyte infiltration.....	25
1.4.3. Epithelial to mesenchymal transition.....	28
1.4.4. Fibrosis.....	29
1.4.5. Treatment.....	30
1.5. The NLRP3 inflammasome	31
1.5.1. Priming.....	34
1.5.2. Activation.....	36
1.5.3. Action of proinflammatory cytokines	41
1.5.4. Current and future therapeutics for diabetic nephropathy	43
1.6. Connexin-mediated cell-cell communication	45
1.6.1 Gap Junctions	47
1.6.2 Hemichannels.....	47
1.6.3. Role of connexin-43 in inflammatory diseases.....	48
1.6.4. The role of Cx43 in diabetic nephropathy	51
1.7. Hypothesis.....	53
1.8. Aims	53
2.0. Methods and materials	55
2.1. Materials	55
2.1.1. Cell culture	55
2.1.2. Carboxyfluorescein dye uptake	55
2.1.3. Reverse transcription polymerase chain reaction	56
2.1.4. Western blotting	56

2.1.5. Assay reagents and kits	57
2.2. Cell culture.....	57
2.2.1. Clonal human kidney cell line	57
2.2.2. Human kidney 2 cell maintenance	58
2.2.3. Maintenance of primary human proximal tubule epithelial cells	60
2.2.4. Cell revival.....	63
2.2.5. Cell passaging.....	63
2.2.6. Freezing cells	65
2.3. Animal model of diabetic nephropathy	65
2.4. Evaluation of renal morphology, interstitial fibrosis, and immunohistochemistry	65
2.5. Phase contrast microscopy	66
2.6. Crystal violet assay	67
2.7. The 3-(4,5-Dimethylthiazol-2-yl)-2,5-diphenyltetrazolium bromide assay	68
2.8. Carboxyfluorescein uptake assay	68
2.9. Real-time quantitative polymerase chain reaction	70
2.9.1. RNA extraction	71
2.9.2. Complementary DNA conversion.....	72
2.9.3. Polymerase chain reaction	73
2.10. Whole cell protein extraction	75
2.11. Bradford Assay	75
2.12. Western blotting.....	76
2.12.1. Sample preparation	77
2.12.2. Gel electrophoresis.....	78
2.12.3. Transfer to membrane	80
2.12.4. Antibody probing	81
2.12.5. Visualisation and analysis.....	84
2.13. Proteome profiler human cytokine array.....	84

2.14. ATP-lite luminescence assay	85
2.15. Caspase Glo-1 inflammasome assay	85
2.16. IL1 β enzyme linked immunosorbent assay	86
2.17. Transcriptomic analysis.....	87
2.18. Statistical analysis.....	88
3.0. The role of pro-inflammatory cytokines and glucose in mediating tubular injury.....	90
3.1. Introduction	90
3.2. Aims	94
3.3. Results.....	95
3.3.1. Evaluating the effect of pro-inflammatory cytokines IL1 β , IL18 and TNF α on human proximal tubule cell viability under conditions of basal and high glucose.	95
3.3.2. Inflammatory factors associated with the NLRP3 inflammasome are upregulated following pro-inflammatory cytokine and glucose challenge in tubule epithelial cells.....	98
3.3.3. Pro-inflammatory cytokines and glucose mediate altered cell morphology and phenotype in proximal tubule epithelial cells.....	101
3.3.4. Expression of extracellular matrix and fibrosis associated proteins is increased in pro-inflammatory cytokine and glucose treated proximal tubule cells.....	104
3.3.5. Inflammatory cytokines and glucose stimulate upregulated release of multiple pro-inflammatory cytokines and chemokines associated with diabetic nephropathy.	106
3.4. Discussion	112
4.0. Effects of high glucose/cytokines on hemichannel activity and actions of Tonabersat in protecting against inflammatory-induced damage in proximal tubule epithelial cells.	119
4.1. Introduction	119
4.2. Aims	127
4.3. Results.....	128
4.3.1. Pro-inflammatory cytokines combined with high glucose alter expression of connexins and pannexins.....	128

4.3.2. Connexin 43 is upregulated in diabetic nephropathy.....	131
4.3.3. Evaluating the effect of Tonabersat on cell viability in the presence of high glucose and inflammatory cytokines.....	132
4.3.4. Tonabersat reduces hemichannel-mediated dye uptake and ATP release, stimulated by IL1 β , TNF α and 25mmol/L glucose.....	133
4.3.5. High glucose in combination with inflammatory cytokines increased IL6 expression through aberrant Cx43 hemichannel activity.....	135
4.3.6. Blocking Cx43 hemichannel activity protects against increased expression of partial-EMT and fibrosis markers.....	136
4.3.7. Tonabersat and BAPTA block Cx43 hemichannel-mediated ATP release and reduce markers for tubular injury in IL1 β and TNF α stimulated RPTECs under conditions of high glucose.	140
4.3.8. Blocking ERK/MAPK and p38 signalling prevents Cx43 expression and hemichannel-mediated ATP release in IL1 β , TNF α and high glucose treated RPTECs.	144
4.3.9. Aberrant Cx43 hemichannel activity upregulates markers of tubular injury in part through ERK and p38 MAPK signalling.	147
4.4. Discussion	149
5.0. Elucidating the role of connexin 43 hemichannel activity in priming and activation of the NLRP3 inflammasome, initiating a perpetual inflammatory cycle.	156
5.1. Introduction.....	156
5.2. Aims-	160
5.3. Results-	161
5.3.1. Markers of inflammasome priming and activation are increased in diabetic and non-diabetic kidney disease.	161
5.3.2. Increased tubule connexin 43 is linked to increased levels of NLRP3 in a mouse model of advanced interstitial inflammation and fibrosis.	164
5.3.3. Pro-inflammatory cytokines IL1 β and TNF α stimulate both priming and activation of the NLRP3 inflammasome in primary human RPTECs under conditions of high (25mmol/L) glucose.	167

5.3.4. Hemichannel blocker Tonabersat blocks an NFκB-mediated increase in NLRP3 inflammasome priming and activation in treated RPTECs.	169
5.3.5. Alterations in calcium and inhibition of non-canonical signalling intermediaries reduced Cx43 hemichannel associated inflammasome activation.	171
5.3.6. Aberrant Cx43 hemichannel activity is linked to an increase in Cx43 expression, a mechanism blocked through inhibition of transcription factor NFκB.	173
5.3.7. Blocking inflammasome activation reduces Cx43 expression and hemichannel activity.	176
5.3.8. Tubule Cx43 deletion in the mouse UUO model ameliorates an increase in tubule injury, inflammation and fibrosis.	178
5.3.9. Tonabersat negates an increase in pro-inflammatory markers associated with diabetic nephropathy in an <i>in vitro</i> model of diabetic kidney disease.	182
5.3.10. Blocking inflammasome activation prevents downstream changes in EMT and fibrosis marker expression.	184
5.4. Discussion-	187
6.0. Discussion.	196
7.0. References.	205

List of Figures

Figure 1.1. The mechanism of insulin secretion and action under physiological conditions.

Figure 1.2. Insulin signalling transduction pathways.

Figure 1.3. The different mechanisms underlying insulin release and action in physiological (healthy) conditions as compared to type 1 and type 2 diabetes.

Figure 1.4. The involvement of immune cells in autoimmune mediated destruction of pancreatic beta cells in type 2 diabetes.

Figure 1.5. The contributions of obesity to development of type 2 diabetes.

Figure 1.6. The mechanisms through which diabetes contributes to development of secondary macrovascular complications.

Figure 1.7. The impact of diabetes induced sustained hyperglycaemia on vasculature in the eye, resulting in diabetic retinopathy.

Figure 1.8. Schematic demonstrating the four stages on wound healing under physiological conditions.

Figure 1.9. The structure of the kidney.

Figure 1.10. Diabetes contributed to structural and functional changes in the renal glomerulus, an early clinical manifestation of diabetic nephropathy.

Figure 1.11. Homotypic and heterotypic interactions driving the presence of different inflammatory and fibrotic cell types in the proximal tubule, ultimately contributing to progression of diabetic nephropathy.

Figure 1.12. Injury induced partial epithelial to mesenchymal transition as demonstrated in proximal tubule epithelial cells in late stage diabetic nephropathy.

Figure 1.13. Structure of the NLRP3 inflammasome complex.

Figure 1.14. Schematic demonstrating priming of the NLRP3 inflammasome.

Figure 1.15. Schematic illustrating canonical (classical) activation of the NLRP3 inflammasome.

Figure 1.16. Illustration of the mechanisms of non-canonical NLRP3 inflammasome activation.

Figure 1.17. Schematic illustrating mechanisms of alternate NLRP3 inflammasome priming and activation in monocytes.

Figure 1.18. Simplified downstream signalling mechanisms of IL1 β and IL18 after binding to their respective receptors.

Figure 1.19. Cycle of connexin hemichannel and gap junction formation and degradation.

Figure 2.1. Image of a haemocytometer.

Figure 2.2. Steps carried out for a crystal violet assay.

Figure 2.3. MTT assay protocol.

Figure 2.4. Carboxyfluorescein uptake assay protocol.

Figure 2.5. Extraction of RNA from cell lysates.

Figure 2.6. Conversion of messenger RNA to complementary (c)DNA.

Figure 2.7. Example of a standard curve produced using known concentrations of BSA in Bio-Rad protein assay reagent.

Figure 2.8. Methodology for immunoblotting.

Figure 2.10. Assembly of the transfer cassette.

Figure 2.10. Proteome profiler human cytokine array protocol.

Figure 2.11. Caspase Glo-1 inflammasome assay substrate reaction.

Figure 2.12. IL1 β enzyme linked immunosorbent assay protocol.

Figure 3.1. The effect of pro-inflammatory cytokines on proximal tubule cell viability in 5mmol/L glucose conditions.

Figure 3.2. The effect of pro-inflammatory cytokines and 25mmol/L glucose on proximal tubule cell viability.

Figure 3.3. Inflammatory cytokines and glucose increase expression of inflammatory markers in proximal tubule epithelial cells.

Figure 3.4. The combined effect of pro-inflammatory cytokines and 25mmol/L glucose on proximal tubule epithelial cell morphology.

Figure 3.5. Pro-inflammatory cytokines and high glucose alter expression of epithelial adherens junction proteins.

Figure 3.6. Expression of fibrosis and extracellular matrix markers was increased in proximal tubule cells following treatment with pro-inflammatory cytokines and glucose.

Figure 3.7. Cytokines IL1 β , TNF α and 25mmol/L glucose increase secretion of pro-inflammatory cytokines and chemokines in primary proximal tubule epithelial cells.

Figure 3.8. Pro-inflammatory cytokines and chemokines secretion is increased in primary proximal tubule epithelial cells after treatment with IL1 β , TNF α and 25mmol/L glucose.

Figure 3.9. Inflammatory markers are elevated in kidney biopsies of people with CKD and proximal tubule epithelial cells treated with IL1 β , TNF α and 25mmol/L glucose.

Figure 3.10. A schematic demonstrating the proposed vicious cycle of chronic inflammation, partial EMT and fibrosis in IL1 β , TNF α and 25mmol/L glucose treated RPTECs and HK-2 cells.

Figure 4.1. Hemichannel forming proteins, connexin 43, connexin 26 and pannexin 1 increased in expression following treatment with high glucose and inflammatory cytokines in proximal tubule epithelial cells.

Figure 4.2. Connexin 43 is elevated in human diabetic nephropathy, and correlates to increased proteinuria.

Figure 4.3. The effect of Tonabersat on proximal tubule cell viability in 25mmol/L glucose conditions, with and without the addition of IL1 β and TNF α .

Figure 4.4. Tonabersat negates an IL1 β , TNF α and 25mmol/L glucose-induced increase in Cx43-mediated dye uptake and ATP release in proximal tubule epithelial cells.

Figure 4.5. Tonabersat blocks an IL1 β , TNF α and 25mmol/L glucose-mediated upregulation of inflammatory marker IL6 in proximal tubule epithelial cells.

Figure 4.6. Tonabersat blocks IL1 β , TNF α and 25mmol/L glucose-mediated upregulation of select markers of pEMT in proximal tubule epithelial cells, but not all.

Figure 4.7. Tonabersat blocks an IL1 β , TNF α and 25mmol/L glucose-mediated upregulation of key ECM proteins associated with fibrosis in proximal tubule epithelial cells.

Figure 4.8. A pro-inflammatory cytokine IL1 β , TNF α and 25mmol/L glucose-induced Cx43-mediated dye uptake, ATP release and protein expression is reduced in primary proximal tubule epithelial cells when co-incubated with Tonabersat or BAPTA.

Figure 4.9. An IL1 β , TNF α and 25mmol/L glucose-induced increase in expression of injury markers is associated with [Ca²⁺]_i gating of Cx43 hemichannel activity, which is negated by Tonabersat.

Figure 4.10. IL1 β , TNF α and 25mmol/L glucose induced Cx43-mediated dye uptake, ATP release and Cx43 protein expression is partially mediated through ERK/MAPK signalling.

Figure 4.11. An IL1 β , TNF α and 25mmol/L induced increase in Cx43 expression and hemichannel-mediated dye uptake is partially mediated through p38 signalling.

Figure 4.12. Tonabersat blocks an IL1 β , TNF α and 25mmol/L glucose-mediated upregulation an adherens junction and fibrosis associated marker in proximal tubule epithelial cells.

Figure 5.1. Increased expression of NLRP3 inflammasome proteins in human diabetic nephropathy biopsies correlate to measures of reduced renal function.

Figure 5.2. Increased caspase 1 (CASP1) expression in biopsies isolated from patients with diabetic nephropathy and chronic kidney disease correlates to measures of reduced renal function.

Figure 5.3. Confirming a connexin 43 gene deletion in the renal proximal tubules of mice following unilateral ureteral obstruction.

Figure 5.4. Tubule-specific deletion of Cx43 (Cx43^{-/-}) negates increased expression of inflammasome markers following UUO.

Figure 5.5. The NLRP3 inflammasome is primed and activated by IL1 β and TNF α in 25mmol/L glucose in primary human proximal tubule cells.

Figure 5.6. Priming of the NLRP3 inflammasome lies downstream of Cx43 hemichannel activity in IL1 β , TNF α and 25mmol/L glucose treated RPTECs, effects negated following pre-incubation with Tonabersat.

Figure 5.7. Pro-inflammatory cytokines IL1 β , TNF α and 25mmol/L glucose activate the NLRP3 inflammasome via increased Cx43 hemichannel activity, effects blocked when RPTECs are pre-incubated with Tonabersat.

Figure 5.8. Pro-inflammatory cytokines IL1 β , TNF α and 25mmol/L glucose activate the NLRP3 inflammasome via increased Cx43 hemichannel activity, effects blocked when RPTEC Ca²⁺ gating, ERK and P38 signalling are inhibited.

Figure 5.9. Blocking NF κ B mediated priming of the inflammasome reduces Cx43 expression and hemichannel activity.

Figure 5.10. Tonabersat negates a proinflammatory cytokine and 25mmol/L glucose-induced increase in Cx43 expression.

Figure 5.11. Blocking caspase 1 activity reduces pro-inflammatory cytokine-induced increases in Cx43 expression and hemichannel activity.

Figure 5.12. Tubule-specific Cx43 knockout reduces markers of kidney injury in a mouse model of tubulointerstitial fibrosis.

Figure 5.13. Tubule-specific Cx43 knockout reduces markers of inflammation in a mouse model of diabetic nephropathy.

Figure 5.14. Tonabersat blocks a pro-inflammatory cytokine and high glucose-mediated increase in the expression of pro-inflammatory markers.

Figure 5.15. N-cadherin is elevated in human chronic kidney disease and reduced by caspase 1 inhibition

Figure 5.16. Fibronectin is elevated in human diabetic nephropathy and chronic kidney disease, correlating to measures of reduced renal function.

Figure 5.17. Schematic demonstrating some of the therapeutic compounds that have been/are in clinical trial targeting components of the inflammasome.

Figure 5.18. A schematic outlining the proposed mechanisms through which Cx43 hemichannel activity and NLRP3 inflammasome activation exacerbate each other resulting in downstream inflammation and fibrosis, characteristic of diabetic nephropathy.

List of Tables

Table 1.1. The 5 pathological stages of diabetic nephropathy.

Table 1.2. The effect of blocking connexin hemichannel activity in different *in vivo* models of chronic inflammatory diseases.

Table 2.1. List of stimulants and inhibitors utilised for tissue culture experiments.

Table 2.2. Primary human proximal tubule epithelial cell media supplements.

Table 2.3. List of stimulants and inhibitors utilised for tissue culture experiments.

Table 2.3. HK-2 seeding densities.

Table 2.4. Reverse transcriptase master mix.

Table 2.5. PCR reaction master mix.

Table 2.6. Amplification primers for RT qPCR.

Table 2.7. Lysis buffer recipe.

Table 2.8. Sample buffer recipe.

Table 2.9. Resolving gel recipe.

Table 2.10. Stacking gel recipe.

Table 2.11. Electrode running buffer (10x) recipe.

Table 2.12. Transfer buffer (10x) recipe.

Table 2.13. List of primary antibodies used for western blotting.

Table 2.14. List of secondary antibodies used for western blotting.

Table 4.1. Cx43 hemichannel blockers and their use in chronic inflammatory diseases.

Abbreviations

AIF-1	Allograft inflammatory factor 1
AMD	Age-related macular degeneration
Ang II	Angiotensin II
APS	Ammonium persulfate
ARPE	Human retinal pigment epithelial
asODN	Anti-sense oligodeoxynucleotide
ATCC	American Type Culture Collection
BPB	Bromophenol blue
BSA	Bovine serum albumin
BSS	Balanced salt solution
BUN	Blood urea nitrogen
C5aR1	C5a receptor 1
CALLA	Common acute lymphoblastic leukaemia antigen
CANTOS	Canakinumab Anti-Inflammatory Thrombosis Outcomes Study
CARD	Caspase recruitment domain
CASP	Caspase
cDNA	Complementary DNA
CHI3L1	Chitinase-3-like 1
CKD	Chronic kidney disease
COX-2	Cyclooxygenase-2
Cx26	Connexin 26
Cx43	Connexin 43
DAMP	Danger-associated molecular pattern
DMEM	Dulbecco's Modified Eagles Medium
DMEM/F12	DMEM/Hams F12
DMSO	Dimethyl Sulphoxide
DN	Diabetic nephropathy
dNTP	Deoxynucleotide triphosphates

DPPIV	Dipeptidyl peptidase-IV
DTT	Dithiothreitol
E	Epithelial
ECM	Extracellular matrix
EDTA	Ethylenediaminetetraacetic acid
EGF	Epidermal growth factor
eGFR	Estimated glomerular filtration rate
EMT	Epithelial to mesenchymal transition
EndoMT	Endothelial-mesenchymal transition
ERK	Extracellular signal related kinase
ESRD	End stage renal disease
FADD	Fas-associated death domain protein
FAO	Fatty acid oxidation
Fc	Fragment crystallisable
FCS	Foetal Calf Serum
FISH	Fluorescence <i>in situ</i> hybridization
FSP1	Fibroblast-specific protein 1
Gab	GRB2-associated-binding protein
GAD	Glutamate decarboxylase
GBM	Glomerular basement membrane
G-CSF	Granulocyte colony stimulating factor
GDF-15	Growth differentiation factor 15
GJIC	Gap junction intercellular communication
GLP-1	Glucagon-like peptide 1
GLUT	Glucose transporter
GM-CSF	Granulocyte-macrophage colony-stimulating factor
gp	Glycoprotein
GSDMD	Gasdermin D
GSDMD-NT	GSDMD amino terminal fragment
HbA1c	Haemoglobin A1c

HK-2	Human kidney-2
HNF1alpha	Hepatocyte nuclear factor
HPV-16	Human papilloma virus 16
HRPT	Hypoxanthine phosphoribosyl transferase
ICAM-1	Intercellular adhesion molecule 1
IFN γ	Interferon gamma
IKK	I κ B kinase
IL18	Interleukin 18
IL18R	IL18 receptor
IL1-R	IL1-receptor
IL1R1	IL1-receptor 1
IL1R3	IL1 type 3-receptor
IL1ra	IL1 receptor agonist
IL1 β	Interleukin 1-beta
IL6	Interleukin 6
IL6R	IL6 receptor
IP ₃	Inositol triphosphate
IRAK	IL1 receptor associated kinase
IRI	Ischaemia reperfusion injury
I κ B	Inhibitor of nuclear factor kappa B (I κ B)
JAK	Janus kinase
JNK	c-Jun N-terminal kinase
KIM-1	Kidney injury molecule-1
LDLR-/-	LDL receptor-deficient
LPS	Lipopolysaccharide
LRR	Leucine-rich repeat
MAPK	Mitogen-activated protein kinases
MCP3	Monocyte chemotactic protein-3
MCSF	Macrophage colony-stimulating factor
MIP-1 α /1 β	Macrophage inflammatory protein 1-alpha/ 1-beta

miR-10	MicroRNA-10
MMP	Matrix metalloproteinase
MODY	Maturity onset diabetes of the young
mRNA	Messenger RNA
MTT	3-(4,5-Dimethylthiazol-2-yl)-2,5-diphenyltetrazolium bromide
MYD88	Myeloid differentiation primary response protein 88
N	Neural
NAC	N-acetyl-L-cysteine
NEK7	NIMA-related kinase-7
NEMO	NFκB essential modulator
NFκB	Nuclear factor kappa B
N-GAL	Neutrophil gelatinase-associated lipocalin
NLR	Nod-like receptor
NLRP	NLR protein containing a pyrin domain
NLRP3	NOD-like receptor protein 3
NOD	Nucleotide-binding oligomerisation domain containing protein
NTN	Nephrotoxic serum–induced nephritis
OGTT	Oral glucose tolerance test
P2X7R	P2x7 receptor
PAMP	Pathogen-associated molecular pattern
Panx1	Pannexin 1
PBS	Phosphate buffered saline
PCR	Polymerase chain reaction
PDX-1	Pancreatic and duodenal homeobox 1
pEMT	Partial-EMT
PFA	Paraformaldehyde
PMSF	Phenylmethylsulfonyl fluoride
PTH	Parathyroid hormone
PVDF	Polyvinylidene difluoride
PYD	Pyrin domain

RAGE	Receptor for advanced glycation end-products
RANTES	Regulated on activation, normal T-expressed and secreted
RIPK1	Receptor-interacting serine/threonine-protein kinase 1
ROS	Reactive oxygen species
RPTEC	Renal proximal tubule epithelial cell
RT	Room temperature
RTase	Reverse transcriptase
RT-q	Real time quantitative
SASP	Senescence associated secretory phenotype
SD	Sprague Dawley
SDS	Sodium dodecyl sulfate
SDS-PAGE	Sodium dodecyl-sulphate polyacrylamide gel electrophoresis
SGLT2	Sodium glucose co-transporter 2
SGLT2i	Sodium-glucose co-transporter-2 inhibitors
sh	Short hairpin
SHP2	Src homology region 2-containing protein tyrosine phosphatase 2
Smad	Suppressor of mothers against decapentaplegic
SODD	Silencer of death domains
STAT	Signal transducer and activator of transcription
STZ	Streptozotocin
T1DM	Type 1 diabetes mellitus
T2DM	Type 2 diabetes mellitus
TGFβ1	Transforming growth factor beta 1
TLR	Toll-like receptors
TMB	Tetramethylbenzidine
TNFR	Tumour necrosis factor receptor
TNFα	Tumour necrosis factor alpha
TRADD	Type-1-associated death domain
TRAF6	TNF receptor-associated factor 6
TRIF	TIR domain containing adaptor molecule 1

Tris	Tris aminomethane
Twist1	Twist Family BHLH Transcription Factor 1
U-IRI	Unilateral ischemia/reperfusion injury
Upar	Urokinase plasminogen activator surface receptor
UUO	Unilateral ureteral obstruction
VGCC	Voltage gated calcium (Ca ²⁺) channels
Wnt	Wingless and integration site
WT	Wild type
WT-CTL	Wild type control
ZnT	Zinc transporter
ZO-1	Zonula occludens-1
αCT1	Alpha connexin carboxyl terminus 1
αSMA	Alpha-smooth muscle actin

1.0. Introduction

1.1. Introduction to diabetes

1.1.1. Incidence

Diabetes mellitus is a severe, chronic condition that occurs when the body cannot produce enough insulin or use the insulin it does produce effectively, resulting in dangerously elevated blood glucose levels (hyperglycaemia; Leslie *et al.*, 2016; World Health Organisation, 2019). Among the most rapidly increasing global health concerns of the 21st century, approximately 537 million people, equating to 10.5% of 20–79-year-olds, suffer from diabetes worldwide, around 50% of which are undiagnosed (International Diabetes Federation., 2021). The number of cases is expected to rise to 643 million by 2030 and cost over one trillion US\$ in direct health expenses (International Diabetes Federation., 2021). In the UK, treatment of diabetes and its secondary complications, including cardiovascular disease, retinopathy, and nephropathy (Harding *et al.*, 2019), cost the NHS ~£10 billion a year, 10% of the total budget (Whicher, O'Neill and Holt, 2020). Identifying novel ways in which to treat and prevent diabetes and halt the development of its secondary complications is essential in tackling this global health crisis.

1.1.2. Role of insulin

Produced by pancreatic beta cells located in the islets of Langerhans, insulin is an essential anabolic hormone primarily involved in mediating glucose uptake. Under physiological conditions, when blood glucose increases it enters pancreatic beta cells through a membrane bound glucose transporter (GLUT)2 (Thorens *et al.*, 2015) before undergoing glycolysis and the formation of pyruvate and ATP through the action of glucokinase, the rate-limiting step for insulin secretion (Guo *et al.*, 2012). As a result of a change in the intracellular ATP-to-ADP ratio, ATP-dependant potassium channels (K^{+}_{ATP}) close, causing membrane depolarisation and opening of voltage gated calcium (Ca^{2+}) channels (VGCC). Subsequent Ca^{2+} -influx triggers the calcium-dependent exocytotic process and leads to insulin secretion. Circulating biologically active insulin binds to the insulin receptor in peripheral tissue such as skeletal, liver, or adipose tissue, activating

downstream signalling pathways (Peterson *et al.*, 2018). In muscle and fat, one of the earliest responses elicited by activation of the insulin receptor is the rapid translocation and insertion of GLUT4 to the membrane, facilitating rapid glucose uptake and subsequent metabolism (Figure 1.1).

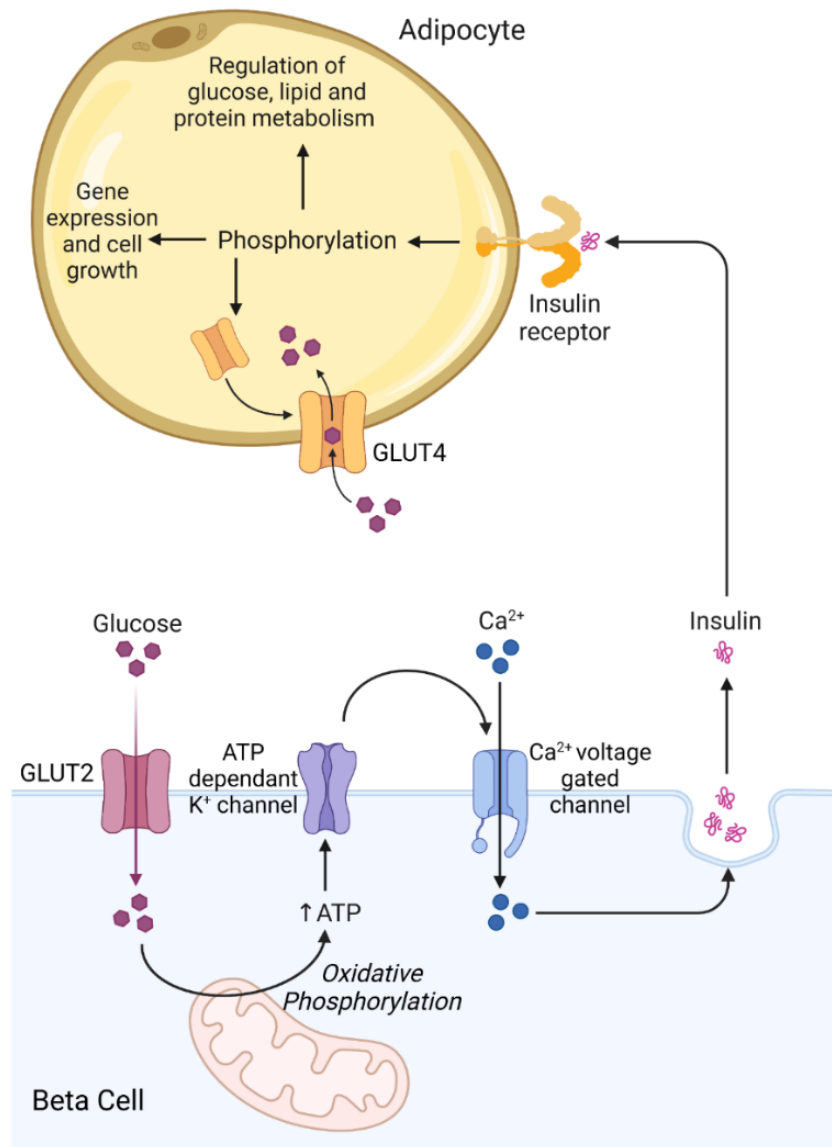


Figure 1.1. The mechanism of insulin secretion and action under physiological conditions. In pancreatic beta cells glucose uptake via glucose transporter (GLUT2) leads to mitochondrial ATP production and closure of ATP-dependant K⁺ channels. As a result, Ca²⁺ voltage channels open and intracellular Ca²⁺ increases, stimulating release of insulin. Insulin triggers insulin receptors on multiple other cell types, including adipocytes, activating downstream pathways that allow the cell to respond appropriately to blood glucose levels. Created in biorender.

In addition to its role in glucose homeostasis, insulin is also important in protein biosynthesis, lipogenesis and potassium uptake into cells, whilst inhibiting fat breakdown (lipolysis) and gluconeogenesis (Peterson *et al.*, 2018). The biochemical pathways through which insulin elicits these effects is called the insulin signalling transduction pathway (Figure 1.2). Insulin binds to the insulin receptor, a tyrosine kinase receptor which upon activation initiates a cascade of phosphorylation events and recruitment of insulin receptor substrates (IRS) and Shc proteins (Haeusler *et al.*, 2017). IRS proteins recruit and activate the PI3K, leading to downstream activation of PIP₃, PDK-1, Akt and PKCs, which mediate metabolic effects including regulation of glucose transport, gluconeogenesis and synthesis of lipids and glycogen, as well as effecting cell cycle control and cell survival. Shc activates the Grb2-Sos-Ras-Raf-MAPK pathway which contributes to cell proliferation/differentiation, cytoskeletal reorganisation and gene transcription (Haeusler *et al.*, 2017). Activation of the p38 MAPK pathway inhibits insulin signalling through phosphorylation of IRS1 and inhibition of PGC1 α and GLUT4 transcription, which blocks insulin-dependent glucose uptake (Bengal *et al.*, 2020). There are multiple forms of diabetes mellitus, the most common of which are type 1 and type 2 diabetes. In all forms of the disease, the mechanism of insulin action is impaired, resulting in sustained hyperglycaemia due to either reduced insulin secretion, insulin resistance or a combination of the two (Bratusch-Marrain, 1983).

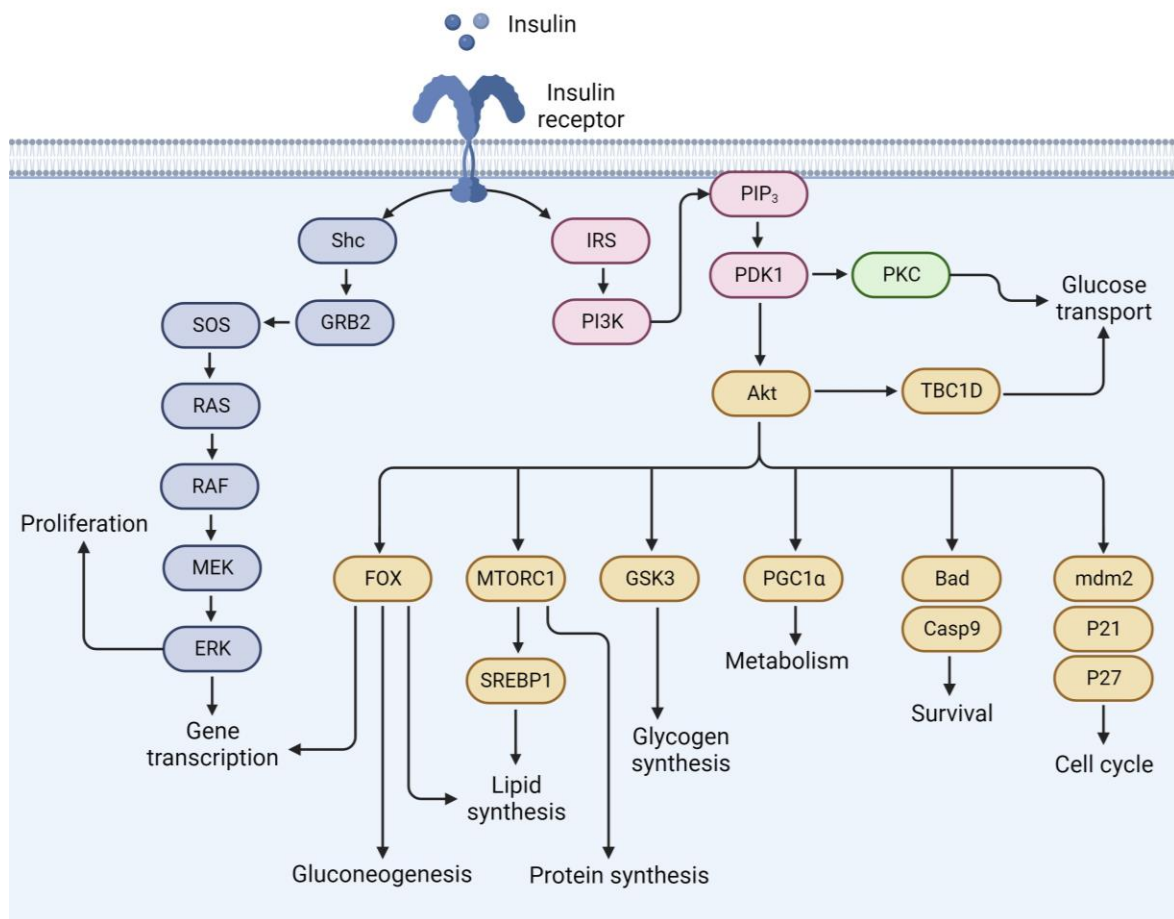


Figure 1.2. Insulin signalling transduction pathways. Binding of insulin to the insulin receptor elicits activation of a number of divergent signalling pathways which regulate cell metabolism, gene expression and proliferation. This schematic shows is a simple summary of the major signalling pathways. Created in biorender.

1.1.3. Type 1 diabetes

Accounting for approximately 10% of cases, type 1 diabetes mellitus (T1DM) is a chronic autoimmune disease characterised by lymphoid infiltration of the islets of Langerhans and destruction of insulin producing pancreatic beta cells, resulting in insulin deficiency and sustained hyperglycaemia (Mobasseri *et al.*, 2020; Figure 1.2).

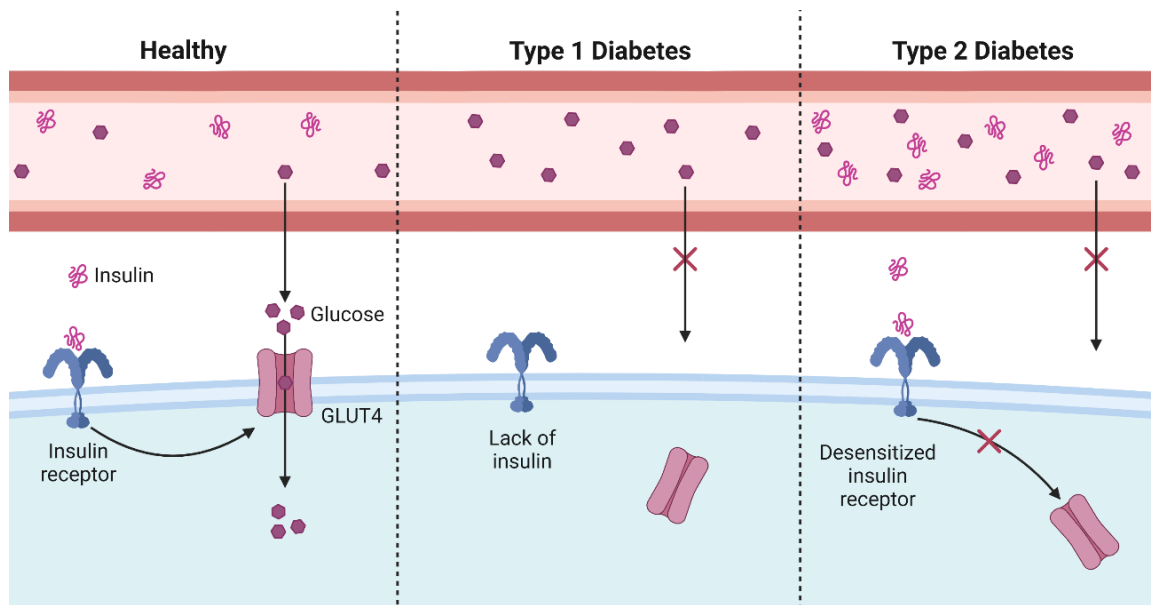


Figure 1.3. The different mechanisms underlying insulin release and action in physiological (healthy) conditions as compared to type 1 and type 2 diabetes. In healthy tissue, detection of insulin via cell membrane insulin receptors stimulates GLUT4 mediated uptake of glucose from the blood into the cell. This mechanism is disturbed in diabetes, preventing uptake of glucose from the blood and subsequent hyperglycaemia. In type 1 diabetes, a lack of insulin results in a lack of cell response to hyperglycaemia, preventing GLUT4-mediated glucose uptake. Similarly in type 2 diabetes, GLUT4-mediated glucose uptake is not initiated due to a lack of cellular response to circulating insulin. Sustained hyperglycaemia occurs in both cases as a result. Created in biorender.

In T1DM, disease is associated with local inflammation in the pancreatic islets, characterised primarily by CD8⁺ cytotoxic T cells in addition to CD4⁺ helper T cells, antibody producing B cells and infiltrating macrophages (Budd *et al.*, 2021). The development of autoimmune disease is linked to the presence of a range of autoantibodies against beta cells, present in more than 90% of individuals (Basu *et al.*, 2020; Richardson *et al.*, 2013). Insulin is the most common target of early autoantibodies, produced by infiltrating B lymphocytes, often followed by other major beta cell antigens including, but not limited to glutamate decarboxylase (GAD; Baekkeskov *et al.*, 1990), tyrosine phosphatase-like protein IA-2 (Hawkes *et al.*, 2000), zinc transporter (ZnT)8 (Wenzlau *et al.*, 2007) and tetraspanin-7 (McLaughlin *et al.*, 2016). Whilst the initial cause of the autoimmune response is not yet fully understood, it is known that B cells play a

major role, through the uptake of beta cell antigens, subsequent release of autoantibodies and presentation to CD4⁺ and CD8⁺ T cells (Christie, 2016). This leads to the activation of CD8⁺ cytotoxic T cells, which mediate beta cell death, and CD4⁺ T helper cells which release an array of pro-inflammatory cytokines to further exacerbate B cell and CD8⁺ T cell responses (Figure 1.3; Christie, 2016).

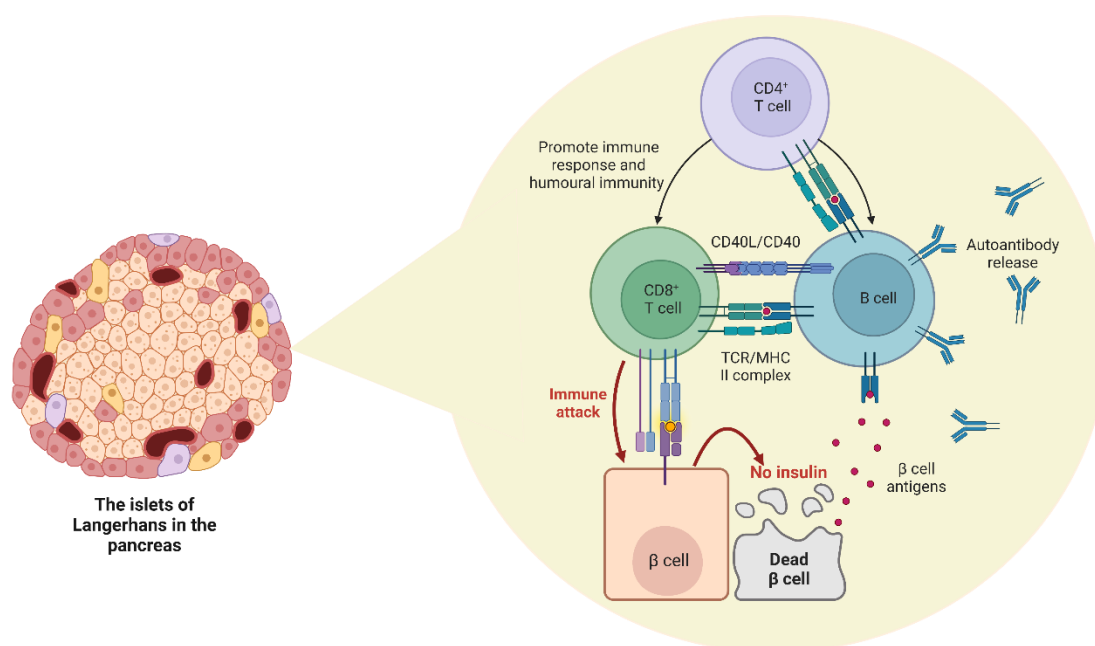


Figure 1.4. The involvement of immune cells in autoimmune-mediated destruction of pancreatic beta cells in type 1 diabetes. Responsible for the death of insulin producing beta (β) cells, CD8⁺ T cell activation and recognition of beta cells is promoted by CD4⁺ T helper cells and B cells. Acting as antigen presenting cells, B cells take up beta cell antigens and present them to activate other immune cells, initiating the immune response, as well as producing autoantibodies labelling beta cells as targets for the immune system. Created in biorender.

Typically, T1DM presents during childhood, with an average age of onset of 13 years, but it can develop later in life (Chiang *et al.*, 2018). While the exact mechanisms leading to T1DM are not fully established, research shows that a combination of genetic susceptibility and environmental triggers, such as a viral infection activating the immune response, drive unregulated autoimmune activity (Norris *et al.*, 2020). The onset of T1DM is often rapid, especially in children, with one third of cases presenting with diabetic

ketoacidosis upon diagnosis, making swift diagnosis and treatment essential (Mencher *et al.*, 2019). Development of disease is classified into three stages. Stage 1 is asymptomatic with normal blood glucose levels but the presence of two or more pancreatic autoantibodies. Individuals diagnosed at stage 2 still present as asymptomatic with two or more autoantibodies but also have high fasting glucose, impaired glucose tolerance or haemoglobin A1c (HbA1c) between 5.7% and 6.4%. Diagnosis criteria at stage 3 include presence of two or more autoantibodies, diabetes or hyperglycaemia and clinical symptoms (Insel *et al.*, 2015). While presentation is diverse, common symptoms include polyuria, caused by hyperglycaemia-induced osmotic imbalance and polydipsia as a result of hyperosmolarity and dehydration (Roche *et al.*, 2005). Osmotic imbalance can lead to swelling of the optic lens resulting in blurred or altered vision (Balaji *et al.*, 2019). Weight loss, polyphagia and fatigue often develop secondary to muscle and fat breakdown, increased lipolysis, and ketone production (Balaji *et al.*, 2019). Increased ketones combined with electrolyte imbalances can lead to diabetic ketoacidosis, a potentially life-threatening complication of diabetes requiring hospitalisation (Mencher *et al.*, 2019).

People with T1DM must closely monitor blood glucose levels and require life-long daily exogenous insulin replacement to survive (Pathak *et al.*, 2019). With effective management of blood glucose, people with T1DM can live healthy lives and diabetes associated complications can be delayed or prevented (Pathak *et al.*, 2019). However self-management can be difficult, especially in young children and teenagers, and is not an effective option for all. In areas of high socio-economic deprivation, access to insulin, healthcare and education are often limited, contributing to poor self-management (Fallon *et al.*, 2022). When blood glucose levels are not maintained, people can develop diabetic ketoacidosis, a result of the build-up of harmful ketones in the body, which can lead to severe disability and death (Mencher *et al.*, 2019). Another acute complication is hypoglycaemia, a result of improper insulin dosage typically presenting as polydipsia, polyuria, fatigue, constant hunger, sudden weight loss and blurred vision. This can result in chronic complications including poor growth and early onset vascular conditions (Kaur and Seaquist, 2023). Associated with high morbidity and mortality, nearly 50% of individuals with T1DM will develop at least one severe secondary complication such as cardiovascular disease, renal disease, vision loss, neuropathy and foot ulcers (Harding *et al.*, 2019). In the absence of an islet or pancreas transplant and with no cure currently

available, maintaining normoglycaemia over a healthy lifespan is challenging and reduces individuals' quality of life (Khadilkar *et al.*, 2022).

1.1.4. Type 2 diabetes

The most common form of diabetes, type 2 diabetes (T2DM) accounts for over 90% of diabetes cases worldwide (International Diabetes Federation., 2021). In T2DM, hyperglycaemia initially develops in response to the bodies inability to respond as effectively to insulin, referred to as insulin resistance (Peterson and Shulman, 2018; Figure 1.2). Symptoms are similar to those of T1DM but typically less severe and can be symptomless (Reinehr, 2005). Risk factors associated with T2DM include increasing age, family history and ethnicity. Lifestyle choices also play a large role, with development linked to lack of physical activity, smoking and high alcohol intake (Bellou *et al.*, 2018). A significant proportion (60-90%) of cases of T2DM are associated with obesity and high percentage body fat (Bhupathiraju and Hu, 2016; Gray *et al.*, 2015) which are strongly linked to insulin resistance and reduced beta cell production (Ormazabal *et al.*, 2018).

Whilst the exact mechanisms underlying insulin resistance are yet to be fully determined, research shows that excessive adipose tissue creates a systemic inflammatory environment which contributes to reduced insulin action (Ahmed *et al.*, 2021; McLaughlin *et al.*, 2002; Nieto-Vazquez *et al.*, 2008; Senn *et al.*, 2003). Obesity is a major risk factor for T2DM because of the knock-on effects of having a disproportionate amount of adipose tissue. As an endocrine organ, adipose tissue plays a role in regulation of energy homeostasis through release of cytokines and chemokines (Dilworth *et al.*, 2021). In obesity, high levels of proinflammatory cytokines and chemokines, including interleukin 1-beta (IL1 β), tumour necrosis factor alpha (TNF α), interleukin 6 (IL6) and interferon gamma (IFN γ) are released, resulting in high levels of systemic inflammation (Figure 1.4; Brennan *et al.*, 2021). Altered function of adipose tissue culminates in dampened sensitivity to insulin, prompting an increase in insulin production and secretion by pancreatic beta cells, which can maintain normoglycaemia despite insulin resistance (Ahmed *et al.*, 2021). Due to this, diabetes often first appears asymptomatic. However, over time as insulin resistance increases and beta cell mass reduces because of excessive production, individuals become hyperglycaemic (Beagley *et al.*, 2014). Furthermore, during obesity

storage of adipose tissue is exceeded leading to lipid spill over into other tissue types including the pancreas, kidneys, liver and skeletal muscle (Figure 1.4). This abnormal release of proinflammatory cytokines contribute to high levels of local inflammation as well as elevated systemic inflammation (Pitere *et al.*, 2022), which then contribute to the development of secondary complications.

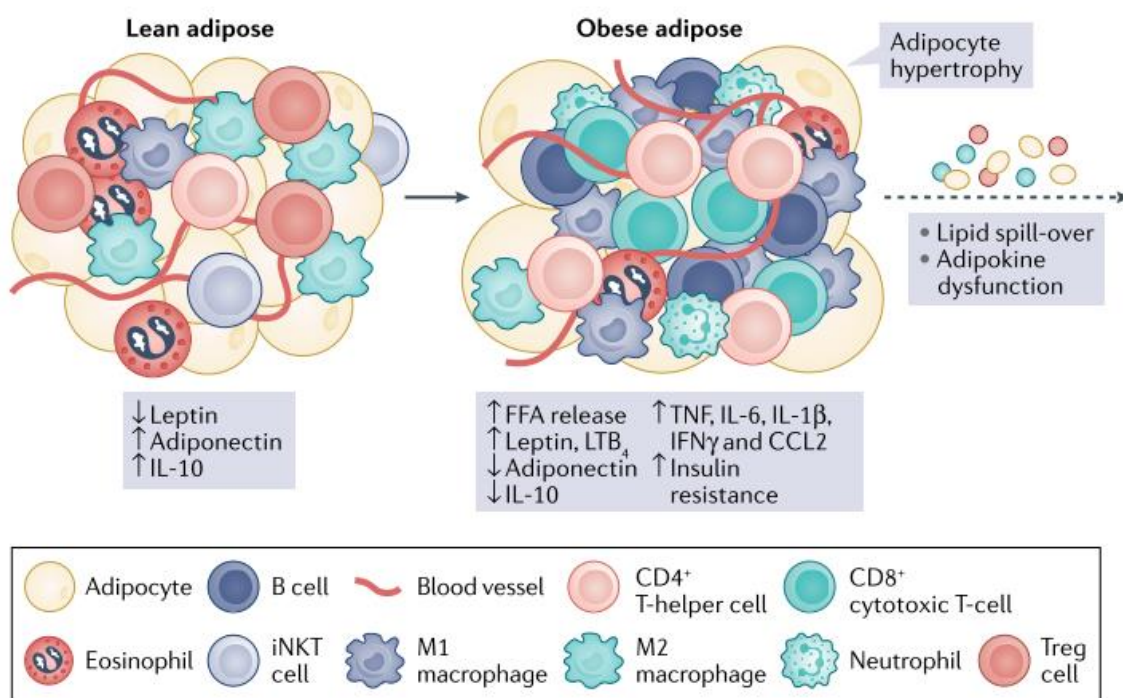


Figure 1.5. The contributions of obesity to development of type 2 diabetes. This schematic demonstrates the differences between healthy ‘lean’ adipose tissue and obese adipose tissue as is often seen in T2DM. Excessive calorie intake leads to adipocyte hypertrophy and dysfunction, lipid spill over into other tissues, increased release of proinflammatory markers and reduced expression of protective proteins adiponectin and IL10. These changes culminate in an increase in insulin resistance leading to increased risk of T2DM. Adapted from Brennan *et al.*, 2021.

1.1.5. Other types of diabetes

In addition to T1DM and T2DM, other types of the disease have also been classified. Gestational diabetes is the development of hyperglycaemia during pregnancy, which affects approximately 3-5% of all pregnancies (McIntyre *et al.*, 2019). Associated with a

hormonal switch to human placental lactogen which acts as an insulin inhibitor (Moore, 2016), gestational diabetes often occurs late in the second trimester and therefore has only a small increased risk of congenital abnormalities (Kc *et al.*, 2015). However, it does increase the risk of both the mother and child developing T2DM later in life and for neonatal macrosomia, defined as a birth weight of over 4000g.

Commonly misdiagnosed as T2DM, latent autoimmune diabetes is similar to T1DM in pathology but develops at a slower rate with onset seen in individuals aged 25 and above (Pozzilli and Pieralice, 2018). In addition, maturity onset diabetes of the young (MODY) is often referred to as genetic diabetes, as it is caused by a single genetic mutation in one of 11 different genes, including GK, HNF1alpha (hepatocyte nuclear factor), PDX-1 (pancreatic and duodenal homeobox 1), also known as insulin promoter factor 1 (Punthakee *et al.*, 2018; Velho *et al.*, 1997). Like T1DM, onset of MODY often occurs before the age of 25 but develops despite pancreatic beta cell function and lack of an autoimmune response (Urakami, 2019). Moreover, obesity is not a risk factor for development of MODY, as seen in T2DM (Urakami, 2019).

1.1.6. Diagnosis

Diagnosis of diabetes is based upon the presence of sustained hyperglycaemia. Criteria for diagnosis include a fasting (no calorie intake for a minimum of 8 hours prior) plasma glucose of ≥ 7.0 mmol/L as the main standard test, which can diagnose asymptomatic diabetes (International Diabetes Federation., 2021). In individuals displaying classical symptoms of diabetes, such as polyuria, polydipsia and sudden weight loss, a random venous plasma glucose concentration of ≥ 11.1 mmol/L is diagnostic, however in those without symptoms, an additional test on a different day will also be required (International Diabetes Federation., 2021). An oral glucose tolerance test (OGTT) is also used in which a two hour plasma glucose concentration of ≥ 11.1 mmol/L following intake of 75g anhydrous glucose is considered diabetic (American Diabetes Association Professional Practice Committee, 2022).

A HbA1c test can also be used to diagnose diabetes, but in the presence of a positive glucose test, it also cannot rule it out. HbA1c ≥ 47 mmol/L (6.5%) is the recommended guidance for diagnosing diabetes (International Diabetes Federation., 2021). For diagnosis

of T1DM, presence of circulating pancreatic beta cell autoantibodies can also indicate diabetes and the stage of development (International Diabetes Federation., 2021). The diagnostic criteria differs for gestational diabetes where a diagnosis can be made based on a fasting plasma glucose ≥ 5.6 mmol/L or a two hour plasma glucose concentration of ≥ 7.8 mmol/L after an oral glucose tolerance test (International Diabetes Federation., 2021).

1.1.7. Treatment

To maintain normal blood glucose levels in people with T1DM, delivery of exogenous insulin is required. Various modes of delivery are now available, from multiple daily injections via syringe or pre-filled pens, or use of an insulin pump (Janež *et al.*, 2020). This requires careful glucose monitoring and therapeutic education to ensure correct dosage and delivery, essential to avoid severe complications such as hypoglycaemia (DiMeglio *et al.*, 2018). Advances in the use of hybrid closed-loop insulin pump systems, also known as an artificial pancreas, have improved glucose control and reduced risk of both hyper and hypoglycaemia through automated glucose-responsive insulin delivery (Weisman *et al.*, 2017; Brown *et al.*, 2021). Insulin replacement therapy may also be required for severe cases of T2DM where beta cells cannot produce enough insulin (MarínPeñalver *et al.*, 2016). Alternatively, pancreas or islet transplantation negates the need for insulin therapy but is associated with risks of its own.

The major way in which T2DM is managed is through lifestyle changes by adopting a healthy diet, exercising regularly and reducing other risk factors. These include high blood pressure, cholesterol, body weight and smoking (Bellou *et al.*, 2018). These changes alone are not always sufficient to maintain normal glucose levels and so oral diabetic medications are also available, which can be used individually or in combination (Marx *et al.*, 2021). An oral anti-hyperglycaemic drug, Metformin is the most common first line treatment for T2DM. A biguanide, it alleviates chronic hyperglycaemia through inhibition of hepatic gluconeogenesis, reducing release of glucose in the liver, whilst additionally reducing insulin resistance and increasing glucose uptake (Foretz *et al.*, 2019). Whilst its mechanisms are yet to be fully identified, several studies demonstrate protective effects of Metformin against diabetes related death (Johnson *et al.*, 2002), cardiovascular

complications (Zhang *et al.*, 2020) and renal injury (Kwon *et al.*, 2020; Zhou *et al.*, 2021a). Other glucose lowering drugs are also sometimes used such as incretin-based agents (for example, glucagon-like peptide 1 (GLP-1) agonists (Sattar *et al.*, 2021) and dipeptidyl peptidase-IV (DPP-IV) inhibitors (Deacon, 2020) and sodium glucose co-transporter 2 (SGLT2) inhibitors (McGuire *et al.*, 2021). Please see Chapter 6 for a more in-depth description.

1.2. Complications of diabetes

1.2.1. Micro and macrovascular complications

Acute and chronic secondary complications develop as a result of both T1DM and T2DM and often occur 5-6 years prior to diagnosis of the disease (Diabetes UK, 2019). Despite good overall management, more than 50% of people with diabetes present with at least one complication at the time of diagnosis (Harding *et al.*, 2019). Long term insulin dysfunction can lead to hyperglycaemic-induced damage of many major organs, also contributed to by hypertension and high cholesterol (Ormazabal *et al.*, 2018). Although acute complications can occur such as diabetic ketoacidosis, chronic secondary complications are most common and are a major cause of high morbidity and mortality rates amongst those with diabetes (Papatheodorou *et al.*, 2018; Deshpande *et al.*, 2008). Debilitating and life-threatening secondary complications include cardiovascular disease, nerve damage, kidney impairment, limb amputation and blindness.

1.2.2. Cardiovascular disease

Diabetes and insulin resistance are major risk factors for cardiovascular complications, contributed to by sustained hyperglycaemia, hypertension, dyslipidaemia, systemic inflammation, and elevated cholesterol (Ohkuma *et al.*, 2019). Acute and chronic cardiovascular complications, such as myocardial events and stroke, are associated with a three-to-four-fold increase in mortality and are the most common cause of diabetes associated death (Einarson *et al.*, 2018), accounting for 44% of deaths associated with T1DM and 52% of deaths associated with T2DM (Raghavan *et al.*, 2019). Despite the

severe impacts of cardiovascular complications, the pathological mechanisms behind disease are complex and not fully elucidated, resulting in limited treatment options.

Atherosclerosis is a common cardiovascular condition associated with diabetes. Hyperglycaemia and insulin resistance lead to endothelial cell dysfunction (Abu-Saleh *et al.*, 2021), increased oxidative stress (Papachristoforou *et al.*, 2020), adhesion molecules, vasoconstriction and systemic inflammation which cause the development of calcified, lipid-rich atherosclerotic plaques containing immune cells and inflammatory proteins (Figure 1.5; Laakso and Kuusisto, 2014). Diabetes is also associated with increased fibrosis in the heart and altered morphology, reducing vascular output, and putting strain on the heart (Tuleta and Frangogiannis, 2021; Feng *et al.*, 2017). In addition, contributing to an array of cardiovascular disorders, hypertension and an obesity-related increase in blood volume (hypervolaemia) increases the force with which blood is pumped through the body, over time damaging artery vasculature and altering cardiac morphology (Grönholm *et al.*, 2005; Montero *et al.*, 2019). Dyslipidaemia, present in approximately 90% of people with diabetes, contributes to hardening of the arteries. Combined, these effects lead to reduced blood flow and oxygen starvation affecting myocardial tissue which can have severe and life-threatening effects such as myocardial infarction and stroke (Kaze *et al.*, 2021; Kane *et al.*, 2021). This can also reduce blood flow to the extremities, contributing peripheral vascular disease, which when left untreated often leads to amputation (Giannopoulos and Armstrong, 2020). These complications are associated with high morbidity and mortality, even after survival of an initial cardiac event, highlighting an urgent need for therapeutic interventions for diabetes (Raghavan *et al.*, 2019).

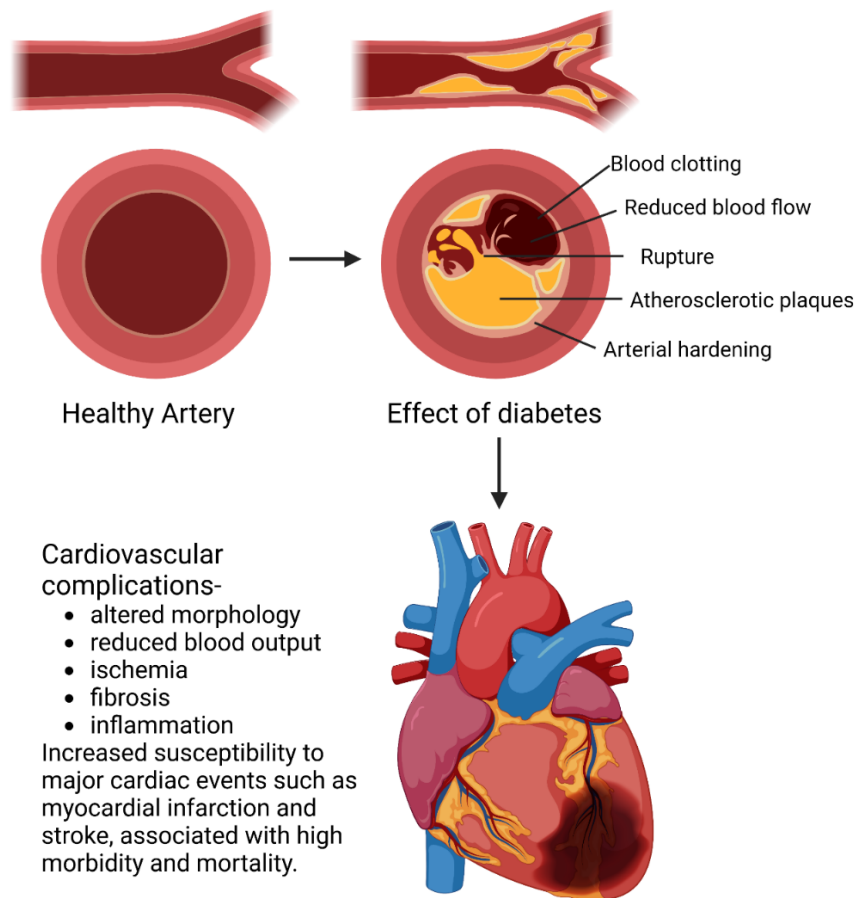


Figure 1.6. The mechanisms through which diabetes contributes to development of secondary macrovascular complications. Created in biorender.

1.2.3. Retinopathy

Diabetic retinopathy affects approximately 30% of individuals with diabetes, and 80% of those who have suffered from diabetes for over 20 years. Diabetes-induced retinopathy is the leading cause of blindness in developed countries and the working age population, accounting for approximately 12% of new cases of blindness in the US (National diabetes statistics report, 2020).

Categorised into two stages of clinical disease (Figure 1.6), diabetic retinopathy initially presents as non-proliferative, characterised by inflammation, ischemia, oedema, hypertrophy, capillary closure and loss of microvascular endothelium integrity leading to

altered blood-retinal barrier permeability. These pathologies are caused by a hyperglycaemic-induced increase in vascular permeability, apoptosis and disruption of retinal homeostasis (Mathebula, 2018). Macula oedema develops in approximately 50% of individuals with diabetic retinopathy, effects of which range from mild to severe visual impairment and is the most common contributor to vision loss in those with diabetic retinopathy (Ixcamey *et al.*, 2021). Other pathologies contributing to diabetic retinopathy include increased vascular permeability (Miloudi *et al.*, 2019; Liu *et al.*, 2019a) and dysfunction of the blood-retinal barrier (Hyun *et al.*, 2018; Hao *et al.*, 2022), which usually protects from toxins and immune cells in the blood (Antonetti *et al.*, 2021). Furthermore, the retinal blood vessel basement membrane thickens, small capillaries degenerate and vascular cells including pericytes and smooth muscle cells are lost. Subsequent reduced blood flow and ischemia leads to formation of microscopic aneurysms, immune cell recruitment and degeneration of retinal neurons and glial cells (Antonetti *et al.*, 2021).

Over time, many individuals progress to the proliferative stage of disease, where increased blood vessel formation leads to haemorrhage and scar tissue formation. Minor bleeds from new vessel breakage partially obstruct vision and major bleeds can be fully obstructive. Perpetual blood vessel formation, swelling and scarring leads to diabetic macular oedema, haemorrhage or retinal detachment, resulting in loss of sight (Cheung *et al.*, 2010; Wang and Lo, 2018).

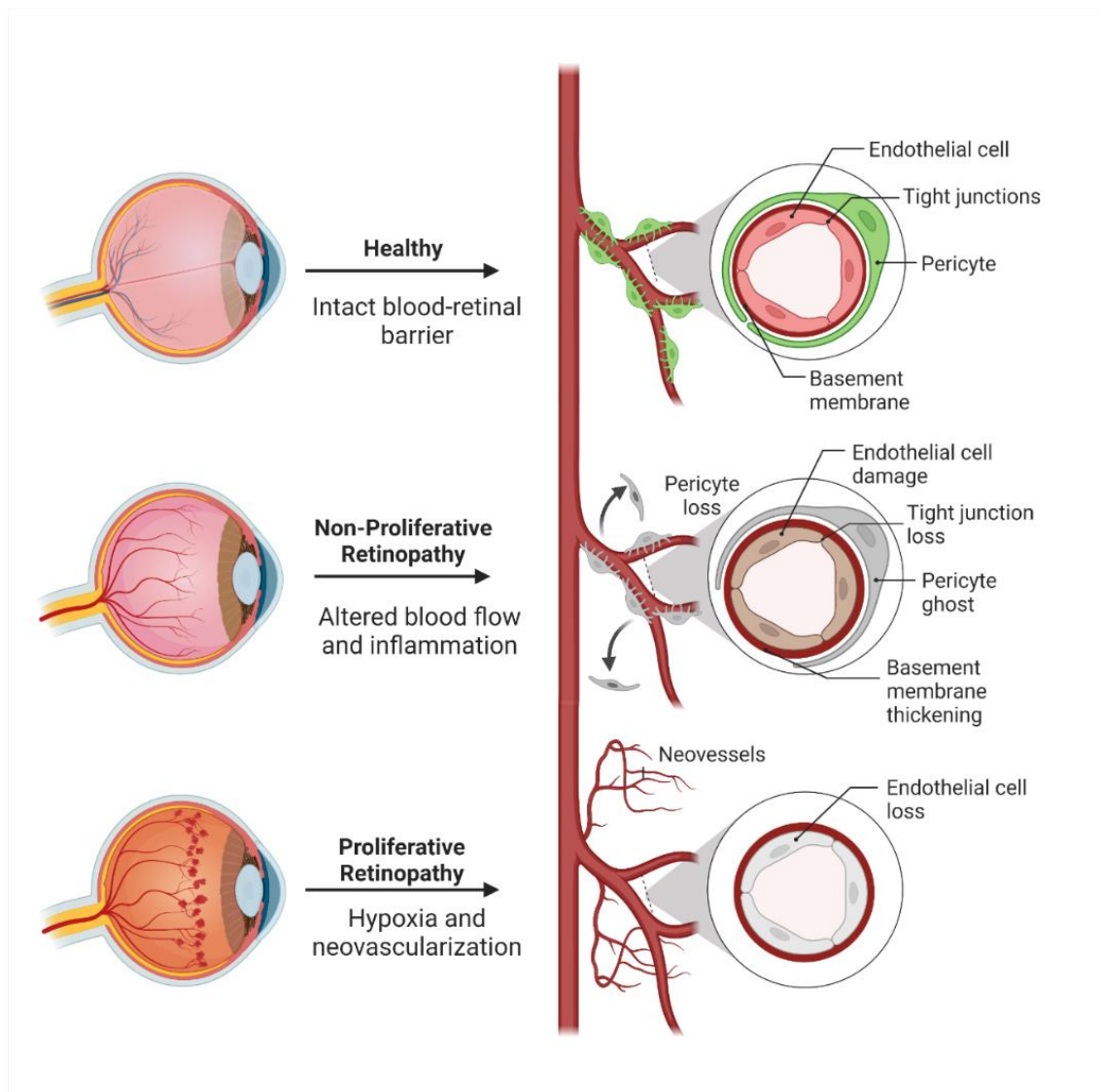


Figure 1.7. The impact of diabetes-induced sustained hyperglycaemia on vasculature in the eye, resulting in diabetic retinopathy. Created in biorender.

Whilst there is no definitive cure for diabetic retinopathy, treatments are available to manage progression and reduce the likelihood of severe vision loss (Duh *et al.*, 2017). In addition to management options used for diabetes including control of blood glucose, pressure and cholesterol, there are four main treatments used to treat diabetic retinopathy: anti-VEGF injections (Arrigo *et al.*, 2022), steroid injections (Lynch *et al.*, 2019), pan-retinal laser photocoagulation (Mukhtar *et al.*, 2016; Everett and Paulus, 2021), and vitrectomy (Yorston *et al.*, 2008; Liao *et al.*, 2020).

To slow progression of non-proliferative diabetic retinopathy anti-vascular endothelial growth factor VEGF drugs and steroids can be injected into the eyes, an option that is effective in slowing progression in approximately 50% of cases. However, this treatment is only partially effective and monthly injections are needed to maintain efficacy (Wang and Lo, 2018). For macular cases of oedema, severe non-proliferative and proliferative diabetic retinopathy, the gold standard treatment is photocoagulation laser therapy (Romero-Aroca *et al.*, 2014). This treatment is used in earlier stages to burn in the retina, reducing cell number and oxygen demand to reduce subsequent ischemia. In more progressed stages of disease, photocoagulation laser therapy targets new abnormal retinal blood vessels and reduces risk of severe vision loss by 50% (Evans *et al.*, 2014). The procedure does however need to be repeated to maintain its protective effects. Recently advances have been made in laser therapy to develop a subthreshold laser which specifically targets blood vessel formation in the retinal pigment epithelium. This treatment avoids adverse effects associated with photocoagulation laser therapy (Mansour *et al.*, 2020). In patients who have suffered a large haemorrhage, vitrectomy surgery is performed in which the obstructed vitreous is removed and replaced with saline solution to reduce risk of severe vision impairment (Newman *et al.*, 2010).

1.2.4. Neuropathy

Caused primarily by hyperglycaemia, diabetic neuropathy encompasses several different types of nerve damage associated with diabetes (Feldman *et al.*, 2019). Approximately 50% of individuals with diabetes also suffer neuronal damage of some kind associated with diabetic neuropathy (Ismail-Beigi *et al.*, 2010; Pop-Busui *et al.*, 2009), which is the cause of approximately 50-75% of non-traumatic amputations (Armstrong *et al.*, 1998). Also linked to microvascular injury, neuropathy occurs because of damage to the small blood vessels supplying the affected nerves. Onset begins with narrowing of the blood vessels and progresses on to capillary basement membrane thickening, endothelial hyperplasia, and hypoxia. Subsequent neuronal ischemia and dysfunction follows (Baum *et al.*, 2021).

Sensorimotor polyneuropathy is characterised by decreased sensation, loss of reflexes and pain in the limbs, usually starting at the toes and working upwards. Sensory loss leads

to increased risk of amputation due to infection or ulcer development, loss of muscle function and multiple fractures, significantly affecting quality of life (Sloan *et al.*, 2021). Alternatively, autonomic neuropathy affects nerves of organ systems including the heart, lungs, adipose tissue, and gastrointestinal system. Therefore, autonomic neuropathy can display as a vast array of symptoms and pathologies dependant on the organ affected (Verrotti *et al.*, 2014). Several other neuropathies can also affect people with diabetes, including cranial neuropathy (Mathew *et al.*, 2019), and whilst therapeutics to relieve symptoms and slow progression exist, there is no cure. The main treatment, as with other complications of disease, is maintenance of hyperglycaemia and hypertension to reduce microvascular damage (Feldman *et al.*, 2019).

1.2.5. Impaired Wound Healing

Many secondary complications of diabetes are associated with microvascular changes (Wong *et al.*, 2016), including chronic wounds and skin lesions, which have a slower healing rate in diabetes, increasing risk of infection and amputation (Patel *et al.*, 2019). Resulting from sustained hyperglycaemia, and associated with diabetic neuropathy, approximately 20% of individuals with diabetes develop diabetic wounds, the largest contributor (50-70%) to non-traumatic limb amputations (International Diabetes Foundation, 2019).

Classified into four individual stages (Figure 1.7), wound healing is essential for the restoration of anatomical integrity to protect against infection and maintain tissue function (Smith *et al.*, 2020). Under physiological conditions, haemostasis is the first stage of the healing process, characterised by blood clotting and scab formation to prevent bleeding and close the wound, protecting against invasion of pathogens (Wilkinson and Hardman, 2020). Followed by the inflammatory stage, immune cells including neutrophils and macrophages (Kim and Nair, 2019) infiltrate the site of injury to fight off potential pathogens, whilst also recruiting and activating fibroblasts (Desjardins-Park *et al.*, 2018). During the proliferation stage, fibroblasts secrete fibronectin, collagen I and collagen III, forming a scaffold structure on which new cells can proliferate, replacing those lost due to cell damage (Worthen *et al.*, 2020). The final stage is maturation, characterised by extracellular matrix (ECM) remodelling and controlled by matrix metalloproteinases

(MMPs). During this stage, cells of the epidermis and dermis; particularly fibroblasts, break down damaged extracellular matrix upon injury and replace it to form mature granulation tissue and build up tensile strength (Wilkinson and Hardman, 2020).

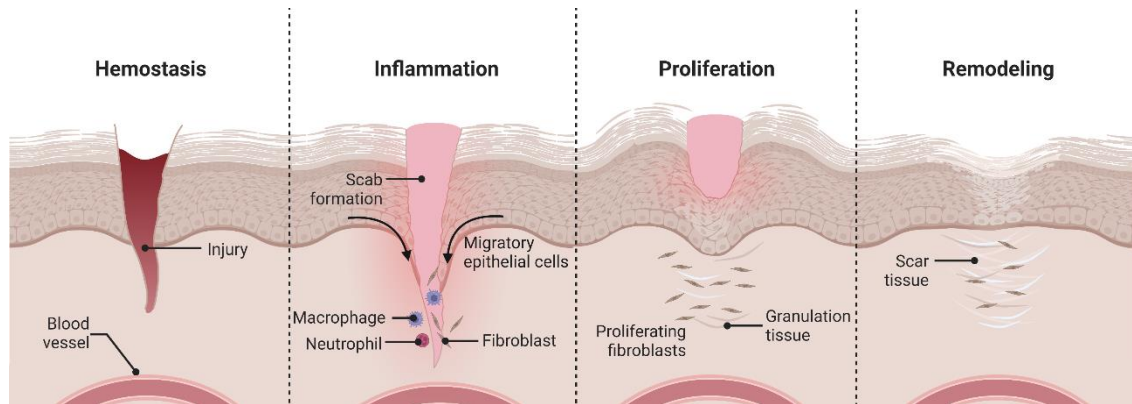


Figure 1.8. Schematic demonstrating the four stages on wound healing under physiological conditions. Consisting of haemostasis, in which the vessels vasoconstrict, blood clots and scab forms rapidly to prevent excessive blood loss and close the wound. Macrophages and neutrophils clear out infection in addition to activation and recruitment of fibroblasts during the inflammatory stage. Fibroblasts secrete extracellular matrix proteins, providing a scaffold for proliferation cells to heal the tissue. Fibroblasts and other cells secrete MMPs for extracellular matrix remodelling and maturation. Created in biorender.

In diabetes, a persistent inflammatory phase is exhibited which delays the formation of mature granulation tissue paralleled by reduced tensile strength. This results in chronic wounds associated with impaired nitric oxide synthesis, reduced cell proliferation and differentiation, dysfunctional fibroblasts slowing extracellular matrix deposition, increased pro-inflammatory cytokines and upregulated MMP-mediated breakdown of ECM components. This leads to increased risk of infection, sepsis, reduced mobility and even amputation, which result in a long-term negative effect on quality of life, morbidity and in some cases, mortality (Wang *et al.*, 2007; Landén *et al.*, 2016). Treatment of diabetic wounds is limited, relying on control of blood glucose, removal of dead tissue through surgical debridement, wound dressings, and wound offloading to relieve pressure (Patel *et al.*, 2019).

1.3. Diabetic nephropathy

Diabetic nephropathy (DN) is a severe secondary microvascular complication of diabetes affecting approximately 40% of people with diabetes (Dagar *et al.*, 2021). Second only to cardiovascular complications, DN has high rates of morbidity and mortality in people with type 1 (~21%) and type 2 diabetes (~11%; Gheith *et al.*, 2016; Morrish *et al.*, 2001). Moreover, DN is the leading cause of end stage renal disease (ESRD), accounting for ~50% of cases (Koye *et al.*, 2018). Despite advances in the clinical management of diabetes, the number of people that experience diabetic nephropathy as a result continues to rise (DeFronzo *et al.*, 2021). In the absence of a definitive treatment, urgent therapeutic approaches are required.

Our kidneys are complex, bean shaped organs located below the ribcage, in the back of the abdomen behind the peritoneum either side of the spine. Their function is to filter and remove waste products and excess fluid from the blood to maintain a healthy homeostasis (Soriano *et al.*, 2022). They also play a role in regulating blood pressure via the secretion of renin, releasing glycoprotein hormone erythropoietin, produced by the peritubular cells of the kidney, that stimulates red blood cell production, and strengthening bones via the production of 1,25 dihydroxyvitamin D3 (calcitriol; 1,25 D3) the most active form of vitamin D. Each kidney is made up of approximately 1 million small filter structures called nephrons (Figure 1.8; Soriano *et al.*, 2022). The proximal structure in the nephron is the renal corpuscle, a cup shaped structure (Bowman's capsule) surrounding a cluster of small blood vessels (the glomerulus), responsible for filtering small molecules, waste, and fluid into the renal tubules whilst larger negatively charged molecules, proteins and blood cells remain in the blood vessel (Scott and Quaggin, 2015). Following glomerular filtration, the proximal tubule passively reabsorbs approximately 60-70% of water and actively reclaims salts along with nearly all nutrients back into the blood (Figure 1.8; Aryal and Jackson, 2020). The Loop of Henle is a long U-shaped portion of the tubule surrounded by peritubular blood vessels which acts as a counter current multiplier with the active and passive transport of sodium and chloride ions lowering water potential and creating a medullary interstitial osmolar gradient (Figure 1.8; Zacchia *et al.*, 2018). This is essential for water and sodium reabsorption, regulation of plasma volume and blood pressure and production of concentrated urine (Zacchia *et al.*, 2018). The distal tubule and collecting duct play a role in hormone-sensitive water (antidiuretic hormone) and electrolyte (aldosterone) uptake and maintain blood acid-base balance (McCormick and Ellison,

2015). Together this allows efficient filtering of toxins, waste products and excess fluid whilst maintaining blood plasma volume and pressure (Soriano *et al.*, 2022).

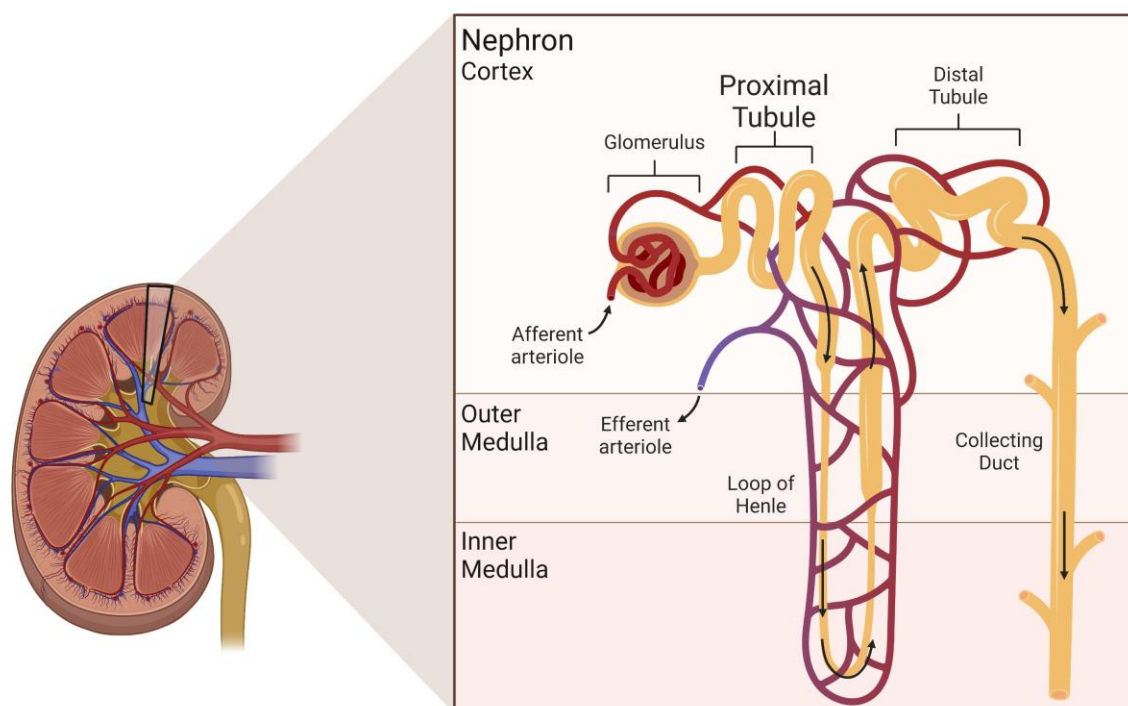


Figure 1.9. The structure of the kidney. Illustration showing a nephron and its components consisting of the afferent arteriole, glomerulus, proximal tubule, Loop of Henle, distal tubule, collecting duct and the efferent arteriole. Created in biorender.

Characterised by several structural and functional changes, DN develops in response to sustained hyperglycaemia, release of pro-inflammatory cytokines/chemokines and infiltration and activation of immune cells (Lin *et al.*, 2012). Central to renal injury, tubulointerstitial inflammation (Takaori *et al.*, 2016; Waikar *et al.*, 2016) drives phenotypic instability of proximal tubule cells and is characterised by upregulation of fibroblast associated proteins, downregulation of epithelial cell markers and excessive ECM deposition, culminating in a loss of renal function (Hills and Squires., 2010; Abed *et al.*, 2014).

1.3.1. Diagnosis

Annual screening for diabetic nephropathy starts 5 years after diagnosis of T1DM and upon diagnosis of T2DM, as approximately 7% of people diagnosed with type 2 will already present with microalbuminuria, associated with a degree of kidney injury (Persson and Rossing, 2018). The standard for diagnosis of diabetic nephropathy is spot urinary albumin (mg/L) measurements or albumin to creatinine ratio (mg/mmol). Urinary albumin levels of 20mg/L and above for diagnosis is recommended by the European Diabetes Policy group, which must be confirmed in two of three samples collected in a 3-6 month period to rule out daily variability. In some individuals with diabetes, a decline in glomerular filtration rate can be present in the absence of microalbuminuria. Therefore, estimated glomerular filtration rate (eGFR) is also routinely measured using clearance of endogenous creatinine, insulin, and other markers (Topf and Inker, 2019). Following diagnosis, further examinations are carried out, including ultrasonography, to determine the stage of disease and how best to treat it.

1.3.2. Clinical Stages

Diabetic nephropathy has been classified into 5 stages, by cause, eGFR and albuminuria by Mogensen *et al.*, in 1983, summarised in the table below (Table 1.1).

Table 1.1. The 5 pathological stages of diabetic nephropathy. Adapted from Mogensen *et al.*, 1983.

Clinical stage	Pathology	eGFR (ml/min/1.73m²)	Albuminuria (mg/g)
1. Early hypertrophy-hyperfunction	Minor kidney damage, usually renal hypertrophy, present but no loss of function.	90% or above	<30mg/g
2. Glomerular lesions without clinical disease	Structural alterations start to occur alongside small loss of function.	60-89%	<30mg/g
3a. Moderate incipient diabetic nephropathy	Mild loss of function, persistent microalbuminuria. Typically occurs 10-15 years after diagnosis (Krolewski <i>et al.</i> , 2017).	45-59%	30-300mg/g
3b. Severe incipient diabetic nephropathy	Severe loss of function, persistent microalbuminuria. Typically occurs 10-15 years after diagnosis.	30-44%	30-300mg/g
4. Overt diabetic nephropathy	Severe loss of function, marked decline in GFR, macroalbuminuria, high diastolic blood pressure. Often occurs 15-20 years after diagnosis.	15-29%	>300mg/g
5. End stage renal disease	Kidney failure, low GFR, macroalbuminuria, 50% of people with stage 4 disease progress to stage 5 within 10 years (Yuan <i>et al.</i> , 2017).	<15%	>300mg/g

1.3.3. Glomerulonephritis

Diabetic nephropathy is widely regarded as a glomerular disease in origin, developing as a result of sustained hyperglycaemia and hypertension (Ilyas *et al.*, 2017). A consequence of abnormal accumulation of ECM, composed of collagen proteins, fibronectin, and laminin, the first structural change to develop is thickening of the glomerular basement membrane (GBM), which increases with disease progression (Figure 1.9; Liu *et al.*, 2020). Also contributed to by excessive ECM deposition, mesangial expansion is a structural abnormality associated with diabetic nephropathy, causing restriction and distortion of glomerular capillaries and a reduced capillary filtration surface. Often developing in parallel to mesangial expansion, formation of crescent shaped lesions occurs associated with detachment of endothelial cells from the GBM and lytic changes in the mesangial space (Figure 1.9; Nunes *et al.*, 2020).

Glomerular injury is contributed to by other cell types including monocyte infiltration and macrophage differentiation (Zhang *et al.*, 2019), exacerbating local chronic inflammation through the release of pro-inflammatory factors (Mistry, Dabhi and Joshi, 2020). Moreover, podocytes, essential in maintaining glomerular structure and filtration function, undergo injury causing hypertrophy, loss of foot effacement processes and apoptosis (Figure 1.9; Kravets and Mallipattu, 2020; Weil *et al.*, 2012). These changes cumulatively drive progression to glomerulosclerosis, the end point of pathological mechanisms contributing to glomerular injury, characterised by severe scarring, lesion formation and loss of function (Thomas *et al.*, 2015; Yasuda *et al.*, 2018).

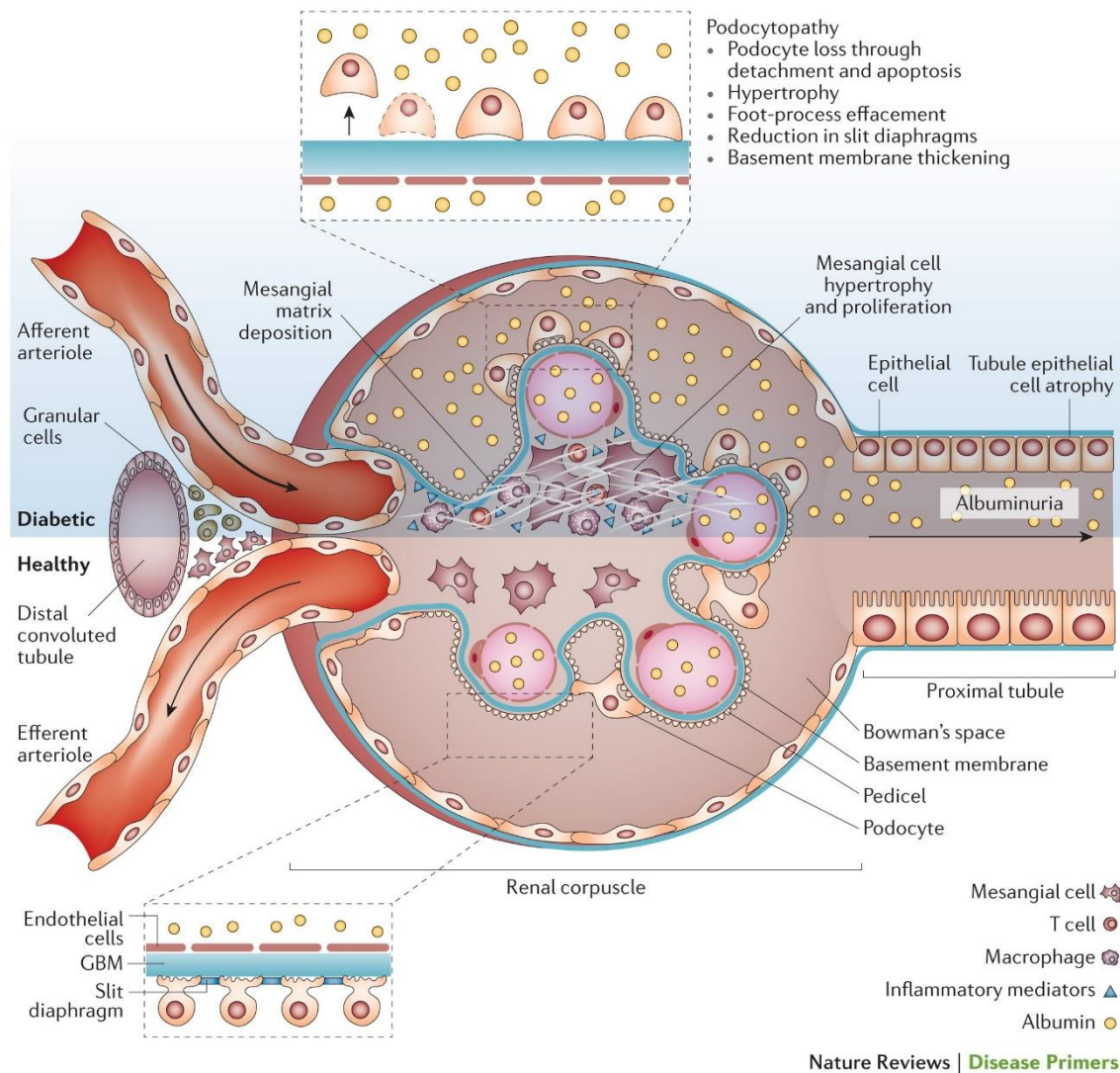


Figure 1.10. Diabetes contributed to structural and functional changes in the renal glomerulus, an early clinical manifestation of diabetic nephropathy. Adapted from Thomas *et al.*, 2015.

1.4. Tubulointerstitial injury

1.4.1. Proximal tubule inflammation

In diabetes, high blood glucose has been linked to elevated systemic concentrations of inflammatory cytokines; an effect which is compounded in individuals with high levels of adipose tissue, as evidenced by increased serum and urine IL1 β (Koleva Georgieva, Sivkova and Terzieva, 2011), interleukin 18 (IL18; Nakamura *et al.*, 2005) and TNF α

(Moriwaki *et al.*, 2003; Wong *et al.*, 2007; Navarro *et al.*, 2006; Hotamisligil *et al.*, 1993). Referred to as low-grade systemic inflammation (Alexandraki *et al.*, 2008), these inflammatory mediators have been linked to altered cell function in several secondary complications of diabetes including retinopathy, cardiovascular disease, and diabetic nephropathy (Schram *et al.*, 2005). In addition to these systemic effects, epithelial and immune cells of the diabetic kidney secrete increased levels of proinflammatory cytokines, creating a sustained local environment of high inflammation (Donate-Correa *et al.*, 2015; Pérez-Morales *et al.*, 2019).

It is inflammation and subsequent injury of the proximal tubule that dictates the rate of disease progression, leading to onset of end-stage renal disease (Takaori *et al.*, 2016). The innate immune response is activated in all forms of kidney inflammation, whether it be microbial or sterile, and it is the loss of regulation of this response that drives excessive inflammation in diabetic nephropathy (Anders and Muruve, 2011). A key mediator of innate immunity is activation of the NOD-like receptor protein-3 (NLRP3) inflammasome, through which aberrant activity in diabetic nephropathy results in excessive release of proinflammatory cytokines, as discussed in section 1.5. Chronic inflammation has been linked to infiltration and activation of immune cells, altered cell phenotype, fibrosis, and loss of tissue function (Calle and Hotter., 2020). However, our understanding of the exact mechanisms driving this inflammation in diabetic kidney disease is rudimentary, hindering our ability to treat this damage and delay progression onto end stage renal disease.

1.4.2. Monocyte infiltration

The principal source of pro-inflammatory mediators in diabetic nephropathy are resident kidney cells and infiltrating macrophages (Mathew *et al.*, 2011). The pathogenic role of infiltrating and resident macrophages has been demonstrated in various forms of chronic kidney disease with studies demonstrating therapeutic effects of kidney specific macrophage deletion and attenuation of these effects following macrophage repletion (Jo *et al.*, 2006; Kitamoto *et al.*, 2009). Macrophages are a major source of pro-inflammatory cytokines and chemokines including IL1 β , IL18 and TNF α , all of which contribute to development of tubulointerstitial injury (Taylor *et al.*, 2009). In multiple forms of chronic kidney disease, the degree of macrophage infiltration correlates to the severity of kidney

injury (Lee *et al.*, 2011; Eardley *et al.*, 2006; Eardley *et al.*, 2008). Findings from experimental models and observational studies in humans demonstrate a key role for macrophages in islet beta cell inflammation in obesity and T2DM, driven largely by synergistic responses to IFN γ , TNF α and IL1 β (Ying *et al.*, 2020). In diabetic nephropathy, damage to the proximal tubule is linked to recruitment of circulating monocytes into the interstitium, where the local environment can trigger cell differentiation and polarisation into either M1 or M2 macrophages (Figure 1.4), processes shown in models of chronic kidney disease (CKD; Abed *et al.*, 2014) and DN (Cao *et al.*, 2015).

Whilst the definitive characterisation of macrophages is controversial, M1 and M2 characterisation is a simplistic representation of two different types of macrophages based on inflammatory function (Calle and Hotter, 2020). Pro-inflammatory M1 macrophages are classically activated macrophages that secrete pro-inflammatory cytokines, recruit neutrophils and induce apoptosis, whereas M2 macrophages are alternatively activated, anti-inflammatory macrophages that promote wound healing but can lead to fibrosis during sustained injury (Cao *et al.*, 2015). Macrophage polarisation is dependent on environmental stimuli; thus, macrophages have a phenotypic plasticity, allowing them to adapt to the needs of the tissue in response to injury and inflammation. For example, in adipose tissue, macrophages convert from an M2 to M1 phenotype in response to increased obesity and inflammation (Lumeng, Bodzin and Saltiel., 2007). Dysregulated heterotypic cell communication between adipocyte cells and activated M1 macrophages augments the release of pro-inflammatory factors and exacerbates inflammation through increasing monocyte recruitment and inflammation within adipose tissue (Boutens *et al.*, 2018). Furthermore, in the kidney IFN γ stimulated macrophages undergo phenotypic switch from M1 to M2 during the repair phase of kidney injury (Lee *et al.*, 2011). In diabetic nephropathy, studies suggest that sustained hyperglycaemia evokes a switch from an M2 to M1 phenotype, with M1 macrophage infiltration linked positively to DN progression (Zhang, Yang and Zhao., 2019). Co-culture experiments indicate that this switch is induced by tubule cell derived factors (Figure 1.10). Despite this, the mechanisms which underlie this conversion are not fully understood (Lee *et al.*, 2011).

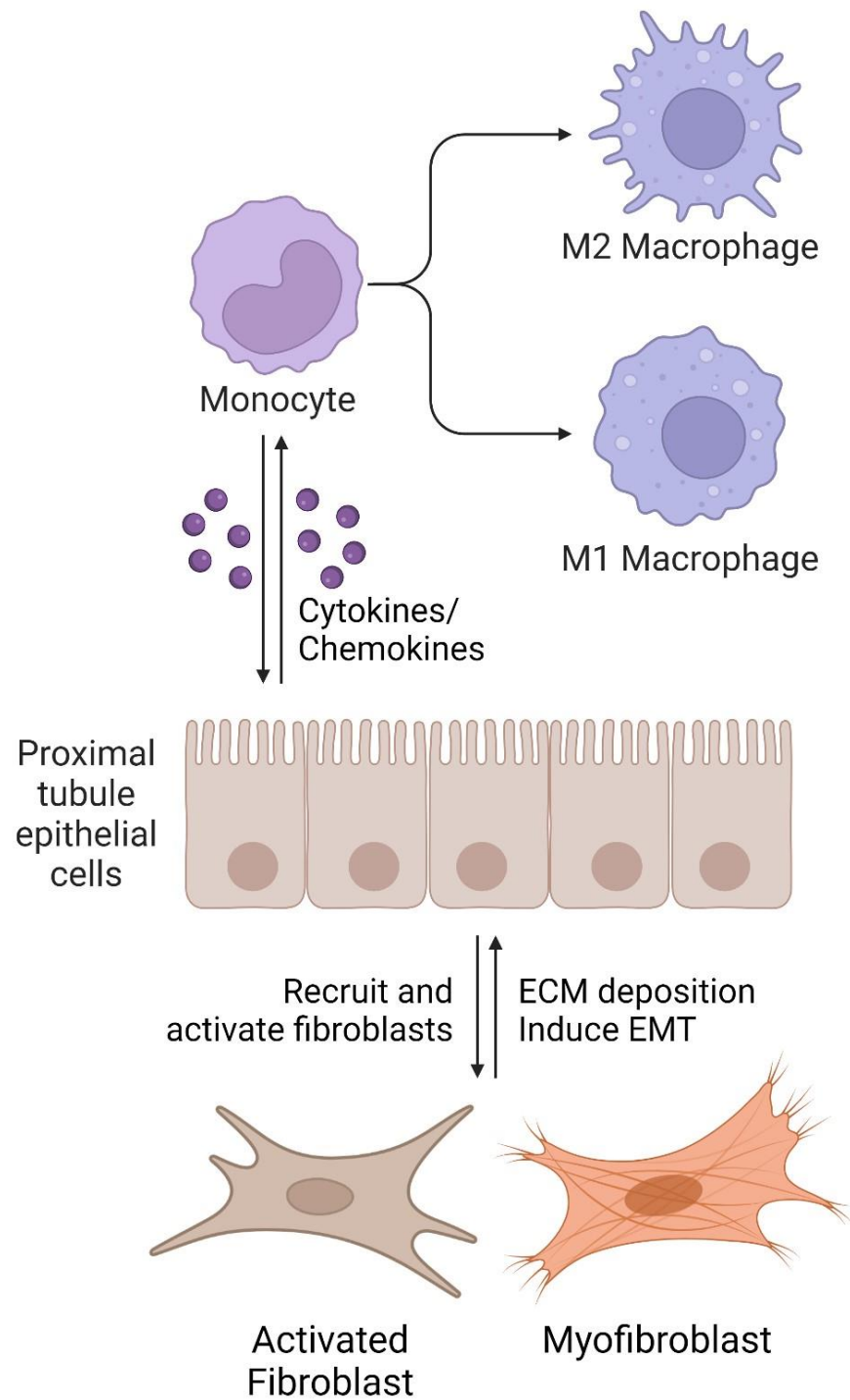


Figure 1.11. Homotypic and heterotypic interactions driving the presence of different inflammatory and fibrotic cell types in the proximal tubule, ultimately contributing to progression of diabetic nephropathy. Created in biorender.

1.4.3. Epithelial to mesenchymal transition

The damaging effects of chronic inflammation in the kidney extends to induction of epithelial to mesenchymal transition (EMT), a process in which injured proximal tubule epithelial cells evade apoptosis and undergo phenotypic conversion to a more mesenchymal phenotype (Figure 1.10; Rout-Pitt *et al.*, 2018). In healthy tissue, the process of EMT is tightly regulated, initiated primarily to aid wound healing. However chronic, sustained inflammation can disturb this balance, leading to EMT-mediated injury (Masola *et al.*, 2019). Key to the induction of EMT, glucose-mediated release of pro-inflammatory cytokine transforming growth factor beta-1 (TGF β 1) in diabetes activates suppressor of mothers against decapentaplegic (Smad)2/3/4 and downstream transcription factors stimulate mesenchymal cell protein synthesis (Hills *et al.*, 2012; Singh *et al.*, 2019). Epithelial cells have apical-basal polarity and form adherens and tight junctions between neighbouring cells to maintain cell integrity and stability (Hartsock and Nelson, 2008). During disease, epithelial cells take on a more fibroblast like appearance, exhibiting signs of altered cell morphology as evidenced by increased elongation and acquisition of a spindle shape. In addition, cells lose their cell-to-cell interactions, facilitated by disassembly of adherens and tight junction complexes (Hills *et al.*, 2012), culminating in disrupted polarity, which when combined with increased expression of fibroblast-specific protein 1 (FSP1) and alpha-smooth muscle actin (α SMA), enables cells to migrate into the interstitium, exacerbating the state of fibrosis (Burn and Thomas, 2010).

As an adherens junction protein, epithelial (E)-cadherin ligates partner proteins on neighbouring cells and binds β -catenin to link to the actin cytoskeleton (Tian *et al.*, 2011). Downregulation of E-cadherin is paralleled by a compensatory increase in neural (N)-cadherin (the cadherin-switch), with loss of E-cadherin-mediated cell tethering associated with the early stages of EMT (Figure 1.11; Hills *et al.*, 2012; Stone *et al.*, 2016). In parallel, cells acquire expression of mesenchymal markers such as α SMA and vimentin. There is controversy around the induction of full EMT in diabetic nephropathy, as this requires detachment from the basement membrane in order for the transformed cells to infiltrate the interstitial matrix as myofibroblasts (Yang *et al.*, 2020a). A proportion of tubular epithelial cells stay attached to the basement membrane during injury and do not acquire a full mesenchymal protein expression profile, with some cells not expressing key markers such as α SMA and FSP1, referred to as partial-EMT (Qi and Yang, 2018). In order to migrate into the interstitial space, expression of α SMA and FSP1 is essential for gain of

traction and motility in cells, indicative of full EMT. Following EMT, cells synthesize matrix proteins including fibronectin, collagen-I and collagen-IV, which are deposited into the extracellular space (Sheng and Zhuang, 2020).

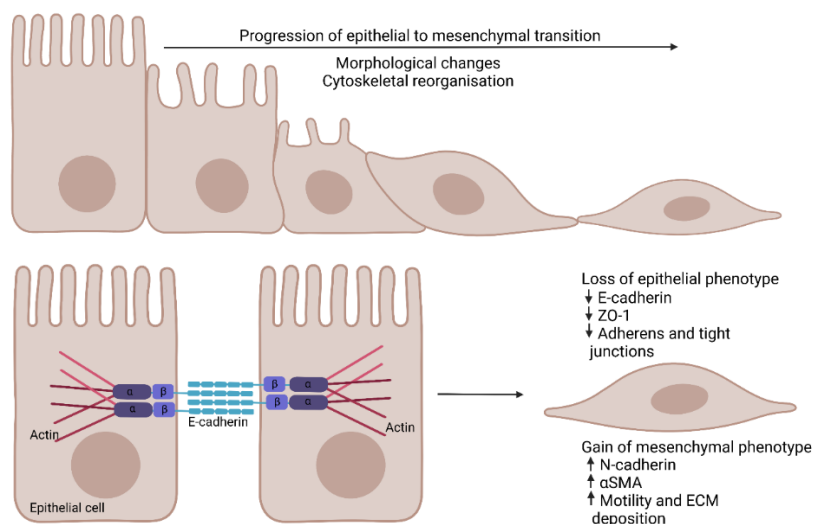


Figure 1.12. Injury-induced partial epithelial to mesenchymal transition as demonstrated in proximal tubule epithelial cells in late stage diabetic nephropathy. Created in biorender.

1.4.4. Fibrosis

Tubulointerstitial fibrosis is the final common pathway leading to end stage renal disease. Contributed to by resident fibroblasts and myofibroblasts, excessive secretion of ECM is a hallmark of tubular injury (Qi and Yang, 2018; Lam *et al.*, 2004). Composed predominantly of fibronectin, laminin and collagen proteins, the ECM plays several physiological roles including physical/structural support and regulation of cell functions (Zhang *et al.*, 2021c). In health, ECM deposition is a dynamic process, consisting of both breakdown and remodelling. In injury, an upregulation in expression and secretion of ECM proteins promotes healing with protracted periods of illness and injury each associated with a loss of regulation, which leads to excessive deposition, irreversible scarring and loss of tissue function (Frantz, Ewart and Weaver, 2010).

1.4.5. Treatment

Despite the high risk of morbidity and mortality associated with diabetic nephropathy (González-Pérez *et al.*, 2021), and the increased risk of co-morbidities such as cardiovascular disease (Cabrera *et al.*, 2020) and retinopathy (Jeng *et al.*, 2016), current treatments for DN are limited to changes in lifestyle, management of blood glucose and reduction of blood pressure to reduce disease progression (Brenneman, Hill and Pullen, 2016). However, approximately 7% of people diagnosed with diabetes already present with a degree of kidney injury, and many individuals will progress to late-stage renal disease regardless of effective glycaemic control. Despite this, there is a lack of available treatments to target late-stage kidney disease (Tonna *et al.*, 2010). Consequently, progression onto end stage kidney disease is inevitable, with dialysis or transplantation the only options currently available (Bello *et al.*, 2019). Since, these treatments are not curative options, they do not improve the patient's quality of life. Furthermore, the patients cardiovascular risk remains high. Undoubtedly, therapies targeting and preventing inflammation in the proximal tubule could slow or stop disease progression. However, for this to be achieved, the underlying molecular mechanisms driving this sterile inflammation need to be defined.

The newest compounds to receive FDA approval for the treatment of DN are a class of drugs called sodium-glucose co-transporter-2 inhibitors (SGLT2i). Acting by reducing renal glucose reabsorption in the proximal tubule, SGLT2i's prevent hyperglycaemia whilst allowing other mechanisms of glucose reabsorption to remain active, thereby avoiding unintended hypoglycaemia. In addition to beneficial effects in diabetes, use of SGLT2i's has also improved renal and cardiovascular outcomes for individuals with cardiovascular disease and nephropathy (Schmidt *et al.*, 2021; Liu *et al.*, 2021; Thirunavukarasu *et al.*, 2021). Initially the beneficial effects observed were believed to be a result of decreased glomerular hyperfiltration however, several studies demonstrate that SGLT2i's mediate protection through suppression of inflammation and fibrosis, although the mechanisms through which they act remain to be fully elucidated (D'Onofrio *et al.*, 2021; Xu *et al.*, 2021; Madonna *et al.*, 2020). Despite these promising findings, SGLT2i are not a one size fits all, with prescription targeted primarily to individuals with T2DM and associated possible side effects linked to ketoacidosis (Musso *et al.*, 2020), increased risk of amputation (Lin *et al.*, 2021) and increased genitourinary tract infection (Unnikrishnan *et al.*, 2018).

Instrumental to the pathogenesis of diabetes and its secondary complications, targeted anti-inflammatory therapy has been investigated in order to treat and prevent complications such as nephropathy (Pollack *et al.*, 2016; Tsalamandris *et al.*, 2019; Teodoro *et al.*, 2019). Central to disease progression across multiple chronic inflammatory conditions e.g., diabetes (Jourdan *et al.*, 2013), obesity (Cañadas-Lozano *et al.*, 2020) and age-related macular degeneration (Tseng *et al.*, 2013), there is a large body of ongoing research dedicated to the design of pharmacological therapeutics aimed at blocking inflammation and key drivers of these changes. Major targets include the NLRP3 inflammasome (MCC950; Zhang *et al.*, 2019), cell senescence (senolytics; Palmer *et al.*, 2021) and its senescence associated secretory phenotype (SASP; Cuollo *et al.*, 2020) or glucose reabsorption (SGLT2i; Li *et al.*, 2021; Lee *et al.*, 2021; Petrie, 2020). Breakthrough clinical trials include the Canakinumab Anti-Inflammatory Thrombosis Outcomes Study (CANTOS) trial (Clinical Trials Identifier: NCT01327846; Ridker *et al.*, 2017) which demonstrated the therapeutic effects of targeting IL1 β for atherosclerosis, and the ongoing phase III ZEUS trial (Clinical Trials Identifier: NCT05021835) in which the effects of IL6 inhibitor Ziltivekimab are to be established in individuals with cardiovascular disease, chronic kidney disease and inflammation. Based on the limitations of the available treatments, more therapeutic approaches are required.

1.5. The NLRP3 inflammasome

Upregulated in immune and epithelial cells across various tissues, the NLRP3 inflammasome is linked to a variety of inflammatory conditions including atherosclerosis (van der Heijden *et al.*, 2017), Alzheimer's disease (Lonnemann *et al.*, 2020), inflammatory bowel disease (Khatri and Kalyanasundaram, 2021), and non-alcoholic steatohepatitis (Torres *et al.*, 2021). Activation culminates in secretion of pro-inflammatory cytokines IL1 β and IL18 which in turn activate TNF α and IL6, both of which exhibit increased serum levels in disease and mediate inflammation/fibrosis in multiple secondary complications of diabetes (Ram *et al.*, 2020; Sharma *et al.*, 2021; Gora *et al.*, 2021; Ge *et al.*, 2021; Huang *et al.*, 2020).

The inflammasome is an inflammatory complex acting as part of the innate immune system to induce maturation and release of pro-inflammatory cytokines, first evidenced in 2002 by Martinon *et al.*, (Martinon *et al.*, 2002). The innate immune system can respond to

both pathogen-associated molecular patterns (PAMPs; Fusco *et al.*, 2020) and non-microbial stimuli known as danger associated molecular patterns (DAMPs; Sandall *et al.*, 2020). In sterile injury, the release of DAMPs can trigger inappropriate inflammatory responses that contribute to tissue injury (Land, 2015). One such way in which the innate immune system is known to contribute to kidney injury is through activation of the nod-like receptor (NLR) gene family which form multiprotein proteolytic complexes within injured cells called inflammasomes.

There is a total of 22 NLR proteins identified in humans of which, all have conserved NACHT domains that allow nucleotide dependant protein oligomerisation. Most have a pyrin domain (PYD) and C-terminal leucine-rich repeat (LRR) domains that function in ligand sensing. Some NLRs also have a caspase recruitment domain (CARD). When NLRs oligomerise to form an inflammasome complex, their primary role is caspase or NF κ B activation. The LRR domain plays a role in self-inhibition by folding back onto the NACHT domain, which has ATPase activity essential for protein oligomerisation (Leu *et al.*, 2023). Best characterised are NLRC1 and NLRC2 in which NLRC is an NLR protein containing a caspase recruitment domain. The primary role of these proteins is to activate NF κ B following bacterial protein stimulation, which is shown to also contribute to Crohn's disease (Maeda *et al.*, 2005)

Alternatively, NLR proteins containing a pyrin domain (NLRPs), are a sub family, consisting of 14 proteins (NLRP1-14). Upon activation by various stimuli, NLRP proteins form an oligomerised protein complex with the PYD-CARD adaptor protein (ASC) and caspase 1, known as the inflammasome (Guey *et al.*, 2014). Caspase 1 consists of a large catalytic domain (p20), a carboxy-terminal small catalytic domain (p10) and an amino terminal CARD. A proteolytic complex, inflammasome formation leads to caspase 1 activation and subsequent cleavage of multiple substrates, key of which are pro-inflammatory cytokines IL1 β and TNF α (Swanson *et al.*, 2019). Believed to be the final common pathway sensing cellular stress and/or injury, knowledge of the NLRP inflammasomes is limited and the ligand and functions of many NLRP proteins are yet to be established.

The best characterised inflammasome, and a key mediator of chronic inflammation in several diseases (Fusco *et al.*, 2020) including diabetic nephropathy (Yang *et al.*, 2021), is the NLRP3 inflammasome (Blevins *et al.*, 2022). Made up of a sensor protein (NLRP3) an

adaptor (ASC) and an effector enzyme (caspase 1), the inflammasome is implicated in the pathogenesis of multiple sterile chronic inflammatory diseases (Milner *et al.*, 2021; Shimizu *et al.*, 2019; Takahashi, 2019). In fact, evidence suggests that NLRP3 inflammasome activity is essential to altered glucose tolerance, insulin resistance and inflammation which underlies type 1 and type 2 diabetes (Ding *et al.*, 2019). Furthermore, it is also shown to play a key role in secondary microvascular complications of diabetes, including diabetic nephropathy (Feng *et al.*, 2021; Ram *et al.*, 2020), diabetic retinopathy (Ge *et al.*, 2022) and impaired wound healing (Huang *et al.*, 2020). Under physiological conditions NLRP3 is maintained in a stable inhibited state by interactions with the ubiquitin ligase-associated protein SGT1 and heat shock protein 90 (Mayor *et al.*, 2007). Upon activation, NLRP3 is released and oligomerises via homotypic molecular interactions of the NACHT domain, which leads to recruitment of ASC through homotypic PYD-PYD interactions (Figure 1.12). These PYD-PYD interactions also lead to formation of helical ASC filaments which coalesce into a single micromolar focus called the ASC speck. Subsequent caspase 1 recruitment through homotypic CARD interactions with ASC completes the inflammasome formation (Figure 1.12). From here, the inflammasome induces self-cleavage of caspase 1 into its active p10-p20 enzyme form which cleaves immature pro-IL1 β and pro-IL18 to their mature forms to be secreted from the cell. Found to be an essential part of NLRP3 inflammasome formation, the serine threonine kinase NIMA-related kinase-7 (NEK7) interacts and oligomerises with NLRP3 upon inflammasome activation, where it is shown to be essential for ASC speck formation and caspase1 activation (Sun *et al.*, 2020).

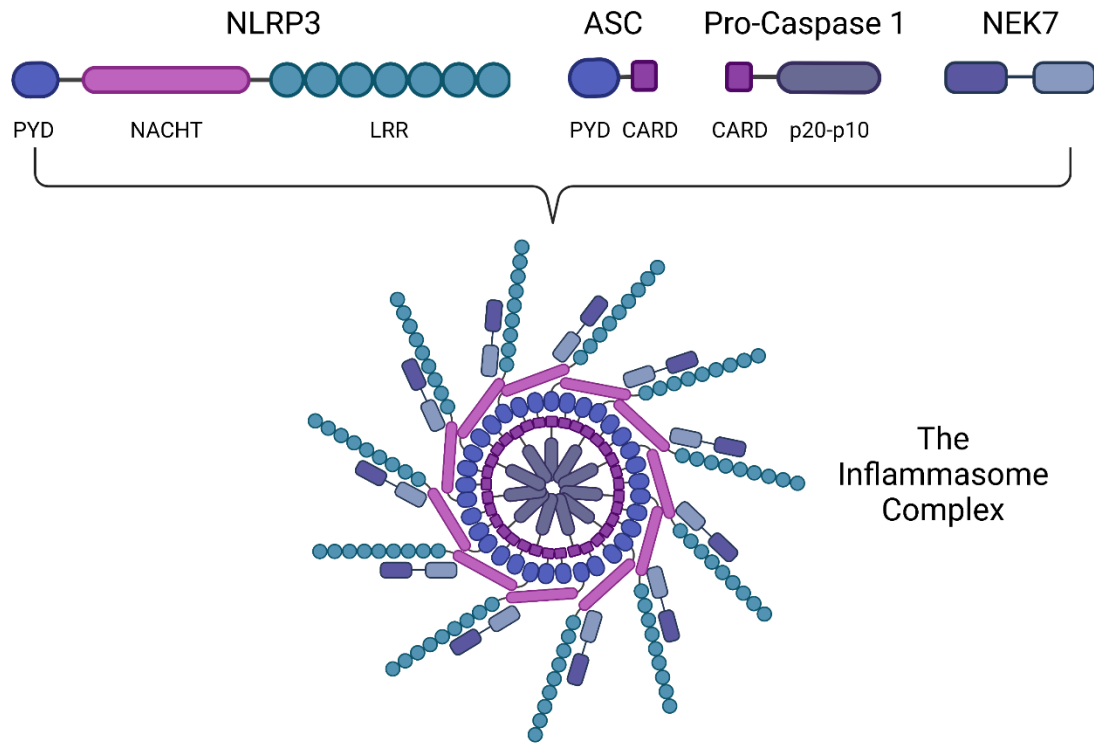


Figure 1.13. Structure of the NLRP3 inflammasome complex. Consisting of NLRP3, ASC, pro-caspase 1 and NEK7. Created in biorender.

1.5.1. Priming

Activation of the inflammasome is a two-step process whereby priming (step 1) precedes activation, a mechanism which allows tight regulation of inflammasome activity. Priming is initiated through DAMP/PAMP engagement with pattern recognition receptors such as toll-like receptors (TLRs) and nucleotide-binding oligomerisation domain containing protein (NOD)2 (Figure 1.13; Kelley *et al.*, 2019). Another mechanism includes cytokine activation of receptors including IL1 (Xing *et al.*, 2017) and TNF receptors (Jämsen *et al.*, 2020). Stimulation of these receptors leads to activation of the inhibitor of nuclear factor kappa B (IκB) kinase (IKK) enzyme complex. A regulator of nuclear factor kappa B (NFκB), IκB sequesters NFκB in an inactive state in the cytoplasm by masking nuclear localisation signals. Following receptor activation, IKK phosphorylates IκB which then dissociates from NFκB, allowing it to migrate into the nucleus. Acting as a transcription factor, NFκB

upregulates the transcription of inflammasome components including NLRP3 and pro-IL1 β (Figure 1.13; Blevins *et al.*, 2022)

A second and lesser-known function of inflammasome priming is the induction of post-translational modifications of NLRP3 (Song *et al.*, 2017). The covalent addition of functional groups is an essential mechanism through which NLRP3 protein folding, localisation and functional abilities are regulated. These modifications stabilise NLRP3 into a self-inhibitory, inactive state, whilst also being able to rapidly respond to activating stimuli. Key among these regulatory modifications are phosphorylation, ubiquitination and sumoylation (Song *et al.*, 2017).

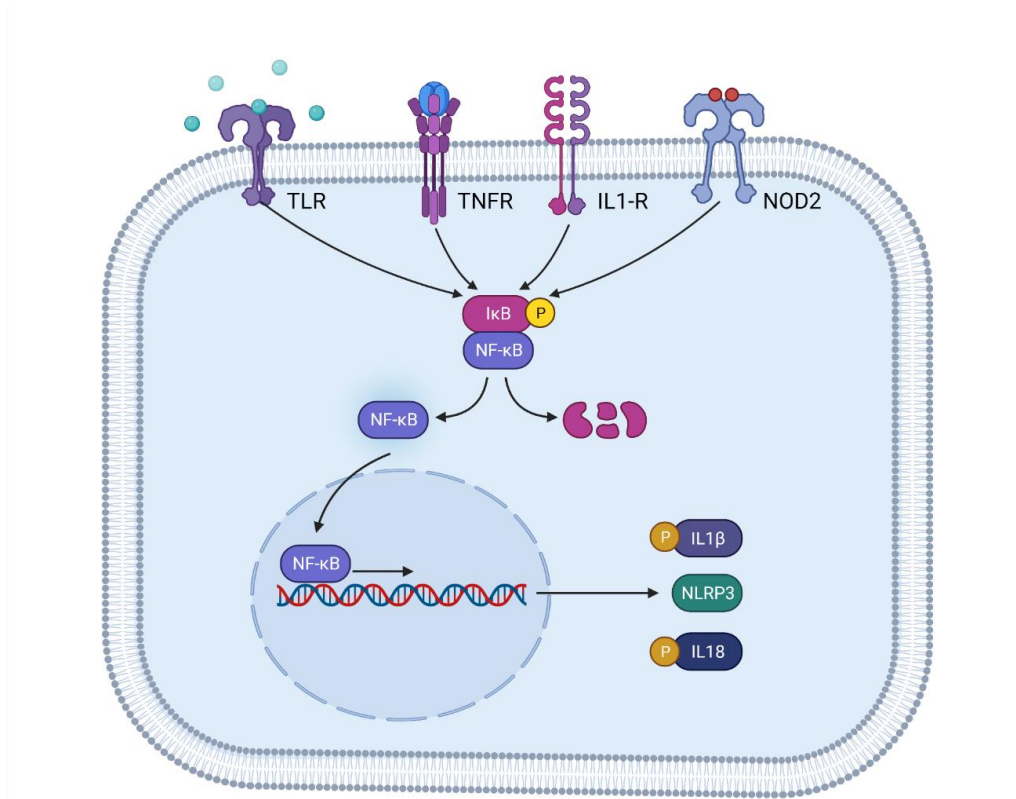


Figure 1.14. Schematic demonstrating priming of the NLRP3 inflammasome. Cell surface receptors such as Toll like receptors (TLRs), nucleotide-binding oligomerisation domain containing protein 2 (NOD2), and receptors for TNF α (TNFR) and IL1 β (IL1-R) are activated by extracellular danger associated molecular patterns (DAMPs) and pathogen associated molecular patterns (PAMPs). This leads to phosphorylation of inhibitor of NF κ B (I κ B), allowing NF κ B dissociation and translocation to the nucleus. Here, NF κ B acts as a transcription factor, upregulating the transcription of components essential for inflammasome activity, key of which include IL1 β and NLRP3. Created in biorender.

1.5.2. Activation

The NLRP3 inflammasome can be activated by a vast array of DAMPs and PAMPs associated with disease. In sterile inflammation, release of endogenous cellular components including reactive oxygen species (ROS; Chatterjee and Tao, 2019), nucleic acids (Shimada *et al.*, 2012), uric acid (Braga *et al.*, 2017), ECM component biglycan (Babelova *et al.*, 2009), and extracellular ATP (Zha *et al.*, 2016; Amores-Iniesta *et al.*, 2017) have all been implicated as activators of the inflammasome. In diabetes, evidence shows that release of ROS following hyperglycaemia stimulates inflammasome activation (Zhou *et al.*, 2010; Iyer *et al.*, 2009), whilst interleukin 1-receptor (IL1-R) inhibition dampened diabetes progression via decreased hyperinsulinemia in a phase II clinical trial (Clinical Trials Identifier: NCT00303394), likely via increased pancreatic beta cell survival (Larsen *et al.*, 2007). Stimulation by these endogenous cellular components is thought to lead to inflammasome activation through initiation of several upstream signals including influx of calcium (Ca^{2+}) ions, efflux of potassium (K^+) or chloride (Cl^-) ions, mitochondrial dysfunction and metabolic alterations either individually or simultaneously (Gong *et al.*, 2018). Currently data shows evidence for a vast array of pathways, some data consistent and coinciding, whilst some contradictory, meaning a consensus model for NLRP3 activation is yet to be confirmed.

Thus far, three main pathways of NLRP3 inflammasome activation have been elucidated, the canonical (classical) pathway, the non-canonical pathway, and the alternative pathway. Of these, the canonical pathway is the most established (Kelley *et al.*, 2019):

1.5.2.1. Canonical Activation

Activation is-mediated via an array of DAMPs, including extracellular ATP. Traditionally associated with sterile injury, the canonical pathway is initiated via activation of purinergic P2x7 receptor (P2X7R). Upon sensing extracellular DAMPs, P2X7Rs open creating an influx of Ca^{2+} and an efflux of K^+ . These changes release NLRP3 from its state of regulation within the cell, allowing it to oligomerise and recruit inflammasome components ASC and caspase 1 as previously described in Section 1.5, leading to complex formation (Blevins *et al.*, 2022). Upon formation caspase 1 is cleaved and the activated subunit mediates the cleavage of pro-IL1 β and pro-IL18 to their mature forms. In addition to these

proinflammatory cytokines, caspase 1 also cleaves gasdermin D (GSDMD). The resulting GSDMD amino terminal fragment (GSDMD-NT) forms pores within the membrane through which mature IL1 β and IL18 are released, as well as other endogenous cell components which can act as DAMPs to activate other neighbouring cells. The formation of these pores in sufficiently high quantities can also lead to excessive release of cell components and pyroptosis, a pro-inflammatory, necrotic form of programmed cell death (Figure 1.14; Tsuchiya, 2020).

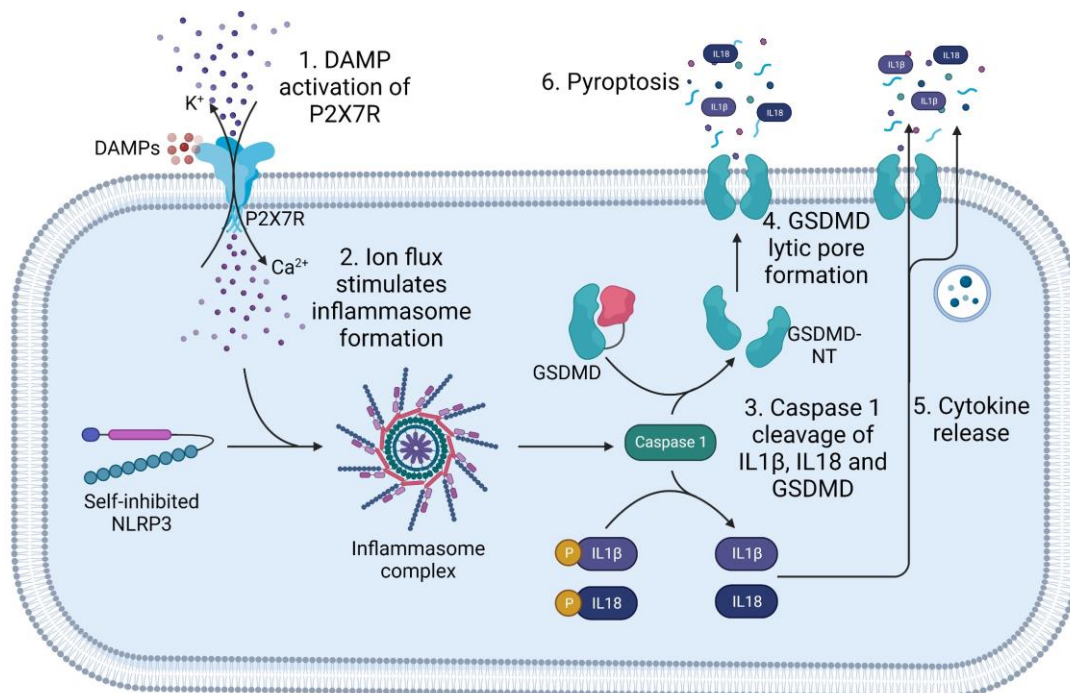


Figure 1.15. Schematic illustrating canonical (classical) activation of the NLRP3 inflammasome. (1) Purinergic P2X7 receptors are activated by extracellular danger associated molecular patterns (DAMPs) such as ATP. (2) Receptor activation stimulates an influx of Ca²⁺ paralleled by a K⁺ efflux which initiated NLRP3 oligomerisation and inflammasome complex formation. (3) During complex formation caspase 1 is cleaved, releasing an active subunit which then cleaves proinflammatory cytokines pro-IL1 β and pro-IL18, in addition to gasdermin D (GSDMD). (4) Amino terminal fragments of GSDMD (GSDMD-NT) oligomerise in the cell membrane forming lytic pores. (5) Mature IL1 β and IL18 are released from the cell via GSDMD pores along with other cell components, or lysosomal or exosomal secretion (6) resulting in a programmed form of cell death known as pyroptosis. Created in biorender.

1.5.2.1. Non-canonical activation

The non-canonical pathway, typically associated with activation via PAMPs such as lipopolysaccharide (LPS), achieves the same outcome as the canonical pathway but via different mechanisms. This route relies on the activation of human caspase 4 and 5 (or caspase 11 in mouse models) by LPS-mediated stimulation of TLR4, which then cleave GSDMD inducing formation of lytic GSDMD-NT pores and subsequent pyroptosis (Downs *et al.*, 2020). The pyroptosis-mediated efflux of K^+ then activates formation of the NLRP3 inflammasome, caspase 1 activation and release of pro-inflammatory cytokines IL1 β and IL18 (Figure 1.15; Downs *et al.*, 2020).

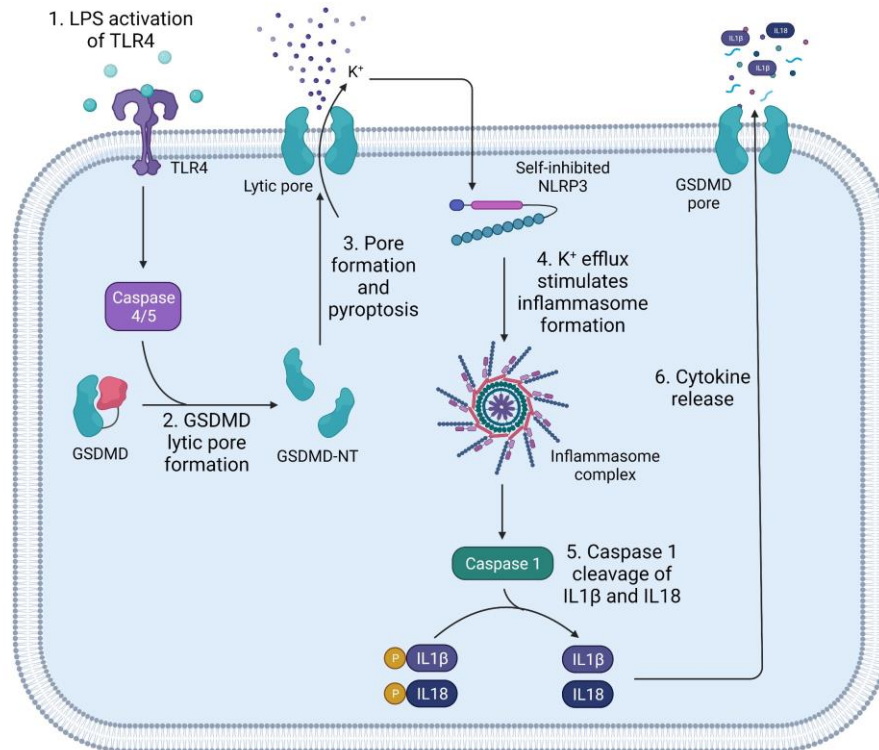


Figure 1.16. Illustration of the mechanisms of non-canonical NLRP3 inflammasome activation. (1) Toll like receptor 4 (TLR4) is activated by the PAMP lipopolysaccharide (LPS) which leads to activation of caspases 4 and 5 (or caspase 11 in mice). (2) Caspase 4 and 5 both mediate the cleavage of GSDMD (3) leading to formation of lytic GSDMD-NT pores and pyroptosis. (4) An efflux of K^+ associated with GSDMD pores initiates NLRP3 oligomerisation and formation of the inflammasome complex, (5) resulting in activation of caspase 1 and subsequent cleavage of pro-IL1 β and pro-IL18 into their mature forms. (6) Mature cytokines are secreted from the cell into the extracellular space. Created in biorender.

1.5.2.3. Alternative activation

The alternative pathway occurs specifically in monocytes and is independent of potassium influx. Unlike the canonical and non-canonical pathways, the alternative pathway consists of just one signal to induce both priming and activation of the inflammasome simultaneously (Gaidt *et al.*, 2016). Activation of TLR4 via LPS primes NLRP3 in human and porcine monocytes via myeloid differentiation primary response protein 88 (MYD88) activation of NF κ B and subsequent, whilst also activating through the TLR4– TIR domain containing adaptor molecule 1 (TRIF)– Receptor-interacting serine/threonine-protein kinase 1 (RIPK1)– Fas-associated death domain protein (FADD)– Caspase (CASP)8 signalling axis, which cannot induce K⁺ efflux, ASC speck formation, or pyroptosis (Figure 1.16). This one step rapid response to LPS alone is thought to be essential for maintaining sterility of the blood and protecting against sepsis (Gaidt *et al.*, 2016).

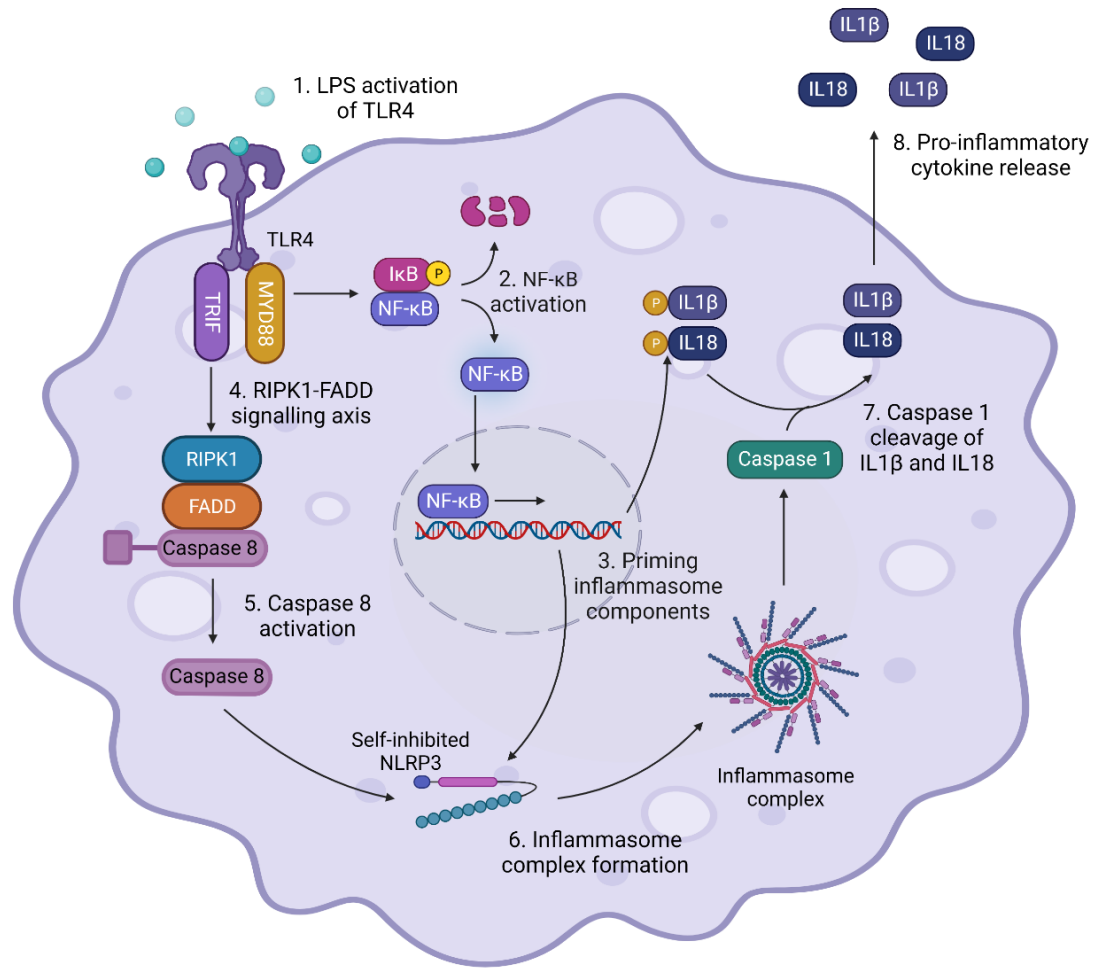


Figure 1.17. Schematic illustrating mechanisms of alternate NLRP3 inflammasome priming and activation in monocytes. (1) Toll like receptor 4 (TLR4) is activated by the PAMP lipopolysaccharide (LPS) activating downstream signalling. (2) This leads to inflammasome priming through downstream MYD88 signalling and phosphorylation of IκB which dissociates from NFκB. (3) Upon being released from its regulated state NFκB translocates to the nucleus where it upregulates the transcription of components essential for inflammasome activity, including pro-IL1β and pro-IL18. In addition, (4) TRIF-mediated activation of the RIPK1-FADD pathway leads to (5) cleavage of caspase 8. (6) Activation of caspase 8 initiates NLRP3 oligomerisation and inflammasome complex formation, (7) resulting in cleavage of caspase 1. The resulting active caspase 1 cleaves pro-IL1β and pro-IL18 into their mature forms prior to secretion into the extracellular space. Created in biorender.

1.5.3. Action of proinflammatory cytokines

The NLRP3 inflammasome mediates its downstream pathological effects via the release of IL1 β and IL18. These proteins are both pro-inflammatory cytokines with pleiotropic effects associated with injury in states of chronic inflammation (Kaneko *et al.*, 2019).

One of the most powerful proinflammatory cytokines, IL1 β affects nearly every organ in the human body and excessive release is the primary cause of several inflammatory diseases (Galozzi *et al.*, 2021). To initiate downstream signalling cascades, IL1 β binds to interleukin 1-receptor 1 (IL1R1) which forms a heterodimer with IL1 type 3-receptor (IL1R3), associated with adaptor IL1 receptor associated kinase (IRAK), MyD88 and TNF receptor-associated factor 6 (TRAF6; Muroi and Tanamoto, 2008). Through these mechanisms transcription factor NF κ B is activated, dependant on IKK α , IKK β and NF κ B essential modulator (NEMO) complex formation, as well as p38, c-Jun N-terminal Kinase (JNK)s, extracellular signal related kinases (ERKs) and mitogen-activated protein kinases (MAPKs; Figure 1.17). These signalling pathways drive increased expression of pro-inflammatory cytokines, chemokines, and mediators of the inflammatory response, including but not limited to TNF α , IL1 β , IL18, and granulocyte-macrophage colony-stimulating factor (GM-CSF; Liu *et al.*, 2017). Through these mechanisms, IL1 β mediates a wide array of effects including proliferation, differentiation, apoptosis, immune cell recruitment, activation of endothelial adhesion molecules and stimulation of adaptive immunity (Kaneko *et al.*, 2019). These effects, combined with the potency of IL1 β , make it one of the most potentially harmful pro-inflammatory cytokines in the body. As such, the body has several mechanisms to regulate its activity through strict control of the inflammasome and use of IL1 receptor agonist (IL1ra) and the type II decoy receptor to inhibit its receptor binding (Dinarelloo *et al.*, 2018).

Also, from the IL1 family, IL18 binds to the IL18 receptor (IL18R), made up of a ligand binding chain and a co-receptor chain, both of which are required for signalling. Whilst both cytokines act through very similar mechanisms and have many of the same effects such as upregulating expression of proinflammatory cytokines and chemokines, there are some differences, compounded by a reduced potency associated with IL18 (Figure 1.17; Dinarelloo *et al.*, 2018). For example, both cytokines induce cyclooxygenase-2 (COX-2) gene expression but whilst IL1 β induces COX-2 dependant fever, IL18 does not. A primary function of IL18 is to upregulate IFN γ expression in addition to other pro-inflammatory

cytokines. As a result, IL18 contributes to inflammation through increased immune cell infiltration, proliferation, and activation, which is linked to chronic inflammatory disease progression (Kaneko *et al.*, 2019).

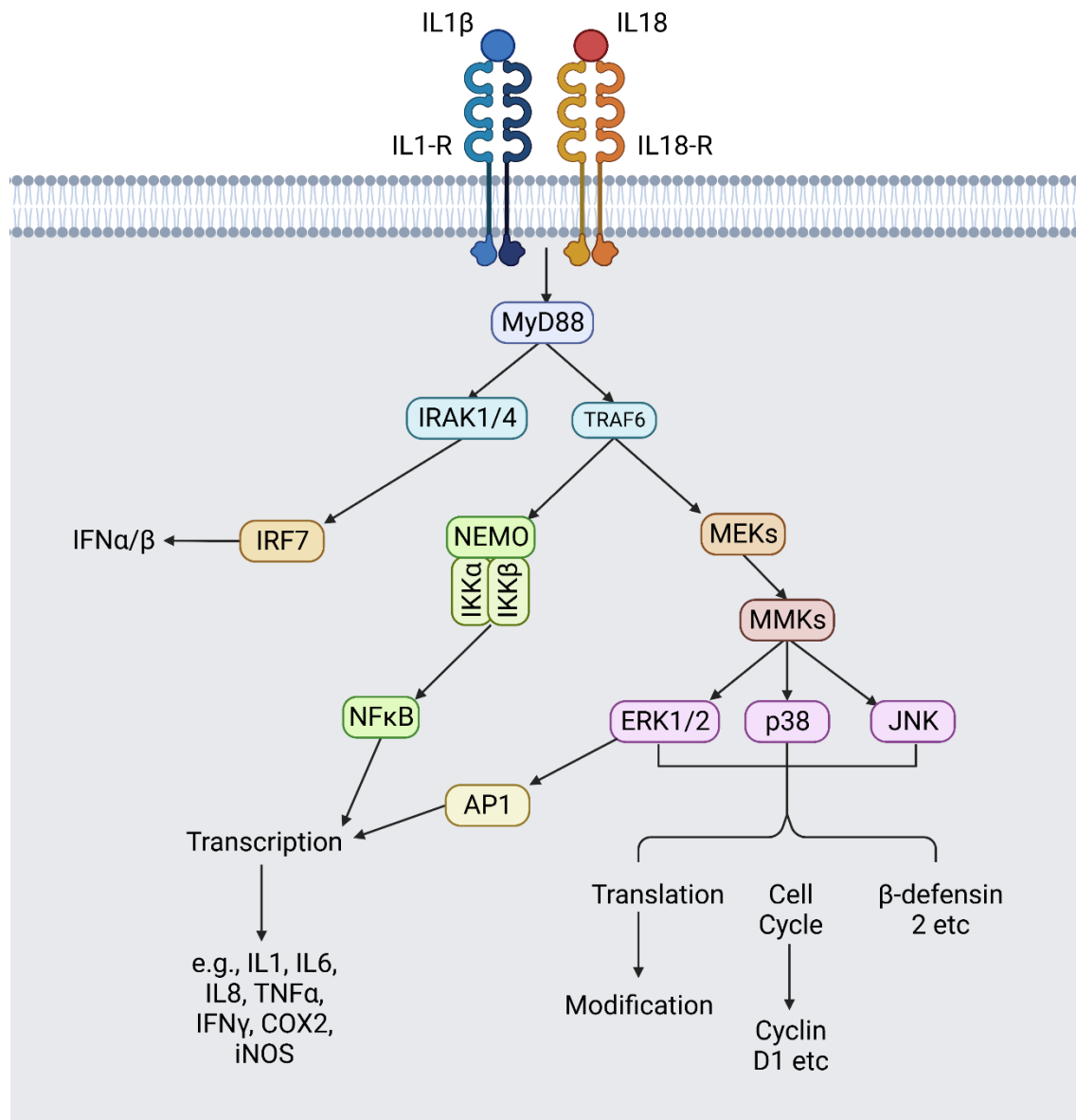


Figure 1.18. Simplified downstream signalling mechanisms of IL1β and IL18 after binding to their respective receptors. Created in Biorender.

Downstream to the release of IL1β and IL18 (Netea *et al.*, 2000), TNFα is a proinflammatory cytokine that activates several signalling pathways inducing a plethora of

cellular functions (Van Loo and Bertrand, 2022). Binding to tumour necrosis factor receptors (TNFR) TNFR1 and TNFR2, receptors form a trimer inducing dissociation of inhibitory protein silencer of death domains (SODD; Morton *et al.*, 2019) and subsequent activation of adaptor protein, tumour necrosis factor receptor type-1-associated death domain (TRADD) to initiate three main signalling cascades (Li *et al.*, 2020c). Activated by TNF α as well as IL1 β , MAPK activation mediates changes associated with cell differentiation, proliferation and apoptosis (Morton *et al.*, 2019). In addition, transcription factor NF κ B is activated driving not only increased expression of pro-inflammatory cytokines, but also priming of the NLRP3 inflammasome (Zhou *et al.*, 2019). Binding of TNF α also mediates apoptosis through binding of TRADD to FADD which recruits pro-caspase 8 for proteolytic activation and subsequent cleavage of effector caspases, driving apoptosis, a form of programmed cell death (Li *et al.*, 2020c). Pro-inflammatory cytokine TNF α plays a pivotal role in various inflammatory diseases including rheumatoid arthritis (Guo *et al.*, 2018) and Crohn's disease (Holbrook *et al.*, 2019).

1.5.4. Current and future therapeutics for diabetic nephropathy

Aberrant activation of the NLRP3 inflammasome and upregulation of pro-inflammatory cytokines play a key role in the progression of chronic kidney disease, with NLRP3 expression linked to reduced renal function in human and animal models of disease (Vilaysane *et al.*, 2010). This is supported by studies demonstrating that pharmacological inhibition and genetic knockout of NLRP3 has significant therapeutic effects in rat models of disease (Foresto-Neto *et al.*, 2018). Moreover, in a mouse model of renal ischaemia reperfusion injury (IRI), the genetic depletion of NLRP3 decreased IL1 β and IL18 secretion, paralleled by reduced apoptosis and necrosis in the renal proximal tubule (Shigeoka *et al.*, 2010). This is further evidenced in a mouse NLRP3 knockout model of advanced interstitial inflammation, which exhibited reduced caspase 1 activation, decreased IL1 β and IL18 maturation, resulting in diminished levels of inflammation and fibrosis (Vilaysane *et al.*, 2010). Subsequently, targeting NLRP3 has received considerable clinical interest (Yang *et al.*, 2021). Several inhibitors including SGLT2 inhibitors, DPPIV inhibitors, small molecule inhibitor MCC950 and ginsenoside compound K are shown to attenuate progression of DN in mice models of diabetes via inhibition of NLRP3 inflammasome activation (Birnbaum *et al.*, 2018; Zhang *et al.*, 2019; Song *et al.*,

2018), highlighting the importance of reducing NLRP3 activation and cytokine production in the injured kidney.

Since chronic inflammatory conditions are amplified and perpetuated by inflammasome activity, blocking the NLRP3 inflammasome directly (e.g., MCC950) alleviates inflammation (Sharma *et al.*, 2021; Li *et al.*, 2021; He *et al.*, 2021). Despite these encouraging findings, complete blockade of a complex integral part of our innate immune response is also associated with undesirable side effects (Ridker *et al.*, 2017; Li *et al.*, 2021). The NLRP3 inflammasome mediates both sterile and non-sterile inflammation, meaning while its inhibition may protect against sterile inflammation-induced by DAMPs, this could render individuals susceptible to microbial infection (Surabhi *et al.*, 2020; Zhao and Zhao, 2020). Regardless, playing a key role in inflammation in over 80 different *in vivo* models of injury (Zheng *et al.*, 2020; Feng *et al.*, 2020; Yang *et al.*, 2019; Kelley *et al.*, 2019; He *et al.*, 2016), several compounds targeting the NLRP3 inflammasome have entered clinical trials e.g., Inzomelid (Clinical Trials Identifier: NCT04015076), IFM-2427 (DFV890; Clinical Trials Identifier: NCT04382053) and Dapansutrile (OLT1177; Clinical Trials Identifier: NCT04540120; Klück *et al.*, 2020; Wohlford *et al.*, 2021). Unfortunately, no drug has yet reached its primary endpoint in clinical trials (El-Sharkawy *et al.*, 2020).

Therapeutics targeting downstream mediators such as IL1 β and TNF α have also been investigated. Canakinumab (ACZ885, Ilaris) is a recombinant human monoclonal antibody that selectively inhibits IL1 β receptor binding (Dhimolea, 2010). After demonstrating positive primary outcomes in the CANTOS trial (Ridker *et al.*, 2018), the drug became licensed for the treatment of rare inflammatory conditions, including juvenile arthritis (Ruperto *et al.*, 2018). However, it lacked efficacy for the treatment of inflammation in diabetic retinopathy (Clinical Trials Identifier: NCT01589029), T1DM (Clinical Trials Identifier: NCT00947427; Moran *et al.*, 2013) and atherosclerosis (Clinical Trials Identifier: NCT00900146; Ridker *et al.*, 2012), and was associated with significantly more deaths attributable to infection, suggesting that anti-inflammatory strategies might compromise patient immune responses (Ridker *et al.*, 2017). Similarly, efforts to target TNF α include drugs which contain either receptor fusion proteins (etanercept; Kiyoshi *et al.*, 2021) that suppress the physiologic response to TNF α or monoclonal antibodies (golimumab, infliximab, adalimumab certolizumab pegol), which have shown limited success (Stevenson *et al.*, 2016). Currently, IL6 inhibitor ziltivekimab is undergoing phase III trials,

called the ZEUS trial (Clinical Trials Identifier: NCT05021835), in individuals with cardiovascular risk and chronic kidney disease (Ridker *et al.*, 2021).

A possible cause explaining the lack of efficacy that some drugs have shown at clinical trial is because whilst one inflammatory pathway is blocked, several others remain open and functioning. Subsequently, targeting multiple inflammatory targets has also been considered. However, concerns have also been raised over targeting inflammatory mediators directly due to compromising the innate immune response to pathogenic threat, a particular concern for those who already have an elevated risk of bacterial and viral infection compared to healthy individuals, including individuals with diabetes (Carey *et al.*, 2018). Therefore, it is essential to consider alternative approaches that reduce inflammation whilst leaving the innate immune system active to pathological infection. Therefore, targeting the pathways and mediators underpinning chronic inflammation is essential to prevent downstream effects such as tissue remodelling and fibrosis.

1.6. Connexin-mediated cell-cell communication

Recent studies suggest that inflammation is, in part, mediated by altered expression and function of a class of proteins called connexins (Peng *et al.*, 2022). Unsurprisingly, this field of research has received considerable interest, with many studies demonstrating that reduced connexin expression prevents the progression of chronic inflammatory diseases *in vivo*, including atherosclerosis (Chadjichristos *et al.*, 2006), sepsis (Dosch *et al.*, 2019) and rheumatoid arthritis (Tsuchida *et al.*, 2013).

The connexin family of transmembrane proteins are made up of 21 different isoforms in humans and mice, named according to their molecular mass (Wagner, 2008). Each connexin consists of four transmembrane domains, connected by a cytoplasmic loop and two extracellular loops (Beyer and Berthoud, 2017). Oligomerising as clusters of six named connexons, these hexameric structures are transported from the endoplasmic reticulum to the plasma membrane in vesicles that transit along the cells secretory pathway (Evans *et al.*, 1999; Laird, 2006). In the membrane, connexons form pores, known as hemichannels which allows passive diffusion of small molecules and ions between cells and the extracellular environment. A highly conserved cytoplasmic, NH₂-terminus has a putative calmodulin-binding motif, required for membrane insertion, as well

as playing a role in channel conductance regulation with the cytoplasmic COOH terminus (Sáez *et al.*, 2003). Connexin serine and threonine or tyrosine residues are phosphorylated to alter channel permeability and conductance, which also affects the assembly, biosynthesis, and degradation of connexons (Aasen *et al.*, 2019). Connexins are removed from the cell membrane forming a connexosome, which then fuse with lysosomes for connexin degradation (Figure 1.18; Falk *et al.*, 2014). This enables a rapid connexin turnover of an approximate 1-2.5 hour half-life (Leithe *et al.*, 2012; Su and Lau, 2014).

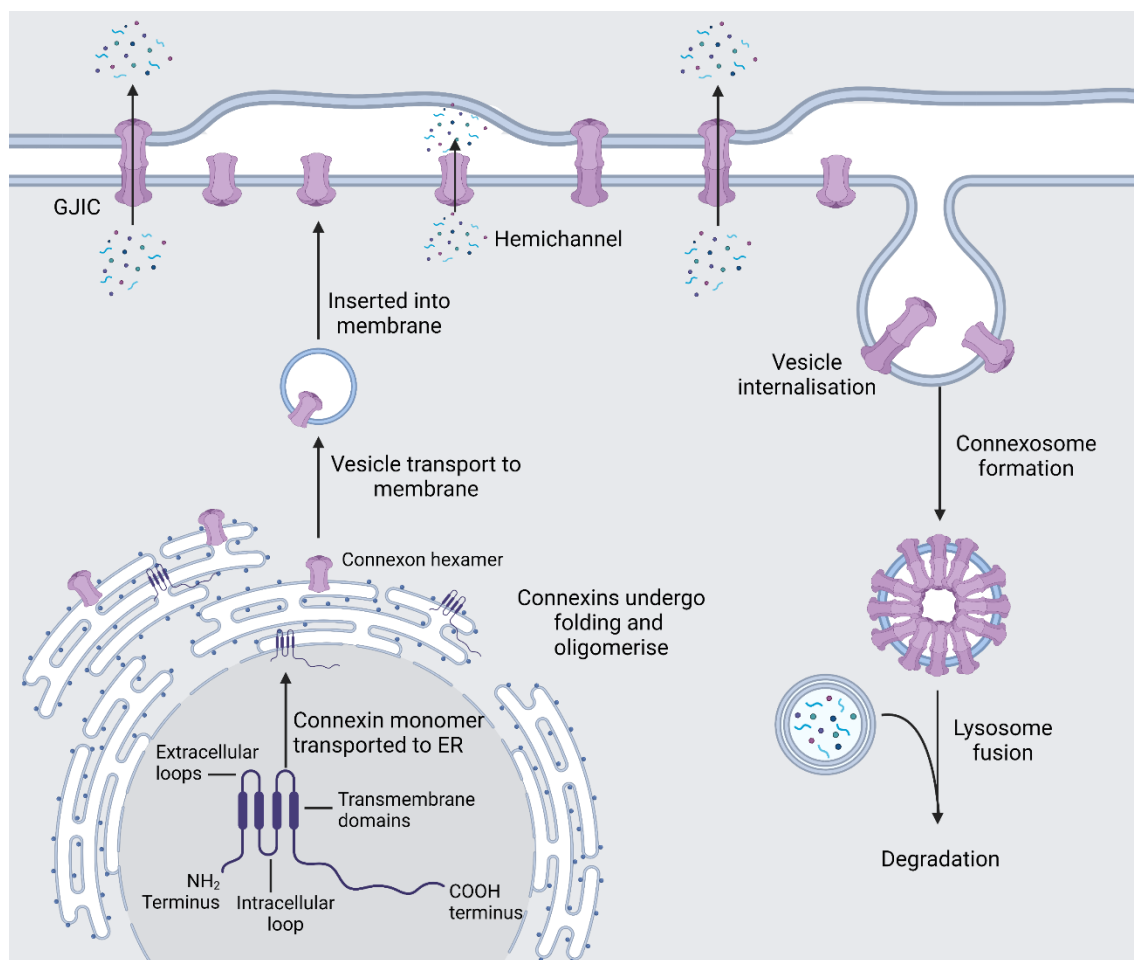


Figure 1.19. Cycle of connexin hemichannel and gap junction formation and degradation. Created in Biorender.

1.6.1 Gap Junctions

When connexons on neighbouring cells align, they dock forming a gap junction. These gap junctions function as conduits of 1-2nm in diameter between cells, allowing direct, bidirectional flow of ions, metabolites and secondary messengers including Ca^{2+} , ATP, Na^+ and inositol triphosphate (IP_3), between adjacent cells (Dong *et al.*, 2018; Retamal *et al.*, 2015; Ribeiro-Rodrigues *et al.*, 2017) via chemical gradient diffusion (Kumar and Gilula, 1996; Nagy *et al.*, 2018). Referred to as gap junction intercellular communication (GJIC), exchange of molecules and signals between adjacent cells is essential for cell differentiation, growth, and function. Allowing cells to synchronise their activity maintains tissue homeostasis and is crucial for mediating a co-ordinated tissue action/response.

1.6.2 Hemichannels

Central to the pathology of several chronic diseases, connexin hemichannels open predominantly under pathophysiological conditions including oxidative stress (Retamal *et al.*, 2007) and inflammation (Willebrords *et al.*, 2016; Retamal *et al.* 2015). When open, hemichannels release aberrant levels of small molecules such as ATP into the extracellular space where they act as DAMPs, activating danger recognition receptors on nearby cells including purinergic receptors and toll like receptors. Unregulated hemichannel activity has been linked to the pathology of chronic conditions including deafness (Mhaske *et al.*, 2013), brain ischaemia (Ma *et al.*, 2018) and chronic pain (Yang *et al.*, 2018; Wang and Sun, 2017).

The opening of connexin hemichannels is tightly regulated by several different mechanisms such as mechanical stimulation, pH, Ca^{2+} , voltage and phosphorylation (Van Campenhout *et al.*, 2021). Cytoplasmic and extracellular calcium ion concentration is a key mechanism through which connexin hemichannels are regulated (Van Campenhout *et al.*, 2021). When intracellular calcium ions ($[\text{Ca}^{2+}]_i$) are elevated ($>200\text{nM}$), hemichannels open via activation of a calmodium-dependant signalling cascade and intermediate signalling pathways (Sáez and Green, 2018). Furthermore, extracellular calcium ($[\text{Ca}^{2+}]_e$) at a concentration of 1mmol/L prevents the release of ATP through binding of Ca^{2+} to extracellular regions of hemichannels inducing a conformational change to prevent their opening (Krebs, 2018). Subsequently, a decrease in $[\text{Ca}^{2+}]_e$ is paralleled by gradual

enlargement of hemichannel pore diameter (Torres *et al.*, 2012) and increased ATP release (Cotrina *et al.*, 1998).

Connexins are phosphoproteins and with the exception of connexin 26 (Cx26), activity is regulated by a variety of phosphorylation mechanisms, which vary between isoforms (Pogoda *et al.*, 2019). Fluctuations in pH have also been shown to affect hemichannel gating, with findings showing extracellular acidity temporarily closes open hemichannels (Sáez *et al.*, 2005) and alkaline conditions steadily increase connexin 43 (Cx43) hemichannel activity from pH 7.4 to 8.5 in Cx43 transfected human cervical cancer cells (Schalper *et al.*, 2010). Another potential mechanism contributing to hemichannel open probability is voltage gating whereby electrical differences between the cytoplasmic and extracellular environment alter the position of amino acids, driving changes in connexin formation (Verselis, 2019; Pinto *et al.*, 2017).

1.6.3. Role of connexin-43 in inflammatory diseases

Dysregulation of physiological connexin activity has been linked to disease pathologies through altered connexin expression, a breakdown in gap junction formation (Wong *et al.*, 2017) and intercellular communication and an increase in connexin hemichannel activity (Li *et al.*, 2018). Usually closed in physiological conditions, the opening of connexin hemichannels causes a 'leaky' membrane through which small cytoplasmic components are released. Of these, some molecules such as nucleotides and ATP act as danger associated molecular patterns, triggering an inflammatory response in nearby cells via paracrine-mediated purinergic signalling (Xu *et al.*, 2022). This is associated with an increase in the release of proinflammatory cytokines and chemokines, immune cell infiltration and loss of function.

The protective effects of blocking connexin hemichannel activity has been demonstrated in *in vivo* models of over twenty-six chronic inflammatory diseases, associated with reduced tissue injury and loss of function (Peng *et al.*, 2022) summarised in table 1.2. The mechanism through which protection is conferred is often through attenuation of inflammation due to diminished release of DAMPs (Peng *et al.*, 2022). Studies in chronic inflammatory diseases and secondary complications of diabetes, such as diabetic retinopathy, demonstrate a link between connexin hemichannel-mediated ATP release

and subsequent activation of the NLRP3 inflammasome, culminating in upregulation of proinflammatory cytokine release (Tonkin *et al.*, 2018; Huang *et al.*, 2019; Louie *et al.*, 2021). Secondary to inflammasome activation and key to the pathophysiology of most chronic inflammatory diseases, the activation and infiltration of immune cells is increased in response to increased hemichannel-mediated ATP release (Dosch *et al.*, 2019; Choi *et al.*, 2022; Abed *et al.*, 2014).

Table 1.2. The effect of blocking connexin hemichannel activity in different *in vivo* models of chronic inflammatory diseases. Adapted from (Peng *et al.*, 2022).

Disease	Model	Species	Connexin Blocker	Effects	Reference
Alzheimer's disease	APP _{swe} /PS1 _{dE9} mice	Mouse	Gap26	Reduced gliotransmitter release	(Yi <i>et al.</i> , 2017)
Cardiac injury	Left ventricle cryoinjury	Mouse	ACT1	Reduced inducible arrhythmia (O'Quinn <i>et al.</i> , 2011)	(O'Quinn <i>et al.</i> , 2011)
Cerebral Ischemia	Carotid artery occlusion and reperfusion	Rat, sheep	Gap19, Gap26, Gap27, Peptide5	Reduced cerebral infarct volume and neuron loss; improved functional recovery	(Chen <i>et al.</i> , 2019; Li <i>et al.</i> , 2015; Davidson <i>et al.</i> , 2014)
Diabetic foot	Neuropathic foot ulcer in diabetic patients	Human	ACT1	Improved ulcer re-epithelialization	(Grek <i>et al.</i> , 2015)
Chronic pain	Chronic constriction injury; peripheral neuropathy	Mouse	Peptide5	Reduced mechanical pain	(Ghatnek ar <i>et al.</i> , 2009)
Corneal epithelial wounding	Ex vivo human cornea, suture-induced corneal inflammation, corneal wounding by isopropyl alcohol	Human, rat	Gap27, ACT1	Improved healing and reduced inflammation	(Moore <i>et al.</i> , 2013; Elbadawy <i>et al.</i> , 2016)
Diabetic retinopathy	Intravitreal injection of IL1 β and TNF- α	Mouse	Peptide5	Improved function and reduced inflammation	(Mugisho <i>et al.</i> , 2019)

				and microglia infiltration	
Duchenne muscular dystrophy	Isoproterenol challenge in DMD mice	Mouse	Gap26, Gap19	Decreased animal death and cardiac arrhythmogenesis	(Gonzalez <i>et al.</i> , 2015)
Foetal asphyxia	Complete umbilical cord occlusion (25 min)	Sheep	Peptide5	Reduced neuron and oligodendrocyte death	(Davidson <i>et al.</i> , 2014)
Gingival wound healing	Gingival wound healing	Human	Gap19	Faster wound healing	(Tarzema <i>ny et al.</i> , 2017)
Heart ischemia	Cardiac ischemia/reperfusion	Rat, mouse	Gap26, Gap27, Gap19	Reduced infarct size	(Shintani-Ishida <i>et al.</i> , 2007; Iyyathurai <i>et al.</i> , 2018; Hawat <i>et al.</i> , 2012)
Hepatic ischemia	Ischemia/reperfusion	Mouse	Peptide5	Reduced transaminases and LDH	(Li <i>et al.</i> , 2018)
Intracerebral haemorrhage	Collagenase IV injection	Mouse	Gap19	Reduced cytokine levels and neurological deficits	(Yu <i>et al.</i> , 2020)
Liver fibrosis	Thioacetamide	Mouse	Gap19	Reduced fibrosis and inflammation	(Crespo Yanguas <i>et al.</i> , 2018)
Parkinson's disease	1-methyl-4-phenyl-1,2,3,6 tetrahydropyridine-triggered dopamine neuron degeneration	Mouse	Gap26, Gap19	Reduced dopamine neuron loss and microglial activation	(Maatouk <i>et al.</i> , 2019)
Retinal ischemia	Ischemia	Rat	Peptide5	Reduced vascular leakage and retinal ganglion cell loss	(Chen <i>et al.</i> , 2015; Danesh-Meyer <i>et al.</i> , 2012)
Sepsis	Peritonitis	Mouse	Gap27, Peptide5	Reduced mortality	(Li <i>et al.</i> , 2018; Dosch <i>et al.</i> , 2019)

Septic shock	TNF-induced septic shock	Mouse	Gap19	Reduced mortality	(Delvaeye <i>et al.</i> , 2019)
Skin scarring	Skin incision	Human	ACT1	Less scarring, improved scar pigmentation	(Grek <i>et al.</i> , 2017)
Spinal cord injury	Mild contusion injury at T10	Rat	Peptide5	Improved motor neuron survival and hind limb function	(O'Carroll <i>et al.</i> , 2013)
Steatohepatitis (non-alcoholic)	Choline-deficient high-fat diet	Mouse	Gap19	Reduced inflammatory markers	(Willebrords <i>et al.</i> , 2017)
Type 1 diabetes	Streptozotocin injection	Rat	ACT1	Improved wound closure and reduced inflammation	(Moore <i>et al.</i> , 2014)
Venous leg ulcers	Ulcer patients	Human	ACT1	Faster ulcer closure	(Ghatnagar <i>et al.</i> , 2009)

1.6.4. The role of Cx43 in diabetic nephropathy

In diabetes, hyperglycaemia has been shown to alter connexin expression (Zhang *et al.*, 2021a; Tien *et al.*, 2013), GJIC (Tien *et al.*, 2013) and hemichannel opening (Sáez *et al.*, 2018). Of the 21 isoforms expressed, Cx43 is the predominant form and is associated with the pathology of multiple secondary complications of disease, including diabetic retinopathy, diabetic wound healing and diabetic nephropathy. Levels of renal Cx43 are elevated in mouse models of CKD (Abed *et al.*, 2014; Toubas *et al.*, 2011) and biopsies from individuals with diabetic nephropathy (Hills *et al.*, 2018), suggesting their involvement in disease.

Whilst a role for Cx43 hemichannel activity is demonstrated in chronic inflammatory conditions such as diabetic retinopathy (Shi *et al.*, 2022; Lyon *et al.*, 2021a; Mugisho *et al.*, 2018a), the involvement of Cx43 in inflammation and inflammasome activation in the diabetic kidney is yet to be established. Downstream of inflammasome activation studies indicate a role for Cx43 in immune cell infiltration (Abed *et al.*, 2014) and activation (Dosch *et al.*, 2019) with Cx43 expression increased in macrophages in multiple chronic immune diseases (Choi *et al.*, 2022; Dosch *et al.*, 2019; Rodjakovic). Genetic reduction of Cx43 in

hypercholesterolemic LDL receptor-deficient (LDLR^{-/-}) mice (Chadjichristos *et al.*, 2006) and hypertension-induced CKD mouse models (RenTgCx43^{+/-}; Abed *et al.*, 2014) is shown to reduce immune cell infiltration and inflammation in the kidney.

Additionally, in LPS treated macrophages (Huang *et al.*, 2019) and TGFβ1 treated fibroblasts (Williams *et al.*, 2022), both ATP and caspase 1 activity increased, indicating increased inflammasome activity. Further to this, inflammasome activation mediated an increase in fibronectin expression (Jun *et al.*, 2012), whilst increased fibronectin expression was also shown to drive caspase 1 activation in macrophages, fibroblasts and epithelial cells (Jun, Jung and Choi, 2016), suggesting the presence of a feedback loop between inflammasome activation and ECM deposition, increasing inflammation and fibrosis in multiple cell types. Recent findings show that high glucose and TGFβ1 mediate altered adherens junctions and extracellular matrix expression in fibroblasts (TK173) and proximal tubule epithelial cell line, human kidney-2 (HK-2), via increased connexin hemichannel activity. Moreover, indirect co-culture studies demonstrated that high (25mmol/L) glucose conditioned media transfer from HK-2 cells and onto renal fibroblasts, evoked an increase in Cx43 hemichannel activity and downstream phenotype. Blocking Cx43 hemichannel-mediated communication in HK-2 cells (Tonabersat) prevented the conditioned media-induced effects in fibroblasts and protected against cell injury (Williams *et al.*, 2022).

Upregulated in tubulointerstitial fibrosis, collagen I and TGFβ1 have been shown to evoke increased hemichannel-mediated ATP release in tubule HK-2 cells, paralleled by altered cell morphology and increased extracellular matrix deposition. Further corroborating a role for Cx43 in fibrosis (Potter *et al.*, 2021a) these changes were significantly blunted when cells were pre-treated with hemichannel blocker Peptide5. A major contributor to tubulointerstitial fibrosis is disassembly of the adherens junction and tight junction complex. Studies in primary proximal tubule cells and the unilateral ureter obstruction (UUO) mouse model of advanced interstitial inflammation showed that reducing Cx43 through genetic (*in vivo*) or pharmacological (*in vitro*) blockade restored hemichannel-mediated changes in adherens junction protein expression, protecting against induction of partial EMT (Price *et al.*, 2020). Whilst these findings collectively highlight a role for Cx43 in the pathology of diabetic nephropathy, further work is required to determine the mechanism by which a reduction in Cx43 expression confers protection in the diseased kidney. If Cx43 exhibits its deleterious effects via aberrant hemichannel activity, then the

use of Cx43 hemichannel blockers, may represent a viable therapeutic in management of late stage nephropathy.

1.7. Hypothesis

High levels of proinflammatory cytokines associated with elevated glucose mediate an increase in proximal tubule inflammation and fibrosis through aberrant Cx43 hemichannel ATP release and subsequent NLRP3 inflammasome activation, pathological changes that can be negated through use of Cx43 hemichannel blocking therapeutics.

1.8. Aims

This project aims to:

- I. Elucidate the effects of inflammation combined with high glucose on proximal tubule epithelial cells.
- II. Determine the role that Cx43 hemichannels play in mediating these pathological effects.
- III. Assess the impact of inflammatory cytokines and high glucose on priming and activation of the NLRP3 inflammasome complex.
- IV. Investigate the ability of hemichannel blocker Tonabersat to negate changes induced by pro-inflammatory cytokines and high glucose, including inflammasome activity, in proximal tubule epithelial cells.

2.0. Methods and materials

2.1. Materials

2.1.1. Cell culture

Human primary renal proximal tubule epithelial cells (RPTECs), HK-2 proximal tubule epithelial cells and RPTEC media supplements were sourced from the American Type Culture Collection (ATCC) Bio-resource Centre (LGC Standards, Middlesex, UK) and Lonza (Basel, Switzerland). Cell culture plasticware was purchased from Sarstedt (Nümbrecht, Germany) and fluorodishes from Thistle Scientific (Uddingston, Scotland). Dulbecco's Modified Eagles Medium (DMEM), Ham's Nutrient Mixture F-12 (F-12), DMEM/F-12 + GlutaMAX mixture and RPMI-1640 media were all purchased from Thermo Fisher Scientific (Massachusetts, US). Foetal Calf Serum (FCS), Penicillin-Streptomycin solution and Trypsin-ethylenediaminetetraacetic acid (EDTA) solution were purchased from R&D Systems (Minneapolis, US), Sigma-Aldrich (Poole, UK) and Thermo Fisher Scientific (Massachusetts, US) respectively. Dimethyl Sulphoxide (DMSO), epidermal growth factor (EGF) and a 'Neubauer Improved' haemocytometer cell counter were purchased from Sigma-Aldrich (Poole, UK). Suppliers for stimulants and inhibitors used can be found listed in table 2.1. Motic AE31E phase contrast microscope with a Moticom 3+ camera attached (Wetzlar, Germany) and a TC20 Automated Cell Counter from Bio-Rad (California, USA) were used.

2.1.2. Carboxyfluorescein dye uptake

Balanced salt solution components D-Glucose ($C_6H_{12}O_6$), magnesium sulphate heptahydrate ($MgSO_4 \cdot 7H_2O$), sodium bicarbonate ($NaHCO_3$) and sodium chloride (NaCl) were purchased from Thermo Fisher Scientific (Massachusetts, US). Carboxyfluorescein, calcium chloride dihydrate ($CaCl_2 \cdot 2H_2O$), EGTA (ethylene glycol-bis (β -aminoethyl ether)-N,N,N',N'-tetraacetic acid), HEPES (4-(2-hydroxyethyl)-1-piperazineethanesulfonic acid) and potassium chloride (KCl) were purchased from Sigma-Aldrich (Poole, UK). Potassium dihydrogen phosphate (KH_2PO_4) and sodium phosphate dibasic dihydrate ($Na_2HPO_4 \cdot 2H_2O$) were obtained from BDH Laboratories (Dubai, UAE). A metafluor

imaging workbench (Universal Imaging Corp Ltd; Marlow, Buckinghamshire, UK), a Lambda 10-2 optical filter changer (Sutter instrument; California, US), CoolSnap HQ CCD camera (Roper Scientific; Lange Dreef, Netherlands), an Axiovert 200 Research Inverted Microscope (with heated stage), an XBO 75 lamp housing unit with EBX 75 isolated power supply and a Tempcontrol 37 (Carl Zeiss Ltd; Welwyn Garden City, UK) were used to obtain results which were analysed using Fiji software (v1.0, ImageJ Studio Ltd, Wisconsin, US).

2.1.3. Reverse transcription polymerase chain reaction

Plasticware including polymerase chain reaction (PCR) plates, microtubes and pipette tips were obtained from Sarstedt (Nümbrecht, Germany). TRIZOL reagent and UltraPure DNase/RNase free distilled water were from Invitrogen (Waltham, US). Chloroform and custom DNA Oligos were purchased from Thermo Fisher Scientific (Massachusetts, US). Ethanol and isopropanol/propan-2-ol were obtained from VWR International (Radnor, US). A high-capacity complementary (c)DNA reverse transcription kit was purchased from Applied Biosystems (Waltham, US) and qPCRBIO SyGreen Blue Mix and ROX dye from PCR Biosystems (London, UK). A NanoDrop 2000 Spectrophotometer from Thermo Fisher Scientific (Massachusetts, US), BioRad T100 Thermo Cycler (BioRad, California, US), Stepone Plus Real-Time PCR instrument (Applied Biosystems, Massachusetts, US) and StepOne software v2.3 (Applied Biosystems, Massachusetts, US) were used.

2.1.4. Western blotting

Protein extraction reagents NP-40 (IGEPAL), phenylmethylsulfonyl fluoride (PMSF) and bovine serum albumin (BSA) were purchased from Sigma (Poole, UK) whilst Bio-Rad protein assay was obtained from Bio-Rad (California, USA). Western blotting reagents ammonium persulfate (APS), bromophenol blue, dithiothreitol (DTT), glycerol, glycine, sodium dodecyl sulphate (SDS), hydrochloric acid (HCl), sodium hydroxide, Tween-20 and N,N,N',N'-Tetramethylethylenediamine (TEMED) were purchased from Sigma (Poole, UK). Chameleon duo pre-stained protein ladder, fluorescent secondary antibodies and Intercept PBS blocking buffer were purchased from Licor Biosciences (Lincoln, US). Primary

antibody providers are listed in tables 2.13 and 2.14. Methanol, stripping buffer and 3mm chromatography paper were obtained from Thermo Fisher Scientific (Massachusetts, US). Bis/Acrylamide (30%) 37.5:1, Immobilon-FL membranes and Tris were purchased from Bio-Rad (California, USA), Millipore (Watford, UK) and Glentham Life Sciences (Corsham, England) respectively. Blots were run using a Mini-PROTEAN Tetra cell western blotting kit from Bio-Rad (California, USA). Licor Odyssey Fc imager and Licor Image Studio software v5.2.5. from Licor Biosciences (Lincoln, US) were used to obtain and analyse results.

2.1.5. Assay reagents and kits

Crystal violet, MTT 3-(4,5-dimethylthiazol-2-yl)-2,5-diphenyltetrazolium bromide and paraformaldehyde (PFA) were purchased from Sigma-Aldrich (Gillingham, Dorset, UK). The human proteome profiler human XL cytokine array kit and human IL1 β /IL1F2 quantikine enzyme linked immunosorbent assay were purchased from R&D Systems (Minnesota, US). An ATP-lite luminescence assay system and a Caspase Glo-1 Inflammasome assay were obtained from Perkin Elmer (Waltham, US) and Promega (Madison, US) respectively. A SpectraMax iD3 plate reader (Molecular Devices, California, US) and an iMark microplate reader from Bio-Rad (California, USA) were used to obtain results.

2.2. Cell culture

2.2.1. Clonal human kidney cell line

Human kidney 2 (HK-2) cells, a proximal tubule epithelial cell line derived from normal adult male human kidneys, were purchased and termed passage 1 on arrival from the ATCC Bio-resource Centre (LGC Standards, Middlesex, UK). Transduction of human papilloma virus 16 (HPV-16) E6/E7 genes, confirmed by PCR, induced cell immortalisation and the resulting cell line survived over a year in culture (Ryan *et al.*, 1994). This is achieved through E6/E7 protein interaction with negative cell proliferation regulators P53 and product of the retinoblastoma tumour-suppressor gene (p105-RB; Scheffner *et al.*,

1990; Münger *et al.*, 1989). Southern hybridisation and fluorescence *in situ* hybridization (FISH) analysis confirm that the cell line is derived from a single cell (Ryan *et al.*, 1994).

Taken from the normal region of a renal carcinoma, HK-2 cells retain phenotypic and functional characteristics of well differentiated proximal tubular epithelial cells and can reproduce experimental results obtained using freshly isolated primary proximal tubule epithelial cells (Ryan *et al.*, 1994). Phenotypic markers include expression of brush border membrane enzymes (acid and alkaline phosphatase), cytokeratin, vimentin, fibronectin, $\alpha 3/\beta 1$ integrin and a lack of factor VIII and common acute lymphoblastic leukaemia antigen (CALLA) endopeptidase, indicating normal proximal tubule epithelial cell phenotype (Ryan *et al.*, 1994). The possession of proximal tubule epithelial functional characteristics including parathyroid hormone (PTH) adenylate cyclase content, sodium ion (Na^+) dependant glucose uptake, glycolytic activity and gluconeogenesis further confirm a proximal tubule epithelial cell origin and normal functionality. These markers combined with their requirement for anchorage and EGF to induce polarity demonstrate that these cells are immortalised, not highly transformed, and are a suitable model for studying mechanisms of injury and repair in the proximal tubule.

2.2.2. Human kidney 2 cell maintenance

HK-2 cells were incubated at 37°C and a humidified 5% CO_2 atmosphere. HK-2 cells were cultured (passages 3-30) in T75 flasks with DMEM/Hams F12 (DMEM/F12) medium supplemented with FCS (10%) to provide nutrients and growth factors, Penicillin-Streptomycin (100IU/mL) to prevent bacterial infection and EGF (5ng/mL) to induce epithelial cell polarity. Media was replaced with fresh culture media every 2 days and cells were passaged every 3-4 days.

Before treatment HK-2 cells were split and seeded at the desired density and cultured in DMEM/F12 (17.5mmol/L glucose) medium for 24 hours. Whilst 17.5mmol/L glucose media is used for cell culture to encourage cell growth and healthy viability, sustained blood glucose levels above 11.1mmol/L would be considered diabetic (IDF Diabetes Atlas, 2021), which raises concerns as to the effect this can have on experiments *in vitro* such as promoting altered metabolic rates and protein expression, such as increased levels of TGF- $\beta 1$, a key fibrotic cytokine in diabetic nephropathy (Perlman *et al.*, 2015). Therefore,

a 1:1 combination of DMEM (no Glucose) and Ham's F12 Nutrient Mix, GlutaMAX Supplement (10mmol/L glucose) was used to create a basal (5mmol/L) glucose medium in which cells were cultured in for 48 hours. This glucose concentration falls within the range of a healthy individual's normal fasting blood glucose of 4-5.4mmol/L (Güemes *et al.*, 2016) which was used to negate any pre-stimulatory effects of the culture media.

After a 48 hour period in which cells were cultured in 5mmol/L glucose media, cells were serum starved overnight in FCS-free DMEM/F12 basal (5mmol/L) glucose medium. This was used to induce quiescence, a state of growth arrest which resets baseline activity and removes any confounding stimulatory factors.

Basal glucose (5mmol/L) media was supplemented with D-Glucose and filter sterilised to create a high (25mmol/L) glucose media, used to mimic the hyperglycaemic environment of diabetes for experiments. At a confluency of ~80%, HK-2 cells were treated with basal (5mmol/L) or high (25mmol/L) glucose \pm IL1 β (10ng/mL), TNF α (10ng/mL) and IL18 (10ng/mL) for 48 hours. Cells were also pre-treated for 30 minutes with inhibitors Tonabersat (50 μ M), Peptide 5 (25 μ M) and YVAD CMK (10-100 μ M) to evaluate the effects of Cx43 hemichannels and the NLRP3 inflammasome (Table 2.1).

Table 2.1. List of stimulants and inhibitors utilised for tissue culture experiments. A full list of reagents used in cell culture experiments for HK-2, RPTEC and primary macrophage cells, with their function, concentration and the supplier products were sourced from.

Treatment	Function	Concentration	Supplier
IL1 β	Pro-inflammatory cytokine	10ng/mL	Miltenyi Biotec, Bergisch Gladbach, Germany
IL18	Pro-inflammatory cytokine	10ng/mL	R&D Systems, Minneapolis, US
TNF α	Pro-inflammatory cytokine	10ng/mL	Miltenyi Biotec, Bergisch Gladbach, Germany
Tonabersat	Cx43 hemichannel blocker	1-100 μ M	Sigma Aldrich, St. Louis, US
Peptide 5	Cx43 hemichannel	25 μ M	Sigma Aldrich, St.

	blocker		Louis, US
YVAD CMK	Caspase 1 inhibitor	10-100µM	Sigma Aldrich, St. Louis, US
BAY11 7082	NFκB inhibitor	5µM	Sigma Aldrich, St. Louis, US
A 438079 hydrochloride	Competitive P2X7 inhibitor	10-100µM	Tocris Bioscience, Bristol, UK
PD 98059	Cell permeable ERK/MEK1/MEK2 inhibitor	50µM	Tocris Bioscience, Bristol, UK
SB 203580	Pyridinyl imidazole P38/Akt MAPK inhibitor	10µM	Tocris Bioscience, Bristol, UK
BAPTA-AM	Calcium chelator	5µM	Abcam, Cambridge, UK
Macrophage colony-stimulating factor (M-CSF)	Monocyte to M0 macrophage differentiation	10-20ng/mL	R&D Systems, Minnesota, US
Lipopolysaccharides (LPS)	Pathogen-associated molecular pattern	10ng-1µg/mL	Sigma Aldrich, St. Louis, US
Adenosine 5'-triphosphate disodium salt (ATP)	Danger-associated molecular pattern	0.1-10mmol/L	Sigma Aldrich, St. Louis, US

2.2.3. Maintenance of primary human proximal tubule epithelial cells

Human primary renal proximal tubule epithelial cells (RPTECs) isolated from a normal, healthy kidney were purchased from ATCC (Manassas, US) and Lonza (Basel, Switzerland). Primary RPTECs were cultured (passage 0-3) in Renal Epithelial Cell Basal Medium supplemented with the Renal Epithelial Cell Growth Kit and Penicillin-Streptomycin-Amphotericin B Solution (Table 2.2) at 37°C in a humidified environment

with 5% CO₂. Media was replaced every 2 days and cells were passaged when they reached 90-95% confluency.

Table 2.2. Primary human proximal tubule epithelial cell media supplements. Components of the Renal Epithelial Cell Growth Kit and Penicillin-Streptomycin-Amphotericin B Solution added to Renal Epithelial Cell Basal Medium to ensure healthy growth.

Supplement	Volume (mL)	Final Concentration
Fetal Bovine Serum	2.5	0.5%
Triiodothyronine	0.5	10nM
rh EGF	1.0	10ng/mL
Hydrocortisone Hemisuccinate	0.5	100ng/mL
rh Insulin	0.5	5ug/mL
Epinephrine	0.5	1.0uM
Transferrin	0.5	5ug/mL
LAlanylL Glutamine	6.0	2.4mmol/L
Penicillin Streptomycin Amphotericin B Solution	0.5	Penicillin: 10 Units/mL Streptomycin: 10 µg/mL Amphotericin B: 25 ng/mL

To set up for experiments cells were seeded at 5000 cells per cm² of the appropriate vessel and cultured in normal culture media until they reached 85-90% confluency. Cells were then treated with growth media adjusted to contain basal (5mmol/L) or high (25mmol/L) glucose ± IL1β (10ng) and TNFα (10ng; Table 2.1). Cells were also pre-treated for 30 minutes with inhibitors Tonabersat (50µM), YVAD CMK (10-100µM), BAY11 7082 (5µM; Sigma Aldrich, St. Louis, US), A 438079 hydrochloride (100µM), PD98059 (50µM), SB203580 (10µM; Tocris Bioscience, Bristol UK) and BAPTA-AM (5µM; Abcam, Cambridge, UK; Table 2.3).

Table 2.3. List of stimulants and inhibitors utilised for tissue culture experiments. A full list of reagents used in cell culture experiments for HK-2, RPTEC and primary macrophage cells, with their function, concentration and the supplier products were sourced from.

Treatment	Function	Concentration	Supplier
IL1 β	Pro-inflammatory cytokine	10ng/mL	Miltenyi Biotec, Bergisch Gladbach, Germany
IL18	Pro-inflammatory cytokine	10ng/mL	R&D Systems, Minneapolis, US
TNF α	Pro-inflammatory cytokine	10ng/mL	Miltenyi Biotec, Bergisch Gladbach, Germany
Tonabersat	Cx43 hemichannel blocker	1-100 μ M	Sigma Aldrich, St. Louis, US
Peptide 5	Cx43 hemichannel blocker	25 μ M	Sigma Aldrich, St. Louis, US
YVAD CMK	Caspase 1 inhibitor	10-100 μ M	Sigma Aldrich, St. Louis, US
BAY11 7082	NF κ B inhibitor	5 μ M	Sigma Aldrich, St. Louis, US
A 438079 hydrochloride	Competitive P2X7 inhibitor	10-100 μ M	Tocris Bioscience, Bristol, UK
PD 98059	Cell permeable ERK/MEK1/MEK2 inhibitor	50 μ M	Tocris Bioscience, Bristol, UK
SB 203580	Pyridinyl imidazole P38/Akt MAPK inhibitor	10 μ M	Tocris Bioscience, Bristol, UK
BAPTA-AM	Calcium chelator	5 μ M	Abcam, Cambridge, UK
Macrophage colony-stimulating factor (M-CSF)	Monocyte to M0 macrophage differentiation	10-20ng/mL	R&D Systems, Minnesota, US
Lipopolysaccharides (LPS)	Pathogen-associated molecular pattern	10ng-1 μ g/mL	Sigma Aldrich, St. Louis, US
Adenosine 5'-triphosphate (ATP) disodium salt	Danger-associated molecular pattern	0.1-10mmol/L	Sigma Aldrich, St. Louis, US

2.2.4. Cell revival

Stocks of HK-2 and RPTEC cells were stored in liquid nitrogen. To revive, cells were defrosted rapidly in 37°C water and diluted in 10mL culture media to prevent ice crystal formation and cell lysis (Pegg, 2015). The cells were centrifuged at 2500g to pellet cells, the supernatant removed, and cells were resuspended in 6mL culture media in a T25 flask. Cells are incubated at 37°C, 5% CO₂ overnight to allow cells to adhere to the flask, before the media is removed and replaced with fresh culture media the following morning to ensure all DMSO is removed.

2.2.5. Cell passaging

Passaging is a process which involves the transfer of cells into new culture media at a lower density, to maintain cells at an optimum density, enabling further propagation of the cell line. Regular passaging of HK-2 and RPTEC cells was performed by removing the culture media, ahead of washing the cells in 3mL of PBS to remove excess FCS, a known inhibitor of trypsin-EDTA. Cells were then incubated at 37°C with 6mL trypsin-EDTA for 2-3 minutes. Trypsin-EDTA is a digestive protease used for cell dissociation from the surface of the flask. Trypsin-mediated cleavage of proteins at their C-termini (Mótyán *et al.*, 2013) disrupts focal adhesion complexes, through removal of Ca²⁺ and Mg²⁺, ions essential for cadherin and integrin dependant cell adhesion (Alberts *et al.*, 2002). After confirming that all cells had detached from the vessel surface, cells were added to 5mL culture media containing FCS to neutralise the trypsin and centrifuged at 2500g to pellet the cells (Mótyán *et al.*, 2013). The supernatant was removed, and cells were resuspended in 4mL culture media as advised by ATCC. A cell count, performed using a haemocytometer, was used to calculate the dilution factor needed for the appropriate seeding density (Figure 2.1; Table 2.3). Resuspended cells (100µL) were added to the counting chamber of the haemocytometer and covered with a coverslip. The number of cells in each of the four outermost large squares (highlighted in red), made up of 16 smaller squares, was counted and the average of the four calculated. The dilution factor was calculated using the formula:

$$\text{Volume of cells to dilute} = \frac{\text{Volume of media needed}}{\left(\frac{\text{Average cell count}}{\text{Desired seeding density}} \right)}$$

The cells were diluted in the appropriate amount of culture media and seeded into a flask/plate as required at the appropriate dilution. Maximum passages of 3 for RPTECs and 30 for HK-2 cells was used to prevent phenotypic drift and genetic instability (Geraghty *et al.*, 2014).

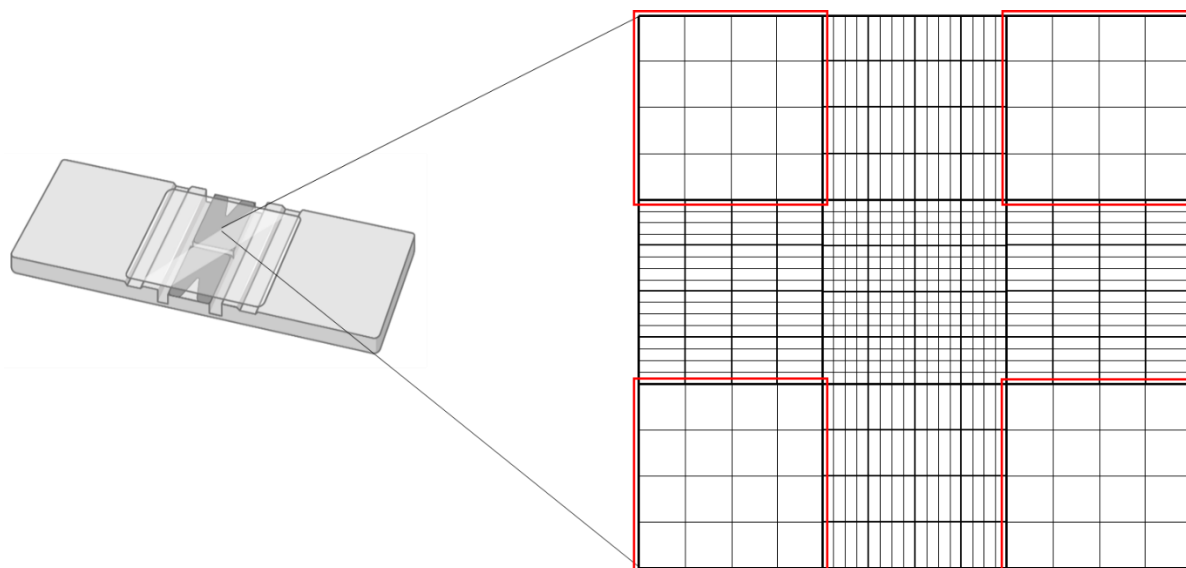


Figure 2.1. Image of a haemocytometer. A haemocytometer used for performing a cell count. Cells in the outer four quadrants, highlighted in red, are counted and an average of the four is calculated to be used to calculate the dilution factor required for the desired seeding density.

Table 2.3. HK-2 seeding densities. A table summarising the seeding densities used for HK-2 cells when setting up treatments.

Cell Vessel	Seeding Density	Experiment
Plastic T75 flask	4×10^4	Western blotting
Plastic T25 flask	2×10^4	Western blotting
Plastic 6-well plate	2×10^4	RNA isolation
Plastic 12-well plate	2×10^4	Crystal violet assay, RNA isolation
Plastic 96-well plate	1×10^4	MTT, Caspase Glo-1 Assay, ATP-Assay
Glass Fluorodish	1×10^4	Carboxyfluorescein

2.2.6. Freezing cells

Frozen stocks of HK-2 cells were prepared by trypsinising a T75 flask of confluent cells as previously described (Section 2.2.4) and resuspending cells in 1.5mL FCS + DMSO (10%). Formation of ice crystals during freezing was prevented by the addition of DMSO (Pegg, 2015). Cells were transferred to cryovials and frozen slowly over several hours for long term storage in liquid nitrogen.

2.3. Animal model of diabetic nephropathy

All *in vivo* animal work and experiments using animal tissue was carried out by our collaborators Dr Chadjichristos and colleagues at INSERM, Paris. All procedures regarding whole animal studies were in accordance with the ARRIVE (Animal Research: Reporting *In Vivo* Experiments) guidelines 2.0 and within the European Union Guidelines for the Care and Use of Laboratory Animals and approved by the local ethics committee of INSERM. Mice were housed at a constant temperature with free access to water and food. All mice used were male C57BL/6. The Cx43^{flox/flox} mice were purchased from the European Mouse Putant Archive- consortium. The Cx43 tubular-specific deletion strain was created as previously described (Kormann *et al.*, 2020). The Pax8-rtTA-LC1 mice were interbred with Cx43^{flox} mice (Pax8-rtTA-LC1/Cx43^{flox/flox}). Deletion of Cx43 specifically in renal tubule epithelial cells was induced by administration of 0.2 mg/mL doxycycline in drinking water, containing 2.5 % sucrose for 2 weeks starting 1 month after birth. Then, 3–4-month-old mice were subjected to UUO as already described (Abed *et al.*, 2014). This procedure involves ligation of the ureter of one kidney with silk thread. To examine the effect of Cx43 deletion alone sugar was administered to Pax8-rtTA-LC1/Cx43^{flox/flox} transgenic mice, serving as controls for up to 4 months.

2.4. Evaluation of renal morphology, interstitial fibrosis, and immunohistochemistry

Harvested by collaborators at INSERM, kidneys were fixed in 4% formalin solution and embedded in paraffin as described previously (Abed *et al.*, 2014). Sections of 4mm thick were stained with varying histological and immunological stains by collaborators at

INSERM. Masson's trichrome staining produces three colours and is often used to differentiate cells from connective tissue. Nuclei are stained blue, collagen is stained green or blue and cytoplasm are stained bright red allowing histological evaluation of kidney samples. Tubular dilation was scored as previously reported (Abed *et al.*, 2014) by collaborators at INSERM. Scoring was performed blind on coded slides. Used primarily for staining collagen fibers and amyloid, serius red staining was used to semi-quantitatively assess interstitial fibrosis. Analysis morphometric software (Olympus) that allowed the formation of a binary image was used to assess fibrosis, calculating the stained area as percentage of the image area. Ten fields that covered the entire cortex were randomly selected per section.

Immunostaining was performed on paraffin embedded sections as described in Kavvadas *et al.*, 2017, by collaborators at INSERM. Staining of F4-80 (1:200; Serotec), a cell surface glycoprotein expressed at high levels on macrophages, was used as a measure of monocyte infiltration and differentiation to macrophages. FSP1 (1:200; Abcam) was stained as a marker of the abundance of fibroblasts within kidney sections. Furthermore, staining of NLRP3 (1:200; AdipoGen) was performed to determine changes in NLRP3 expression, a protein associated with activation of the NLRP3 inflammasome. Immunofluorescence for transmembrane protein, Cx43 (1:200; Sigma-Aldrich) was performed on methanol fixed cryosections as described in Abed *et al.*, 2017. Alexa Fluor secondary antibodies were used for detection (1:500). Sections were counterstained with Evans Blue. Negative controls included omission of first antibodies or preincubation of first antibodies with immunogenic peptides.

2.5. Phase contrast microscopy

High resolution images of HK-2 and RPTEC cell morphology were captured at a 10x and 20x objective using a Moticam 3+ camera attached to a Motic AE31E phase contrast microscope. Images were saved and exported using the Motic Images Plus 3.0MP (x64) software.

2.6. Crystal violet assay

Crystal violet assays are commonly used for assessing cytotoxicity and cell viability (Figure 2.2). Using cell adherence as a measure of cell death, dead cells detach and are washed away during the assay whilst remaining living cells take up the crystal violet, staining DNA which can then be quantified and used as a measure of cell viability (Vega-Avila *et al.*, 2011; Feoktistova *et al.*, 2016).

To determine optimum concentration of inflammatory cytokines and Tonabersat for treatments, HK-2 cells were cultured in 12 well plates (2×10^4 cells/well) in 5mmol/L versus 25mmol/L glucose +/- IL1 β (2-50ng/mL), IL18 (2-50ng/mL) and TNF α (2-50ng/mL), +/- Tonabersat at 1-100 μ M. Post treatment, wells were washed in PBS and cells fixed in 4% PFA for 10 minutes at room temperature (RT). Cells were stained with crystal violet (0.1%) at RT for 20 minutes. Excess crystal violet was washed away with distilled water and stain solubilised with SDS (1%). Optical density was read at 595nm using a microplate reader. The values are presented as a percentage of staining in treated cells as compared to control.

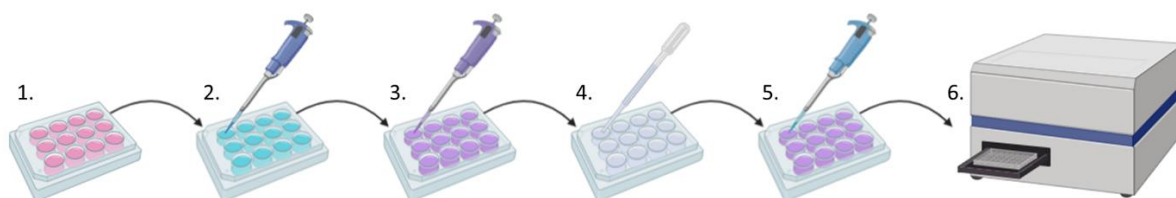


Figure 2.2. Steps carried out for a crystal violet assay. (1) Cells are cultured in a 12 well plate and treated with proinflammatory cytokines +/- high glucose for 48 hours. (2) The media is removed, and cells are fixed in 4% paraformaldehyde. (3) Crystal violet is added to stain cells. (4) Once stained excess crystal violet is removed and thoroughly washed away with distilled water. (5) The remaining crystal violet stain is solubilised in 1% SDS and (6) the optical density of each well is measured.

2.7. The 3-(4,5-Dimethylthiazol-2-yl)-2,5-diphenyltetrazolium bromide assay

The 3-(4,5-Dimethylthiazol-2-yl)-2,5-diphenyltetrazolium bromide (MTT) assay is a colorimetric assay that measures reduction of MTT to formazan crystals by mitochondrial succinic dehydrogenases. Formazan is insoluble and purple in colour (Figure 2.3). This purple stain is quantified and used as an indicator of cell viability and proliferation (Nikzad *et al.*, 2014).

HK-2 cells were cultured in 96 well plates (2×10^4 cells/well). Cells were stimulated with 5mmol/L versus 25mmol/L glucose +/- IL1 β , IL18 and TNF α (2-50ng/mL) +/- Tonabersat (1-100 μ M) in DMEM/F12 for 48 hours. At 48 hours, MTT (5mg/mL) was added to each well and incubated for 4 hours at 37°C in a dark, humidified 5% CO₂ atmosphere. Following MTT reduction, the media was removed and DMSO added to solubilise the stain. The optical density was measured using a microplate reader at a dual wavelength (595-655nm). The values are presented as a percentage of MTT uptake in treated cells as compared to control cells.

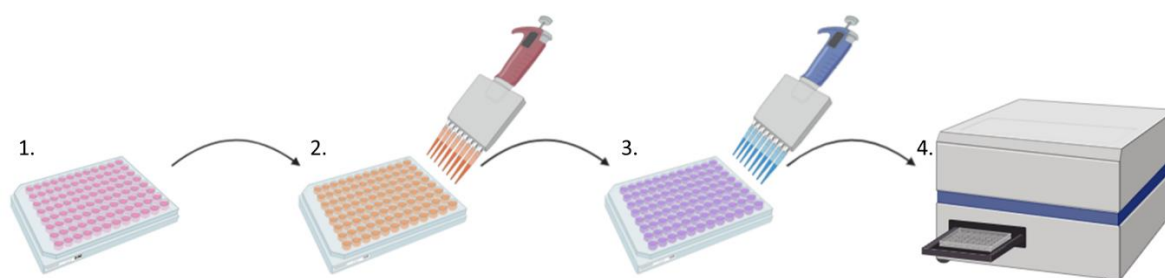


Figure 2.3. MTT assay protocol. (1) Cells are cultured in a 96 well plate and treated with high proinflammatory cytokines +/- high glucose for 48 hours. (2) MTT was added to each well and incubated for 4 hours. (3) DMSO was added to solubilise the stain. (4) The optical density of each well is measured.

2.8. Carboxyfluorescein uptake assay

Carboxyfluorescein dye uptake studies are used as a measure of functional hemichannels in the cell membrane, where increased dye uptake exhibits a positive correlation to hemichannel number (Figure 2.4). This technique utilises 376Da polyanionic fluorescent probe, 5(6)-carboxyfluorescein, a membrane impermeant dye which is permeable to

connexin hemichannels, which allow small molecules up to 1kDa to pass through (Potter *et al.*, 2021b). Connexin hemichannels are tightly gated by extracellular levels of calcium, where Ca^{2+} binds and forms a Ca^{2+} binding ring near the extracellular entrance of the pore, disrupting salt bridges within the hemichannel, thereby changing the shape and closing the channel (Lopez *et al.*, 2016). Therefore, Ca^{2+} -containing and Ca^{2+} -free balanced salt solution (BSS) were used to artificially gate Cx43 hemichannels. Under Ca^{2+} -free conditions hemichannels opened allowing dye uptake, whilst Ca^{2+} -containing BSS closed hemichannels and trapped the dye inside the cells ahead of imaging (Potter *et al.*, 2021b).

HK-2 and RPTEC cells were preincubated with hemichannel inhibitors Peptide 5 (25 μM) and Tonabersat (10-100 μM) for 30 minutes prior to treatment with either IL1 β (10ng/mL), TNF α (10ng/mL) or a combination of the two. Cells were incubated with Ca^{2+} -free BSS and 5,6-carboxyfluorescein (200 μM) for 10 minutes, allowing uptake of the fluorescent dye through hemichannels forced open by the artificial (experimental) removal of extracellular Ca^{2+} . Calcium-containing BSS with carboxyfluorescein was added to cells for 5 minutes to close the hemichannels whilst preventing wash out of dye within the cells. A subsequent wash in Ca^{2+} -containing BSS maintained the hemichannels in the closed state and removed excess dye from the cell exterior. Images of cells were captured using a Cool Snap HQ CCD camera (Roper Scientific) and Metamorph software (Universal Imaging Corp., Marlow, Bucks, UK). ImageJ was used to quantify dye uptake by drawing a region of interest around each cell (10-15 cells/dish) and measuring the mean pixel intensity.

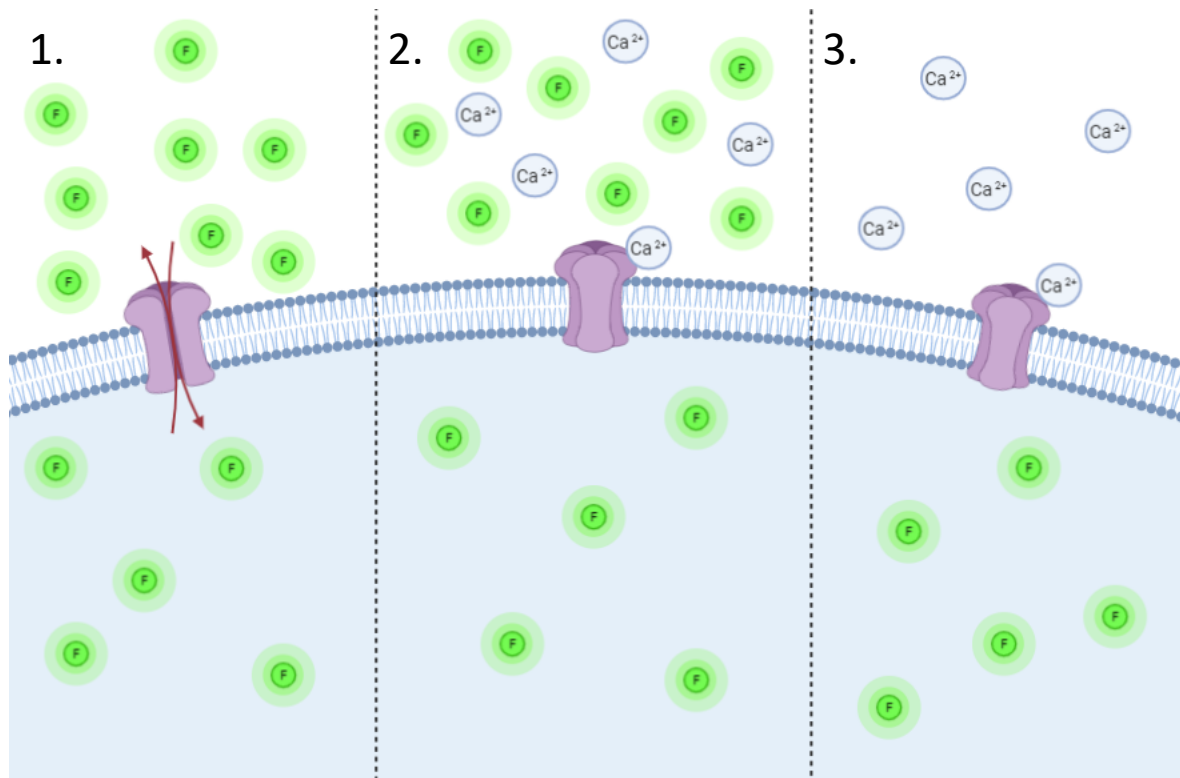


Figure 2.4. Carboxyfluorescein uptake assay protocol. On the basis that calcium gates hemichannel activity, a Ca^{2+} -free/containing BSS was used to open and close hemichannels. (1) Following treatment, cells were incubated with carboxyfluorescein in a Ca^{2+} -free BSS to open hemichannels and allow for carboxyfluorescein dye uptake. (2) Ca^{2+} -containing BSS supplemented with carboxyfluorescein dye is added. This closes hemichannels without causing intracellular carboxyfluorescein to be released from cells. (3) Cells are washed in Ca^{2+} -containing BSS prior to imaging to wash away excess carboxyfluorescein whilst maintaining closed hemichannels to prevent carboxyfluorescein leakage.

2.9. Real-time quantitative polymerase chain reaction

Expression of genomic messenger (m)RNA levels is measured using real time quantitative (RT-q) PCR, a highly specific and sensitive technique which combines reverse transcription of RNA into cDNA, and amplification of specific DNA targets (Wong *et al.*, 2018).

2.9.1. RNA extraction

For the *in vivo* mouse model mRNA was isolated from the renal cortex. Alternatively, *in vitro* cells were cultured in 12 well plates. Total RNA was isolated using TRIzol reagent (Invitrogen, Waltham, US) following the manufacturer's instructions (Fig.2.5). TRIzol is an acid-guanidinium-phenol based reagent used to break down cells and cell components. The low pH allows RNA to be separated from DNA and protein, whilst its ability to inactivate RNases maintains RNA integrity during cell homogenisation. At the end of the cell treatment period cell media was removed and replaced with TRIzol (1mL) to lyse cells, which were then collected into an Eppendorf (1.5mL) using a cell scraper. Chloroform (200µL) was added to each sample, mixed well and incubated for 2 minutes at room temperature (RT) to allow alcohol phase separation to start. Samples were then centrifuged for 15 minutes at 13,000RCF and 4°C separating the RNA from the rest of the cell lysate. The clear aqueous phase containing the cellular RNA was transferred to a fresh Eppendorf containing isopropanol (500µL) and incubated for 10 minutes at RT to allow RNA to precipitate prior to centrifugation at 13,000RCF for 10 minutes. The supernatant was removed, and the pellet was washed in 75% ethanol, left to dry and resuspended in 100µL dH₂O. RNA yield was increased by heating the sample at 65°C for 5 minutes. Spectrophotometric analysis to determine RNA concentration and purity was performed using a nanodrop.

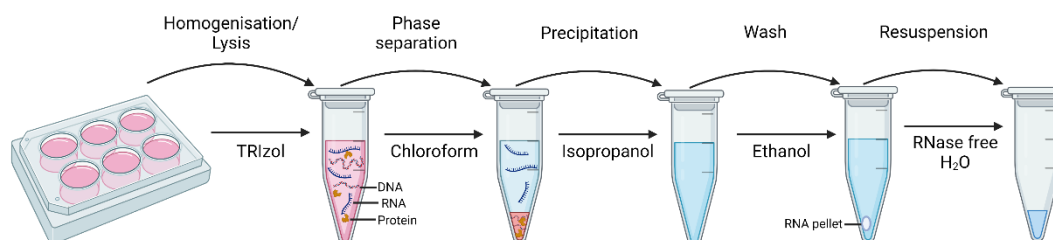


Figure 2.5. Extraction of RNA from cell lysates. TRIzol was used to lyse cells and separate RNA, DNA and protein components. The addition of Chloroform and centrifugation resulted in a clear layer containing only RNA, which was removed and added to isopropanol. In isopropanol, RNA precipitated forming a pellet after centrifugation. The pellet was washed in ethanol prior to resuspension in water.

2.9.2. Complementary DNA conversion

Due to the ubiquitous presence of RNases, mRNA is prone to degradation and so mRNA was converted to cDNA for use in PCR reactions as a more reliable compound. A two-step reaction PCR was carried out, consisting firstly of cDNA synthesis using mRNA samples (Fig.2.6). RNA was converted to single stranded cDNA using a high-capacity cDNA reverse transcription kit (Applied biosystems, Waltham, US) following the manufacturer's instructions. A master mix (Table 2.4) was prepared in a 0.2mL PCR tube, 5.8µL was added to 0.5µg RNA and the solution was made up to a total of 20µL with nuclease-free H₂O. The random primer method was used to initiate cDNA synthesis, ensuring efficient first strand synthesis with all RNA present. The deoxynucleotide triphosphates (dNTP) mix contains A, T, G and C nucleotides essential for building new DNA strands in cDNA synthesis and PCR amplification. Primers and nucleotides were used by multiscribe reverse transcriptase, a recombinant RNA-dependant DNA polymerase that synthesises cDNA from single stranded RNA. The samples were placed into a BioRad T100 Thermo Cycler (BioRad, California, US) following a 3-step protocol; 1) primer annealing- 25°C for 10 minutes, 2) DNA polymerisation- 37°C for 2 hours, 3) enzyme denaturation- 85°C for 5 minutes. A 1:10 dilution was performed on the resultant cDNA which was then stored at 4°C or -20°C.

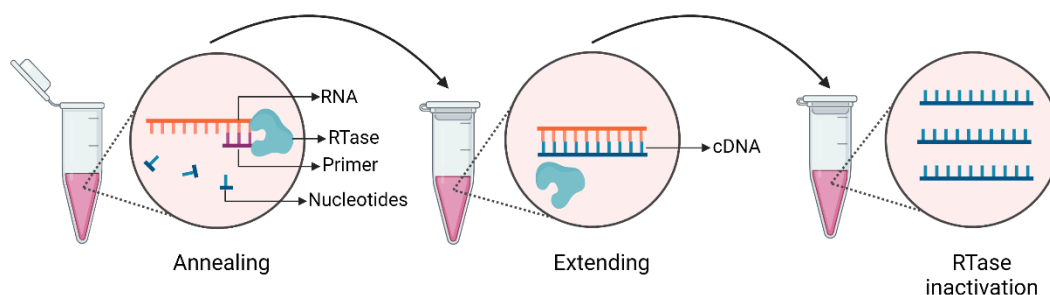


Figure 2.6. Conversion of messenger RNA to complementary (c)DNA. Step one of the RT-qPCR process is the conversion of RNA to cDNA in a thermocycler. Reverse transcriptase (RTase) anneals to RNA with a complementary primer and transcribes cDNA through strand extension. The reaction is terminated by inactivating RTase to prevent it from interfering during qPCR.

Table 2.4. Reverse transcriptase master mix. Components required to make up cDNA conversion master mix. Volumes are per well and should be multiplied by the number of samples being converted, with two extras to ensure volume is sufficient.

Reagent	Amount per cDNA Reaction
10x RT Buffer	2 μ L
25x dNTP Mix	0.8 μ L
10x RT Random Primers	2 μ L
Multiscribe Reverse Transcriptase	1 μ L
Nuclease-free H ₂ O	Make up to total of 20 μ L with RNA

2.9.3. Polymerase chain reaction

Real time quantitative (RT-q) PCR utilises SYBR green fluorescence, which emits light upon binding to the double stranded DNA of the PCR products. Fluorescence increases proportionally with cDNA amplification, allowing the amplification reaction to be monitored in real time giving semi-quantifiable results. RT-qPCR was performed using qPCRBIO SyGreen Blue Mix and ROX dye (PCR Biosystems, London, UK). A master mix (Table 2.5) containing forward and reverse primers for target genes (Table 2.6) was prepared and 7.5 μ L was added to 2.5 μ L cDNA in each well of a PCR plate (Sarstedt, Nümbrecht, Germany). Passive reference dye, ROX was used for signal normalisation to reduce variability between variable replicates. A standard curve was used to give relative cDNA concentrations which were normalised against expression of housekeeping gene GAPDH. Using a Stepone Plus Real-Time PCR instrument (Applied Biosystems, Massachusetts, US) cDNA was denatured at 95°C for 2 minutes, followed by 40 amplification cycles of 60°C for 20 seconds to allow primer annealing and extension and 95°C for 5 seconds for denaturation. A melt curve analysis of 95°C for 15 seconds, 60°C for 1 minute, temperature ramping by 1°C over 20 minutes and 95°C for 15 seconds confirmed primer specificity and detected possible contamination. Results were analysed using StepOne software v2.3 (Applied Biosystems, Massachusetts, US). For *in vivo* work, relative gene expression was analysed using $2^{-\Delta\Delta CT}$. Results are expressed as arbitrary units, representing the ratio of the target gene to the internal control gene hypoxanthine phosphoribosyl transferase (HRPT). For *in vitro* work, results are expressed as percentage values of the cDNA quantity as compared to treated cells, following normalisation to housekeeping gene GAPDH.

Table 2.5. PCR reaction master mix. Amount of reagent needed per reaction to make up PCR master mix. Volume was made up for number of reactions plus two to ensure sufficient volume.

Reagent	Amount
SyGreen Blue Mix	5 μ L
Forward Primer	0.1 μ L
Reverse Primer	0.1 μ L
ROX Dye	0.2 μ L
RNase/DNase free H ₂ O	2.1 μ L

Table 2.6. Amplification primers for RT qPCR. List of amplification (5'–3') primer sequences used for the RT qPCR reaction, obtained using the NCBI Primer Blast.

Target Genes	Species	Forward Primer	Reverse Primer
GAPDH	Human	TTCACCACCATGGAGAAGGC	AGGAGGCATTGCTGATGATCT
Cx43	Human	ATGGGTGACTGGAGCGCCTTAG	CTAGATCTCCAGGTCATCAGG
IL1β	Human	TGGCAGAAGTACCTGAGCTCGC	GCCGCCATCCAGAGGGCAGA
NLRP3	Human	GGAAGTGAAGCACCTGTTGTGCA	TCCTGAGTCTCCCAAGGCATTCT
IL6	Human	CCTGAGAAAGGAGACATGTAACAAGA	GGAAGGTTTCTGAGTTGTTTCTGCTGC
MCP1	Human	GCTCGCTCAGCCAGATGCAA	TCCTGAACCCACTTCTGCTTG
GCSF	Human	AAGCTGTGCCACCCGAGGA	GTGGGACCCAACTCGGGGGA
TNFα	Human	GTGATCGGCCCCCAGAGGGAA	TGGAGCTGCCCCTCAGCTTGA
IL1α	Human	CCAGCCAGAGAGGGAGTCATT	CATGGAGTGGGCCATAGCTT
HPRT	Mouse	GGAGCGGTAGCACCTCCT	CTGGTTCATCATCGCTAATCA
Cx43	Mouse	GTGCCGGCTTCACTTTCA	GGAGTAGGCTTGGACCTTGTC
NLRP3	Mouse	TGCTCTTCACTGCTATCAAGCCCT	ACAAGCCTTTGCTCCAGACCCTAT
IL1β	Mouse	CCACAGACCTTCCAGGAGAATG	GTGCAGTTTCTGAGTATCGTACAGG
IL6	Mouse	GCTACCAAAGTGGATATAATCAGGA	CCAGGTAGCTATGGTACTCCAGAA
MCP1	Mouse	GGCTGGAGAGCTACAAGAGG	CTCTTGAGCTTGGTGACAAAAA
NGAL	Mouse	CCATCTATGAGCTACAAGAGAACAAT	TCTGATCCAGTAGCGACAGC

2.10. Whole cell protein extraction

Following treatment of cells, proteins were isolated from cell lysates for quantification of expression using western blotting. Cells were washed in phosphate buffered saline (PBS), scraped into a mix of PBS with PMSF (0.5%), a serine protease inhibitor which prevents protein digestion after cell lysis, and pelleted at 2500g for 5 minutes. Supernatant was removed, and the cell pellet resuspended in lysis buffer (Table 2.7), containing reducing agent DTT, prior to agitation at -4°C for 20 minutes. Cells were centrifuged at 15,000g for 5 minutes at 4°C to pellet cell debris and the supernatant (protein) aliquoted and stored at -80°C.

Table 2.7. Lysis buffer recipe. Recipe for lysis buffer used to lyse cells for protein extraction.

Reagent	Amount
0.5M Tris-HCl pH 7.8	5ml
NP-40 (IGEPAL)	50µL
1M DTT	50µL
dH ₂ O	5ml
PMSF	100µL

2.11. Bradford Assay

Bradford protein assays, a colorimetric assay utilising Coomassie brilliant blue G-250 dye was used to determine the concentration of protein samples. When bound to protein, the maximum absorption spectrum of the Coomassie brilliant blue G-250 within the Bio-Rad protein assay reagent shifts from 465nm to 595nm, a shift that can be quantified to give sensitive protein concentration measurements (Bradford, 1976). The concentration of each sample was determined using a standard curve, generated using solutions of BSA of a known concentration. A standard curve was generated by adding Bio-Rad protein assay dye to 800µL BSA at a range of concentrations (0-20µg/mL) in quartz cuvettes and measuring the optimal density at 595nm using a SpectraMax iD3 (Molecular Devices, California, US; Figure 2.7). Results were plotted in Microsoft Excel to produce the equation for the standard curve. Protein samples (5 and 10µL) were added to Bio-Rad Dye (200µL) and dH₂O to a total of 1mL in quartz cuvettes. Optical density was measured at 595nm, and the results were used along with the equation of the standard curve to calculate the protein concentration.

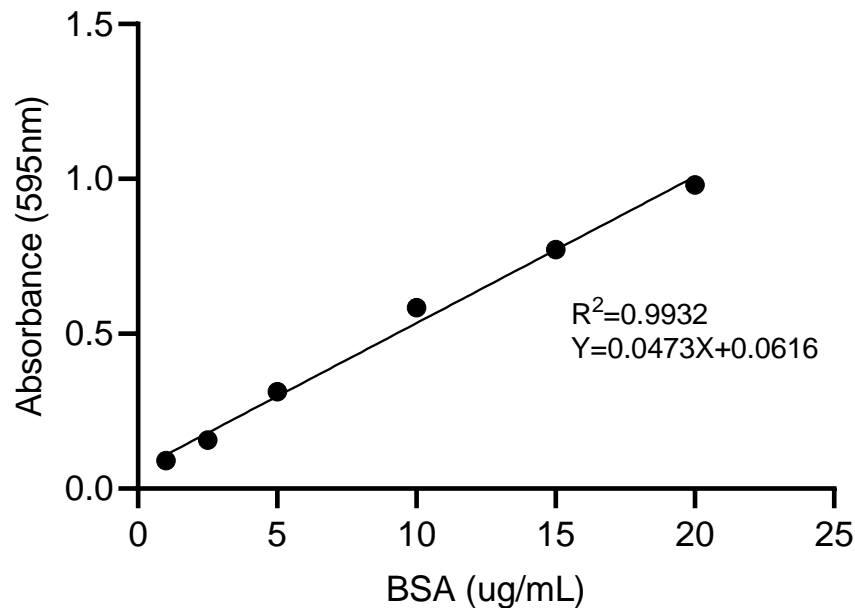


Figure 2.7. Example of a standard curve produced using known concentrations of BSA in Bio-Rad protein assay reagent. The absorbance of protein samples (5 μ L and 10 μ L) of unknown concentrations represented the Y value. The equation of the curve was then rearranged to give the value for X. This value was divided by the volume of protein added and the average of the two replicates was taken to give the concentration of protein in μ g/mL.

2.12. Western blotting

Western blotting, also known as immunoblotting, is a common method used for the separation of proteins based on size and detection of specific proteins from a mixed protein sample. This method is semi-quantifiable, providing a relative comparison of protein concentration in each sample run on each blot rather than an absolute measure (Towbin *et al.*, 1979). The method consists of several stages: sample preparation, sodium dodecyl-sulphate polyacrylamide gel electrophoresis (SDS-PAGE), transfer of protein to a solid membrane, membrane blocking, antibody detection and imaging (Figure 2.8; GE Healthcare, 2014).

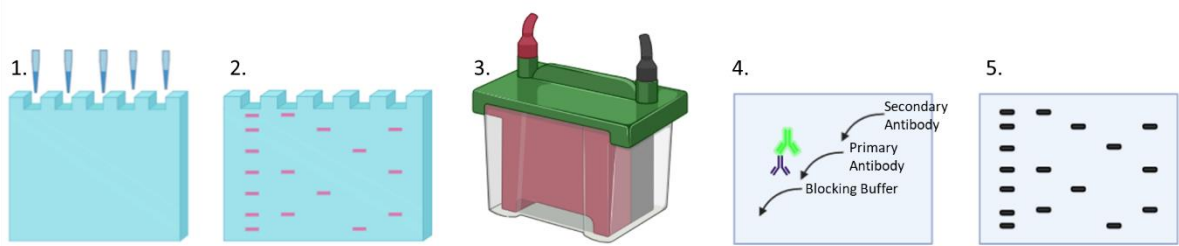


Figure 2.8. Methodology for immunoblotting. (1) Acrylamide gels are made, and protein is loaded into each well. (2) Proteins are separated using SDS-PAGE gel electrophoresis. (3) Proteins are transferred by electroblotting onto an immobilon FL PVDF membrane. (4) Membranes are blocked to prevent non-specific binding, probed overnight with primary antibody and probed for one hour with secondary antibodies. (5) The membrane is developed using a LICOR Odyssey Fc Imager.

2.12.1. Sample preparation

Following protein extraction, cell lysate samples were prepared for separation via sodium dodecyl-sulphate polyacrylamide gel electrophoresis (SDS-PAGE; GE Healthcare, 2014). Sample buffer (Table 2.8) was added at a 1:1/2:1 ratio to cytosolic protein from treated cells, up to a maximum of 40µL. Sample buffer consisted of sodium dodecyl sulfate (SDS), a detergent that unfolds proteins into linear chains and coats them with a negative charge allowing proteins to migrate down the gel when a current is passed through (Bass *et al.*, 2017). This negative charge means that proteins are separated on the basis of molecular weight, with smaller proteins able to migrate through the gel at a faster rate than large proteins. The reducing agent DTT was added to further reduce and disrupt disulphide bonds within proteins. Glycerol increases the density of the sample relative to the surrounding running buffer, which makes the samples easier to load into the wells of the gel, whilst bromophenol blue creates a dye front allowing visualisation of protein migration throughout the gel. Samples were then heated at 95°C for 5 minutes to denature proteins, breaking down the secondary, tertiary and quaternary structure. This opens proteins into their single chain primary structure for more accurate separation based on molecular weight and also increases antibody epitope availability to improve antibody binding. Samples were not heated when probing for collagen I and collagen IV as the antibody does not recognise their epitope in the proteins denatured form.

Table 2.8. Sample buffer recipe.

Reagent	Volume
Trisaminomethane (tris) hydrogen chloride (HCl) pH6.8 (0.5%)	625µL
SDS (10%)	1000µL
Glycerol	500µL
DTT (1M)	16.2µL
Bromophenol Blue (BPB; 0.05%)	125µL
dH ₂ O	250µL

2.12.2. Gel electrophoresis

The gels are made of a large resolving polyacrylamide gel (Table 2.9) formed of small pores to allow protein separation, and a smaller stacking polyacrylamide gel (Table 2.10) in which a plastic well comb was placed whilst the gel set, to form the wells into which the samples would be pipetted into, lining them up so they enter the resolving gel at the same time. Consisting of polymerized acrylamide monomers with cross-linking N,N0-methylene-bisacrylamide monomers, polyacrylamide gels are formed of uniformly sized pores through which proteins migrate, as an electrical current is passed, at different speeds based in size-mediated frictional resistance (Bass *et al.*, 2017). The percentage of acrylamide used to make the resolving gel was dependant on the molecular weight of the protein, large molecular proteins (>100kDa) are run on a 7.5% gel and small molecular weight proteins (<50kDa) on a 12.5% gel so the size of the pores within the gel allow optimal separation for these proteins. The resolving gel was cast first in between two glass plates in a gel solidification rack and left to set for 40 minutes, before the addition of the stacking gel and well comb for 20 minutes. Once set gels were placed into a Bio-Rad mini protean II tank, and the space between the two gels was filled with 1x electrophoresis running buffer (Table 2.11). Protein samples were then loaded into each well and the rest of the tank filled with running buffer to aid current flow and maintain pH (Bass *et al.*, 2017). The gel was run at 125 volts (V) for approximately 90 minutes to allow proteins to migrate laterally down the gel from cathode (-) to anode (+) and separate into compact molecular weight-based bands.

Table 2.9. Resolving gel recipe. Recipe for two resolving gels of 7.5, 10 and 12.5% acrylamide.

	7.5%	10%	12.5%
Acrylamide (30%)	3mL	4mL	5mL
Tris HCl pH 8.8 (1.5M)	3mL	3mL	3mL
SDS (10%)	120μL	120μL	120μL
dH ₂ O	5.84mL	4.84mL	3.84mL
APS	40μL	40μL	40μL
TEMED	10μL	10μL	10μL

Table 2.10. Stacking gel recipe. Recipe for 4x stacking gels.

Reagent	Volume
Acrylamide (30%)	1.5mL
Tris HCl pH 6.8 (0.5M)	2.5mL
SDS (10%)	100μL
dH ₂ O	5.8mL
APS	100μL
TEMED	10μL

Table 2.11. Electrode running buffer (10x) recipe. Reagents for 10x running buffer. Buffer is diluted 1:10 in dH₂O for use.

Reagent	Volume/Weight
Tris	30g
Glycine	144g
SDS	10g
dH ₂ O	Make up to 1L

2.12.3. Transfer to membrane

After complete protein separation via SDS-PAGE, proteins were transferred by electroblotting onto an Immobilon fluorescence (FL) polyvinylidene difluoride (PVDF) membrane using the wet transfer technique. Membranes were firstly soaked in methanol for a few seconds to remove the hydrophobic interactions of the membrane, washed in dH₂O for 5 minutes. Transfer 'sandwiches' were assembled in cassettes (Figure 2.9), where the gel and membrane were held together between 3mm chromatography paper and fibre pads after each was equilibrated in transfer buffer (Table 2.12) for 10-20 minutes to reduce possible interference caused by contaminants such as SDS or ions. The cassettes were then placed in a BioRad mini protean II gel transport tank filled with transfer buffer to maintain current flow and pH. The transfer was run at 100V for 60-90 minutes allowing transfer of negatively charged proteins from the gel to the membrane, to immobilise proteins and provide solid structural support prior to antibody detection. In order to maintain appropriate temperatures to avoid membrane deformation, an ice pack was placed in the tank prior to running and transfer buffer was kept at 4°C, with use of a magnetic flea to ensure an even temperature throughout.

Table 2.12. Transfer buffer (10x) recipe. Reagents for 10x transfer buffer. For 1x buffer

Reagent	Volume/Weight
Trisaminomethane	30.3g
Glycine	144g
dH ₂ O	Make up to 1L

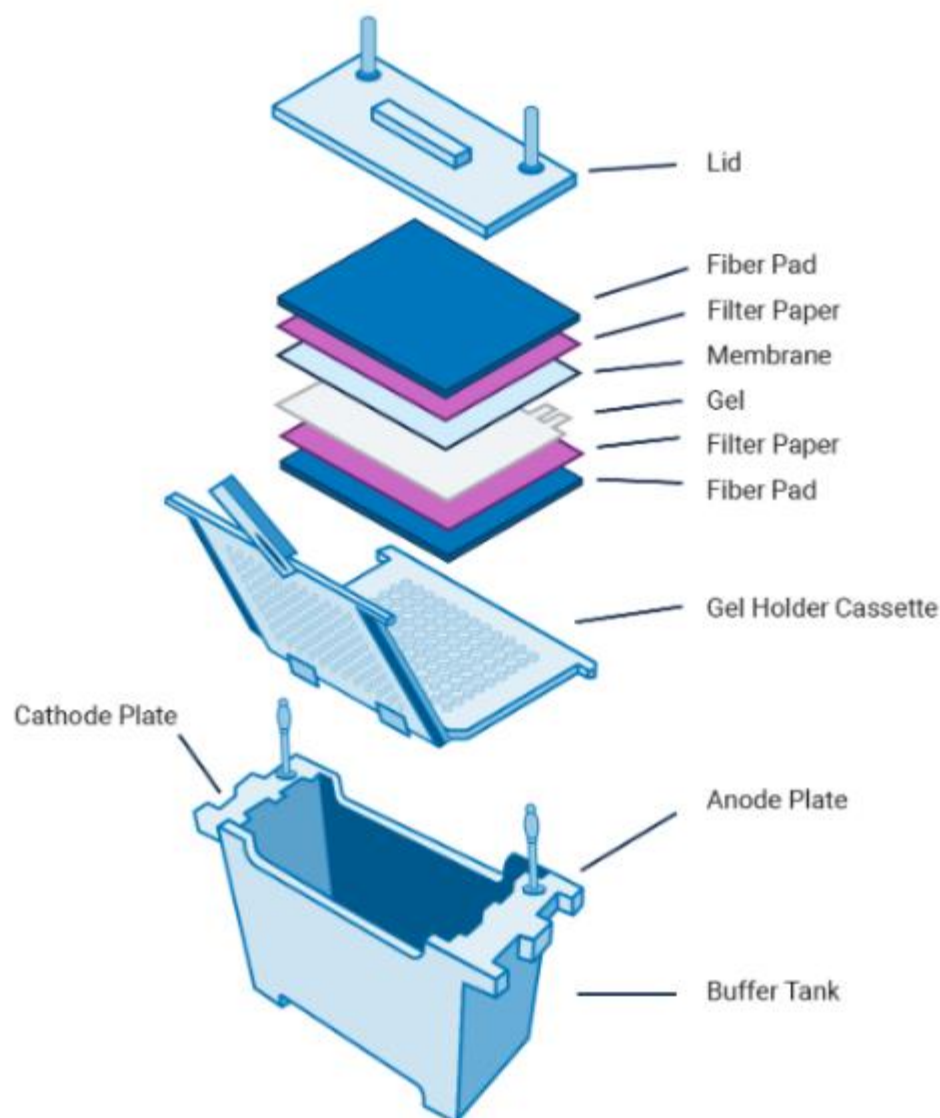


Figure 2.9. Assembly of the transfer cassette. Transfer sandwiches are made up of a gel holder cassette holding the membrane and gel held between filter paper and fibre pads within a gel holder cassette placed within the buffer tank (Licor, 2020).

2.12.4. Antibody probing

Protein bound membranes were blocked using Intercept PBS blocking buffer to prevent non-specific antibody binding to other lysate antigens in the membrane, reducing background levels. Blots were then probed with highly specific monoclonal or polyclonal antibodies (Table 2.13) against proteins of interest diluted in 1:1 PBS and Intercept PBS

blocking buffer at -4°C overnight. Following an overnight incubation, blots were washed in PBS+0.1% Tween, a detergent that acts as a surfactant blocking non-specific antibody binding and reducing background. Blots were probed with a housekeeping anti- α -Tubulin antibody (1:40,000) for 30 minutes at room temperature. Blots were then washed for 3x 10 minutes in PBS with 10% tween and probed with designated fluorescent secondary antibodies (Table 2.14), which bind to the fragment crystallisable (Fc) region of the corresponding primary antibody. The secondary antibodies were tagged with a fluorophore, which could be detected and quantified, of two excitation wavelengths (700nm or 800nm) to allow multiplex detection. An additional 3x wash steps were carried out to remove excess fluorescence prior to imaging.

Table 2.13. List of primary antibodies used for western blotting.

Primary Antibody	Molecular Weight (kDa)	Secondary Antibody	Dilution	Manufacturer
Tubulin		Goat anti-Mouse IgG 680	1:40,000	Thermo-fisher, Leicester, UK
Cx43	43	Goat anti-Rabbit IgG 800	1:1000	Abcam, Cambridge, UK
Cx26	26	Donkey anti-Goat IgG 800	1:1000	Abcam, Cambridge, UK
Panx1	48	Goat anti-Rabbit IgG 800	1:1000	Abcam, Cambridge, UK
NLRP3	118	Goat anti-Rabbit IgG 800	1:500	Abcam, Cambridge, UK
IL1 β	21	Goat anti-Rabbit IgG 800	1:500	Abcam, Cambridge, UK
IL18	22	Goat anti-Rabbit IgG 800	1:2000	Abcam, Cambridge, UK
IL6	21	Goat anti-Rabbit IgG 800	1:1000	Abcam, Cambridge, UK
Fibronectin	212	Goat anti-Rabbit IgG 800	1:2000	Santa Cruz Biotechnology, Texas, US
Collagen I	134	Goat anti-Rabbit IgG 800	1:1000	Abcam, Cambridge, UK
Collagen IV	300	Goat anti-Rabbit IgG 800	1:1000	Abcam, Cambridge, UK
E-Cadherin	135	Goat anti-Rabbit IgG 800	1:500	Abcam, Cambridge, UK
N-Cadherin	140	Goat anti-Rabbit IgG 800	1:1000	Abcam, Cambridge, UK
β -Catenin	92	Goat anti-Rabbit IgG 800	1:2000	Santa Cruz Biotechnology, Texas, US

Table 2.14. List of secondary antibodies used for western blotting.

Secondary Antibody	Dilution	Manufacturer
Goat anti-Mouse IgG 680	1:20,000	Licor Biosciences, Lincoln, US
Goat anti-Rabbit IgG 800	1:20,000	Licor Biosciences, Lincoln, US
Donkey anti-Goat IgG 800	1:20,000	Licor Biosciences, Lincoln, US

2.12.5. Visualisation and analysis

Blots were imaged using the Licor Odyssey Fc imager for detection of membrane bound antibodies. Results were analysed and quantified using Licor Image Studio software v5.2.5. Values were normalised against anti-tubulin and presented as percentage of protein expression in treated cells as compared to control.

2.13. Proteome profiler human cytokine array

Protein expression levels of 105 human cytokines and chemokines were detected using a human proteome profiler human XL cytokine array kit (R&D Systems, Minnesota, US) following the manufacturer's instructions (Figure 2.10). Cell supernatant was used to detect changes in cell secretion following treatment. Array membranes were firstly blocked for 1 hour at room temperature before cell supernatant samples were diluted in blocking buffer and incubated with the membranes overnight at 2-8°C. Membranes were then washed 3x in 20mL wash buffer for ten minutes at RT. A detection antibody cocktail was incubated with the membranes for one hour at RT followed by another 3x wash steps and a 30 minute incubation with streptavidin-HRP at RT. After a further 3x wash steps, excess buffer was removed, and membranes were incubated with a chemi-reagent mix for 1 minute. Excess chemi-reagent was removed, and blots exposed using the Licor Odyssey Fc imager for detection of membrane bound antibodies. Pixel density was analysed and quantified using Licor Image Studio software v5.2.5.

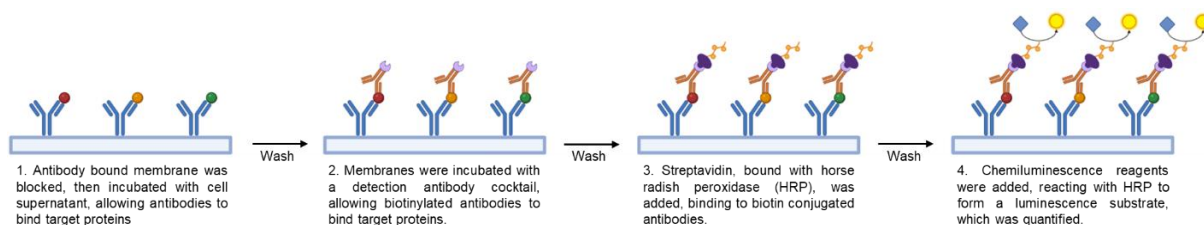


Figure 2.10. Proteome profiler human cytokine array protocol. A diagram illustrating the steps of the proteome profiler human cytokine array on a molecular level. Target proteins in cell supernatant bound to membrane bound antibodies, followed by biotin tagged antibodies. Protein concentration was quantified using streptavidin bound horseradish peroxidase which bound to biotin tagged antibodies and reacted with chemiluminescence to form a luminescent substrate in proportion to the amount of protein present.

2.14. ATP-lite luminescence assay

The ATP-lite luminescence assay system (Brucklacher-Waldert, 2017; Perkin Elmer, Waltham, US) measured extracellular ATP, in response to the luminescent signal generated as in response to ATP reacting with D-luciferin in the presence of luciferase. Cells were seeded in 96-well white-walled plates and pre-incubated with 300 μ M anti-ectonucleotidase ARL 67156 trisodium salt (R&D Systems, Minneapolis, US) in 100 μ L treatment media for 30 minutes before and during the treatment period to prevent rapid hydrolysis of ATP. After reagents were equilibrated to room temperature, 50 μ L of substrate reagent was added to each well and mixed using a plate shaker at 300-500rpm for 5 minutes. Plates were incubated in the dark at room temperature for 10 minutes and luminescence was detected using a SpectraMax iD3 plate reader (Molecular Devices, California, US).

2.15. Caspase Glo-1 inflammasome assay

Activation of the NLRP3 inflammasome leads to caspase 1-mediated cleavage of pro-inflammatory cytokines IL1 β and IL18, therefore caspase 1 activity was quantified using the Caspase Glo-1 Inflammasome assay as a measure of inflammasome activity (O'Brien *et al.*, 2017; Promega, Madison, US; Figure 2.11). Following treatment, reagents were equilibrated to room temperature and 50 μ L of the caspase 1 substrate inhibitor, Z-WEHD-

aminoluciferin (40 μ M) containing protease inhibitor MG-132 (120 μ M) was added to cells cultured in 96 well white-walled plates in a total volume of 50 μ L of media.

This reagent triggers cell lysis, caspase 1-mediated cleavage of the substrate and subsequent recombinant luciferase-based luminescence, the latter of which correlates directly to NLRP3 inflammasome activity. The plate contents were mixed using a plate shaker at 300-500rpm for 30 seconds before incubation in the dark at RT for one hour to allow the luminescent signal to stabilise. Luminescence was detected using a SpectraMax iD3 plate reader (Molecular Devices, California, US).

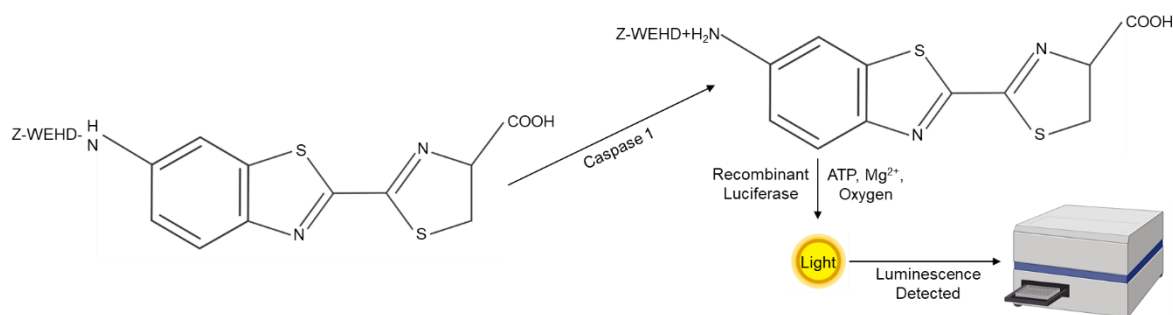


Figure 2.11. Caspase Glo-1 inflammasome assay substrate reaction. The substrate reaction in which caspase 1 from lysed cells mediates the cleavage of a Z-WEHD-aminoluciferin substrate leading to the formation of a luminescent recombinant luciferase. Luminescence is quantified using a SpectraMax iD3 plate reader and used as a measure of caspase 1 activity.

2.16. IL1 β enzyme linked immunosorbent assay

An enzyme linked immunosorbent assay (ELISA) is a commonly used immunoassay which utilises highly specific antibody-antigen reactions to detect the presence of target antigens in a sample. Whilst there are four types of ELISA, direct, indirect, sandwich and competitive, sandwich ELISAs are most used as they have increased sensitivity and specificity over other methods (Alhajj and Farhana, 2022). Sandwich ELISAs detect target proteins using two layers of antibodies, capture antibodies which are immobilised to the bottom of the well and detect antibodies which are added following the capture of the target, which bind to a different antigenic site to the capture antibody. Detection antibodies are conjugated to fluorophores or enzymes which produce colour changes allow the detection of the target antigen (Shah and Maghsoudlou, 2016).

Secretion of active human IL1 β from cells was assessed using a human IL1 β /IL1F2 quantikine enzyme linked immunosorbent assay (ELISA; R&D Systems, Minnesota, US), a sandwich ELISA which utilises a monoclonal antibody specific for active human IL1 β , following the manufacturer's instructions (Figure 2.12). Cell supernatant and human IL1 β standards were added to each well of the microplate strips and incubated for 2 hours at RT, allowing capture antibodies to bind IL1 β . Wells were washed x3 to remove excess supernatant. Polyclonal human IL1 β detection antibodies conjugated to horse radish peroxidase (HRP; 200 μ L) was added each well for 1 hour at room temperature to bind captured IL1 β . Each well was washed 3x and substrate solution composed of tetramethylbenzidine (TMB) and hydrogen peroxide and was added to each well for 20 minutes at RT in the dark, inducing a blue colour change as a result of the product formed from the HRP and TMB reaction. Sulphuric acid stop solution was added to each well to stop the reaction, inducing a colour change from blue to yellow, proportional to the amount of IL1 β in each sample. The optical density at 540nm with wavelength correction was measured using a SpectraMax iD3 plate reader (Molecular Devices, California, US). Standard values were used to create a line of best fit.

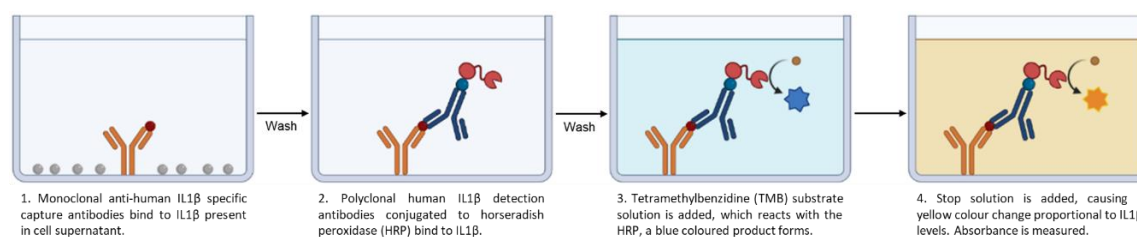


Figure 2.12. IL1 β enzyme linked immunosorbent assay protocol. A diagram illustrating the steps involved in the human solid phase IL1 β sandwich ELISA. Human IL1 β is captured between monoclonal IL1 β capture antibodies and polyclonal IL1 β antibodies with a horseradish peroxidase tag. The amount of IL1 β present is quantified using a TMB substrate and a stop solution inducing a yellow colour change proportional to IL1 β levels.

2.17. Transcriptomic analysis

Data from the Nephroseq (www.nephroseq.org, University of Michigan, Ann Arbor, MI, USA) database were extracted to examine changes in gene expression in healthy human kidneys compared to kidneys from people with DN or CKD. Expression data was obtained

from the 'Woroniecka Diabetes TubInt' (Woroniecka *et al.*, 2011) dataset in which a total of 12 healthy human donors and 10 diabetic nephropathy patients' micro-dissected human tubulointerstitium kidney samples were analysed using affymetrix human genome U133A 2.0 arrays. Database and expression levels were normalised using the GC robust multichip analysis (RMA) algorithm. Expression data was also obtained from the 'Schmid Diabetes TubInt (22)' (Schmid *et al.*, 2006) dataset in which 11 human renal tubulointerstitium biopsy samples were analysed also using an affymetrix human genome U133A microarray. Data was normalised against Cyclophilin A expression and RMA was performed using RMAexpress. This dataset was previously named Schmid Diabetes. Data also obtained using the affymetrix human genome U133A plus 2.0 array from tubulointerstitial biopsy samples from a cohort of 170 European renal cDNA Biobank (ERCB) CKD patients and 31 healthy donors in the 'Ju CKD TubInt (201)' was used (Ju *et al.*, 2015). Data was normalised using an RMA normalisation algorithm. Data from the 'Nakagawa CKD Kidney' dataset consisted of biopsies from 53 individuals with CKD and 8 healthy controls. Gene expression profiles were analysed using Agilent Whole Human Genome Microarrays (Nakagawa *et al.*, 2015).

2.18. Statistical analysis

Statistical analysis of data was performed using a one-way ANOVA with Tukey's multiple comparison post-test. Significance was determined using $P < 0.05$ and data is displayed as percentage mean \pm standard error of the mean (SEM). Each experiment was performed a minimum of three ($n=3$) times. Analysis and graphs were produced using GraphPad Prism 7.0. An unpaired t-test with Welch's correction analysis and simple linear regression were used for statistical analysis of transcriptomics data.

3.0. The role of pro-inflammatory cytokines and glucose in mediating tubular injury

3.1. Introduction

There are several risk factors, of which obesity and hypertension are key for the development and progression of CKD (Evangelista *et al.*, 2018; Tuttle *et al.*, 2019). Of note, several large-scale studies have demonstrated high circulating levels of pro-inflammatory cytokines, including IL1 β and TNF α in people with diabetes and kidney disease (Niewczas *et al.*, 2019; Fernández-Juárez *et al.*, 2017; Chen *et al.*, 2017; Allison, 2019). Contributed to by obesity (Khanna *et al.*, 2022) and glycaemic injury (Esposito *et al.*, 2002; Hoffman *et al.*, 2016), this results in chronic systemic inflammation. Whilst inflammation is an essential component of the body's immune response, protecting against pathogens and removing damaged tissue to facilitate tissue repair, dysregulated and sustained chronic inflammation can lead to fibrosis, loss of function, and organ failure (Furman *et al.*, 2019). Sterile, chronic inflammation is a major driver of disease across multiple conditions including atherosclerosis (Soehnlein and Libby, 2021), obesity and diabetes (Rohm *et al.*, 2022). In diabetic nephropathy, inflammation drives tubule injury through multiple mechanisms, including NLRP3 inflammasome activation as well as recruitment and activation of immune cells, primarily macrophages (Birnbaum *et al.*, 2020; Klessens *et al.*, 2017; Williams *et al.*, 2022; Rayego-Mateos *et al.*, 2020).

Adipose tissue is an endocrine organ that secretes cytokines, chemokines and adipokines to regulate energy homeostasis. When the storage capacity of white adipose tissue is exceeded, as a result of high calorie intake, lipids accumulate in non-adipose tissues including the skeletal muscle, liver, kidneys and pancreas, contributing to high local and systemic levels of pro-inflammatory signalling in both obesity (Pitere *et al.*, 2022) and T2DM (Hotamisligil *et al.*, 1993; Burhans *et al.*, 2018). This inflammation is partly contributed to by dysregulated heterotypic cell communication between adipocyte cells and activated M1 macrophages, events which augment the release of pro-inflammatory factors and exacerbate inflammation through increasing monocyte recruitment and inflammation within adipose tissue (Boutens *et al.*, 2018). Inter-organ crosstalk between adipose tissue and other organs is a key driver of systemic sterile inflammation (Huang and Xu, 2021; Jahng *et al.*, 2016; Ghigliotti *et al.*, 2014; Romacho *et al.*, 2014; Shirakawa

et al., 2017; Stern *et al.*, 2016). Commonly referred to as the adipo-renal axis, interactions between adipose tissue and the kidneys are essential in maintaining normal renal function. However, in the face of adipose hypertrophy, M1 macrophage accumulation, and insulin resistance, the balance between the adipo-renal axis is lost and kidney dysfunction occurs. (Ying *et al.*, 2017; Zhu *et al.*, 2018). Consequently, obesity related lipid accumulation occurs in all major cell types of the kidney, (De Vries *et al.*, 2014) where adipose-derived paracrine and endocrine signals including leptin, TNF α and angiotensin II impair kidney function via inflammation, fibrosis and oxidative stress (Zhu and Scherer, 2018). Together, increased local and systemic pro-inflammatory cytokine build up contributes to the inflammatory environment, which correlates with poor renal outcomes and mortality in people with diabetic nephropathy (Hofherr *et al.*, 2022).

The damaging effects of chronic inflammation in the kidney extend to induction of EMT, a key contributor to tubulointerstitial fibrosis (Stone *et al.*, 2016) and the underlying pathology of diabetic nephropathy. Myofibroblasts (activated fibroblasts) within the kidney are responsible for producing large amounts of ECM proteins, which promote fibrosis. The myofibroblast population is contributed to by activation and proliferation of resident and infiltrating fibroblasts and pericytes in addition to the transition of tubular epithelial and endothelial cells to a mesenchymal phenotype, through endothelial-mesenchymal transition (EndoMT) and EMT (Sun *et al.*, 2016). First identified in CKD (Nadasdy *et al.*, 1994), sustained epithelial cell injury activates cells and initiates a phenotypic conversion in which cells display characteristics of ECM producing myofibroblasts. Events linked to EMT include disassembly of the adherens junction, loss of polarity, cytoskeletal reorganisation and altered cell morphology. These changes are associated with a downregulation of epithelial proteins such as E-cadherin and zonula occludens-1 (ZO-1) paralleled by an upregulation of mesenchymal markers including α SMA, vimentin and FSP1 (Alyaseer *et al.*, 2020).

A major component of the adherens junction, E-cadherin mediates ligation to partner proteins on neighbouring cells and binds β -catenin to link to the actin cytoskeleton (Tian *et al.*, 2011). Loss of E-cadherin-mediated cell tethering, linked to the early stages of EMT (Hills *et al.*, 2012), is commonly associated with a compensatory increase in expression of N-cadherin. This is termed the 'cadherin switch' (Wheelock *et al.*, 2008; Loh *et al.*, 2019), resulting in a loss of adherence between epithelial cells and the favouring of a more mesenchymal cell phenotype (Kim *et al.*, 2017). Although the underlying molecular

mechanisms behind the cadherin switch are largely unknown, multiple studies have demonstrated a link between increased N-cadherin expression and enhanced invasive traits (Mrozik *et al.*, 2018; László *et al.*, 2020); ultimately driving cell migration into the interstitial space where they actively contribute to ECM accumulation and fibrosis (Loh *et al.*, 2019).

Whilst the role of full EMT in contributing to diabetic nephropathy is controversial, with research showing anywhere between 5% and 36% of the myofibroblast pool contributed to by EMT (Lebleu *et al.*, 2013, Iwano *et al.*, 2002), many studies demonstrate a large population of partially differentiated renal tubular epithelial cells that co-express epithelial and mesenchymal markers, known as pEMT. In the kidney, epithelial cells undergoing pEMT exhibit cell-cycle arrest, altered metabolism, inflammation, altered cell communication and fibrosis (Sheng and Zhuang, 2020). Research by Lovisa *et al.* (2015) showed that pEMT inhibition through Twist Family BHLH Transcription Factor 1 (Twist1) and zinc finger transcriptional repressor (Snail) deletion maintained tubule epithelial cell integrity whilst reducing immune cell infiltration and tubulointerstitial fibrosis in mice subjected to UUO, nephrotoxic serum-induced nephritis (NTN) or folic acid-induced nephropathy. (Lovisa *et al.*, 2015). Additionally, inhibition of pEMT promoted tissue repair and improved kidney function in these models of kidney disease (Lovisa *et al.*, 2015).

Renal proximal tubule epithelial cells are highly metabolically active, with high energy demand met through fatty acid oxidation (FAO)-mediated ATP production. This process is altered during injury, with reduced expression of FAO regulators and increased extracellular lipid deposition in both mouse and human models, resulting in immune cell infiltration, cytokine secretion and fibrosis (Kang *et al.*, 2015). Lipid accumulation promoted morphological changes and a cytoskeletal switch, involving loss of E-cadherin and a compensatory upregulation of N-cadherin in RPTECs following glucose stimulation (Kang *et al.*, 2015). Studies examining the link between inflammation and EMT show that in addition to a causal role for inflammation in the development of EMT, inhibition of EMT in the fibrotic kidney reduced immune cell infiltration (Lovisa *et al.*, 2015) and cytokine and chemokine release (Grande *et al.*, 2015), suggesting that the two processes feed into each other to exacerbate disease.

In addition to disassembly of the adherens junction, ECM secretion from both tubule cells and activated fibroblasts is a hallmark of tubular injury (Qi and Yang, 2018; Lam *et al.*, 2004). Consisting predominantly of collagens, fibronectin, laminin and fibrinogen, the ECM

provides physical support and regulates cell behaviour including adhesion and communication (Zhang *et al.*, 2021c). Although usually associated with wound healing, a loss of regulation leads to increased ECM deposition, scar formation and ultimately a decline in function (Frantz, Stewart, & Weaver, 2010). Diabetic nephropathy is characterised by glomerular basement membrane thickening and increased pro-inflammatory and pro-fibrotic factors, including TGF β 1 which drives ECM accumulation and kidney fibrosis, the final common pathology of diabetic nephropathy (Zhao, Zou and Liu, 2020; Sharma *et al.*, 1996). Whilst there are no specific therapies which target fibrosis within the kidney, evidence of the interplay between inflammation, EMT and fibrosis, events compounded by systemic inflammation in diabetes, suggests that targeting upstream of chronic inflammation represents a hopeful therapeutic option in combatting all three associated pathologies.

3.2. Aims

This chapter utilises an *in vitro* model of kidney disease to investigate the hypothesis that inflammatory cytokines IL1 β , IL18 and TNF α in the presence of high glucose induce proximal tubule epithelial cell injury through increased inflammation, partial epithelial-mesenchymal transition and fibrosis.

The aims are to-

- Establish the optimal concentration of inflammatory cytokines IL1 β , IL18 and TNF α to appropriately model proximal tubule injury without compromising epithelial cell viability.
- Investigate the effects of 5mmol/L (basal) or 25mmol/L (high) glucose +/- IL1 β , IL18 and TNF α individually and in combination on cell morphology and expression of inflammatory, EMT and fibrotic markers in proximal tubule epithelial cells.
- Examine the effects of IL1 β and TNF α in the presence of glucose on the release of a host pro-inflammatory cytokines in primary proximal tubule epithelial cells.
- Elucidate how IL1 β and TNF α in the presence of glucose affect the release of inflammatory markers associated with CKD in primary proximal tubule epithelial cells.

3.3. Results

3.3.1. Evaluating the effect of pro-inflammatory cytokines IL1 β , IL18 and TNF α on human proximal tubule cell viability under conditions of basal and high glucose.

The effects of pro-inflammatory cytokines IL1 β , IL18 and TNF α on HK-2 cell morphology and cell viability was assessed using crystal violet staining (Figure 3.1a) as a measure of cell number and an MTT assay (Figure 3.1b) to indicate changes in metabolic (succinate dehydrogenase) activity. Cells were treated with either IL1 β , IL18 or TNF α over a range of concentrations (2-50ng/mL) in 5mmol/L (basal) glucose for 48 hours. Under 5mmol/L glucose conditions, there was no significant change in cell viability when cells were treated with IL1 β , IL18 or TNF α at 2-50ng/mL, as evidenced by the lack of cytotoxic effect observed in the crystal violet (Figure 3.1a) and MTT assays (Figure 3.1b). Similarly, cells treated with IL1 β , IL18 or TNF α (2-50ng/mL) and 25mmol/L glucose for 48 hours, to assess the impact of cytokines in the presence of high glucose, failed to identify any significant impact on HK-2 cell viability when using crystal violet (Figure 3.2a) and MTT assays (Figure 3.2b).

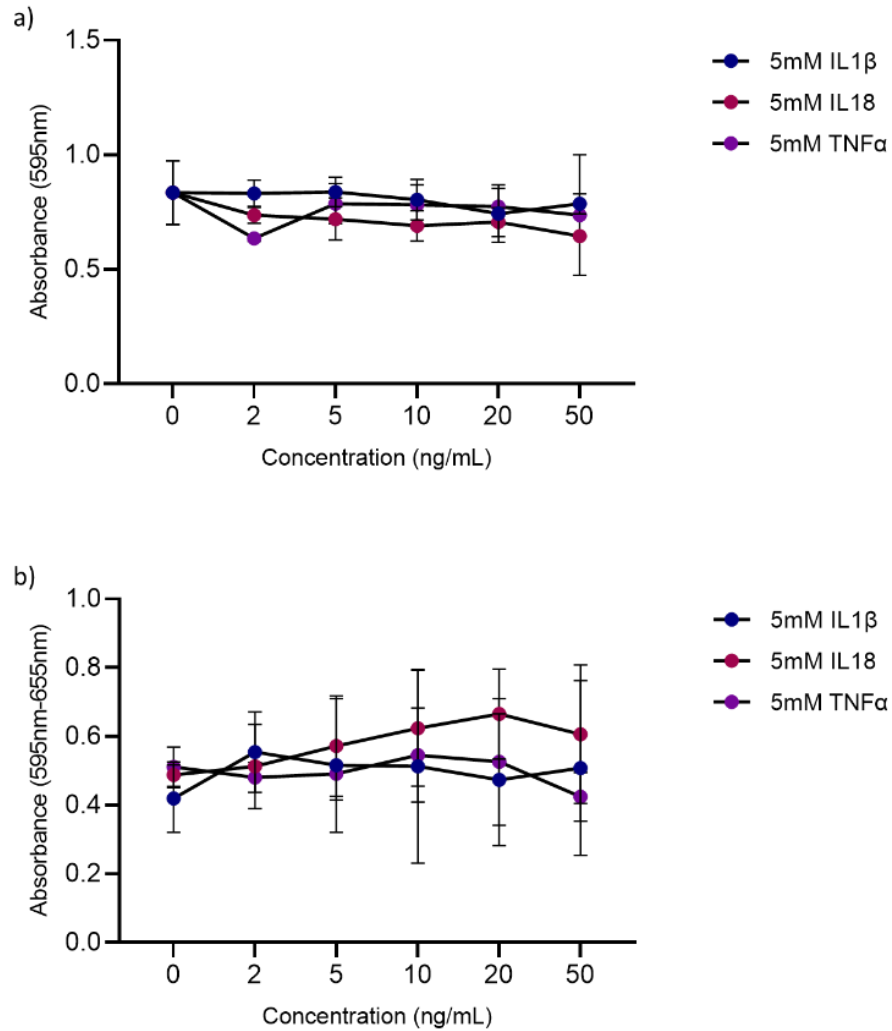


Figure 3.1. The effect of pro-inflammatory cytokines on proximal tubule cell viability in 5mmol/L glucose conditions. HK-2 cells were treated in 5mmol/L (basal) glucose +/- IL1 β (2-50ng/mL), IL18 (2-50ng/mL) or TNF α (2-50ng/mL) for 48 hours. The effect on cell viability was assessed using crystal violet staining (a) and an MTT assay (b). n=3.

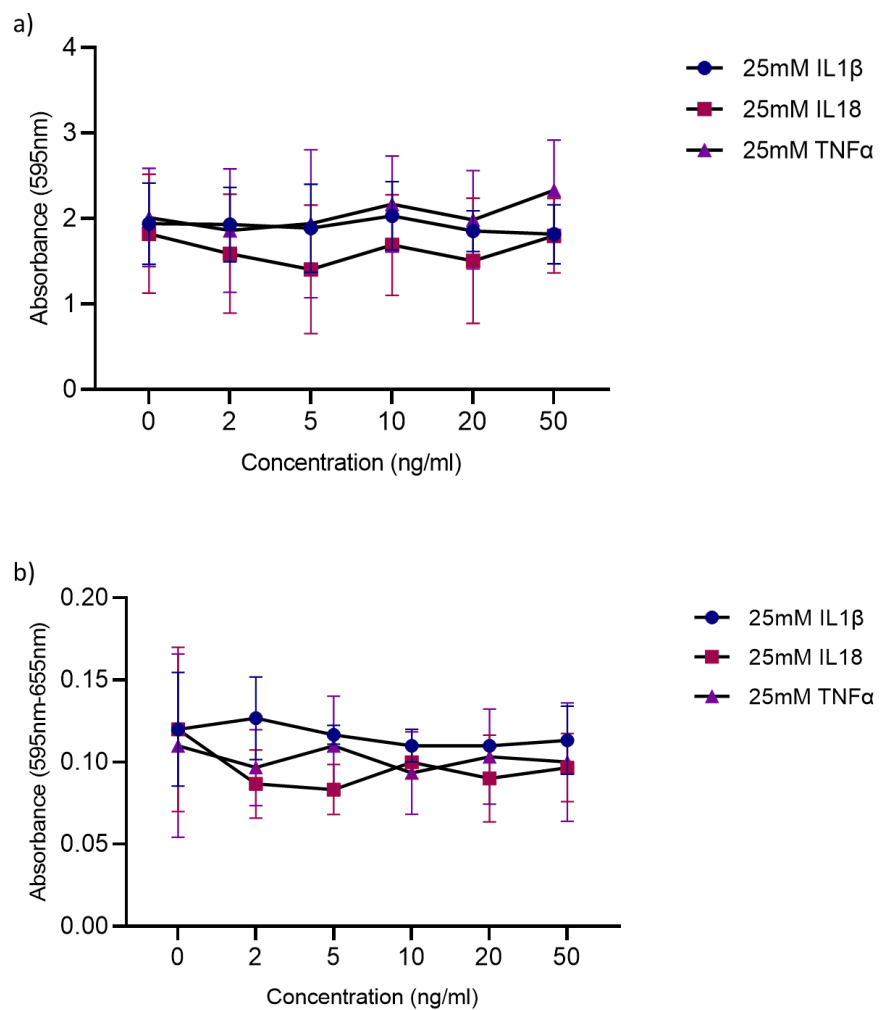


Figure 3.2. The effect of pro-inflammatory cytokines and 25mmol/L glucose on proximal tubule cell viability. HK-2 cells were treated in 25mmol/L (high) glucose +/- IL1 β (2-50ng/mL), IL18 (2-50ng/mL) or TNF α (2-50ng/mL) for 48 hours. The effect on cell viability was assessed using crystal violet staining (a) and an MTT assay (b). n=3.

3.3.2. Inflammatory factors associated with the NLRP3 inflammasome are upregulated following pro-inflammatory cytokine and glucose challenge in tubule epithelial cells.

Following confirmation that inflammatory cytokines, IL1 β , IL18 and TNF α (2-50ng/mL) are not cytotoxic in 5mmol/L or 25mmol/L glucose conditions, an optimised concentration of 10ng/mL was selected for further experiments. This concentration was selected in order to accurately model the inflammatory conditions observed in diabetic nephropathy (Chen *et al.*, 2017; Koleva-Georgieva *et al.*, 2011; Perlman *et al.*, 2015), and its use is well established in several other models of injury (Mugisho *et al.*, 2018a; Mugisho *et al.*, 2018b). Moving forward, HK-2 cells were treated with IL1 β , IL18 and/or TNF α (10ng/mL each) with 5 or 25mmol/L glucose, to determine the cumulative effects of these cytokines on downstream parameters.

Inflammatory cytokines are major initiators of downstream chronic inflammation (Awad *et al.*, 2015), with activation of the NLRP3 inflammasome underlying sterile inflammation in a wide range of diseases, including Alzheimer's (Milner *et al.*, 2021), arthritis (Unterberger *et al.*, 2021) and diabetic kidney disease (Foresto-Neto *et al.*, 2018). To determine the impact of pro-inflammatory cytokines in the presence of glucose on inflammation, expression of the NLRP3 inflammasome and downstream mediators (IL6 and IL18) were assessed.

Whilst inflammatory cytokines at 5mmol/L glucose, failed to significantly change NLRP3 expression (Figure 3.3a), a significant increase was observed at 25mmol/L glucose when cells were stimulated with IL18 (162 \pm 17%, P <0.05) or a combination of both IL18 and IL1 β (193 \pm 10%, P <0.001), as compared to 25mmol/L glucose alone (Figure 3.3b). Interestingly, IL1 β and TNF α significantly reduced NLRP3 expression (38 \pm 19%, P <0.05) in 25mmol/L glucose conditions.

Contrary to the lack of effect on NLRP3 expression at 5mmol/L glucose, a significant increase in expression of the inflammatory mediator IL6, was observed in cells treated with IL18+TNF α (277 \pm 70%, P <0.05) as compared to 5mmol/L control. The effect of IL18 was significantly augmented when co-applied with TNF α (176 \pm 70%, P <0.05), a response that appeared amplified in the presence of 25mmol/L glucose where IL1 β +TNF α significantly increased IL6 expression (491 \pm 164%, P <0.01) as compared to 25mmol/L glucose. These results suggest that high glucose potentiates the effect of these

inflammatory cytokines on IL6 expression (Figure 3.3d). Lastly, whilst no change in IL18 expression was observed at 5mmol/L glucose in the presence of inflammatory cytokines (Figure 3.3e), IL1 β +IL18 at 25mmol/L glucose significantly increased expression as compared to 25mmol/L glucose control, a response which was cumulative when compared to the application of either IL1 β or IL18 alone (Figure 3.3f).

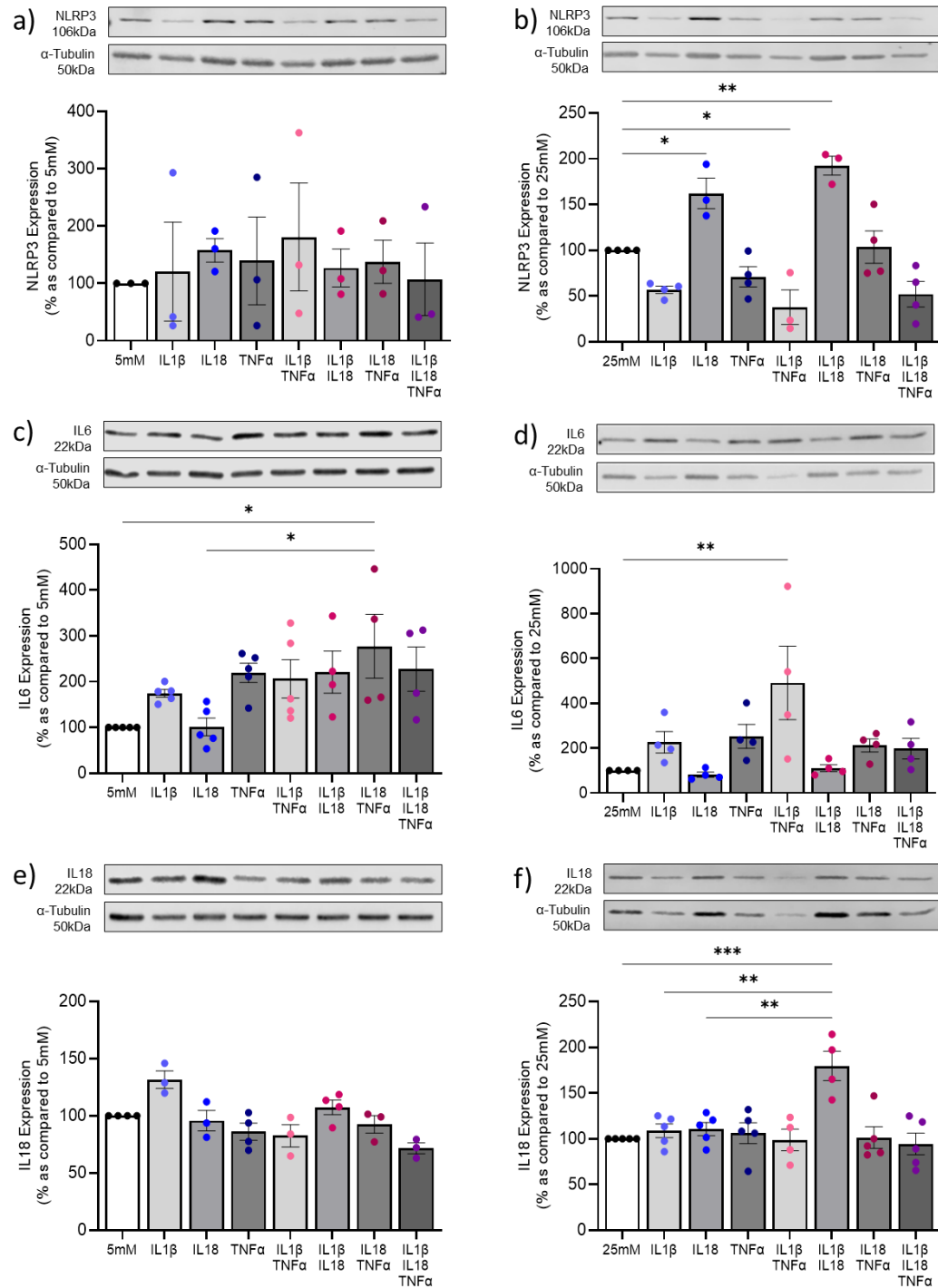


Figure 3.3. Inflammatory cytokines and glucose increase expression of inflammatory markers in proximal tubule epithelial cells. HK-2 cells were treated with 5mmol/L (basal) or 25mmol/L (high) glucose +/- IL1 β (10ng/mL) +/- IL18 (10ng/mL) +/- TNF α (10ng/mL) for 48 hours. Western blotting determined changes in protein expression of NLRP3, IL6 and IL18 in 5mmol/L glucose media (a, c and e respectively) and 25mmol/L glucose media (b, d and f respectively). Results were normalised against expression of housekeeping protein, α -Tubulin as a loading control. n=3-5. Significance is displayed as * P <0.05, ** P <0.01, *** P <0.001.

3.3.3. Pro-inflammatory cytokines and glucose mediate altered cell morphology and phenotype in proximal tubule epithelial cells.

Sustained inflammation has been shown to drive proximal tubule cell injury, contributing to a loss of cell integrity, disassembly of the adherens junctions and an altered phenotype, known as partial EMT (Masola *et al.*, 2019). Phase contrast morphology (Figure 3.4) showed that cells treated in 5mmol/L glucose had a rounded 'cobblestone' morphology, typical of tubular epithelial cells. When treated with 25mmol/L glucose combined with TNF α , IL1 β +TNF α or IL1 β +IL18+TNF α , cells take on a more elongated, spindle shape associated with a more mesenchymal/fibroblast like phenotype. When treated with 25mmol/L glucose +/- IL1 β and/or IL18 there was little to no noticeable change in cell morphology.

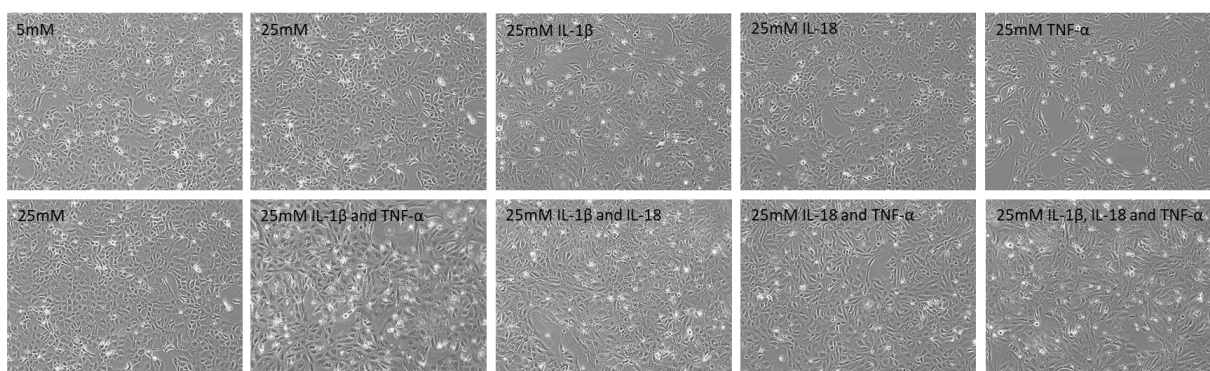


Figure 3.4. The combined effect of pro-inflammatory cytokines and 25mmol/L glucose on proximal tubule epithelial cell morphology. HK-2 cells were treated with 5mmol/L (basal) or 25mmol/L (high) glucose +/- IL1 β (10ng/mL), +/- IL18 (10ng/mL) +/- TNF α (10ng/mL) for 48 hours. Changes in cell morphology were assessed using phase contrast microscopy (magnification x20).

Characterised by phenotypic changes associated with the loss of an epithelial phenotype and acquisition of fibroblast like characteristics, pEMT is associated with the breakdown of adherens junctions, identifiable through the cadherin switch (Masola *et al.*, 2019; Hills *et al.*, 2012) and subsequent translocation of β -catenin to the nucleus (Anthony *et al.*, 2020). The impact of inflammatory cytokines on adherens junction protein expression was assessed by evaluating changes in expression of E-cadherin, N-cadherin and β -catenin. HK-2 cells were treated with IL1 β , IL18 and/or TNF α for 48 hours in 5mmol/L and 25mmol/L glucose media.

At 5mmol/L glucose, E-cadherin expression decreased in response to incubation with all inflammatory cytokines alone and in combination, with the exception of IL18, which significantly increased expression to $193 \pm 14\%$, $P < 0.05$ as compared to control (Figure 3.5a) and TNF α . At 25mmol/L glucose there was a significant reduction in E-cadherin expression in cells treated with IL1 β ($47 \pm 10\%$, $P < 0.001$), TNF α ($44 \pm 5.7\%$, $P < 0.001$), IL1 β +TNF α ($25 \pm 8.1\%$, $P < 0.001$), IL1 β +IL18 ($41 \pm 12\%$, $P < 0.001$), TNF α +IL18 ($44 \pm 5.7\%$, $P < 0.001$) and a combination of all three ($14 \pm 1.7\%$, $P < 0.001$) as compared to 25mmol/L glucose control (Figure 3.5b).

HK-2 cells compensate for a loss of E-cadherin by upregulating expression of N-cadherin. N-cadherin expression significantly increased when cells were treated with 5mmol/L glucose + IL1 β ($213 \pm 24\%$, $P < 0.05$), IL1 β +TNF α ($291 \pm 42\%$, $P < 0.001$) and a combination of all three cytokines ($258 \pm 41\%$, $P < 0.05$) as compared to 5mmol/L glucose control (Figure 3.5c). An amplified response was observed at 25mmol/L glucose, when cells were treated with TNF α ($336 \pm 39\%$, $P < 0.001$), IL1 β +TNF α ($409 \pm 57\%$, $P < 0.001$) and IL18+TNF α ($263 \pm 22\%$, $P < 0.05$) as compared to control (Figure 3.5d). Whilst no significant change in β -Catenin was observed at 5mmol/L glucose (Figure 3.5e), TNF α increased expression ($207 \pm 24\%$, $P < 0.05$) in 25mmol/L glucose as compared to control (Figure 3.5f).

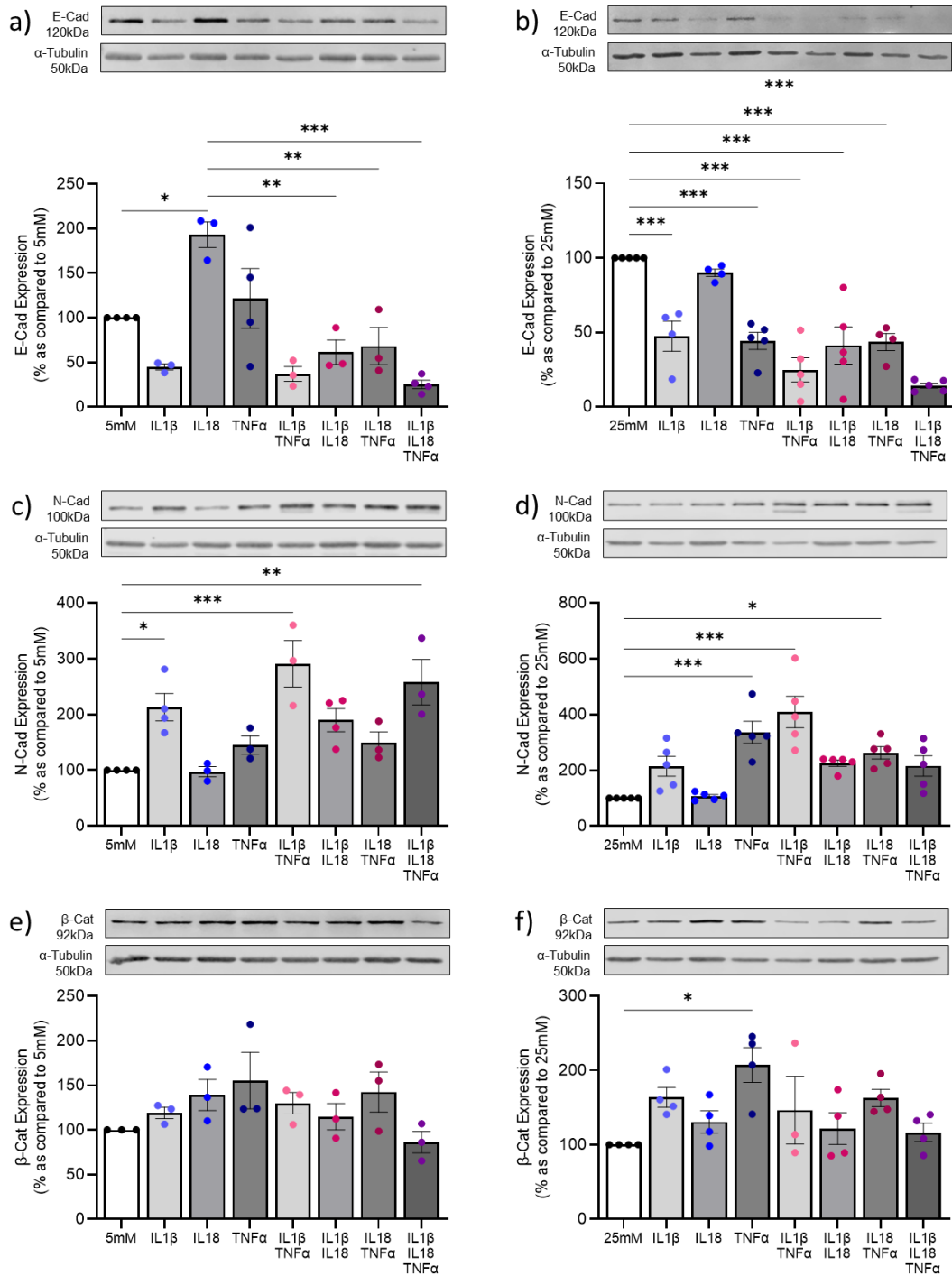


Figure 3.5. Pro-inflammatory cytokines and high glucose alter expression of epithelial adherens junction proteins. HK-2 cells were treated with 5mmol/L (basal) or 25mmol/L (high) glucose +/- IL1β (10ng/mL), +/- IL18 (10ng/mL) +/- TNFα (10ng/mL) for 48 hours. Western blotting determined changes in protein expression of E-Cadherin, N-Cadherin and β-Catenin in 5mmol/L glucose media (a, c and e respectively) and 25mmol/L glucose media (b, d and f respectively). Results were normalised against expression of housekeeping protein, α-Tubulin as a loading control. n=3-5. Significance is displayed as * $P<0.05$, ** $P<0.01$, *** $P<0.001$.

3.3.4. Expression of extracellular matrix and fibrosis associated proteins is increased in pro-inflammatory cytokine and glucose treated proximal tubule cells.

In response to sustained injury and inflammation, excessive deposition of extracellular matrix from both proximal tubule cells and activated fibroblasts leads to scarring and loss of kidney function (Chen *et al.*, 2018; Sharma *et al.*, 2019). To determine how elevated levels of inflammatory cytokines may exacerbate fibrosis *in vitro*, western blotting was used to assess changes in expression of ECM proteins, fibronectin, collagen I and collagen IV in HK-2 cells when treated with IL1 β , IL18 and TNF α (10ng/mL) individually and in combination for 48 hours at both 5mmol/L and 25mmol/L glucose media.

Fibronectin, a marker of fibrosis, was significantly upregulated in cells treated at 5mmol/L glucose with IL1 β (370 \pm 54%, P <0.05) and IL1 β +TNF α (365 \pm 81%, P <0.05) as compared to 5mmol/L control (Figure 3.6a). At 25mmol/L glucose, a significant increase in expression (580 \pm 119%, P <0.05) was observed when cells were treated with IL18+TNF α as compared to 25mmol/L glucose alone (Figure 3.6b). Contrary to the effects of the cytokines on fibronectin, collagen I expression significantly increased in response to all treatments except IL18, IL1 β (440 \pm 33%, P <0.001), TNF α (348 \pm 33%, P <0.01), IL1 β +TNF α (516 \pm 36%, P <0.001), IL1 β +IL18 (392 \pm 63%, P <0.01), IL18+TNF α (314 \pm 67%, P <0.05) and a combination of all three (368 \pm 50%, P <0.01) as compared to control under 5mmol/L glucose conditions (Fig.6c). This response was amplified at 25mmol/L glucose, where collagen I expression significantly increased to 365 \pm 60%, (P <0.05) and 725 \pm 85%, (P <0.001) in TNF α and IL1 β +TNF α treated cells respectively as compared to control. Whilst neither TNF- α or IL1 β alone evoked a change in collagen I expression, co-incubation of IL1 β and TNF- α significantly increased collagen I expression by 416 \pm 36% (P <0.001) as compared to IL1 β alone, highlighting the additive, cumulative effect of these cytokines when added in combination.

Similarly, IL1 β +TNF α increased expression of collagen IV to 830 \pm 217%, (P <0.01) at 5mmol/L glucose as compared to control (Figure 3.6e), whilst treatment with IL1 β +TNF α (868 \pm 77%, P <0.001), IL1 β +IL18 (488 \pm 106%, P <0.01) and a combination of all three (709 \pm 88%, P <0.001) significantly increased expression as compared to 25mmol/L glucose in the absence of cytokine stimulation (Figure 3.6f). As observed with collagen I, expression of collagen IV was significantly higher in cells treated with IL1 β +TNF α

compared to cells treated with either IL1 β or TNF α alone, further supporting an additive effect of combining these two cytokines on the expression of ECM proteins.

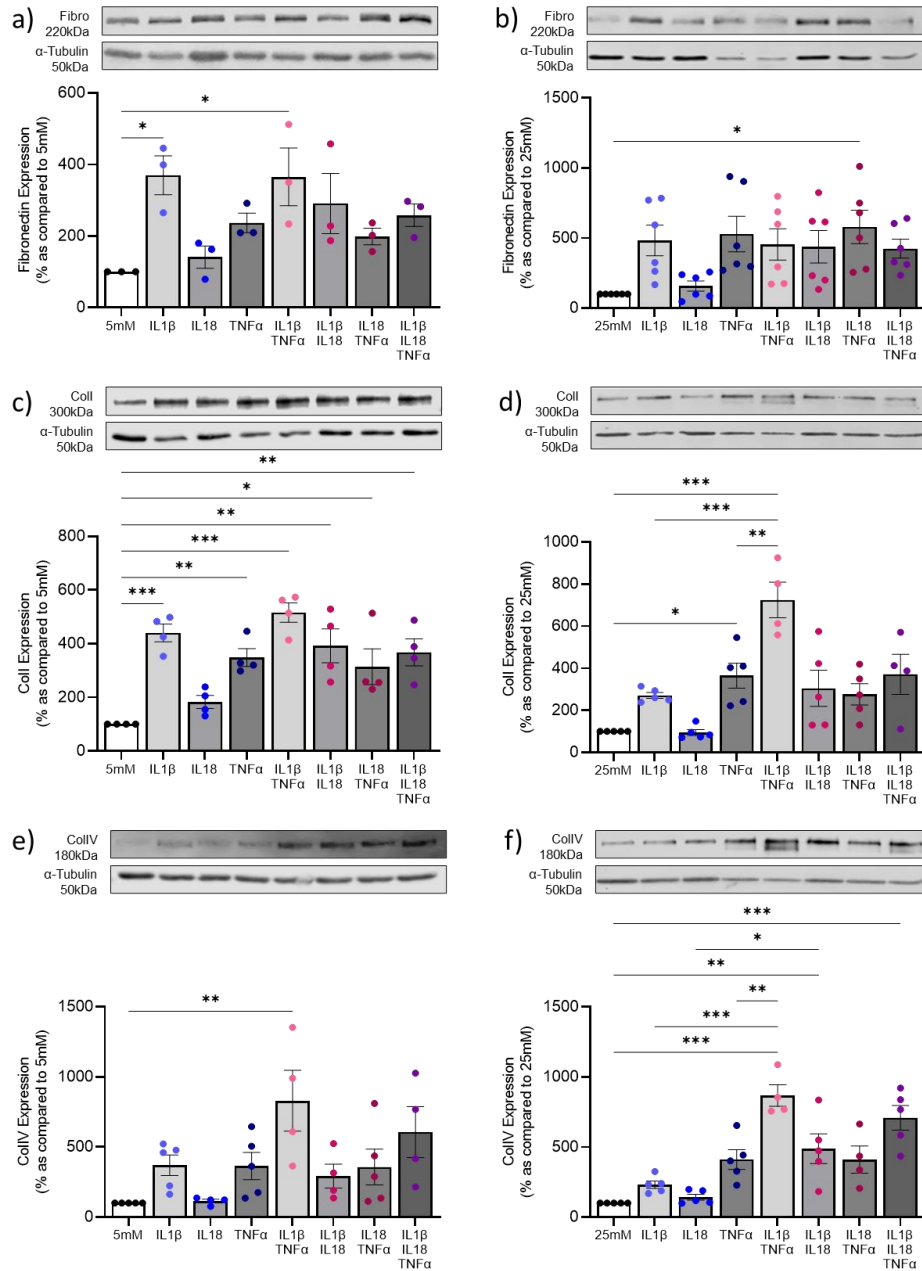


Figure 3.6. Expression of fibrosis and extracellular matrix markers was increased in proximal tubule cells following treatment with pro-inflammatory cytokines and glucose. HK-2 cells were treated with 5mmol/L (basal) or 25mmol/L (high) glucose +/- IL1 β (10ng/mL), +/- IL18 (10ng/mL) +/- TNF α (10ng/mL) for 48 hours. Western blotting determined changes in protein expression of fibronectin, Collagen-I and Collagen-IV in 5mmol/L glucose media (a, c and e respectively) and 25mmol/L glucose media (b, d and f respectively). Results were normalised against expression of housekeeping protein, α -Tubulin as a loading control. n=3-6. Significance is displayed as * P <0.05, ** P <0.01, *** P <0.001.

3.3.5. Inflammatory cytokines and glucose stimulate upregulated release of multiple pro-inflammatory cytokines and chemokines associated with diabetic nephropathy.

Having determined the effects of inflammatory markers IL1 β , IL18 and TNF α on proximal tubule cells at both basal and high glucose, outcomes of these experiments informed and allowed for streamlining of the cytokines and combinations to be used for future experiments. Moving forward cells were treated with IL1 β , TNF α and 25mmol/L glucose for 48hours (unless otherwise specified) in the presence of a 5mmol/L glucose control. Cytokines IL1 β and TNF α were applied in combination at 25mmol/L glucose on the basis that both exhibit elevated circulating levels in diabetes and induced a significant and additive response when co-applied in our *in vitro* model of diabetic kidney disease.

Many cytokines and chemokines are rapidly secreted from the cell into the extracellular space, where they act as signalling molecules activating cell surface receptors on neighbouring cells. When this occurs, changes in whole cell expression should be corroborated and investigated further by assessment of changes in secretion. A proteome profiler human XL cytokine array kit was used to determine the relative concentrations of 105 inflammatory cytokines/chemokines in the supernatant of pro-inflammatory cytokine and glucose treated primary human renal proximal tubule epithelial cells (RPTECs; Figure 3.7a). Building on data from our immortalised model, human primary proximal tubule cells isolated from the normal portion of a renal carcinoma were treated with 5mmol/L glucose, 25mmol/L glucose and IL1 β +TNF α at 25mmol/L glucose for 48 hours, prior to the removal of the cell supernatant which was stored at -80°C ahead of performing cytokine array analysis.

In summary and represented by heatmap analysis (Figure 3.7b), there was a significant increase in 72 of the 105 cytokines measured when cells were stimulated with IL1 β , TNF α and 25mmol/L glucose as compared to the 5mmol/L glucose control. A product of NLRP3 inflammasome activation, IL1 β secretion significantly increased (2869 \pm 300%, P <0.001) in IL1 β , TNF α and 25mmol/L glucose treated cells as compared to 5mmol/L glucose control (Figure 3.8a), whilst further evidence of potential inflammasome activation was supported by elevated expression of downstream mediator IL6 (236 \pm 23%, P <0.001) as compared to control (Figure 3.8b).

Dipeptidyl peptidase IV (DPPIV), functions of which include immune regulation and glucose homeostasis, plays a role in the progression of T2DM and inflammatory conditions. Here we show an IL1 β , TNF α and 25mmol/L glucose dependant increase in DPPIV (700 \pm 94%, P <0.001) as compared to 5mmol/L glucose control (Figure 3.8c). Furthermore, a member of the TGF β 1 superfamily and strongly associated with inflammation and cellular injury, growth differentiation factor 15 (GDF-15) is increased (221 \pm 21%, P <0.01) in the supernatant of RPTECs treated with IL1 β , TNF α and 25mmol/L glucose (Figure 3.8d). Together these findings suggest increased inflammation following high glucose and cytokine treatment as compared to 5mmol/L glucose controls.

In addition to increased release of pro-inflammatory mediators, data demonstrate an increase in cytokines and chemokines associated with monocyte recruitment and macrophage activation following cytokine stimulation, both an effect and a perpetuator of inflammation, including GM-CSF (1028 \pm 127%, P <0.001; Figure 3.8e), IFN γ (227 \pm 20%, P <0.01; Figure 3.8f), macrophage inflammatory protein 1-alpha/ 1-beta (MIP-1 α /1 β ; 397 \pm 55%, P <0.01; Figure 3.8g), receptor for advanced glycation end-products (RAGE; 317 \pm 58%, P <0.01; Figure 3.8h) and regulated on activation, normal T-expressed and secreted (RANTES; 1627 \pm 415%, P <0.01; Figure 3.8i). A further consequence of IL1 β , TNF α and 25mmol/L glucose stimulation is the significant increase in cytokines and chemokines associated with EMT and fibrosis, including chitinase-3-like 1 (374 \pm 44%, P <0.01; Figure 3.8j), emmprin (262 \pm 28%, P <0.01; Figure 3.8k), and urokinase plasminogen activator surface receptor (uPAR; 312 \pm 21%, P <0.001; Figure 3.8l) which are involved in ECM deposition and cellular remodelling, associated with pEMT.

Proteins not associated with a significant change include adiponectin, angiopoietin-1, CD30, CD40 ligand, complement factor D, crypto-1, cystatin C, Dkk-1, EGF, endoglin, fas ligand, FGF-7, FGF-19, Flt-3 ligand, GRO α , HGF, IL-3, IL-12 p70, IL-17A, IL-18 Bpa, IL-23, IP-10, MCP-1, MIP-3a, myeloperoxidase, osteopontin, PDGF-AB/BB, RPB-4, Serpin-E1, ST2, TGF- α , thrombospondin-1 and TIM-3 (Figure 3.7b).

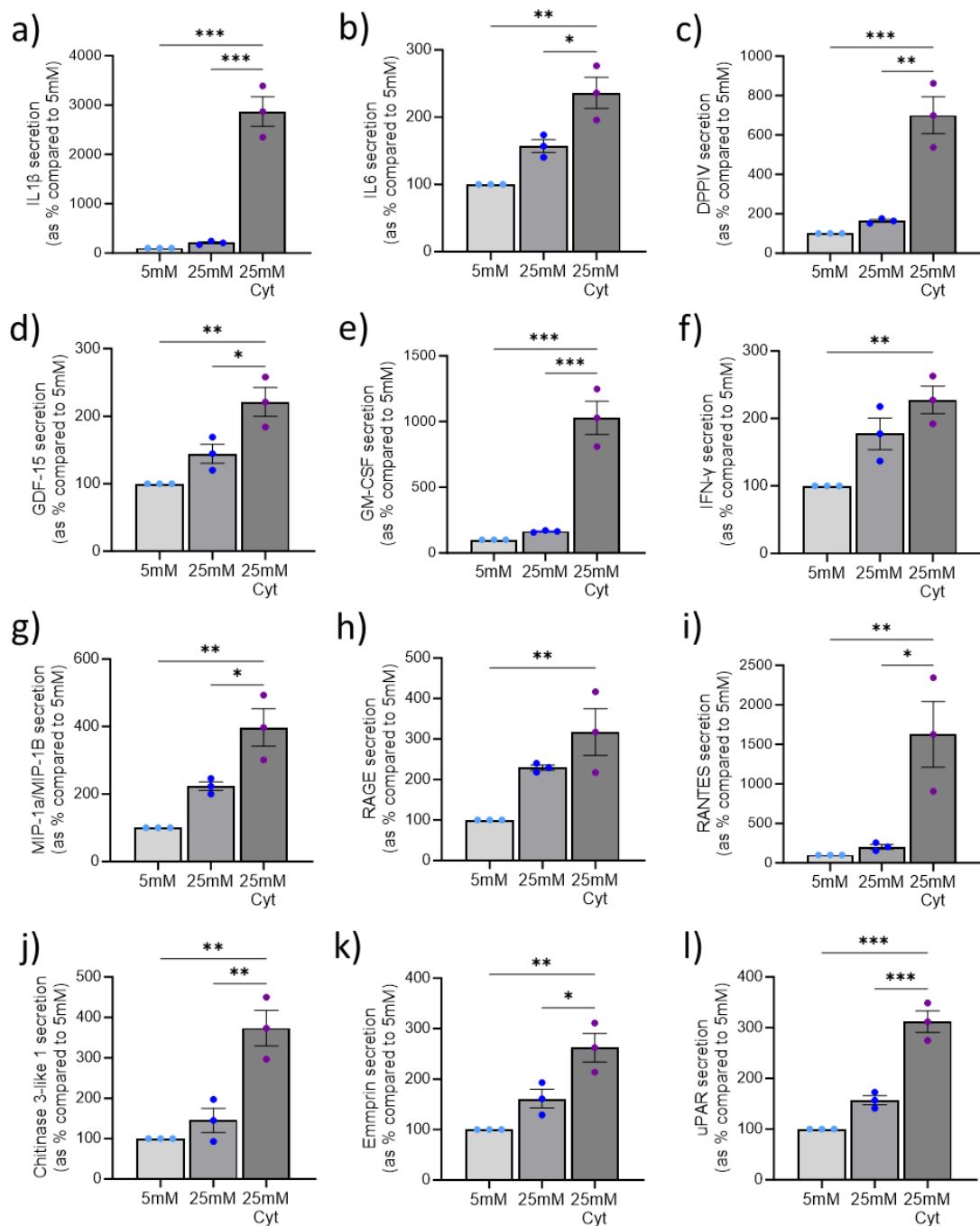


Figure 3.8. Pro-inflammatory cytokines and chemokines secretion is increased in primary proximal tubule epithelial cells after treatment with IL1 β , TNF α and 25mmol/L glucose. Human primary renal proximal tubule epithelial cells were treated with 5mmol/L (basal) glucose or 25mmol/L (high) glucose +/- IL1 β (10ng) and TNF α (10ng) for 48 hours. Secretion of 105 human cytokines and chemokines were detected in cell supernatant using a human proteome profiler human XL cytokine array kit. n=3. Significant increases were detected in secretion of several cytokines and chemokines including IL1 β (a), IL6 (b), DPPIV (c), GDF-15 (d), GM-CSF (e), IFN γ (f), MIP-1 α /MIP-1 β (g), RAGE (h), RANTES (i), chitinase 3-like 1 (j), emmprin (k) and uPAR (l). n=3. Significance is displayed as *P<0.05, **P<0.01, ***P<0.001.

In screening inflammatory mediators secreted by our treated primary tubule cells, data was extrapolated to human datasets using Nephroseq transcriptomic analysis of published datasets obtained from studies of people with CKD (Figure 3.9a). For example, there is a significant increase in supernatant levels of inflammatory markers complement component C5/C5a ($423 \pm 71\%$, $P < 0.01$; Figure 3.9c), C-reactive protein ($321 \pm 66\%$, $P < 0.05$; Figure 3.9e) and matrix metalloproteinase 9 (MMP-9; 665 ± 123 , $P < 0.01$; Figure 3.9g) in $IL1\beta$, $TNF\alpha$ and 25mmol/L glucose treated cells as compared to 5mmol/L glucose controls, which is supported by statistically significant increases in mRNA levels in the proximal tubule region of people with CKD as opposed to healthy volunteers ($P < 0.001$ for all; Figure 3.9b, 3.9d and 3.9f respectively). Furthermore, there is an increase in the release of proteins associated with recruitment, regulation and activation of immune cells such as monocytes in high glucose and cytokine stimulated cells, including granulocyte colony stimulating factor (G-CSF; $5071 \pm 892\%$, $P < 0.001$; Figure 3.9i), $TNF\alpha$ ($6197 \pm 1198\%$, $P < 0.01$; Figure 3.9k), macrophage colony-stimulating factor (M-CSF; $450 \pm 77\%$, $P < 0.01$; Figure 3.9m), monocyte chemotactic protein-3 (MCP-3; $2065 \pm 213\%$, $P < 0.001$; Figure 3.9o) and intercellular adhesion molecule 1 (ICAM-1; $785 \pm 135\%$, $P < 0.01$; Figure 3.9q) all of which have increased mRNA expression in the proximal tubule region of people with CKD as compared to healthy volunteers ($P < 0.001$ for all; Figure 3.9h, 3.9j, 3.9l, 3.9n and 3.9p respectively).

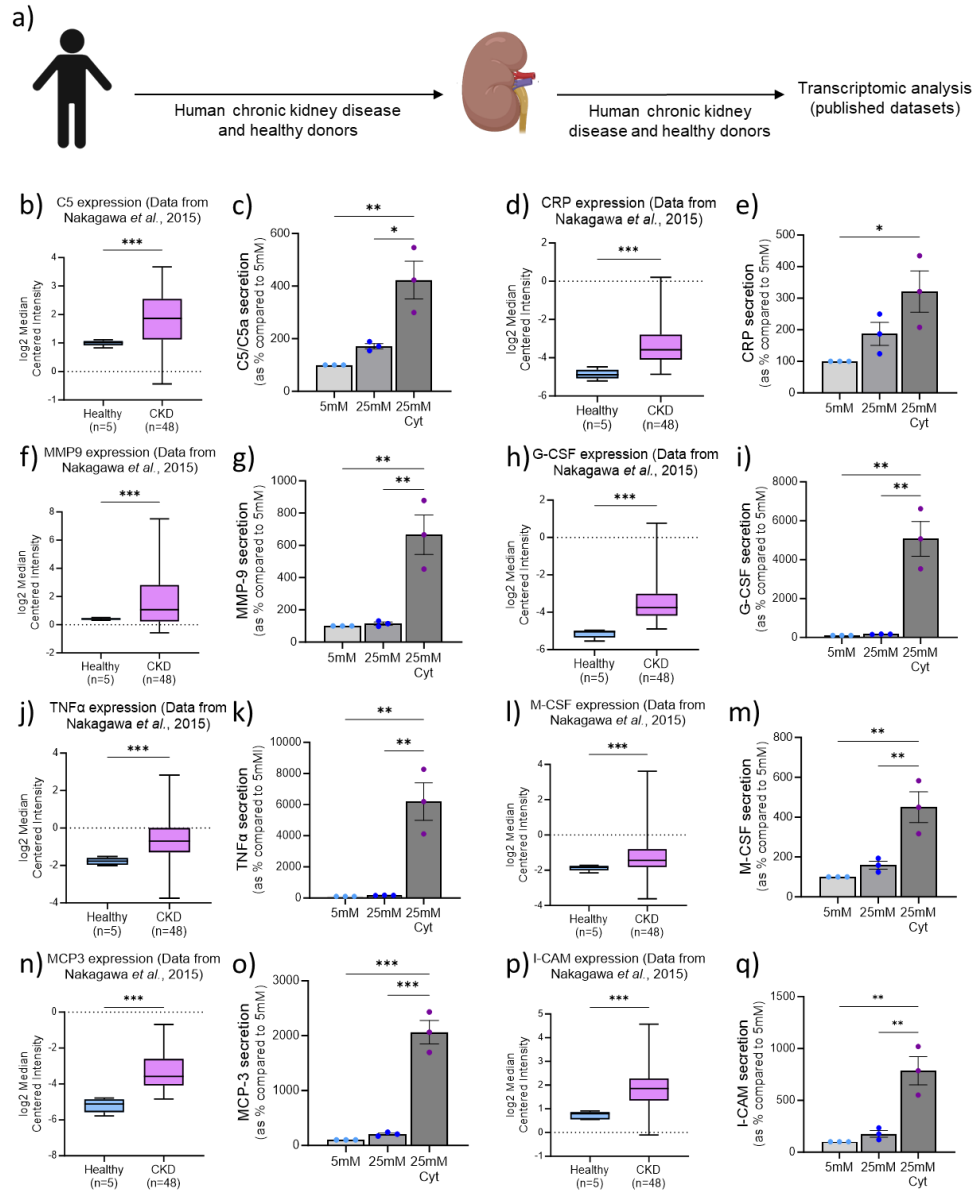


Figure 3.9. Inflammatory markers are elevated in kidney biopsies of people with CKD and proximal tubule epithelial cells treated with IL1 β , TNF α and 25mmol/L glucose. Transcriptomic analysis was performed on publicly available data from Nakagawa *et al.*, 2015 comparing mRNA expression in the tubules of kidney biopsies from healthy donors and donors with CKD (a). Human primary renal proximal tubule epithelial cells were treated with 5mmol/L (basal) glucose or 25mmol/L (high) glucose +/- IL1 β (10ng/mL) and TNF α (10ng/mL) for 48 hours. Cytokine and chemokine secretion were detected in cell supernatant using a human proteome profiler human XL cytokine array kit. Altered expression, identified using transcriptomic analysis and a cytokine array, showed significant increases in complement component C5/C5a (b and c respectively), C-Reactive protein (d and e respectively), MMP-9 (f and g respectively), G-CSF (h and i respectively), TNF α (j and k respectively), M-CSF (l and m respectively), MCP-3 (n and o respectively) and I-CAM (p and q respectively). All groups are n=3 unless specified, with ANOVA and Tukey post-test used for experimental comparisons except transcriptomic data where an unpaired t-test with Welch's correction analysis was used. Significance is displayed as * $P<0.05$, ** $P<0.01$, *** $P<0.001$.

3.4. Discussion

In this chapter, I showed the effect of pro-inflammatory cytokines IL1 β , IL18 and TNF α in the presence of glucose on human proximal tubule epithelial cells. Specifically, I demonstrated their effect on the expression and secretion of markers linked with inflammation, pEMT, and fibrosis, all of which are associated with late stage kidney disease (Gusev *et al.*, 2021). It is well established that inflammation is essential to the progression of diabetic nephropathy (Kelly and Dominguez, 2010), and that activation of the NLRP3 inflammasome plays a key role (Williams *et al.*, 2022b). In this chapter, I elucidated the impact of high glucose and inflammatory cytokines on inflammatory markers in both immortalised HK-2 and primary RPTEC cells. Whilst I observed a decrease in NLRP3 protein expression, this does not reflect inflammasome priming or a downregulation in NLRP3 activity, the latter of which is measured by caspase 1-mediated cleavage of pro-IL1 β and pro-IL18. Results from the proteome profiler cytokine array demonstrated a large ($2869 \pm 300\%$, $P < 0.001$) increase in IL1 β secretion from IL1 β , TNF α and 25mmol/L glucose treated RPTECs, suggesting that IL1 β and TNF α in the presence of high glucose induce NLRP3 inflammasome activation, an observation further supported by increased levels of secretion of downstream NLRP3 mediator IL6. Further investigation into the effects of inflammatory cytokines and high glucose on inflammasome priming and activation are presented in chapter 5.

In addition to changes in expression of proteins of the inflammasome complex, screening of the cytokine array data unveiled a significant increase in multiple inflammatory cytokines and chemokines, each of which possess a range of functions linked to the onset and exacerbation of inflammation and fibrosis. Extrapolation of these observations and transcriptomic analysis of published Nephroseq datasets, demonstrates that many of these cytokines exhibit increased mRNA expression in the proximal tubule of people with chronic kidney disease as compared to healthy volunteers, thus highlighting these proteins and our model as suitable for the study of changes/events observed in the diseased kidney. One such cytokine, C5/5a, is a potent pro-inflammatory cytokine involved in the innate immune response (Pandey *et al.*, 2020; Sommerfeld *et al.*, 2021). Through interactions with the C5a receptor 1 (C5aR1) it is an essential component of tubulointerstitial fibrosis in a murine model of renal ischemia/reperfusion injury, where it plays a role in regulating expression of pro-inflammatory and fibrotic cytokines, ECM (fibronectin and collagen-I) deposition, immune cell infiltration and renal fibroblast

activation (Peng *et al.*, 2019), thus highlighting one of many potential pathways through which elevated levels of high glucose, IL1 β and TNF α can contribute to downstream inflammation and fibrosis in the diseased kidney *in vivo*.

Research by Xu *et al.*, showed whole kidney mRNA expression of chemo-attractants GM-CSF and MCP1 were increased in mice following unilateral ischemia/reperfusion injury (U-IRI), a model of maladaptive kidney repair after transient kidney injury, which positively correlated to progressive macrophage accumulation and collagen-I expression (Xu *et al.*, 2019). Furthermore, using co-cultured naïve bone marrow derived-macrophages with serum-starved mouse proximal tubular cells they established that increased macrophage expression of MCP1 is dependent on tubule expression of GM-CSF (Xu *et al.*, 2019). These results, combined with array data showing increased levels of MCP1, GM-CSF and several other cytokines involved in immune cell recruitment, cellular remodelling and ECM deposition, suggest that IL1 β , TNF α and 25mmol/L glucose contribute and likely exacerbate kidney injury through stimulating proximal tubule release of an array of cytokines and chemokines that drive downstream inflammation and fibrosis through varying mechanisms, including immune cell recruitment and activation.

Research in other models of chronic inflammation show that NLRP3 activation, drives disease progression through the induction of pEMT, associated with downstream fibrosis in CDK. Having ascertained that IL1 β , TNF α and glucose amplifies NLRP3 activation in primary proximal tubule epithelial cells, experiments were carried out to determine whether these effects extended to the induction of pEMT. A combination of phase morphology and western blotting show that treatment with IL1 β , TNF α and glucose initiates partial EMT in tubule epithelial HK-2 cells, which appear more elongated, typical of myofibroblasts and demonstrate protein changes indicative of the cadherin switch. Similarly, in A549 adenocarcinomic human alveolar basal epithelial cells, stimulation with IL1 β and TNF α -induced TGF β 1-mediated EMT as shown by morphological changes and loss of E-cadherin (Liu, 2008).

A combination of IL1 β , TNF α and 25mmol/L glucose exacerbated alterations in the expression of E-cadherin and N-cadherin, highlighting a role for hyperglycaemia in loss of epithelial polarity. This role was also demonstrated by Li *et al.*, where inhibition of aberrant glycolysis using the SGLT2 inhibitor empagliflozin restored pathological changes in streptozotocin (STZ)-induced diabetic mice, including restoration of E-cadherin and α SMA expression (J. Li *et al.*, 2020b). Moreover, *in vitro* (Hills *et al.*, 2012) and *in vivo* (Chen *et*

et al., 2018) studies in human proximal tubule cells and STZ-treated, diabetic gerbil kidneys, show that hyperglycaemia induces a TGF β 1-mediated elongation of cell morphology paralleled by a loss of cell adhesion, caused by the loss of E-cadherin and subsequent upregulation of N-cadherin. The translational implications of these observations are demonstrated in studies which correlate reduced levels of serum E-cadherin to increased albuminuria in people with diabetic nephropathy as compared to healthy controls (El-Dawla *et al.*, 2019). These findings support a role for high glucose and inflammation in contributing to kidney injury through partial EMT of proximal tubule epithelial cells. Additionally, Masola *et al.*, demonstrated the induction of partial EMT in HK-2 cells treated with IL1 β (10ng/mL) for 6 and 24 hours, as evidenced by an altered expression of phenotypic markers including, α -SMA, vimentin and fibronectin, was inhibited in the presence of IL1 β blocker canakinumab (Masola *et al.*, 2019). These data support a clear link between NLRP3 activation and downstream pEMT in my *in vitro* model of injury.

The loss of E-cadherin reflects adherens junction disassembly. Upon breakdown of the junctional complex, β -catenin is either released into the cytosol and targeted for proteasomal degradation (Li *et al.*, 2020a), or interacts with wingless and integration site (Wnt) which translocates β -catenin to the nucleus where it functions to regulate gene transcription, including that of G-CSF (Danek *et al.*, 2020), fibronectin and collagen-I expression (Cao *et al.*, 2018). Genetic depletion of β -catenin within renal tubules significantly reduces myofibroblast activation and renal fibrosis following obstructive and ischaemic reperfusion injury (Zhou *et al.*, 2017). When treated with TNF α , HK-2 cells exhibit increased β -catenin expression, paralleled by altered morphology, typical of changes associated with pEMT. Together these data allude to a role for TNF α in modulating β -catenin/Wnt signalling in HK-2 cells, supported by similar findings in bronchial epithelial cells demonstrating that the WNT/ β -catenin pathway modulates the inflammatory response induced by TNF- α (Jang *et al.*, 2017). Whilst I failed to observe any changes in β -catenin expression in IL1 β , TNF α and 25mmol/L glucose treated cells, further studies are required to assess if a change in localisation reflects altered function. Further experiments utilising immunocytochemistry, or isolation and measurement of nuclear membrane proteins would allow subsequent research to elucidate the underlying mechanisms behind these observations and determine if adherens junction disassembly is paralleled by activation of Wnt signalling and downstream fibrosis.

Contributed to by inflammation and partial EMT, tubulointerstitial fibrosis is the final common pathway of CKD. Characterised by myofibroblast and fibroblast activation and ECM deposition through altered release of cytokines and chemokines, tubulointerstitial fibrosis leads to irreversible scarring and ultimately a decline in kidney function (Rockey, Bell and Hill, 2015; Moeller *et al.*, 2022). The pEMT associated breakdown in cell adherens junctions and change in cell phenotype leads to altered epithelial cell communication which promotes excessive deposition of extracellular matrix proteins, including fibronectin, collagen-I and collagen-IV. Data in this chapter shows an increase in the expression of these ECM proteins in cytokine treated HK-2 cells, building upon findings that allude to the induction of a vicious cycle of inflammation and fibrosis in tubular epithelial cells when treated with conditions modelling the diabetic kidney. Research analysing the genetic profiles of kidney samples taken from humans with CKD and a mouse model of severe tubulointerstitial fibrosis, created by transgenic overexpression of the Notch1 intracellular domain in tubular epithelial cells, show an increase in intracellular lipid accumulation and reduced FAO in fibrotic kidneys (Kang *et al.*, 2015). Combined with my own results, these findings support my hypothesis that high glucose and inflammatory cytokines, released downstream of excessive adipose tissue and kidney lipid accumulation, drives kidney fibrosis.

In addition to fibrosis-associated changes in cell morphology and protein expression, changes in the release of cytokines and chemokines in IL1 β , TNF α and 25mmol/L glucose treated RPTECs was examined. Previously linked to ECM deposition, cell remodelling and inflammation in disease (Zhao *et al.*, 2020), I describe increased release of chitinase-3-like 1 (CHI3L1) from RPTEC cells treated with IL1 β , TNF α and 25mmol/L glucose. Whilst its role in disease is still unclear, CHI3L1 has been linked to kidney disease in diabetes, specifically, where increased expression (Rathcke *et al.*, 2006) positively correlates with the incidence and degree of albuminuria (Røndbjerg *et al.*, 2011; Yasuda *et al.*, 2011; Rathcke *et al.*, 2009) and inflammation (Catalán *et al.*, 2011). The cytokine array also demonstrated a significant increase in the release of extracellular matrix metalloproteinase inducer; EMMPRIN, a protein which has previously been shown to play a role in type-3 EMT, that more commonly associated with various cancers (Kim *et al.*, 2021). With a role ascribed to deposition of the ECM, increased fibrosis and macrophage recruitment, studies have reported that increased EMMPRIN expression is correlated with a declining eGFR in people with T2DM (Chiu *et al.*, 2018), and in renal graft recipients (Nalewajska *et al.*, 2022). Interestingly, these individuals often suffer fibrosis similar to people with CKD,

and EMMPRIN serum concentrations positively correlate with urine protein concentration and increased interstitial fibrosis, thus highlighting EMMPRIN as a biomarker of poor long-term graft function (Nalewajska *et al.*, 2022). Another protein raised in IL1 β , TNF α and 25mmol/L glucose treated RPTEC supernatant is DPPIV. Urinary levels of DPPIV correlate to severity of diabetic nephropathy (Sun *et al.*, 2012). Use of DPPIV inhibitors e.g., sitagliptin (Al-Qabbaa *et al.*, 2023), saxagliptin (Xing *et al.*, 2021), linagliptin (Oraby *et al.*, 2019), and alogliptin (Davidson *et al.*, 2011) have reno-protective effects in both mouse models and people, with several clinical trials demonstrating their therapeutic effects in people with diabetic nephropathy (Coppolino *et al.*, 2018; Muskiet *et al.*, 2020; Hsu *et al.*, 2022; Dalui *et al.*, 2021). As an adjunct to their glucose lowering effects, *in vitro* studies in HK-2 cells demonstrate an ability of DPPIV inhibitors to reduce TGF β 1, collagen and fibronectin-mediated fibrosis in HK-2 cells (Komala *et al.*, 2015). My results demonstrate a role for IL1 β , TNF α and 25mmol/L glucose in inducing expression of DPPIV. As an established mediator of fibrosis in kidney disease, these results further highlight the therapeutic potential of blocking the combined effects of glycaemic injury and inflammation in a bid to slow the inflammatory damage and loss of renal function observed in diabetes.

In conclusion, this chapter characterises the effects of IL1 β , TNF α and 25mmol/L glucose on proximal tubule cell phenotype and function. I observed that hyperglycaemia and inflammation likely contribute to tubulointerstitial injury through NLRP3 inflammasome activation, the release of pro-inflammatory cytokines and chemokines, induction of partial EMT and excessive deposition of ECM. Together these effects culminate in a vicious cycle of chronic inflammation and irreversible fibrosis, both critical to the progression of diabetic nephropathy (Figure 3.10). Moving forward I aim to elucidate the mechanisms through which IL1 β , TNF α and 25mmol/L glucose mediate these effects, how they influence monocyte-derived macrophages and the effects of heterotypic communication between injured epithelial cells and macrophages. Importantly and from a pharmacological perspective, I will also investigate if I can block these harmful effects and inform future treatment of diabetic nephropathy.

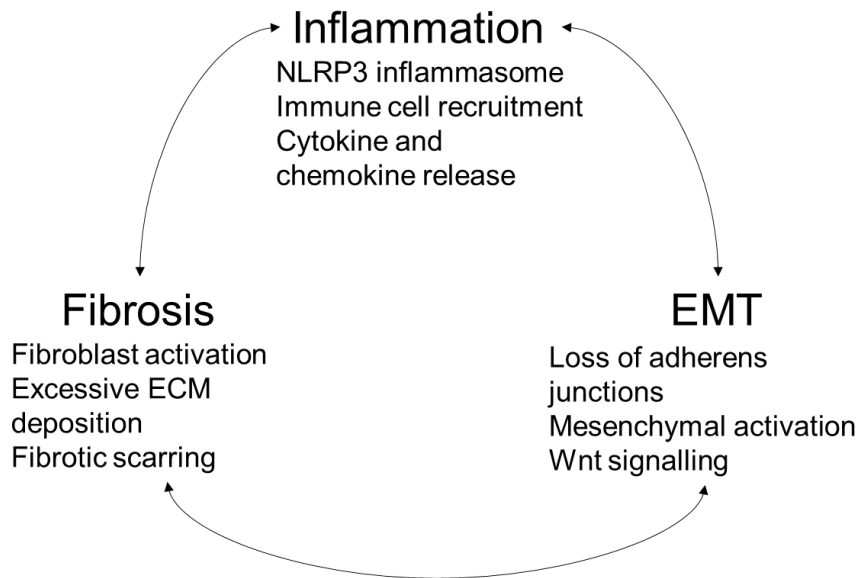


Figure 3.10. A schematic demonstrating the proposed vicious cycle of chronic inflammation, partial EMT and fibrosis in IL1 β , TNF α and 25mmol/L glucose treated RPTECs and HK-2 cells.

4.0. Effects of high glucose/cytokines on hemichannel activity and actions of Tonabersat in protecting against inflammatory-induced damage in proximal tubule epithelial cells.

4.1. Introduction

Hyperglycaemia and systemic inflammation in diabetes drives the development of several debilitating secondary complications, including cardiovascular disease (Paolisso *et al.*, 2021; Paolisso *et al.*, 2022), retinopathy (Mathebula, 2018; Forrester, Kuffova and Delibegovic, 2020) and impaired wound healing (Li *et al.*, 2019; Portou *et al.*, 2020). Interestingly, a strong association exists between disease complications in people with T2DM, and it has been demonstrated that individuals with diabetic nephropathy experience a higher incidence of diabetic retinopathy compared to those without diabetes related kidney disease (Jeng *et al.*, 2016), and vice versa (Zhang *et al.*, 2018). Similarly, a study found that in individuals with heart failure, 40% had CKD, of which 16% of these had diabetes. Diabetes and kidney disease compound the risk of heart failure, leading to higher hospitalisation rates and reduced survival (Lawson *et al.*, 2021). These inter-relationships suggest a common pathway for secondary complications, which drive progressive loss of tissue function across multiple organs. Recent studies examining chronic inflammatory conditions and secondary complications of diabetes demonstrate a role for the family of transmembrane proteins called connexins in mediating disease onset and progression, such as arthritis (Tsuchida *et al.*, 2013), age-related macular degeneration (Guo *et al.*, 2016; Obert *et al.*, 2017), ischemia (Chen *et al.*, 2015; Jiang *et al.*, 2019; Wang *et al.*, 2013; Chen *et al.*, 2019; Zhang *et al.*, 2021b), sepsis (Li *et al.*, 2018), diabetic foot ulcers (Grek *et al.*, 2015) and diabetic retinopathy (Shi *et al.*, 2022; Lyon *et al.*, 2021a; Louie *et al.*, 2021). Since diabetic nephropathy exhibits a similar aetiology to changes observed at both the back of the diabetic eye and in diabetic wounds, connexins have been identified as a possible unifying target for the treatment of inflammation and fibrosis in diabetic kidney disease.

Connexins are transmembrane proteins which oligomerise to form hexameric structures known as connexons (Wang and Liu., 2021). When connexons on neighbouring cells align, they dock forming gap junctions, allowing direct cell-to-cell communication. Unpaired connexons, also referred to as hemichannels, largely remain closed in physiological

conditions (Wang and Liu., 2021), but open in response to pathological conditions such as inflammation where they allow the release of small molecules and ions into the extracellular space (Van Campenhout *et al.*, 2021). It is by this mechanism that connexin hemichannels contribute to injury, releasing DAMPs into the extracellular environment, where they activate receptors (such as Toll-Like Receptor 4) on neighbouring cells (Li *et al.*, 2018; Chen *et al.*, 2018), triggering downstream events linked to oxidative stress (Ma *et al.*, 2020; Zhou *et al.*, 2021b) and inflammation (Tittarelli, 2021; Peng *et al.*, 2022; Huang *et al.*, 2019). Studies utilising human renal biopsy samples show an increase in Cx43 expression in individuals with diabetic nephropathy as compared to those without the disease (Price *et al.*, 2020; Abed *et al.*, 2014). How Cx43 contributes to disease pathology in the kidney remains to be determined.

Similar in aetiology to diabetic nephropathy (Zhang *et al.*, 2018), diabetic retinopathy is a microvascular complication affecting approximately one third of people with diabetes and is the leading cause of blindness in the working age population (National Diabetes Statistics Report, 2020). Comparable to the onset and progression of tubulointerstitial fibrosis in injured proximal tubules, the breakdown of the retinal pigment epithelium is associated with glucose-induced EMT (Che *et al.*, 2016) and NLRP3 inflammasome activation (Mugisho *et al.*, 2018a; Louie *et al.*, 2021), events which drive a loss of epithelial integrity and downstream inflammation. Extensive research in models of diabetic eye disease demonstrate the role of connexin hemichannel activity in mediating NLRP3 inflammasome activation (Mugisho *et al.*, 2018a; Louie *et al.*, 2021), partial/full EMT and fibrosis (Lyon *et al.*, 2021b).

Specifically, *in vitro* studies treating human retinal pigment epithelial (ARPE) cells with high glucose and a combination of inflammatory cytokines e.g., IL1 β (10ng/mL) and TNF α (10ng/mL) determined a role for Cx43 hemichannel activity in the activation of the NLRP3 inflammasome. This was evidenced by a Cx43 hemichannel sensitive increase in NLRP3 and active caspase 1 complex formation, culminating in the release of pro-inflammatory cytokines IL1 β , IL6 and VEGF (Lyon *et al.*, 2021a). Downstream of NLRP3 inflammasome activation, IL1 β and TNF α treated ARPE cells were reported to exhibit morphology typical of a fibroblast-like phenotype, including increased cell motility, a downregulation of epithelial ZO-1 paralleled by increased expression of fibroblast marker α SMA under conditions of high glucose. Pre-incubation of these retinal epithelial cells with connexin hemichannel blocker Tonabersat, reduced the high glucose and cytokine-induced

phenotypic changes in epithelial cells, supporting a role for Cx43 in mediating pEMT at the back of the eye (Lyon *et al.*, 2021b). Tonabersat has been shown to prevent the opening of connexin hemichannels in high glucose and cytokine stimulated ARPE cells, subsequently preventing ATP release (Lyon *et al.*, 2021a). Addition of exogenous ATP negated this protective effect on injury markers including NLRP3 inflammasome assembly (Lyon *et al.*, 2021a), an essential contributor to diabetic retinopathy. Downstream of inflammasome activation, Tonabersat also protects against IL1 β and TNF α -induced pEMT in ARPE cells, further highlighting its potential therapeutic effects in targeting sterile inflammation.

In the kidney, these observations were partly recapitulated in both *in vitro* and *in vivo* models of diabetic nephropathy. Previous studies in our group demonstrate that pro-fibrotic TGF β 1 increases Cx43 hemichannel-mediated dye uptake and ATP release (Price *et al.*, 2020; Squires *et al.*, 2021; Potter *et al.*, 2021a; Williams *et al.*, 2022). These events are paralleled by a loss of cell adhesion and altered expression at both the mRNA and protein level of markers associated with inflammation, pEMT and fibrosis (Price *et al.*, 2020; Squires *et al.*, 2021; Potter *et al.*, 2021; Williams *et al.*, 2022). Interestingly, these changes were significantly reduced when cells were pre-treated with hemichannel blockers Peptide 5 (Price *et al.*, 2020; Potter *et al.*, 2021a), Danegaptide (Squires *et al.*, 2021) and Tonabersat (Williams *et al.*, 2022).

In a UUO model of advanced inflammation and fibrosis, partial deletion of Cx43 (Cx43^{+/-}) reduced UUO-induced changes in adherens and tight junction protein expression, changes commonly associated with pEMT (Price *et al.*, 2020). A form of obstructive injury, UUO is surgically induced via ligation of one of the two ureters. This causes a post-renal effect, damaging the affected kidney by restricting renal drainage to the bladder and increasing retrograde hydrostatic pressure on the kidney. The unligated kidney acts as a paired control. Characterised primarily by tubulointerstitial fibrosis, the UUO mouse model is often used as a model of late-stage kidney disease irrespective of initiating cause. Pathological changes in the ligated kidney include tubular dilation, loss of proximal tubule mass, immune cell infiltration, inflammation, oxidative stress, and progressive renal fibrosis, all of which are relevant to diabetic nephropathy (Martínez-Klimova *et al.*, 2019). The Cx43^{+/-} UUO mouse model exhibits decreased inflammation and fibrosis (Price *et al.*, 2020). Nevertheless, the underlying mechanism behind this protection remains to be determined.

Extensive data has linked increased Cx43 hemichannel activity to disease pathology across multiple age associated conditions of chronic sterile inflammation (Tsuchida *et al.*, 2013; Sáez *et al.*, 2020; Chen *et al.*, 2018), and the potential of Cx43 hemichannel inhibitors as a therapeutic option has received increasing attention. Connexin-43 hemichannel blockers are a class of drugs which bind and prevent the opening of Cx43-hemichannels in response to pathological triggers (King *et al.*, 2021). Reduced hemichannel opening and subsequent inhibition of ATP release prevents the activation of local paracrine (P2X7R)-mediated signalling leading to diminished NLRP3 inflammasome activation (Mugisho *et al.*, 2018a), immune cell recruitment and fibrosis (Lyon *et al.*, 2021a). Several clinical trials are currently assessing the specificity and effectiveness of a range of Cx43 hemichannel blockers in disease and include the use of alpha connexin carboxyl terminus 1 (α CT1; Grek *et al.*, 2017; Clinical trials.gov identifier: NCT02652754), GAP-134 (danegaptide; Clinical trials.gov identifier: NCT01977755) and Tonabersat (Xiflam; Clinical trials.gov identifier: NCT00332007), as summarised in table 4.1.

A gap-junction modifying dipeptide, Danegaptide (GAP-134) was used to experimentally treat myocardial infarction. Three phase I clinical trials (NCT00510029, NCT00783341 and NCT00543946) and a stage II clinical trial (NCT01977755) demonstrated that Danegaptide was well tolerated with only few side effects. However, the primary and secondary endpoints showed no improvement between people treated with Danegaptide compared to control (Engstrøm *et al.*, 2018). Despite this setback, early evidence suggests that Danegaptide may be more effective in secondary complications of diabetes including diabetic retinopathy (Kim *et al.*, 2018) and nephropathy (Squires *et al.*, 2021). In studies of diabetic retinopathy Danegaptide was used as a Cx43 gap junction modifier, preventing the loss of gap junction coupling in injured cells (Kim *et al.*, 2018). This protected against increased apoptosis and cell monolayer permeability in high (30mmol/L) glucose treated rat retinal endothelial cells, highlighting potential therapeutic effects in diabetic retinopathy (Kim *et al.*, 2018). In an *in vitro* model of diabetic nephropathy, lower concentrations of Danegaptide were shown to additionally function as a Cx43 hemichannel blocker, negating a TGF β 1-induced increase in hemichannel-mediated dye uptake and ATP release in primary renal proximal tubule epithelial cells (Squires *et al.*, 2021). This protected against changes associated with inflammation and fibrosis, a consequence of the diminished expression and release of cytokines and chemokines, which collectively are associated with pEMT, immune cell recruitment/activation, matrix deposition and cellular senescence (Squires *et al.*, 2021).

Additional support for the role of Cx43 in secondary complications of diabetes are seen in studies examining wound healing. In a Cx43^{+/-} mouse model of skin injury, Cx43 deficiency promoted re-epithelialisation, activation, and proliferation of dermal fibroblasts with increased expression of ECM proteins, facilitating and accelerating wound closure (Cogliati *et al.*, 2015). In these models, targeting connexins using antisense technology, synthetic mimetic peptides or bioactive materials, including injectable hydrogels, have been used for the treatment of skin wounds/diabetic ulcers (Becker *et al.*, 2012), e.g., a Cx43 anti-sense oligodeoxynucleotide (asODN) in a thermo-reversible, slow release, pluronic gel; has been used in diabetic rat chronic wounds to reduce Cx43 expression in keratinocytes and fibroblasts, subsequently increasing migration and wound healing (Becker *et al.*, 2012). The Cx43 hemichannel blocker Gap27 promotes cell proliferation and migration in keratinocytes and fibroblasts (Faniku *et al.*, 2019), accelerating wound closure in human corneal epithelium both *in vitro* and *ex vivo* (Elbadawy *et al.*, 2016). Alpha connexin carboxyl terminus 1 (α CT1; Grek *et al.*, 2015), siRNA (Gilmartin *et al.*, 2016) and Gap19 (Tarzemany *et al.*, 2017) have all been used to improve wound healing in multiple types of injury. Mimicking the C-terminus of Cx43, α CT1 is a small peptide that has been used in phase I clinical trials for diabetic foot ulcers. Results from a pilot clinical study highlighted the potential for α CT1 in the treatment of diabetic foot ulcers where it significantly accelerated re-epithelialisation, decreasing the time taken for ulcers to close (Grek *et al.*, 2015). Corroborating research in the field of retinopathy and nephropathy, collectively these results highlight Cx43 as an effective, novel target to combat microvascular complications of diabetes, including diabetic nephropathy.

Table 4.1. Connexin 43 hemichannel blockers and their use in chronic inflammatory diseases. Inhibitor sequences, mechanisms of action where elucidated, examples of *in vitro/in vivo* models and progress in clinical trials are detailed. Adapted from Cliff *et al.*, 2022.

Drug	Sequence	Mechanism of action	<i>In vivo/in vitro</i> models	Clinical Trials
Alpha connexin carboxyl terminus 1 (α CT1)	Ant-RPRPDDLEI	Blocks hemichannel activity through binding to the COOH cytoplasmic terminus tail of Cx43 (Montgomery <i>et al.</i> , 2018), leading to Cx43 phosphorylation (Jiang <i>et al.</i> , 2019). Also affects gap junction remodelling (O'Quinn <i>et al.</i> , 2011).	Rat corneal wound model (Moore <i>et al.</i> , 2013). Randomised control trial assessing cutaneous scarring (Grek <i>et al.</i> , 2017). Human biopsy tissue/rat and guinea pig scars (Montgomery <i>et al.</i> , 2021).	Clinical trials for treatment of diabetic foot ulcers as 'Grannexin gel' Phase I- NCT02652754 Terminated at phase III NCT02667327
GAP-134 (Danegaptide)	C ₁₄ H ₁₇ N ₃ O ₄	Modifies gap junctions to maintain gap junction coupling (Butera <i>et al.</i> , 2009; Kim <i>et al.</i> , 2018) and blocks Cx43 hemichannels (Squires <i>et al.</i> , 2021) through unknown mechanisms.	Primary human proximal tubule epithelial cells (Squires <i>et al.</i> , 2021). Rat retinal endothelial cells during high glucose stress (Kim <i>et al.</i> , 2018). Canine (Rossman <i>et al.</i> , 2009) and pig (Skyschally <i>et al.</i> , 2013) myocardial infarction. Canine atrial fibrillation (Rossman <i>et al.</i> , 2009; Laurent <i>et al.</i> , 2009).	Clinical trials treating myocardial infarction Phase I- NCT00510029 NCT00783341 NCT00543946 Phase II- NCT01977755
Gap19	KQIEIKKFK	Binds to the intracellular loop of Cx43, inhibiting hemichannels without affecting gap junction communication (Abudara <i>et al.</i> , 2014).	Primary mouse cardiomyocytes Wang <i>et al.</i> , 2013). Mice cerebral ischaemia/injury (Chen <i>et al.</i> , 2019). Primary mouse astrocytes/hippocampal slices (Abudara <i>et al.</i> , 2014). Immortalised human retinal pigment epithelium cells/ primary human retinal microvascular endothelial cells (hREMC; Coutinho <i>et al.</i> , 2020). Isolated rat hepatocytes (Maes <i>et al.</i> , 2017). Human gingival fibroblasts (Tarzemany <i>et al.</i> , 2017).	N/A
Gap26	VCYDKSFPI	Binds to first	Isolated pig ventricular	N/A

	SHVR	extracellular loop of Cx43, blocking hemichannel activity (Warner <i>et al.</i> , 1995) and gap junctions (Wang <i>et al.</i> , 2012).	cardiomyocytes (Wang <i>et al.</i> , 2013). Cultured microglia, astrocytes and neurons (Orellana <i>et al.</i> , 2011).	
Gap27	SRPTEKTIFI I	Blocks hemichannel activity (Warner <i>et al.</i> , 1995) and gap junction communication (Wang <i>et al.</i> , 2012) through binding to the Cx43 second extracellular loop.	Primary human corneal epithelial cells <i>in vitro</i> , human corneas <i>ex vivo</i> , rat wound healing model <i>in vivo</i> (Elbadawy <i>et al.</i> , 2016). Adult keratinocytes, juvenile foreskin, human neonatal fibroblasts and adult dermal tissue (Faniku <i>et al.</i> , 2018).	N/A
Peptide 5	VDCFLSRP TEKT	Prevents hemichannel opening specifically through binding to the second extracellular loop of Cx43 (Simon <i>et al.</i> , 2020).	Human primary proximal tubule epithelial cells and clonal tubular kidney epithelial cells (Price <i>et al.</i> , 2020; Potter <i>et al.</i> , 2021a). Retinal pigment epithelial cells (Mugiso <i>et al.</i> , 2018; Kuo <i>et al.</i> , 2020). Patch-clamp mice (Delvaeye <i>et al.</i> , 2019). Light-damaged albino rat (Guo <i>et al.</i> , 2016).	N/A
Tonabersat (Xiflam)	C ₂₀ H ₁₉ ClFN O ₄	A benzopyran derivative that blocks Cx43 hemichannels at low concentrations and gap junctions at high concentrations through unknown mechanisms (Lyon <i>et al.</i> , 2021a).	Human retinal pigment epithelial cells (ARPE-19; Lyon <i>et al.</i> , 2021a). Rat model of diabetic retinopathy (Mat Nor <i>et al.</i> , 2020). Human clonal tubular kidney epithelial and fibroblast cells (Williams <i>et al.</i> , 2022)	Phase II clinical trials for treatment of migraines- NCT00311662 NCT00534560 NCT00332007 Phase II clinical trial for diabetic macular edema- NCT05727891

With a good safety profile, the potential for Cx43 hemichannel blockers in the management of microvascular complications of diabetes is undeniable. Specifically, hemichannel blocker Tonabersat has shown potential in both *in vitro* and *in vivo* models of diabetic retinopathy (Lyon *et al.*, 2021a; Lyon *et al.*, 2021b; Green *et al.*, 2019).

As a model of diabetic retinopathy, a spontaneously hyperglycaemic strain of the Sprague-Dawley rat showed significantly reduced Cx43 and inflammation following oral Tonabersat treatment, demonstrated by allograft inflammatory factor 1 (AIF-1) retina staining resulting in improved retinal function (Mat Nor *et al.*, 2020). This study also utilised light damaged Sprague-Dawley rats as a model of dry age-related macular degeneration (AMD). A condition associated with chronic inflammation and increased Cx43, blocking Cx43 hemichannel activity using Tonabersat reduced inflammation in the retina and protected against loss of photoreceptor function (Mat Nor *et al.*, 2020). In the same model of AMD, Tonabersat also prevented thinning of the retina, resulting in significantly improved retinal function (Kim *et al.*, 2017). Well tolerated with a good safety profile in a phase II clinical trial for migraines, Tonabersat is now entering phase II clinical trial for diabetic retinopathy.

Based on the positive outcomes in diabetic retinopathy, I hypothesise that Tonabersat will significantly reduce Cx43 hemichannel activity in an *in vitro* model of proximal tubule injury. Furthermore, I posit that the subsequent decrease in extracellular ATP will negate downstream changes associated with inflammation, pEMT and fibrosis in proximal tubule epithelial cells of the kidney.

4.2. Aims

Using the optimised *in vitro* model of tubulointerstitial inflammation as previously described, I will elucidate the role of Cx43 hemichannel-mediated ATP release in mediating downstream changes associated with inflammation and fibrosis. The efficacy of Tonabersat in blocking these effects will be assessed.

Specifically, I will:

- Investigate the effect of pro-inflammatory cytokines and high glucose on Cx43 hemichannel-mediated ATP release.
- Optimise the concentration of Cx43 hemichannel blocker Tonabersat in my *in vitro* model system.
- Use Tonabersat to evaluate a role for Cx43 hemichannel activity in driving altered protein expression associated with inflammation, pEMT and fibrosis in human primary proximal tubule epithelial cells.

4.3. Results

4.3.1. Pro-inflammatory cytokines combined with high glucose alter expression of connexins and pannexins.

Whilst a wealth of evidence links aberrant connexin hemichannel activity to inflammation across multiple disease states (Peng *et al.*, 2022), our knowledge of a role for connexin hemichannels in orchestrating this response in the kidneys remains rudimentary. Here I investigated the effects of proinflammatory conditions on expression of hemichannel forming proteins, Cx43, Cx26 and pannexin 1 (Panx1). HK-2 cells were treated with 5mmol/L or 25mmol/L glucose +/- IL1 β , IL18 and TNF α (10ng/mL each) either individually or in combination. Western blotting was used to determine changes in protein expression.

Of the 21 isoforms in the human body, Cx43 is the most abundant (Leithe *et al.*, 2018) and has been linked to other secondary complications of diabetes, including diabetic retinopathy (Tien *et al.*, 2016; Shi *et al.*, 2022; Mat Nor *et al.*, 2020; Louie *et al.*, 2021; Mugisho *et al.*, 2019). Elevated levels of expression have been demonstrated in several chronic inflammatory diseases such as diabetic nephropathy (Hills *et al.*, 2018; Abed *et al.*, 2014). Here I showed that IL1 β +TNF α and IL1 β +IL18 increase Cx43 expression in the presence of 5mmol/L glucose (410 \pm 90%, P <0.01 and 386 \pm 75%, P <0.01 respectively; Figure 4.1a). Whilst connexin 26 expression is also elevated in renal biopsy samples isolated from people with diabetic nephropathy (Hills *et al.*, 2018), in HK-2 cells treated with pro-inflammatory cytokines in 5mmol/L or 25mmol/L glucose there were no detectable changes in Cx26 expression (Figure 4.1c&d).

Pannexins are transmembrane proteins that also form hemichannels (but not gap junctions) and release ATP (Narahari *et al.*, 2021). Endothelial and epithelial expression of Panx1, the most abundant pannexin, has been previously associated with acute kidney injury (Jankowski *et al.*, 2018) and inflammation (Yang *et al.*, 2019). Therefore, the effect of inflammatory cytokines on renal epithelial Panx1 expression was determined. In basal glucose, IL1 β (171 \pm 13%, P <0.05), TNF α (173 \pm 9.7%, P <0.05), IL1 β +TNF α (205 \pm 29%, P <0.001), IL18+TNF α (168 \pm 10%, P <0.05) and a combination of all three (175 \pm 7.2%, P <0.05) significantly increased Panx1 expression (Figure 4.1e). Interestingly, in the presence of high glucose, inflammatory cytokines failed to induce an upregulation of Panx1, with IL1 β +TNF α (34 \pm 16%, P <0.05) and all three cytokines in combination (36 \pm 12%, P <0.05) inducing a significant decrease in expression (Figure 4.1f). An ATP

assay was performed in which cells were treated with IL1 β and TNF α in the presence of glucose +/- the pannexin channel blocker probenecid (100 μ M-10mmol/L). Results showed an absence of effect of blocking Panx1 on ATP release, effectively ruling out a role for Panx1 in mediating cytokine and glucose evoked ATP release in this model system (data not shown).

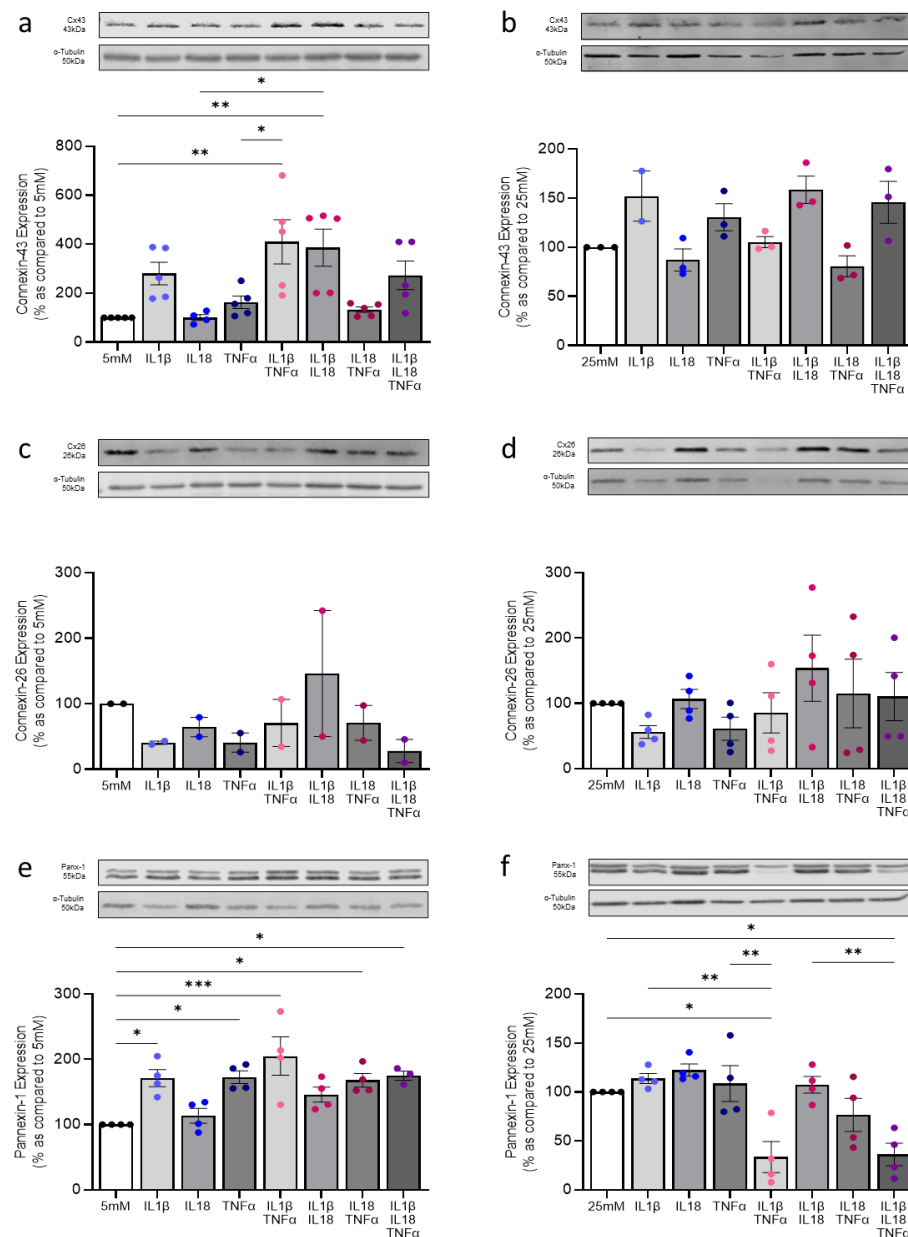


Figure 4.1. Hemichannel forming proteins, connexin 43, connexin 26 and pannexin 1 increased in expression following treatment with high glucose and inflammatory cytokines in proximal tubule epithelial cells. HK-2 cells were treated with 5mmol/L or 25mmol/L glucose +/- IL1 β (10ng/mL), +/- IL18 (10ng/mL) +/- TNF α (10ng/mL) for 48 hours. Western blotting determined changes in protein expression of Cx43, Cx26 and Panx1 in 5mmol/L glucose media (a, c and e respectively) and 25mmol/L glucose media (b, d and f respectively). Results were normalised against expression of housekeeping protein, α -Tubulin as a loading control. n=2-5. Significance is displayed as * P <0.05, ** P <0.01, *** P <0.001.

4.3.2. Connexin 43 is upregulated in diabetic nephropathy

Having determined a role for pro-inflammatory cytokines in the presence of high glucose in regulating Cx43 protein expression in human proximal tubule epithelial cells, data was extrapolated into humans using Nephroseq transcriptomic analysis of publicly available datasets obtained from studies of people with diabetic nephropathy (Figure 4.2a). Analysis revealed a significant upregulation of Cx43 mRNA expression in biopsy samples from people with diabetic nephropathy as opposed to healthy donors ($P<0.05$; Figure 4.2b). This increased expression positively correlates with proteinuria in donors with diabetic nephropathy ($P<0.05$), linking Cx43 to impaired kidney function in disease (Figure 4.2c). On this basis, combined with outcomes from studies in the Cx43^{+/-} UUO mouse and data in 4.3.1, all future experiments focus on Cx43.

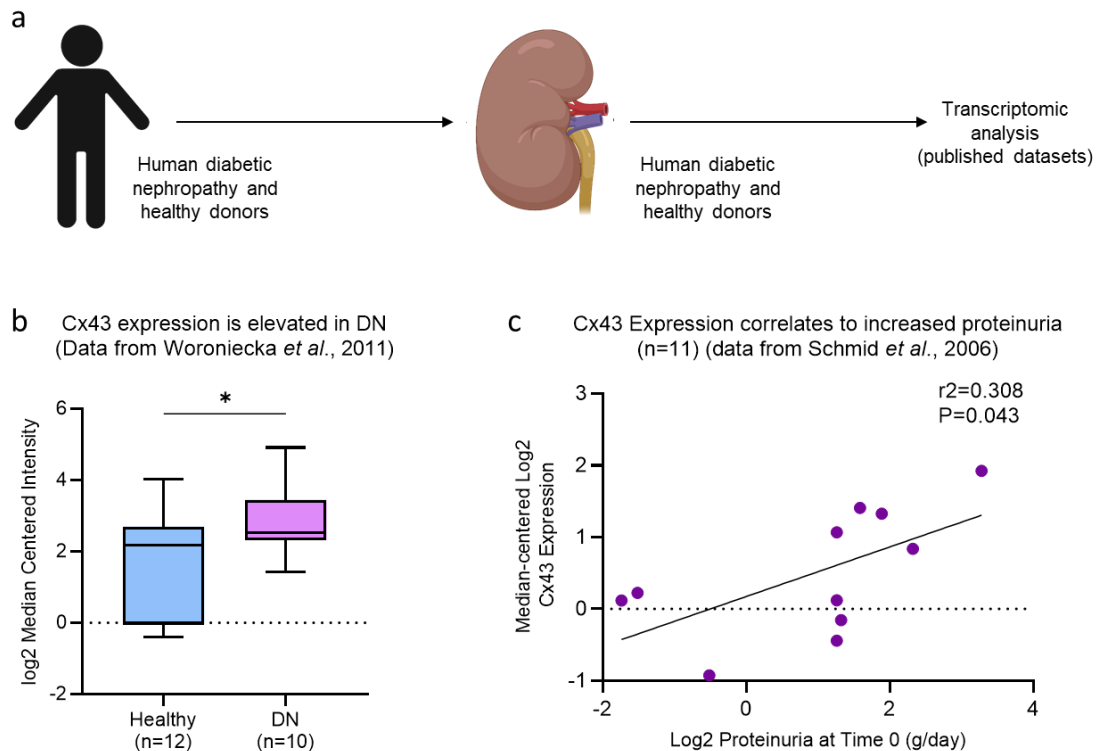


Figure 4.2. Connexin 43 is elevated in human diabetic nephropathy, and correlates to increased proteinuria. Transcriptomic analysis (a) was performed on Nephroseq publicly available data from Woroniecka *et al.*, 2011 (b) and Schmid *et al.*, 2006 (c) comparing mRNA expression in the tubules of kidney biopsies from healthy donors and donors with diabetic nephropathy. n is specified where appropriate. An unpaired t-test with Welch's correction analysis (b) and simple linear regression (c) were used for statistical analysis. Significance is displayed as * $P<0.05$.

4.3.3. Evaluating the effect of Tonabersat on cell viability in the presence of high glucose and inflammatory cytokines

In evaluating a role for Cx43 hemichannel activity in driving epithelial cell damage induced by pro-inflammatory cytokines IL1 β and TNF α under conditions of high glucose, initial experiments assessed the impact of the hemichannel blocker Tonabersat on cell viability, prior to assessing how blocking Cx43 hemichannels impacted on cell phenotype and function. Cell viability was assessed using crystal violet and MTT assays to quantify changes in cell number and metabolic activity respectively. HK-2 cells were treated with 5mmol/L or 25mmol/L glucose +/- IL1 β (10ng/mL) and TNF α (10ng/mL) +/- Tonabersat (1-100 μ M) for 48 hours. There was no significant change in cell viability when cells were treated with Tonabersat, as compared to 5mmol/L glucose control (Figure 4.3a&b).

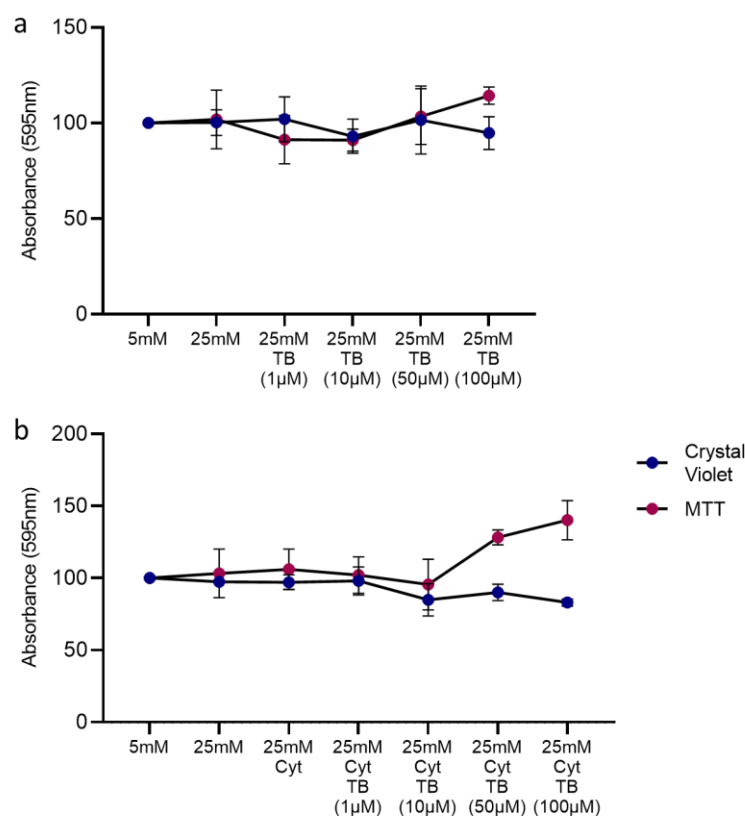


Figure 4.3. The effect of Tonabersat on proximal tubule cell viability in 25mmol/L glucose conditions, with and without the addition of IL1 β and TNF α . HK-2 cells were treated in 5mmol/L or 25mmol/L glucose +/- Tonabersat (1-100 μ M) +/- IL1 β (10ng/mL) and TNF α (10ng/mL) for 48 hours. The effect on cell viability was assessed using crystal violet staining (a) and an MTT assay (b). n=3.

4.3.4. Tonabersat reduces hemichannel-mediated dye uptake and ATP release, stimulated by IL1 β , TNF α and 25mmol/L glucose.

The ability of Tonabersat to reduce Cx43 hemichannel activity has been established in models of diabetic retinopathy (Lyon *et al.*, 2021a; Mat Nor *et al.*, 2020; Louie *et al.*, 2021), but it is yet to be established if Tonabersat can similarly improve outcomes in human proximal tubule epithelial cells in the presence of inflammation and high glucose. Carboxyfluorescein dye uptake was used to determine a change in the number of hemichannels at the cell membrane. This technique relies on manual gating of hemichannels through Ca²⁺ manipulation therefore, an ATP assay was used as a complementary strategy to measure cellular release of ATP. Together these approaches can indicate whether Tonabersat can negate hemichannel activity in response to cytokine and high glucose treatment.

HK-2 cells were treated with 5mmol/L or 25mmol/L glucose +/- IL1 β (10ng/mL) and TNF α (10ng/mL) +/- Tonabersat (50-100 μ M) for 48 hours. Inflammatory IL1 β , TNF α and 25mmol/L glucose increased hemichannel-mediated dye uptake and ATP release by 35 \pm 7.9% (P <0.001) and 77 \pm 6.3% (P <0.001) respectively, as compared to 5mmol/L glucose control (Figure.4.4a-c). Tonabersat significantly reduced an IL1 β , TNF α and 25mmol/L glucose-mediated increase in hemichannel activity by 30 \pm 4.8% (P <0.01) 42 \pm 3.3% (P <0.001) at 50 μ M and 100 μ M respectively. This paralleled a Tonabersat-sensitive reduction in cytokine and high glucose-induced ATP release by 46 \pm 4.6% (P <0.001) seen at 50 μ M (Figure 4.4d&e). The results confirm that in high glucose, IL1 β and TNF α increase dye uptake and ATP release, effects blocked by Tonabersat. Taken together the data indicate an overall increase in Cx43-mediated hemichannel activity.

Peptide5 did not significantly block hemichannel activity and was less effective than Tonabersat in reducing both carboxyfluorescein dye uptake and ATP release (data not shown). Consequently, future experiments utilised Tonabersat as an effective Cx43 hemichannel blocker.

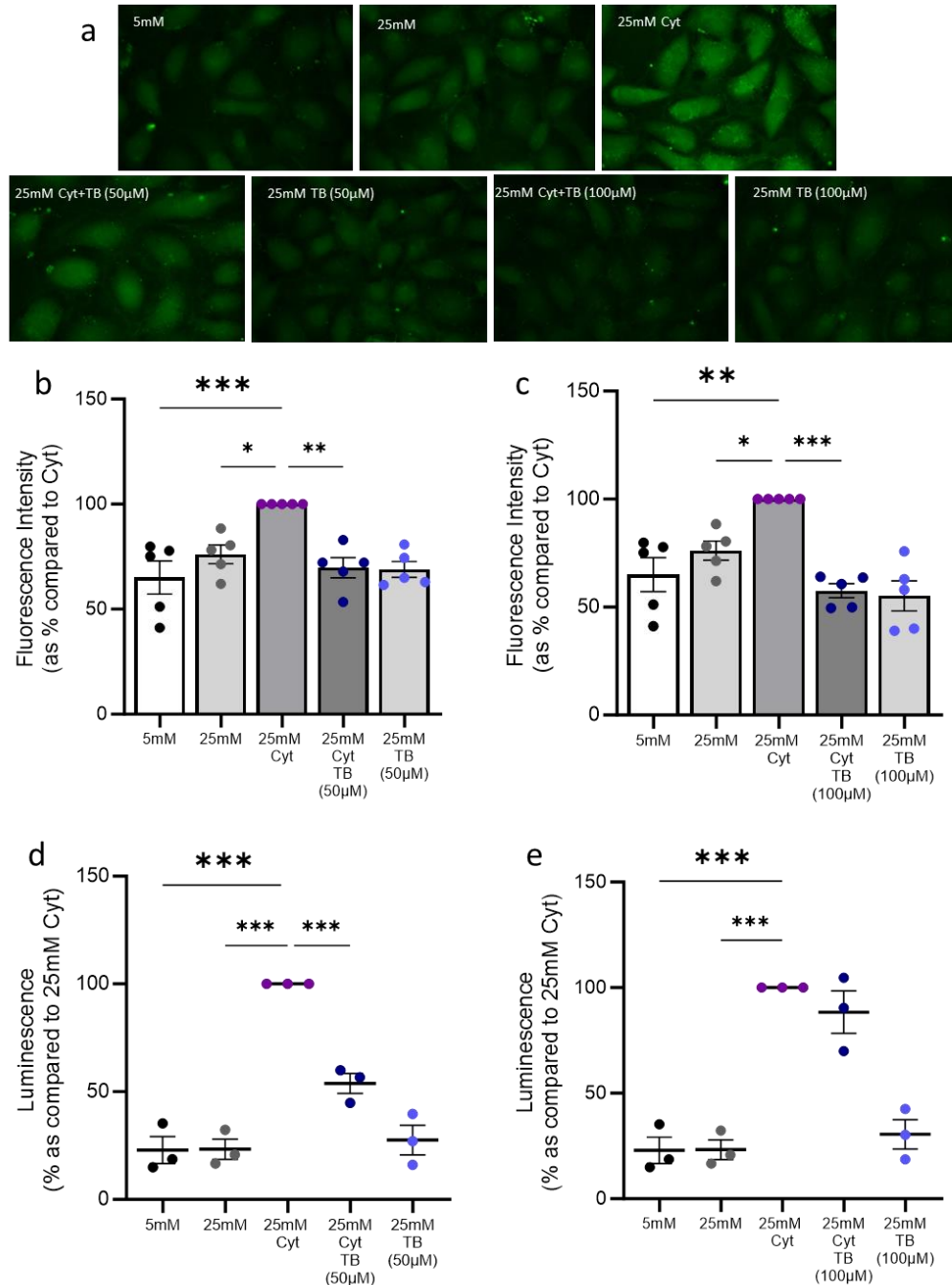


Figure 4.4. Tonabersat negates an IL1 β , TNF α and 25mmol/L glucose-induced increase in Cx43-mediated dye uptake and ATP release in proximal tubule epithelial cells. HK-2 cells were treated with 5mmol/L or 25mmol/L glucose +/- IL1 β (10ng/mL) and TNF α (10ng/mL; Cyt) +/- Tonabersat (TB; 50-100 μ M) for 48 hours. Carboxyfluorescein dye uptake studies determined change in hemichannel number at the cell surface (a) which was quantified using Fiji software (b, c). An ATPlite luminescence assay measured cellular release of ATP into the supernatant (d, e). n=3-5. Significance is displayed as * P <0.05, ** P <0.01, *** P <0.001.

4.3.5. High glucose in combination with inflammatory cytokines increased IL6 expression through aberrant Cx43 hemichannel activity.

Research in other models of disease highlights a mechanistic role for Cx43 hemichannel-mediated ATP release in driving release of pro-inflammatory cytokines, specifically IL6 (Kawano *et al.*, 2015; Zhang *et al.*, 2021b; Zhu *et al.*, 2021). Acting through signalling pathways such as glycoprotein (gp)130, janus kinase (JAK)-signal transducer and activator of transcription (STAT)3 and Src homology region 2-containing protein tyrosine phosphatase 2 (SHP2)/ GRB2-associated-binding protein (Gab)/MAPK, IL6 binds to the IL6 receptor (IL6R) on the cell surface of several cells involved in the immune response including macrophages, neutrophils, CD4+ T-cells and podocytes to contribute to kidney disease (Su *et al.*, 2017). Produced in podocytes, mesangial, endothelial and renal epithelial cells, IL6 is implicated in monocyte differentiation (Chomarat *et al.*, 2000), ROS production (Dong *et al.*, 2018), MCP-1 release (Kang *et al.*, 2020), ECM deposition and tubulointerstitial fibrosis (Chen *et al.*, 2019). I investigated the effect of Tonabersat in reducing production of IL6 (See Chapter 3, Figure 3.3), indicating whether its production in response to inflammatory cytokines and high glucose was Cx43 hemichannel-mediated. Pro-inflammatory cytokines IL1 β , TNF α and 25mmol/L glucose increase expression of IL6 protein by 74 \pm 11%, P <0.001 as compared to 5mmol/L glucose controls, a response successfully reduced by hemichannel blocker Tonabersat at 1 μ M (38 \pm 3.2%, P <0.01), 10 μ M (47 \pm 6.3%, P <0.01), 50 μ M (53 \pm 6.0%, P <0.001) and 100 μ M (65 \pm 2.8%, P <0.001; Figure 4.5).

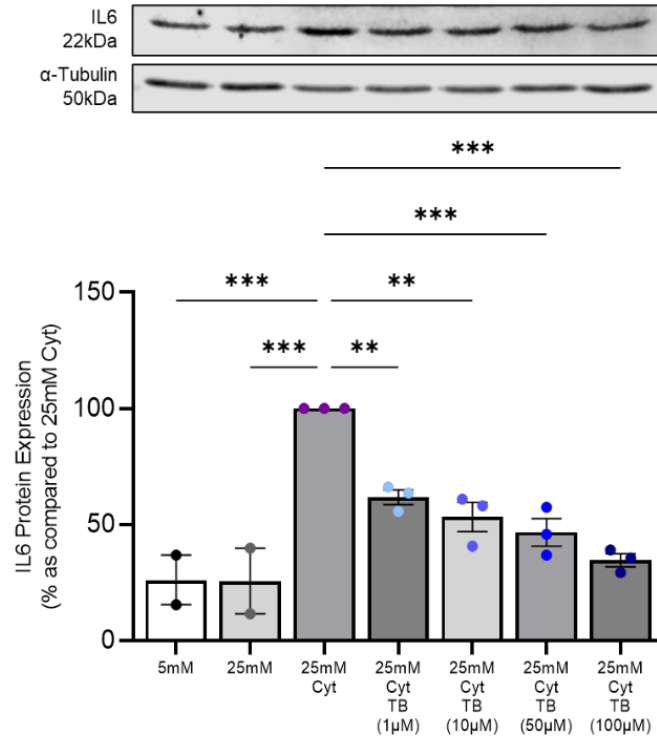


Figure 4.5. Tonabersat blocks an IL1 β , TNF α and 25mmol/L glucose-mediated upregulation of inflammatory marker IL6 in proximal tubule epithelial cells. HK-2 cells were treated with 5mmol/L or 25mmol/L glucose +/- IL1 β (10ng/mL) and TNF α (10ng/mL; Cyt) +/- Tonabersat (TB; 1-100 μ M) for 48 hours. Western blotting determined changes in protein expression of IL6. Results were normalised against expression of housekeeping protein, α -Tubulin as a loading control. n=3. Significance is displayed as ** P <0.01, *** P <0.001.

4.3.6. Blocking Cx43 hemichannel activity protects against increased expression of partial-EMT and fibrosis markers.

As shown previously, treatment of HK-2 cells with IL1 β , TNF α and 25mmol/L glucose leads to protein changes in markers associated with pEMT and fibrosis. Previous work in our group has demonstrated that profibrotic TGF β 1 under euglycaemic conditions, mediates down regulation of epithelial markers and upregulation of fibrotic markers in human proximal tubule cells through increased Cx43 hemichannel activity (Price *et al.*, 2020; Potter *et al.*, 2021a). Furthermore, we have demonstrated the ability of hemichannel blockers Peptide5 (Price *et al.*, 2020; Potter *et al.*, 2021a) and Tonabersat in blocking these effects (Williams *et al.*, 2022). Therefore, having demonstrated an increase in Cx43

hemichannel activity in IL1 β , TNF α and 25mmol/L glucose treated cells, I investigated the consequences of blocking Cx43 hemichannels on cell phenotype, specifically through the assessment of ECM and adherens junction protein expression. HK-2 cells were treated with 5mmol/L or 25mmol/L glucose +/- IL1 β (10ng/mL) and TNF α (10ng/mL) +/- Tonabersat (1-100 μ M) for 48 hours. Western blotting determined changes in protein expression.

Expression of E-cadherin and N-cadherin is typically altered when cells undergo pEMT, with a loss of cytoskeletal E-cadherin and a concomitant upregulation in N-cadherin to maintain cell-cell interactions, known as the cadherin switch (Loh *et al.*, 2019). Treatment of cells with IL1 β , TNF α and 25mmol/L glucose increased N-cadherin expression ($65\pm 8.6\%$, $P<0.001$; Figure 4.6a) paralleled by a decrease in E-cadherin expression ($614\pm 118\%$, $P<0.001$; Figure 4.6b). Treatment with Tonabersat at 10 μ M, 50 μ M and 100 μ M negated IL1 β , TNF α and 25mmol/L glucose-mediated increases in N-cadherin expression ($42\pm 5.4\%$, $P<0.01$; $66\pm 5.1\%$, $P<0.001$ and $4\pm 6.3\%$, $P<0.001$ respectively; Figure 4.6a), but not E-cadherin expression (Figure 4.6b). No significant changes in β -catenin expression were observed following IL1 β , TNF α and 25mmol/L glucose stimulation or Tonabersat inhibition, however this is likely due to previously discussed dual functionality of β -catenin as an integral part of the cytoskeleton in healthy cells, or as a transcription factor in WNT-signalling pathways in injury (Sen *et al.*, 2022; Figure 4.6c). Localisation studies for β -catenin would be needed to confirm this hypothesis.

In addition to altered expression of adherens junction proteins, previous experiments demonstrated an IL1 β , TNF α and 25mmol/L glucose-induced increase in ECM proteins fibronectin, collagen-I and collagen-IV, all of which are markers of fibrosis. Experiments with Tonabersat illustrate that blocking Cx43 hemichannel activity negates an IL1 β , TNF α and 25mmol/L glucose-induced increase in fibronectin ($72\pm 3.9\%$, $P<0.001$; Figure 4.7a), collagen-I ($88\pm 3.0\%$, $P<0.001$; Figure 4.7b) and collagen-IV ($91.7\pm 1.1\%$, $P<0.001$; Figure 4.7c). At concentrations of 50 μ M and 100 μ M, fibronectin expression is decreased by $41\pm 3.2\%$ ($P<0.001$; Figure 4.7a) and $50\pm 10\%$ ($P<0.001$) respectively, collagen-I by $34\pm 3.5\%$ ($P<0.01$) and $44\pm 6.5\%$ ($P<0.001$) respectively (Figure 4.7b) and finally collagen-IV by $49\pm 9.4\%$ ($P<0.05$) and $54\pm 13\%$ ($P<0.01$) respectively (Figure 4.7c). These results highlight a role for Tonabersat-sensitive Cx43 in mediating adherens junction breakdown paralleled by a dysregulation in ECM deposition.

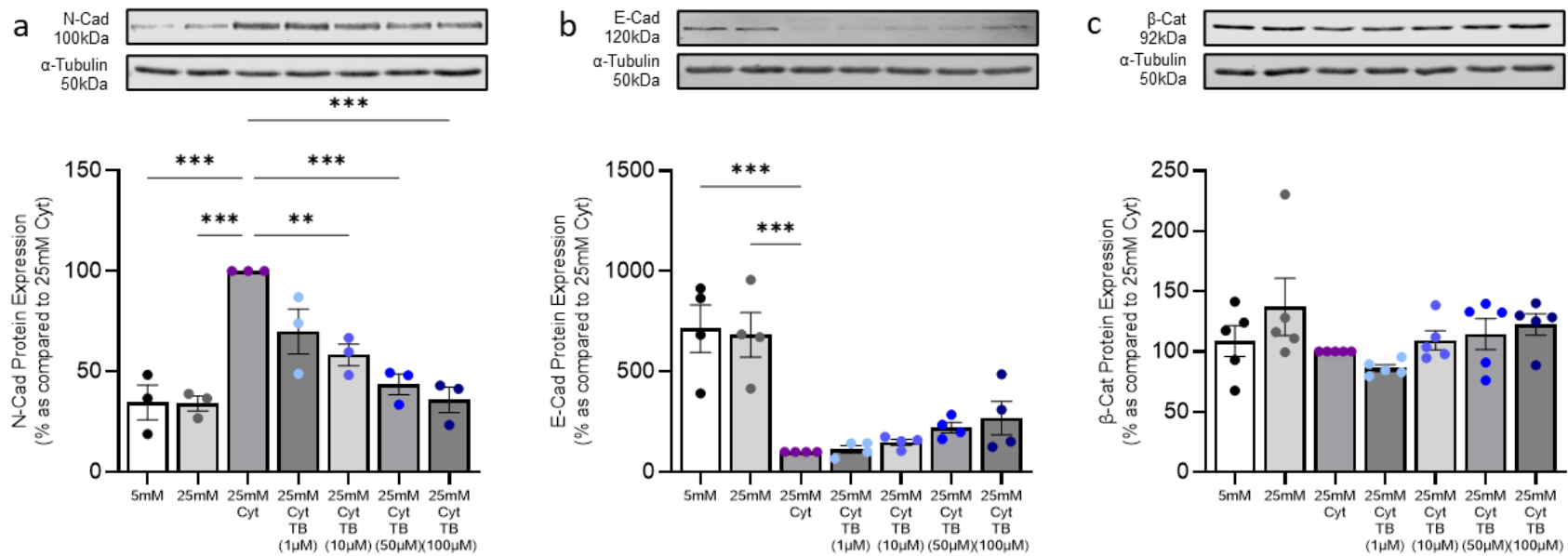


Figure 4.6. Tonabersat blocks IL1 β , TNF α and 25mmol/L glucose-mediated upregulation of select markers of pEMT in proximal tubule epithelial cells, but not all. HK-2 cells were treated with 5mmol/L or 25mmol/L glucose +/- IL1 β (10ng/mL) and TNF α (10ng/mL; Cyt) +/- Tonabersat (TB; 1-100 μ M) for 48 hours. Western blotting determined changes in protein expression of N-Cadherin (a), E-Cadherin (b) and β -Catenin (c). Results were normalised against expression of housekeeping protein, α -Tubulin as a loading control. n=3-5. Significance is displayed as ** P <0.01, *** P <0.001.

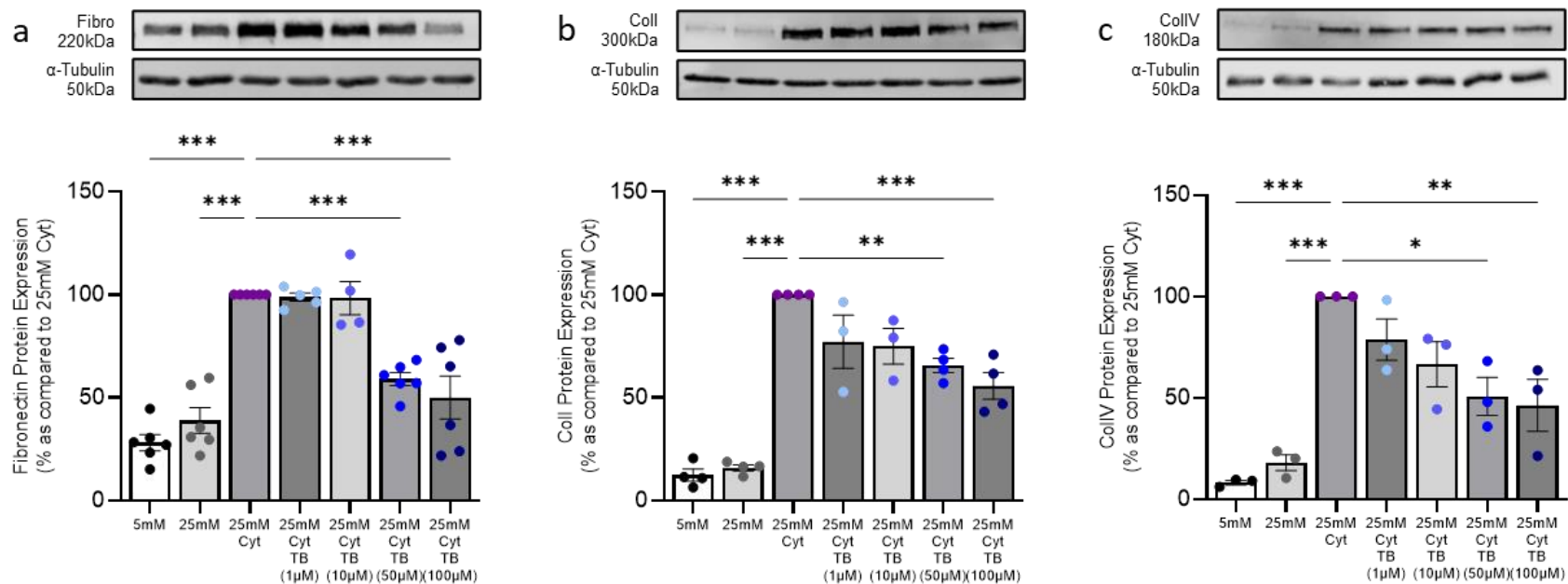


Figure 4.7. Tonabersat blocks an IL1 β , TNF α and 25mmol/L glucose-mediated upregulation of key ECM proteins associated with fibrosis in proximal tubule epithelial cells. HK-2 cells were treated with basal (5mmol/L) or high (25mmol/L) glucose +/- IL1 β (10ng/mL) and TNF α (10ng/mL) +/- Tonabersat (TB; 1-100 μ M) for 48 hours. Western blotting determined changes in protein expression of fibronectin (a), collagen I (Coll; b) and collagen IV (CollIV; c). Results were normalised against expression of housekeeping protein, α -Tubulin as a loading control. n=3-5. Significance is displayed as * P <0.05, ** P <0.01, *** P <0.001.

4.3.7. Tonabersat and BAPTA block Cx43 hemichannel-mediated ATP release and reduce markers for tubular injury in IL1 β and TNF α stimulated RPTECs under conditions of high glucose.

Although HK-2 cells are a well-established human renal epithelial cell line and inform preliminary experiments, the translational aspect of these results are limited by the physiological relevance of this clonal model. Therefore, human primary RPTECs, isolated from the normal region of a renal carcinoma biopsy were used as a more physiologically relevant model to corroborate previous observations. Specifically, I investigated potential signalling mechanisms regulating Cx43 hemichannel-mediated ATP release and downstream injury.

Primary RPTEC cells were treated with 5mmol/L or 25mmol/L glucose +/- IL1 β (10ng/mL) in combination with TNF α (10ng/mL) +/- Tonabersat (50 μ M) +/- BAPTA (5 μ M) for 48 hours. Initial experiments determined that Tonabersat effectively blocked the cytokine and high glucose-induced hemichannel-mediated dye uptake ($61 \pm 3.2\%$ ($P < 0.001$; Figure 4.8a&b) and ATP release $74 \pm 6.4\%$ ($P < 0.001$; Figure 4.8c) by $45 \pm 4.2\%$ ($P < 0.001$) and $44 \pm 5.0\%$ ($P < 0.001$) respectively.

A principal mechanism through which Cx43 hemichannels are gated, is through alterations to intracellular and extracellular Ca²⁺ levels. Increased intracellular calcium positively regulates Cx43 hemichannel opening. Consequently, the calcium chelator, BAPTA, was used to reduce [Ca²⁺]_i prior to assessing the implications that this had on Cx43 expression and hemichannel activity. Treatment with BAPTA significantly reduced an IL1 β , TNF α and 25mmol/L glucose-induced increase in Cx43 protein expression ($62 \pm 7.0\%$, $P < 0.001$; Figure 4.8d) and ATP release ($54 \pm 6.4\%$, $P < 0.001$; Figure 4.8e) by $40 \pm 5.3\%$ ($P < 0.001$) and $38 \pm 8.1\%$ ($P < 0.01$) respectively.

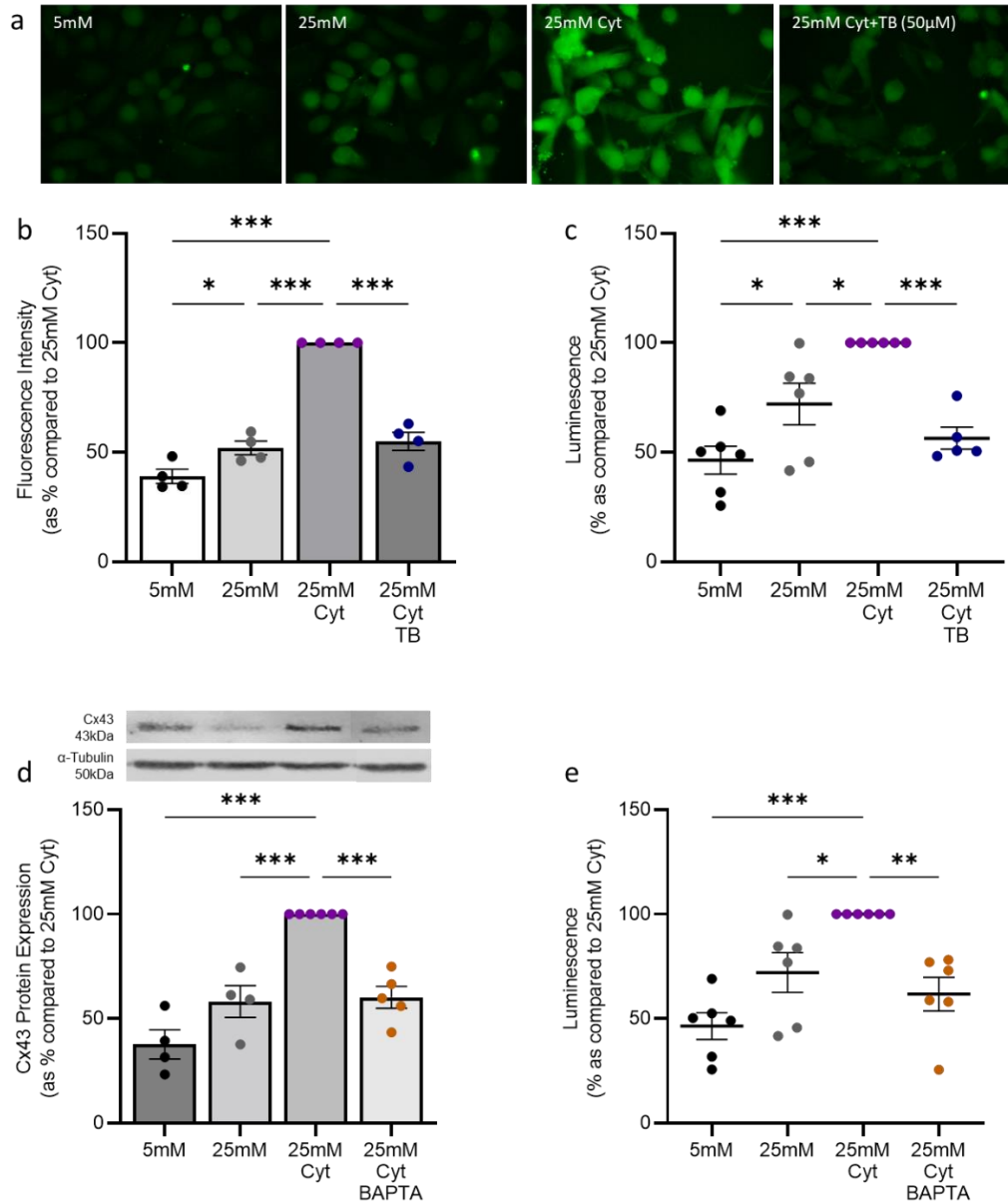


Figure 4.8. A pro-inflammatory cytokine IL1 β , TNF α and 25mmol/L glucose-induced Cx43-mediated dye uptake, ATP release and protein expression is reduced in primary proximal tubule epithelial cells when co-incubated with Tonabersat or BAPTA. Primary RPTEC cells were treated with 5mmol/L or 25mmol/L glucose +/- IL1 β (10ng/mL) and TNF α (10ng/mL; Cyt) +/- Tonabersat (TB; 50μM) +/- BAPTA (5μM) for 48 hours. Carboxyfluorescein dye uptake studies determined change in hemichannel number at the cell surface (a) which was quantified using Fiji software (b). An ATPlite luminescence assay measured cellular release of ATP into the supernatant (c, e). Western blotting determined changes in protein expression of Cx43 (d). Results were normalised against expression of housekeeping protein, α -Tubulin as a loading control. n=4-6. Significance is displayed as * P <0.05, ** P <0.01, *** P <0.001.

Downstream of hemichannel-mediated ATP release is altered expression of injury markers associated with pEMT and fibrosis. Supporting previous experiments in HK-2 cells, data in RPTECs corroborates the finding that Tonabersat effectively blocks a cytokine and high glucose-mediated increase in injury markers fibronectin ($45 \pm 6.4\%$, $P < 0.001$; Figure 4.9a) and N-cadherin ($68 \pm 2.5\%$, $P < 0.001$; Figure 4.9b) by $36 \pm 3.7\%$ ($P < 0.01$) and $38 \pm 9.5\%$ ($P < 0.001$) respectively.

Experiments utilising calcium chelator BAPTA show that alterations to $[Ca^{2+}]_i$ reduced IL1 β , TNF α and high glucose stimulated expression of N-cadherin by $46 \pm 14\%$, $P < 0.001$ in RPTECs (Figure 4.9d). Fibronectin expression was partially reduced by under these conditions, but the change did not attain significance (Figure 4.9c). These data highlight a potential mechanism by which alterations to $[Ca^{2+}]_i$ regulate the gating of Cx43 hemichannel activity and downstream N-cadherin and Fibronectin expression.

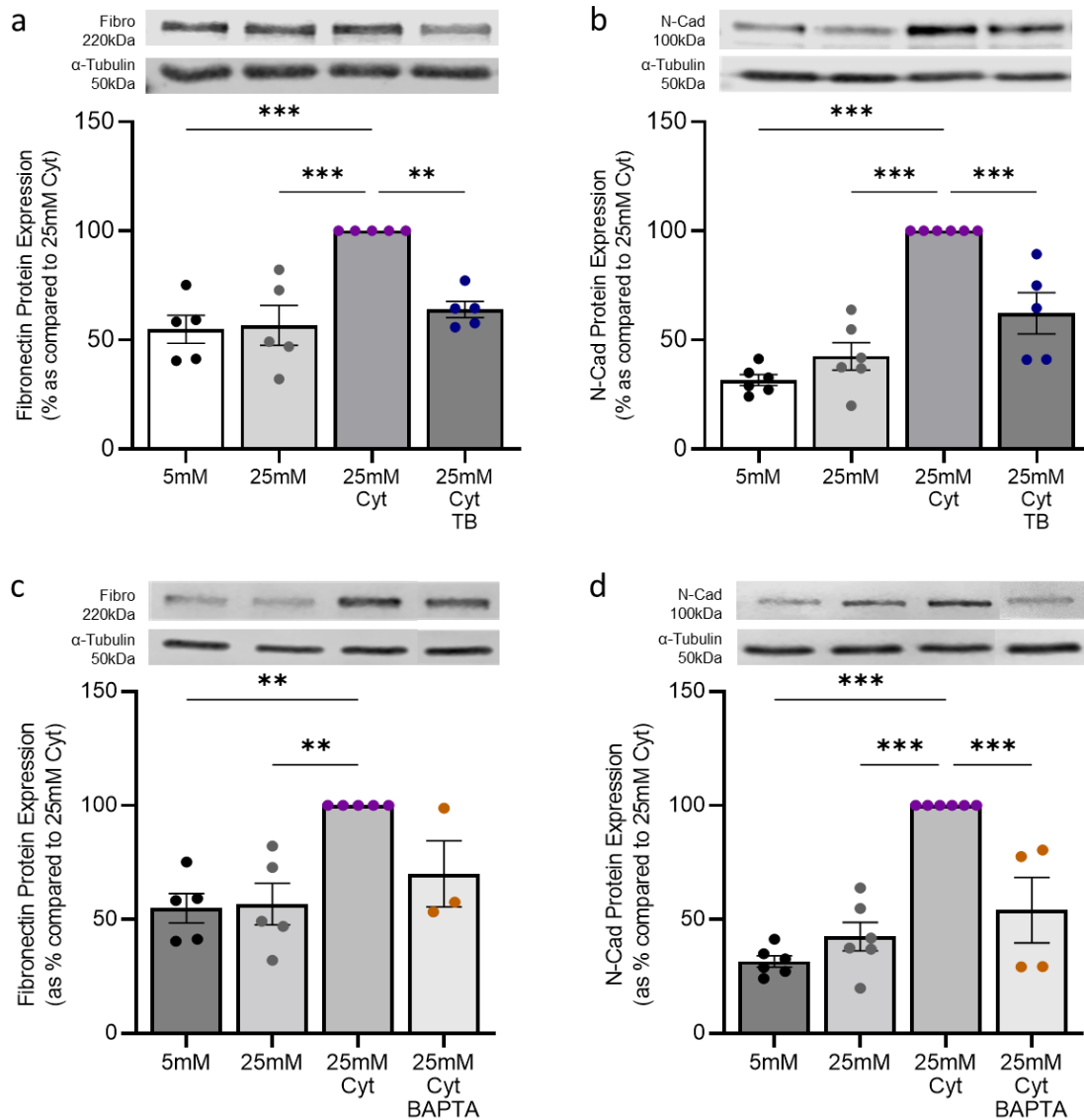


Figure 4.9. An IL1 β , TNF α and 25mmol/L glucose-induced increase in expression of injury markers is associated with [Ca $^{2+}$] $_i$ gating of Cx43 hemichannel activity, which is negated by Tonabersat. Primary RPTEC cells were treated with 5mmol/L or 25mmol/L glucose +/- IL1 β (10ng/mL) and TNF α (10ng/mL; Cyt) +/- Tonabersat (TB; 50 μ M) +/- BAPTA (5 μ M) for 48 hours. Western blotting determined changes in protein expression of fibronectin (a, c) and N-Cadherin (b, d). Results were normalised against expression of housekeeping protein, α -Tubulin as a loading control. n=3-6. Significance is displayed as ** P <0.01, *** P <0.001.

4.3.8. Blocking ERK/MAPK and p38 signalling prevents Cx43 expression and hemichannel-mediated ATP release in IL1 β , TNF α and high glucose treated RPTECs.

Similar to the effect of altered [Ca²⁺]_i on Cx43 hemichannel gating, key signalling pathways involved in diabetic nephropathy, P38 and MAPK have also been linked to altered Cx43 activity in multiple models of disease (Liu *et al.*, 2019c; Wang *et al.*, 2019; Xing *et al.*, 2022). Therefore PD98059, a selective inhibitor of ERK cascades, and SB203580, a p38 MAPK inhibitor, were used to investigate if blocking these signalling pathways modified Cx43 hemichannel activity. Primary RPTEC cells were treated with 5mmol/L or 25mmol/L glucose +/- IL1 β (10ng/mL) and TNF α (10ng/mL) +/- PD98059 (50 μ M) +/- SB203580 (10 μ M) for 48 hours.

Figure 10 illustrates that inhibition of ERK signalling can reduce an IL1 β , TNF α and 25mmol/L glucose-mediated increase in Cx43 protein expression (62 \pm 7.0%, P <0.001) by 48 \pm 8.5% (P <0.001) back towards 5mmol/L control (Figure 4.10b). Evidence for the involvement of ERK in Cx43 hemichannel activity was strengthened by data showing that inhibition of this signalling protein was able to negate a cytokine and high glucose-mediated increase in hemichannel-mediated dye uptake (61 \pm 3.2%, P <0.001; Figure 4.10a&c) and ATP release (54 \pm 6.4%, P <0.001) by 43 \pm 6.4% (P <0.001) and 89 \pm 3.3% (P <0.001; Figure 4.10d) respectively.

Inhibition of p38 significantly suppressed an IL1 β , TNF α and 25mmol/L glucose increase in Cx43 protein expression (62 \pm 7.0%, P <0.001; Figure 4.11b) and hemichannel dye uptake (61 \pm 3.2%, P <0.001) by 48 \pm 7.1% (P <0.001) and 41 \pm 10% (P <0.001; Figure 4.11a&c) respectively. However, this inhibitory effect did not extend to ATP release, which was unaltered by SB203580 (Figure 4.11d). Together, these results support a role for ERK signalling in regulating Cx43 expression and hemichannel activity in cells stimulated with IL1 β and TNF α in high glucose, whilst indicating that p38 signalling regulates Cx43 expression, but does not directly regulate Cx43 gating.

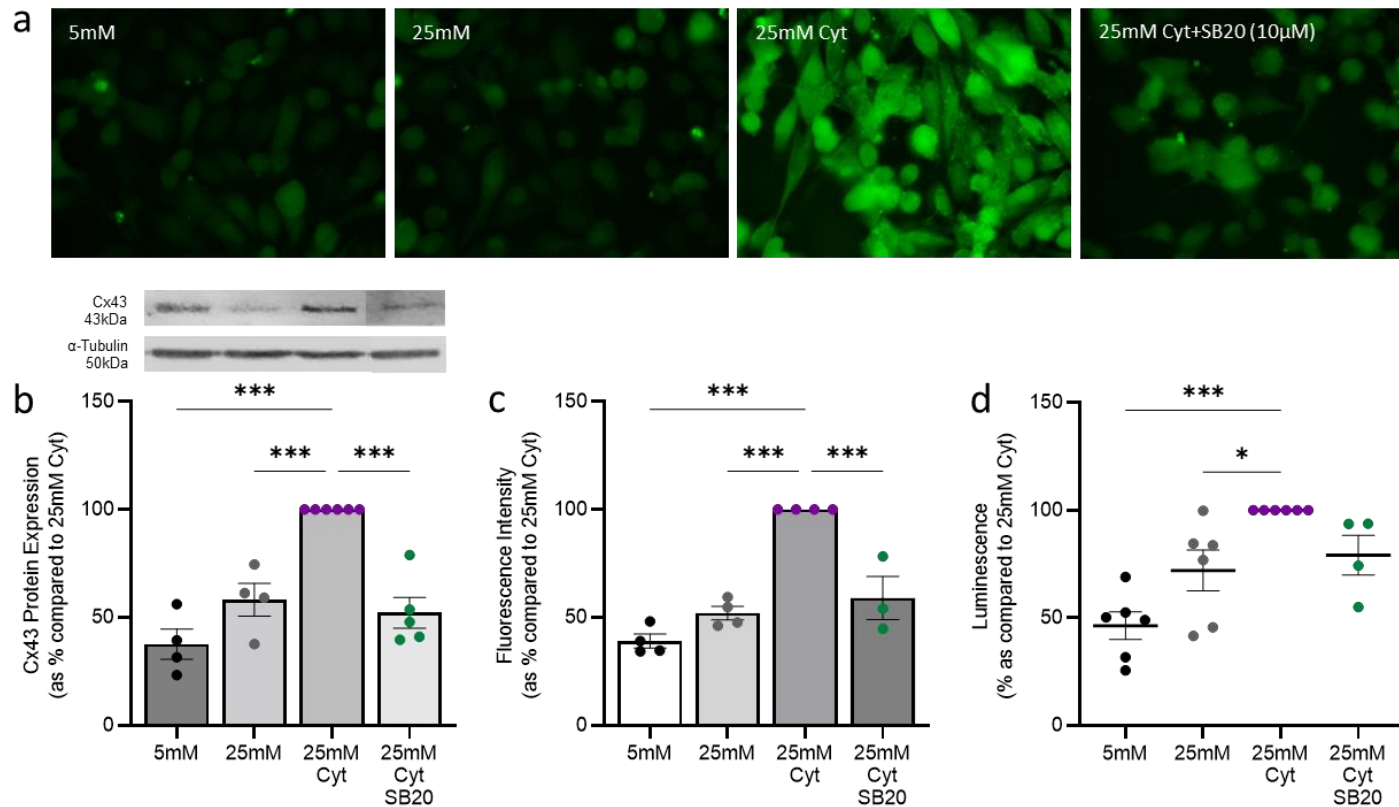


Figure 4.11. An IL1 β , TNF α and 25mmol/L-induced increase in Cx43 expression and hemichannel-mediated dye uptake is partially mediated through p38 signalling. HK-2 cells were treated with 5mmol/L or 25mmol/L glucose +/- IL1 β (10ng/mL) and TNF α (10ng/mL; Cyt) +/- SB203580 (SB20; 10μM) for 48 hours. Western blotting determined changes in protein expression of Cx43 (b). Results were normalised against expression of housekeeping protein, α -Tubulin as a loading control. Carboxyfluorescein dye uptake studies determined change in hemichannel number at the cell surface (a) which was quantified using Fiji software (c). An ATPlite luminescence assay measured cellular release of ATP into the supernatant (d). n=3-6. Significance is displayed as * P <0.05, *** P <0.001.

4.3.9. Aberrant Cx43 hemichannel activity upregulates markers of tubular injury in part through ERK and p38 MAPK signalling.

With evidence that ERK and p38 MAPK signalling are linked to altered Cx43 expression (ERK & p38) and increased hemichannel-mediated ATP release (ERK only), western blotting was used to assess if blocking these pathways impacted on expression of key injury markers, changes previously linked to aberrant Cx43 hemichannel activity (section 4.3.6). Following an IL1 β , TNF α and 25mmol/L glucose-mediated increase in N-cadherin ($45\pm6.4\%$, $P<0.01$) and fibronectin ($68\pm2.5\%$, $P<0.001$) expression, a role for ERK and P38 signalling in contributing to these changes was assessed in cells co-incubated with PD98059 (50 μ M) and SB203580 (10 μ M).

Inhibition of ERK downregulated the IL1 β , TNF α and high glucose-induced increase ($45\pm6.4\%$, $P<0.01$) in N-cadherin expression by $37\pm5.9\%$, ($P<0.001$; Figure 4.12b) but failed to significantly reduce the $68\pm2.5\%$ ($P<0.001$) increase in fibronectin (Figure 4.12a). These data support a role for ERK signalling in regulating changes in injury marker expression whilst highlighting the potential involvement of other signalling pathways. One of these alternative pathways involves p38 signalling, which when inhibited significantly reduced expression of both fibronectin ($47\pm7.7\%$, $P<0.01$; Figure 4.12c) and N-cadherin ($28\pm9.5\%$, $P<0.01$; Figure 4.12c).

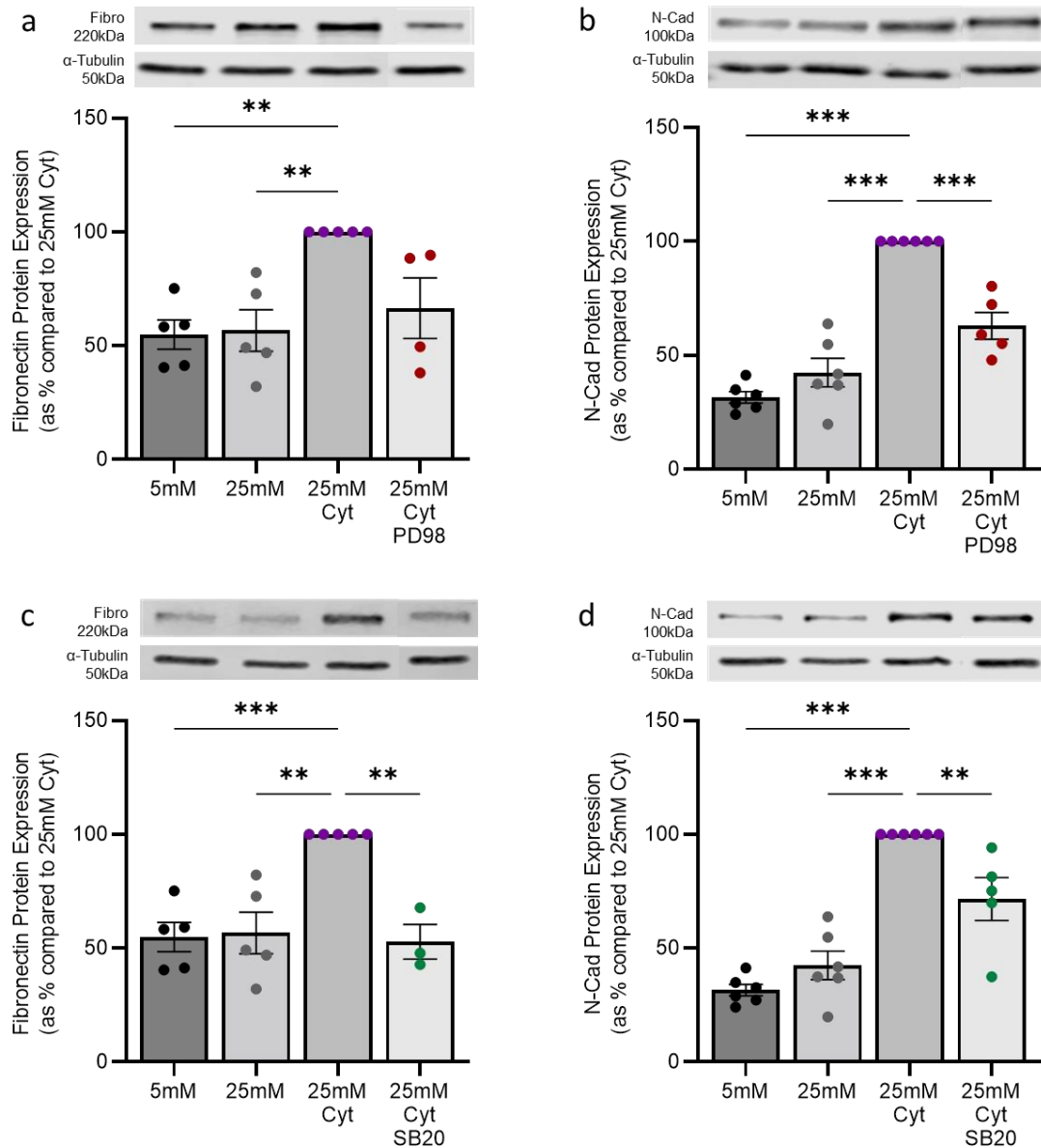


Figure 4.12. IL1 β , TNF α and 25mmol/L glucose-mediated upregulation of adherens junction and fibrosis associated markers is partially mediated by p38 and ERK/MAPK signalling in proximal tubule epithelial cells. HK-2 cells were treated with 5mmol/L or 25mmol/L glucose +/- IL1 β (10ng/mL) and TNF α (10ng/mL; Cyt) +/- PD98059 (PD98; 50 μ M) +/- SB203580 (SB20; 10 μ M) for 48 hours. Western blotting determined changes in protein expression of fibronectin (a, c) and N-Cadherin (b, d). Results were normalised against expression of housekeeping protein, α -Tubulin as a loading control. n=3-6. Significance is displayed as ** P <0.01, *** P <0.001.

4.4. Discussion

Transmembrane protein, Cx43 has been implicated in the pathogenesis of secondary microvascular complications of diabetes including retinopathy (González-Casanova *et al.*, 2021) and impaired wound healing (Montgomery *et al.*, 2018). Previous research by our group has demonstrated elevated levels of tubular Cx43 in renal biopsy material from people with diabetic nephropathy and in TGF β 1 stimulated HK-2 and RPTEC cells (Hills *et al.*, 2018). In the current chapter, I performed transcriptomic analysis of publicly available datasets and present for the first time, novel data which outlines a link between increased Cx43 expression in the tubules of people with diabetic nephropathy to a decline in kidney function, as evidenced by a correlation linking increased Cx43 expression to increased proteinuria. These observations are substantiated by immunostaining which shows elevated Cx43 in renal biopsy from people with CKD, which increases with severity of disease (Abed *et al.*, 2014). Recent findings by Xu *et al.*, also showed that a progressive increase in Cx43 expression correlates with the severity of injury in the mouse UUO model of advanced kidney inflammation and fibrosis (Xu *et al.*, 2022). Having established an association between Cx43 expression and renal injury in human biopsy, I looked to further delineate the role of Cx43 in disease ahead of assessing the therapeutic potential of blocking these effects in an *in vitro* model of CKD.

As a known Cx43 hemichannel blocker (Lyon *et al.*, 2021a; Kim *et al.*, 2017), Tonabersat was used to elucidate the role of Cx43 hemichannels in driving disease progression and evaluate its ability to block Cx43 hemichannel activity and subsequent markers of injury in order to assess its potential efficacy as a therapeutic for diabetic nephropathy. Data in diabetic retinopathy illustrates the ability of multiple hemichannel blockers, primarily Peptide5, in blocking Cx43-mediated ATP release and expression of downstream inflammatory and fibrotic markers (Mugisho *et al.*, 2018a; Mugisho *et al.*, 2019; Kuo *et al.*, 2020). Peptide5 has also been shown to alleviate pEMT and fibrosis through reduced Cx43-mediated ATP release in *in vitro* and *in vivo* models of diabetic nephropathy (Potter *et al.*, 2021a; Price *et al.*, 2020). Interestingly, my experiments demonstrated that whilst Peptide5 significantly reduced Cx43-mediated dye uptake, Tonabersat was more effective in blocking Cx43 hemichannel activity overall. A benzopyran derivative, Tonabersat blocks Cx43 hemichannel opening at low concentrations and Cx43 gap junctions at higher concentrations, though the exact mechanisms are currently unknown (Lyon *et al.*, 2021a). My data demonstrates that ATP release is blocked at a concentration of 50 μ M but not 100 μ M, suggesting that at

100µM Tonabersat may be more efficacious as a gap junction modifier, although this has not been tested in the current programme of investigation.

Use of Tonabersat in diabetic retinopathy has proved beneficial in IL1 β , TNF α and high glucose challenged retinal pigment epithelial cells. Blocking hemichannels reduced phenotypic alterations typical of pEMT (Lyon *et al.*, 2021b), and decreased the release of pro-inflammatory cytokines as a result of diminished NLRP3 inflammasome activation (Lyon *et al.*, 2021a). Additionally, *in vivo* experiments in a spontaneously diabetic strain of Sprague Dawley (SD) rats presenting with diabetic retinopathy, report that Tonabersat treated animals show decreased aneurysms and inflammation whilst preserving vascular integrity and retinal function (Green *et al.*, 2019). Further to this, an *ex vivo* human organotypic retinal model of diabetic retinopathy consisting of human donor retinal explants treated with pro-inflammatory cytokines IL1 β and TNF α in the setting of high (25mmol/L) glucose was used as a more physiologically relevant model (Louie *et al.*, 2021). Again, results showed that treatment with Tonabersat protected against NLRP3 inflammasome assembly and subsequent release of pro-inflammatory cytokines (Louie *et al.*, 2021). These data contributed to the progression of Tonabersat to phase II clinical trials with diabetic retinopathy, a trial to which an amendment has recently been made to now include assessment of changes in kidney function as an exploratory outcome (Clinical Trials Identifier: NCT05727891). This amendment has been made in light of observations linking the incidence of retinopathy to nephropathy and vice versa.

Consistent with these findings, here I demonstrate that Tonabersat negates proximal tubule injury downstream of Cx43 hemichannel activity in an *in vitro* model of diabetic nephropathy (RPTECs and HK-2 cells). Western blotting demonstrated the ability of Tonabersat to significantly block an IL1 β , TNF α and high glucose sensitive increase in the expression of pro-inflammatory cytokine IL6, adherens protein N-cadherin, and fibrosis associated proteins fibronectin, collagen I and collagen IV. The epithelial protein E-cadherin was not affected. In support of these findings, experiments using the Cx43^{+/-} UUO mouse model of renal fibrosis showed that a 50% reduction in Cx43 expression ameliorated changes associated with pEMT and fibrosis, including increased N-cadherin and β -Catenin. Interestingly these changes were paralleled by restoration of expression of ZO-1 and E-cadherin, suggesting that whilst we failed to observe an effect of Cx43 HC blockade on E-cadherin expression, these data suggest that Cx43 may regulate E-cadherin via non hemichannel-mediated effects.

Connexin hemichannels are gated in response to several mechanisms, including the regulation of intracellular or extracellular calcium (Ca^{2+}) ions (Van Campenhout *et al.*, 2021). Concentrations of extracellular calcium ($>1\text{mmol/L}$) maintain hemichannels in the closed state under physiological conditions, preventing the release of small molecules and ions, including ATP (Krebs, 2018). Use of calcium chelator BAPTA reduced intracellular calcium to close hemichannels. The effect mimics that of the Cx43 blocker Tonabersat and supports the role of hemichannel closure in negating the effects of $\text{IL1}\beta$, $\text{TNF}\alpha$ and high glucose stimulation. Chelation of calcium via BAPTA reduced expression of the mesenchymal marker N-cadherin, most likely due to reduced levels of intracellular calcium, which can reduce connexin hemichannel open probability through inhibition of a calmodium-dependant cascade (Sáez and Green, 2018). The effects of BAPTA on N-cadherin have been well established in models of cancer, in which EMT is essential for metastasis and regulated via $[\text{Ca}^{2+}]_i$. In melatonin treated sarcoma cells, a decrease in cytoplasmic and mitochondrial Ca^{2+} reduced expression of markers associated with EMT, including N-cadherin, effects which were enhanced when co applied with BAPTA (Sánchez-Sánchez *et al.*, 2022). Furthermore, BAPTA reduced N-cadherin upregulation in mono-cultured human melanoma A375 cells, mimicking the $[\text{Ca}^{2+}]_i$ effects of human keratinocytes (Chung *et al.*, 2018). Increased N-cadherin was detected in human ovarian cancer samples, along with other EMT markers Vimentin and Twist. Elucidating the mechanisms behind this increase, a BAPTA-mediated reduction in intracellular Ca^{2+} was shown to reduce expression of N-cadherin in human ovarian cancer CAOV-3, A2780, OVCAR3, PA-1 and SKOV3 cells (Liu *et al.*, 2019b)

Whilst not significantly reduced, the cytokine-evoked expression of fibronectin exhibited a clear decrease in expression in cells pre-incubated with BAPTA. Importantly, treatment with BAPTA abolished an increase in fibrosis associated proteins fibronectin, αSMA and collagen I, which were upregulated due to overexpression of S100A16, a gene activated downstream of $\text{TGF}\beta 1$ signalling in tubulointerstitial fibrosis (Jin *et al.*, 2021). Likewise, BAPTA was shown to reduce an angiotensin II (Ang II)-mediated increase in fibronectin and αSMA expression in glomerular mesangial cells (Pedroza *et al.*, 2019). Together these results further support a role for intracellular calcium in the regulation of Cx43 hemichannels and corroborate Tonabersat data, in which closure of Cx43 hemichannels protects against a cytokine-glucose-induced increase in fibronectin and N-cadherin.

To further elucidate how $\text{IL1}\beta$ and $\text{TNF}\alpha$ when in combination with high glucose modulates hemichannel activity, a role for non-canonical signalling intermediates were

assessed utilising inhibitors against ERK cascades and p38. The proteins ERK and p38 are part of the MAPK family of serine/threonine protein kinases that promote intracellular signal transduction in order to regulate cell mechanisms including proliferation (Wei *et al.*, 2002), differentiation (Kurtzeborn *et al.*, 2019) and apoptosis (Yue and López, 2020). Non-canonical MAPK signalling is also implicated in inflammatory, oxidative, and apoptotic processes, all of which are integral to the onset and progression of diabetic nephropathy. In human diabetes and mouse models of diabetes (streptozotocin-induced-T1DM and db/db type 2 diabetic mice), increased phosphorylation of p38 was observed in kidney biopsies, associated with hyperglycaemia, albuminuria and interstitial fibrosis (Adhikary *et al.*, 2004). In addition, inflammatory cytokines IL1 β and TNF α are shown to induce p38-MAPK signalling pathways, as demonstrated in IL1 β treated pericytes (Yun *et al.*, 2021) and rat chondrocytes (Huang *et al.*, 2018) and TNF α treated bronchial epithelial cells (Wang *et al.*, 2022) and osteocytes (Zheng *et al.*, 2020). Evidenced in rat islet cells, IL1 β , TNF α and high glucose initiate a stress-induced cascade of protein kinase activation resulting in phosphorylation of p38 MAPK, activating cellular processes including inflammation, apoptosis, and necrosis (Schwarznau *et al.*, 2009)

To evaluate the involvement of non-canonical signalling, I employed a cell permeable ERK/ERK1/MEK2 inhibitor, PD98059, to investigate the effects of blocking ERK signalling (Alessi *et al.*, 1995). Research by Che *et al.*, 2016 has previously reported that ERK signalling is downstream of high glucose-induced expression of mesenchymal markers in retinal pigment epithelial cells (Che *et al.*, 2016), a process that I have shown to be mediated by Cx43 hemichannel activity in renal epithelial tubule cells. Here I demonstrate that inhibition of non-canonical ERK signalling significantly reduced hemichannel activity, as determined by decreased carboxyfluorescein dye uptake and ATP release in addition to downstream expression of mesenchymal marker, N-cadherin, supporting previous findings by Che *et al.* Interestingly, Abed *et al.*, found that UUO mice treated with a Cx43 antisense (Cx43 AS-ODN), exhibited a decrease in ERK signalling leading to the attenuation of E-cadherin downregulation and collagen I mRNA upregulation (Abed *et al.*, 2014). Whilst our results show that blocking Cx43 hemichannels does not attenuate E-cadherin expression, the use of Cx43 antisense suggests that altered E-cadherin expression occurs as a result of Cx43 hemichannel independent effects (Abed *et al.*, 2014). Together these results suggest the presence of a feedback loop in which ERK phosphorylation and downstream signalling mediates altered Cx43 expression and hemichannel activity, and subsequent increases in ERK signalling. Therefore, blocking

the activity of one inhibits the stimulation of the other, protecting against downstream changes in expression of pEMT and ECM associated proteins linked to progression of DN.

Contrary to these findings, in high glucose treated osteocytes, Cx43 expression and hemichannel activity is reduced, effects dependent on p38/ERK activation and subsequent Cx43 internalisation (Yang *et al.*, 2020b). Also, a member of the MAPK family and often working in tandem with ERK signalling, pyridinyl imidazole P38/Akt MAPK inhibitor, SB203580 (Lali *et al.*, 2000) was used to investigate the effect on Cx43 hemichannel activity in proximal tubule epithelial cells. The data demonstrate that inhibition of p38 significantly inhibits dye uptake, but not ATP release, thus suggesting p38 is involved in Cx43 expression but not gating. Subsequently reduced expression of pEMT and fibrosis markers, N-cadherin and fibronectin suggest p38 may have Cx43 hemichannel independent effects leading to altered expression of injury markers. Similarly, in high glucose treated human endothelial cells, p38 MAPK signalling led to increased intracellular calcium and subsequently increased Cx43 hemichannel-mediated ATP release (Sáez *et al.*, 2018). In renal podocytes, TGF β 1 is shown to drive p38 activation and downstream altered Cx43 expression and function (Kavvadas *et al.*, 2017). A key protein upregulated in CKD and shown to drive proximal tubule damage through increased pEMT and fibrosis, TGF β 1-mediated these effects through activation of ERK and p38 signalling, as well as Wnt/ β -Catenin and NF κ B signalling and subsequent increased Cx43 hemichannel activity (Chakravarthy *et al.*, 2018; Tacheau *et al.*, 2008; Potter *et al.*, 2021a). In addition to reduced Cx43 hemichannel activity, inhibition of p38 and ERK also reduced expression of Cx43. Together these findings highlight the importance of non-canonical p38 and MAPK signalling in regulating Cx43 hemichannel activity.

Due to its plethora of pro-inflammatory effects, p38 is a major target for the treatment of chronic inflammatory diseases. Although evaluated in phase I/II clinical trials, progression to phase III of p38 inhibitors has been hampered by a multitude of contraindications including hepatotoxicity and tumour growth (Singh *et al.*, 2018). Furthermore, whilst the use of ERK inhibitors as a cancer immunotherapy treatment is currently under investigation, with several currently in clinical trials, no selective ERK inhibitors have been approved for the market to date (Pan *et al.*, 2022). This is in-part due to issues with toxicity, with common side effects including diarrhoea, nausea, fatigue, dermatitis acneiform, asthenia and less commonly neurotoxicity (Chin *et al.*, 2019). Targeting up or downstream of P38/ERK signalling could be achieved effectively by Cx43 hemichannel blockers.

In conclusion, this chapter demonstrates an IL1 β , TNF α and high glucose-mediated increase in Cx43 hemichannel activity and resultant ATP release, leading to altered expression of downstream markers associated with inflammation, pEMT and fibrosis in clonal and primary human renal tubule cells. I confirm the ability of Tonabersat to effectively block the opening of Cx43 hemichannels in response to IL1 β , TNF α and 25mmol/L glucose, resulting in reduced extracellular ATP release and expression of injury markers associated with cellular injury in DN. Further to this, Tonabersat treatment reduced injury elicited by cytokines and high glucose through ERK and p38 MAPK signalling pathways and subsequent Cx43 hemichannel opening. Together with findings in other chronic inflammatory diseases, specifically diabetic retinopathy, our data highlight the potential benefit of targeting Cx43 hemichannels using Tonabersat in diabetic nephropathy.

5.0. Elucidating the role of connexin 43 hemichannel activity in priming and activation of the NLRP3 inflammasome, initiating a perpetual inflammatory cycle.

5.1. Introduction

Inflammation is the major pathology underlying tubulointerstitial fibrosis (Albino *et al.*, 2021), key to which is activation of the NLRP3 inflammasome. The inflammasome is an immune complex which regulates the innate inflammatory response to both exogenous and endogenous stimuli such as extracellular ATP and pathogens, including bacteria and fungi (Fusco *et al.*, 2020). In health NLRP3 activity is tightly regulated, whilst dysregulation stimulated by injury is strongly associated with chronic inflammatory diseases (Chen *et al.*, 2021), including atherosclerosis (Sharma *et al.*, 2021), Alzheimer's (Heneka *et al.*, 2013) and rheumatoid arthritis (Yin *et al.*, 2022). Assembly and activation are dependent upon two steps. The first is priming, consisting of NF κ B-mediated transcription of inflammasome components including NLRP3, IL1 β and IL18 in response to extracellular stimuli (Bauernfeind *et al.*, 2009). Activation is the second stage and can occur independently or in conjunction with step 1. Here, activation of purinergic P2X7 receptor triggers an influx of calcium and an efflux of potassium, events which enable the formation of the inflammasome complex (Wang *et al.*, 2020). Consisting of NLRP3, ASC and pro-caspase 1, NLRP3 complex assembly leads to caspase 1-mediated cleavage of pro-IL1 β and pro-IL18 into to their mature forms (Guey *et al.*, 2014).

Research in both type 1 and type 2 diabetes has demonstrated that inflammasome activity is central to changes in insulin resistance, glucose tolerance and inflammation (Ding *et al.*, 2019). Additionally, the effects of NLRP3 activation are integral to the underlying pathology of secondary microvascular complications of diabetes, including diabetic retinopathy (Ge *et al.*, 2022), impaired diabetic wound healing (Huang *et al.*, 2020) and diabetic kidney disease (Ram *et al.*, 2020; Feng *et al.*, 2021). Recent studies link DN and Alzheimer's disease, with inflammasome inhibition via MCC950 mediating reduced insulin resistance, reduced circulating insulin levels and improved regulation of insulin, inflammation and endoplasmic reticulum stress signalling pathways (Hull *et al.*, 2020). Targeting NLRP3 inflammasome activity is of clear therapeutic potential in the future management of both diabetic nephropathy and other microvascular secondary complications of diabetes.

Whilst diabetic nephropathy is considered a glomerular disease in origin, tubulointerstitial injury dictates disease progression, and correlates to the rate of entry into ESRD (Liu *et al.*, 2018). Proximal tubule injury occurs primarily in response to pathological factors including increased inflammation (Pérez-Morales *et al.*, 2019), fibrosis (Zeng *et al.*, 2019), immune cell recruitment (Zheng and Zheng, 2016), EMT (Sheng and Zhuang, 2020) and ECM deposition (Zhao, Zou and Liu, 2020). Specifically, priming and activation of the NLRP3 inflammasome is instrumental to the development and progression of tubulointerstitial inflammation in multiple forms of CKD, including diabetic kidney disease (Ding *et al.*, 2018; Zhang and Wang, 2020). Inflammasome components NLRP3 and IL1 β exhibit increased expression in renal biopsies isolated from people with diabetic nephropathy (Cheng *et al.*, 2021) as compared to healthy controls, with NLRP3 activity significantly higher in people with tubular injury as opposed to those without (Cheng *et al.*, 2021). Furthermore, in renal biopsies isolated from both people with diabetic nephropathy and STZ-induced diabetic mice (C57BL/6J), microRNA-10 (miR-10), a negative regulator of NLRP3 expression, showed reduced expression. These changes were paralleled by increased NLRP3 activity (Ding *et al.*, 2021). In corroboration of these findings, STZ mice overexpressing miR-10 had reduced inflammasome activation as compared to WT STZ-treated mice. This protected against an STZ-induced increase in albuminuria, mesangial expansion and inflammation, improving overall kidney function (Ding *et al.*, 2021). The mechanisms by which inflammasome activation contributes to injury have been determined in part by further *in vivo* and *in vitro* studies.

Inflammasome activity has also been linked to the onset of EMT. A characteristic of tubulointerstitial fibrosis, EMT is the trans-differentiation of epithelial cells to a myofibroblast-like phenotype, increasing tubulointerstitial fibrosis (Sheng and Zhuang, 2020). Research by Song *et al.*, showed that high (30mmol/L) glucose treated HK-2 cells exhibited increased NLRP3 inflammasome activation, as evidenced by increased mRNA and protein expression of NLRP3, ASC, caspase 1, active IL1 β and active IL18 (Song *et al.*, 2018), corroborating previous findings by Hou *et al.*, 2021. In addition, use of NLRP3 short hairpin (sh)RNA and inflammasome blocking antioxidant N-acetyl-L-cysteine (NAC), prevented morphological changes characteristic of EMT and reduced the increase and decrease in expression of EMT markers α SMA and E-cadherin (Song *et al.*, 2018) respectively. A consequence of inflammation and EMT, tubulointerstitial fibrosis culminates in irreversible damage and loss of renal function. Inhibition of NLRP3 activation in STZ-treated mice using antioxidant 4-hydroxy-3-methoxyacetophenone (apocynin) decreased tubular expression of fibrotic markers

TGF β 1, fibronectin and collagen I, culminating in lower urinary creatinine levels and ultimately improved renal function (Xin *et al.*, 2018). These findings further support the hypothesis that inflammasome activation is pivotal in mediating renal tubule damage, through initiation of inflammation, EMT and fibrosis.

Whilst increased Cx43 expression in the UUO kidney has been linked to inflammation, studies in other tissue types have linked Cx43 hemichannel activity to NLRP3 inflammasome activation in multiple chronic inflammatory diseases. Evidencing a relationship between Cx43 and NLRP3, an animal model of peripheral nerve injury previously demonstrated an upregulation of Cx43 and essential NLRP3 inflammasome components (Tonkin *et al.*, 2018). With Cx43 hemichannel-mediated ATP release a known activator of the inflammasome, a role for Cx43 hemichannels in activating downstream inflammasome activity was evaluated through assessment of expression of NLRP3, ASC and Caspase 1 in mice treated with Cx43 hemichannel blocker Peptide5. Expression of all three components were significantly reduced to near basal, effects paralleled by a reduction in spinal glial activation and pain hypersensitivity (Tonkin *et al.*, 2018). Interestingly, in an animal model in which there was no increase in NLRP3 post injury Peptide5 had no effect, suggesting that Peptide5 confers protection through blocking inflammasome activation downstream of Cx43 hemichannel activity (Tonkin *et al.*, 2018).

A microvascular complication of diabetes, changes that occur at the back of the eye in diabetic retinopathy develop in response to similar molecular mechanisms as observed in the kidney tubules of the diabetic kidney (Zhang *et al.*, 2018). Interestingly, the link between Cx43 hemichannel activity and inflammasome activity has been established in multiple models of diabetic retinopathy (Mugisho *et al.*, 2018a), suggesting that a similar relationship may drive inflammation in diabetic kidney disease. Retinal pigment epithelial cells treated with a combination of high glucose, IL1 β and TNF α as an *in vitro* model of diabetic retinopathy, reportedly exhibit an increase in NLRP3 inflammasome complex formation and release of the pro-inflammatory cytokines IL6, IL8, MCP-1, ICAM-1 and VEGF (Mugisho *et al.*, 2018a). Blocking Cx43 hemichannel ATP release using Peptide5 also prevented the upregulation of inflammasome formation and cytokine release, a response negated by the exogenous addition of ATP, confirming a role for Cx43 hemichannel activity in activation of the inflammasome (Mugisho *et al.*, 2018a). Similarly in an *in vivo* model of diabetic retinopathy, Peptide5 treatment negated an IL1 β and TNF α -mediated increase in inflammasome complex formation demonstrated by immunohistological staining of NLRP3 and ASC, in lean diabetic mice (Mugisho *et al.*, 2019). Prevention of Cx43-mediated inflammasome formation resulted

in reduced vascular leak and oedema, protecting against diabetic retinopathy (Mugisho *et al.*, 2019).

Building upon a wealth of *in vitro* and *in vivo* evidence which demonstrates that blocking Cx43 hemichannels can inhibit inflammasome activation in models of diabetic retinopathy, human donor retinal explants treated with high glucose, IL1 β and TNF α were used as an *ex vivo* human organotypic retinal culture model of diabetic retinopathy (Louie *et al.*, 2021). In this physiologically relevant model, treatment with Cx43 hemichannel blocker Tonabersat reduced NLRP3 activation as evidenced by reduced inflammasome complex formation and caspase 1-mediated cleavage of IL1 β and IL18 (Louie *et al.*, 2021). Thus far, research has demonstrated a Cx43-mediated increase in inflammation (Guo *et al.*, 2016; Mugisho *et al.*, 2018a), EMT (Lyon *et al.*, 2021b) and fibrosis (Shi *et al.*, 2022) through activation of the NLRP3 inflammasome in diabetic retinopathy (Louie *et al.*, 2021). Despite being similar in both aetiology and pathogenesis, and incidence of both being linked, suggesting a common underlying mechanism, a link between Cx43 and inflammasome activity remains to be established in the diabetic kidney. Furthermore, there is no evidence outlining the direct role of tubule Cx43 in mediating this damage. Identifying this link could provide a novel therapeutic target for the treatment of late-stage kidney disease where tubulointerstitial fibrosis represents the underlying pathology.

5.2. Aims-

It is well established that priming and activation of the NLRP3 inflammasome plays a pivotal role in numerous chronic inflammatory diseases. On the basis that connexin hemichannels mediate aberrant ATP release leading to inflammasome activation in the diabetic eye, in the current chapter, I determine a role for Cx43 hemichannel activity in regulating inflammasome activity in both an *in vivo* and *in vitro* model of tubulointerstitial inflammation and fibrosis.

Specifically, I aim to-

- Assess expression of NLRP3 inflammasome markers in human renal biopsies isolated from people with DN and determine a correlation between altered expression and kidney function.
- Assess expression of NLRP3 inflammasome markers and associated downstream markers in an *in vivo* mouse model of kidney injury.
- Establish a link between increased tubule Cx43 expression and renal inflammation in an *in vivo* Cx43 tubule knockout mouse model of advanced tubulointerstitial inflammation and fibrosis.
- Establish a link between Cx43 hemichannel-mediated ATP release and inflammasome activation in an *in vitro* model of renal inflammation.
- Investigate the ability of Cx43 hemichannel blocker Tonabersat in negating inflammasome activation and ameliorating downstream inflammatory and fibrotic injury *in vitro*.

5.3. Results-

5.3.1. Markers of inflammasome priming and activation are increased in diabetic and non-diabetic kidney disease.

Research to date demonstrates a clear increase in NLRP3 expression in both T2DM and diabetic nephropathy (Cheng *et al.*, 2021). However, the underlying mechanisms linking NLRP3 to the pathogenesis of diabetic nephropathy are yet to be fully elucidated. With late-stage kidney disease driven by the severity of proximal tubule injury, here, I use transcriptomic analysis of publicly available datasets to show that NLRP3 expression is significantly upregulated in the tubules of people with DN as compared to healthy donors (Woroniecka *et al.*, 2011; Figure 5.1a). This increased NLRP3 expression exhibits a positive correlation to both increased proteinuria (Schmid *et al.*, 2006; Figure 5.1b) and blood pressure (Ju *et al.*, 2015; Figure 5.1c), whilst elevated IL1 β correlates with a declining GFR (Schmid *et al.*, 2006; Figure 5.1d).

Activation of the NLRP3 inflammasome is dependent on caspase 1 cleavage with caspase 1 expression significantly upregulated in people with DN (Woroniecka *et al.*, 2011; Figure 5.2a) and CKD (Nakagawa *et al.*, 2015; Figure 5.2b). Like NLRP3 and IL1 β , increased caspase 1 expression correlates to a declining GFR (Woroniecka *et al.*, 2011; Figure 5.2c) and increasing proteinuria (Schmid *et al.*, 2006; Figure 5.2d). Collectively these observations suggest a key role for the NLRP3 inflammasome in driving loss of kidney function in CKD both with and without diabetes.

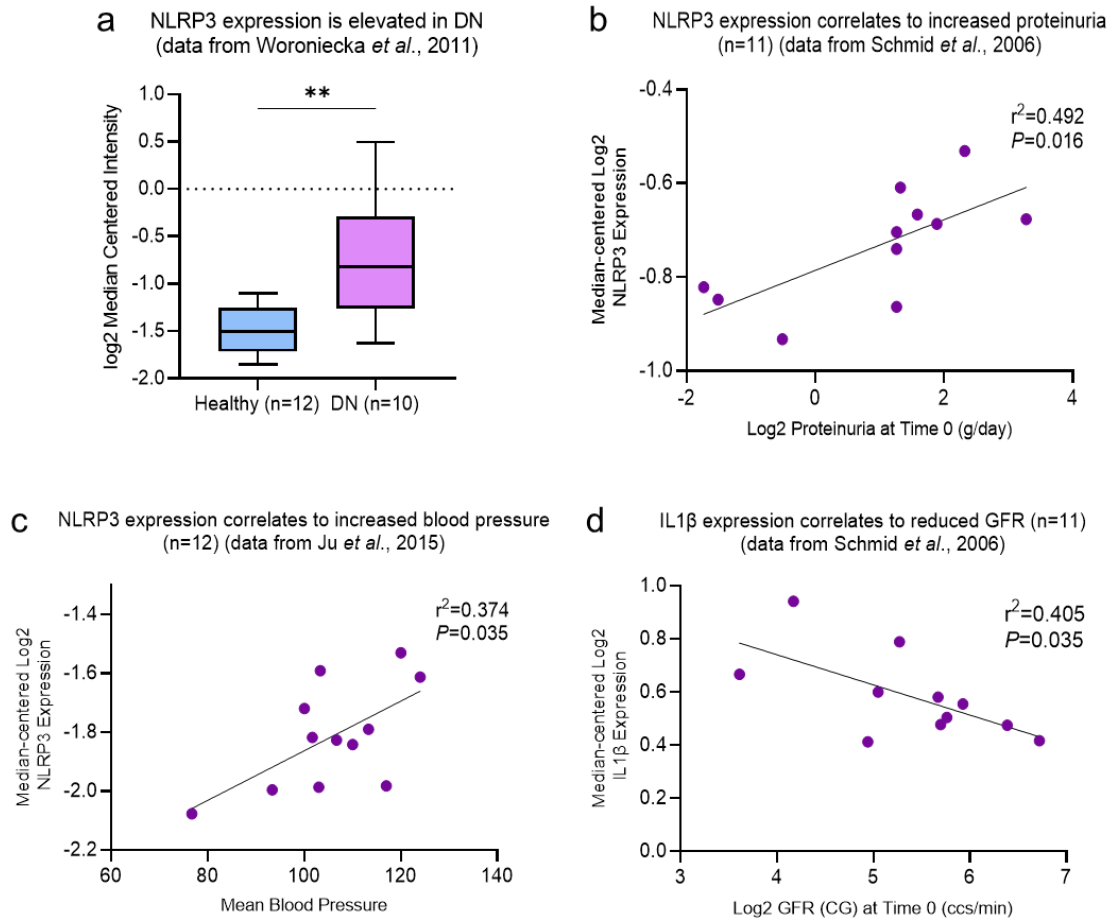


Figure 5.1. Increased expression of NLRP3 inflammasome proteins in human diabetic nephropathy biopsies correlate to measures of reduced renal function. Transcriptomic analysis was performed on Nephroseq publicly available data from Woroniecka *et al.*, 2011 (a) Schmid *et al.*, 2006 (b & d) and Ju *et al.*, 2015 (c) comparing mRNA expression in the tubules of kidney biopsies from healthy donors and donors with diabetic nephropathy. n is specified where appropriate. An unpaired t-test with Welch's correction analysis (a) and simple linear regression (b-d) were used for statistical analysis. Significance is displayed as ** $P<0.01$.

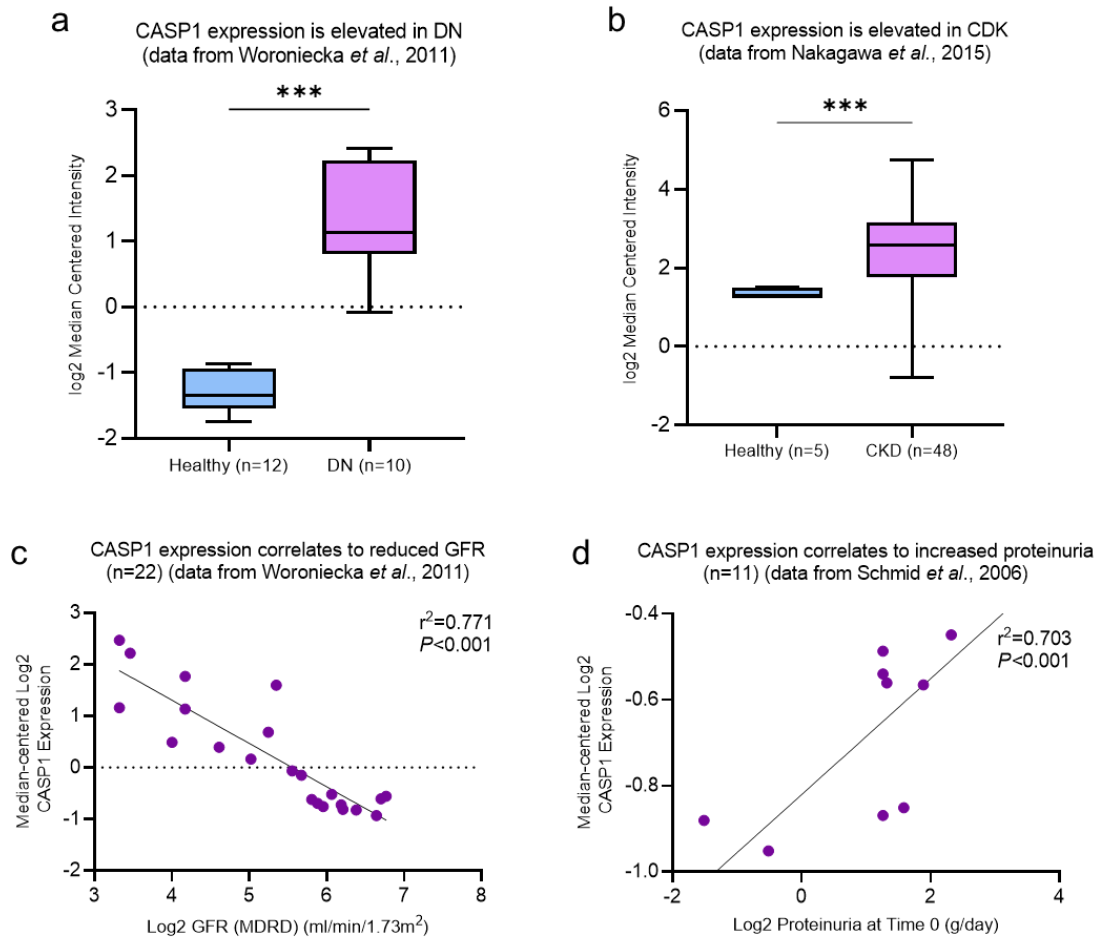


Figure 5.2. Increased caspase 1 (CASP1) expression in biopsies isolated from patients with diabetic nephropathy and chronic kidney disease correlates to measures of reduced renal function. Transcriptomic analysis was performed on Nephroseq publicly available data from Woroniecka *et al.*, 2011 (a & c), Nakagawa *et al.*, 2015 (b) and Schmid *et al.*, 2006 (d) comparing mRNA expression in the tubules of kidney biopsies from healthy donors and donors with diabetic nephropathy or chronic kidney disease. *n* is specified where appropriate. An unpaired t-test with Welch's correction analysis (a & b) and simple linear regression (c & d) were used for statistical analysis. Significance is displayed as *** $P<0.001$.

5.3.2. Increased tubule connexin 43 is linked to increased levels of NLRP3 in a mouse model of advanced interstitial inflammation and fibrosis.

Studies in a Cx43^{+/-} mouse model of CKD have determined that a 50% reduction in global expression of Cx43 is linked to decreased inflammation and fibrosis throughout the kidney (Abed *et al.*, 2014; Kavvadas *et al.*, 2017). The specific contribution of tubule Cx43 to this inflammation however remains to be reported, as does a link between Cx43 hemichannel activity and NLRP3 activation

With kidney tubules the principal site of late-stage kidney damage, our collaborator (Dr Chadjichristos, INSERM, Paris) used male mice of a C57BL/6 background to generate a transgenic tubule-directed Cx43^{-/-} UUO model in which tubule specific deletion of Cx43 allowed for its effect on the inflammasome to be assessed. Cx43^{flox/flox} mice were purchased from “the EMMA -European Mouse Putant Archive- consortium”. The strain of Cx43 tubular-specific deletion was created by Dr Chadjichristos as previously described (Kormann *et al.*, 2020). Briefly, Pax8-rtTA-LC1 were interbred with Cx43^{flox} mice (Pax8-rtTA-LC1/Cx43^{flox/flox}) and Cx43 deletion in renal tubular cells was induced by administering 0.2mg/mL doxycycline in drinking water containing 2.5% sucrose for 4 weeks, starting 1 month after birth. Then, 3-4 month-old mice were subjected to UUO as already described (Abed *et al.*, 2014). The UUO model is a model of advanced chronic kidney disease, that is widely used for studies of advanced interstitial inflammation and fibrosis, irrespective of the initiating cause (Martínez-Klimova *et al.*, 2019). It displays classical pathological features of late-stage disease including tubulointerstitial fibrosis, inflammation and immune cell infiltration (Martínez-Klimova *et al.*, 2019).

To examine the effect of Cx43 deletion alone, sugar was administered to Pax8-rtTA-LC1/Cx43^{flox/flox} transgenic mice, serving as controls for up to 4 months. All procedures regarding whole animal studies were in accordance with the European Union Guidelines for the Care and Use of Laboratory Animals and approved by the local ethics committee of INSERM. Animals were housed at a constant temperature with *ad libitum* access to water and food.

Mice were euthanized and kidneys removed 10 days post UUO and prepared using established methodologies (Abed *et al.*, 2014). Tissue was used for histology, antibody staining, and RNA extraction followed by RT-qPCR (Figure 5.3b), carried out by collaborators at INSERM. Immunostaining of the renal cortex with a Cx43 antibody confirmed an absence of Cx43 antibody staining in the tubules of UUO-Cx43^{-/-} as compared to UUO mice (Figure 5.3c). Analysis of Cx43 mRNA expression via RT-

qPCR confirmed that Cx43 deletion negated a UUO-induced increase in Cx43 mRNA expression from 1.7 ± 0.12 to 1.2 ± 0.11 ($P < 0.01$) as compared to control (1.0 ± 0.056 ; Figure 5.3d).

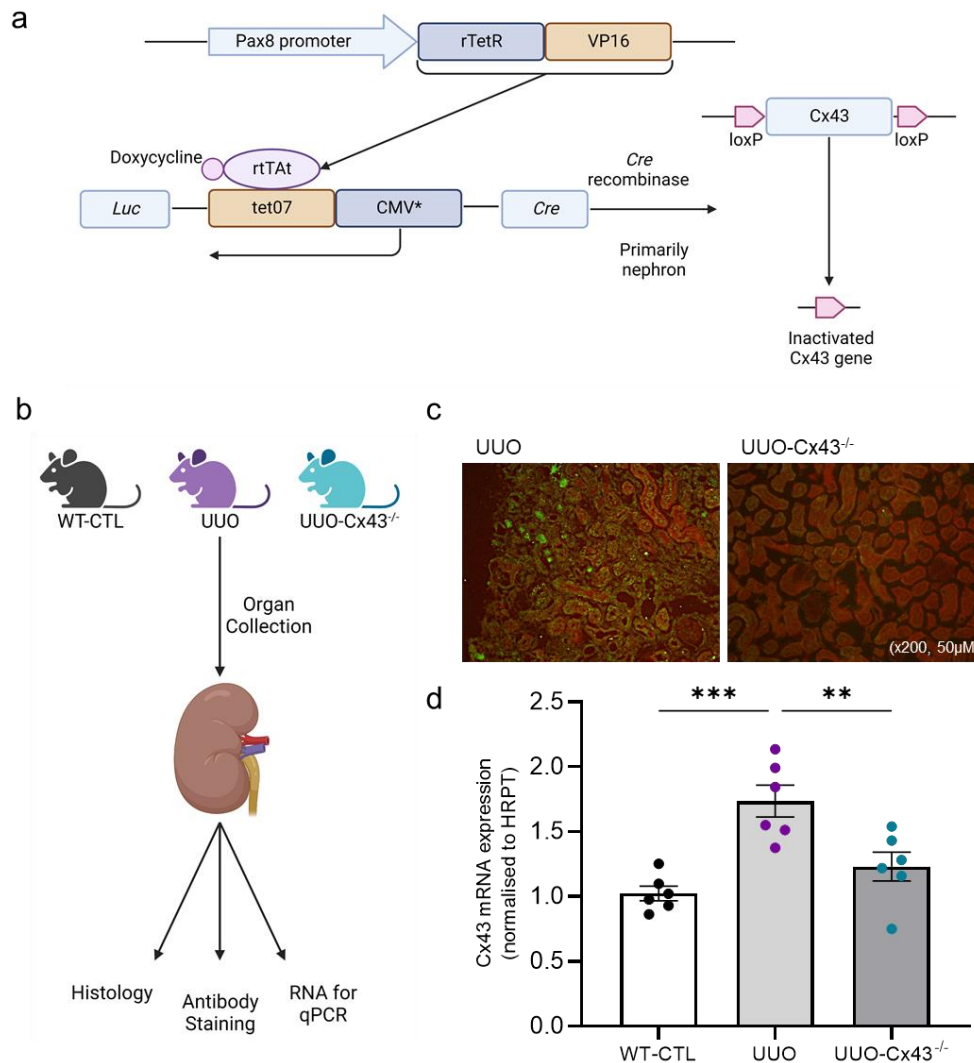


Figure 5.3. Confirming a connexin 43 gene deletion in the renal proximal tubules of mice following unilateral ureteral obstruction. A schematic illustrating the tubule specific Cx43 deletion induced by the administration of doxycycline (0.2mg/mL) in drinking water for 2 weeks in 1 month old Pax8-rtTA-cre:cx43 flox Cx43^{-/-} mice (a). Kidneys were harvested from wild type control (WT-CTL) mice, mice that had undergone UUO and UUO mice with a tubule Cx43 deletion (UUO-Cx43^{-/-}). Tissue was then used for histology and antibody staining in addition to RNA extraction and RT-qPCR to explore changes in tissue structure and mRNA and protein expression and localisation (b). All procedures involving animal material were carried out by collaborators at INSERM. Fluorescent antibody staining for Cx43 is shown in histological sections from both UUO and UUO-Cx43^{-/-} mice (c). Tubule RNA was extracted, and RT-qPCR was performed to determine changes in Cx43 mRNA expression normalised against housekeeping gene hypoxanthine guanine phosphoribosyl transferase (HRPT; d). n=6. Significance is displayed as ** $P < 0.01$ and *** $P < 0.001$.

After confirming tubule Cx43 deletion, the effects on expression of proteins associated with the inflammasome was assessed via multiple parameters. Immunostaining of the renal cortex, by collaborators at INSERM, with an NLRP3 antibody showed that tubule Cx43 deletion successfully reduced a UUO-mediated increase in NLRP3 staining, as compared to control, in addition to helping maintain renal cortex structure and integrity (Figure 5.4a). Specifically, mRNA expression of IL1 β (Figure 5.4b) and NLRP3 (Figure 5.4c), both markers of inflammasome priming, increased after UUO from 3.7 ± 0.98 and non-detectable levels to 48 ± 11 ($P<0.01$) and 1.2 ± 0.11 ($P<0.001$) respectively. Deletion of Cx43 reduced mRNA expression of both IL1 β (22 ± 1.4 , $P<0.05$) and NLRP3 (0.53 ± 0.078 , $P<0.001$) by more than 50% as compared to control, highlighting a role for tubule Cx43 expression in the regulation of inflammasome priming that occurs in response to renal tubule injury.

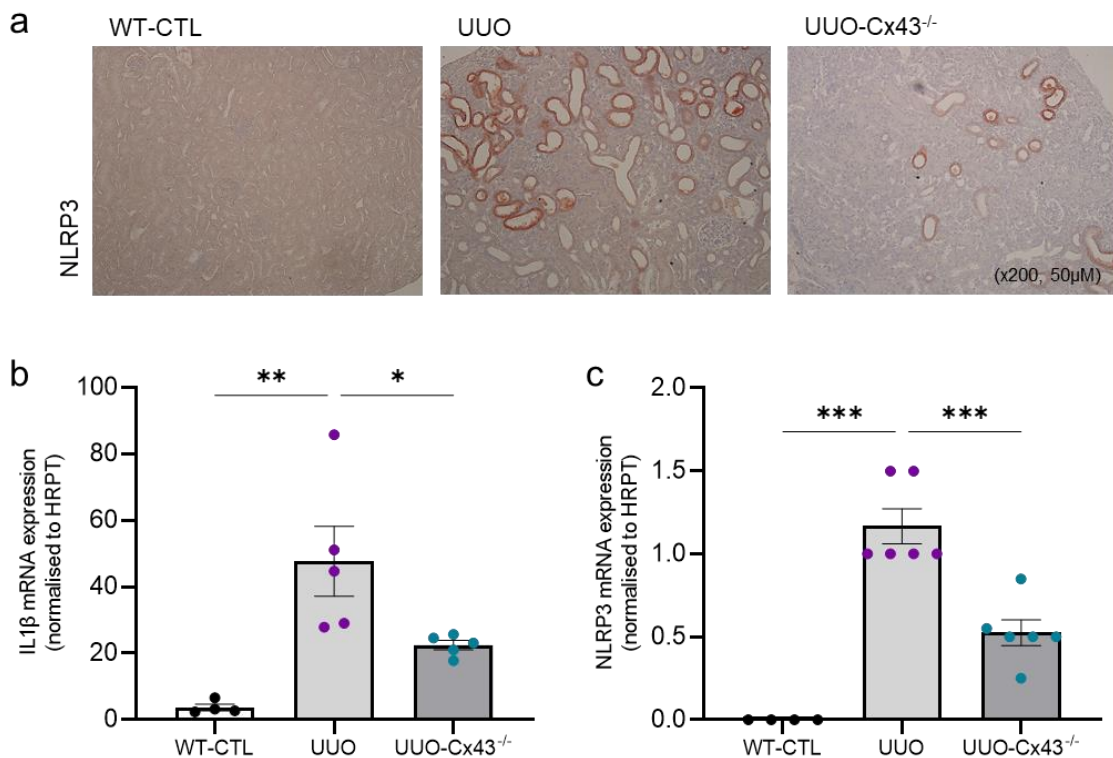


Figure 5.4. Tubule-specific deletion of Cx43 (Cx43^{-/-}) negates increased expression of inflammasome markers following UUO. Collaborators at INSERM carried out immunostaining of the renal cortex and RT-qPCR, illustrating changes in protein expression (a) and mRNA expression (b & c) respectively in Pax8-rtTA-cre:cx43 flox Cx43^{-/-} mice. Housekeeping gene HRPT was used for RT-qPCR. n=6. Significance is displayed as * $P<0.05$, ** $P<0.01$ and *** $P<0.001$.

5.3.3. Pro-inflammatory cytokines IL1 β and TNF α stimulate both priming and activation of the NLRP3 inflammasome in primary human RPTECs under conditions of high (25mmol/L) glucose.

Having determined that tubular Cx43 deletion protects against UUO-induced increases in NLRP3 expression, I utilised my previously established *in vitro* model of diabetic nephropathy to assess if Cx43 regulates NLRP3 expression and activity, via hemichannel-mediated effects. RPTECs were treated with IL1 β , TNF α and 25mmol/L glucose, and IL1 β and NLRP3 mRNA expression assessed as a measure of inflammasome priming. Caspase 1 activity was determined as an indicator of NLRP3 activation. The ability of NF κ B blocker (BAY11 7082) and caspase 1 inhibitor (YVAD CMK) in blocking NLRP3 priming and activation respectively was also assessed.

Treatment with IL1 β , TNF α and 25mmol/L glucose increased mRNA expression of IL1 β by $97.7 \pm 0.69\%$ ($P < 0.001$) as compared to 5mmol/L control (Figure 5.5a) but failed to significantly alter mRNA levels of NLRP3 (Figure 5.5b). Inhibition of transcription factor NF κ B, reduced the increased IL1 β expression by $49 \pm 15\%$ ($P < 0.001$; Figure 5.5a). In addition, IL1 β , TNF α and 25mmol/L glucose significantly increased caspase 1 activity, by $69 \pm 4.7\%$ ($P < 0.001$; Figure 5.5c). Use of caspase 1 inhibitor YVAD CMK reduced this increase by $32 \pm 4.2\%$ ($P < 0.01$; Figure 5.5c), confirming that in this model, NLRP3 activation is caspase 1 specific.

Together these results confirm that IL1 β , TNF α and 25mmol/L glucose-induced priming and activation of NLRP3 are mediated by NF κ B and caspase 1 respectively in primary human RPTECs (Figure 5.5d).

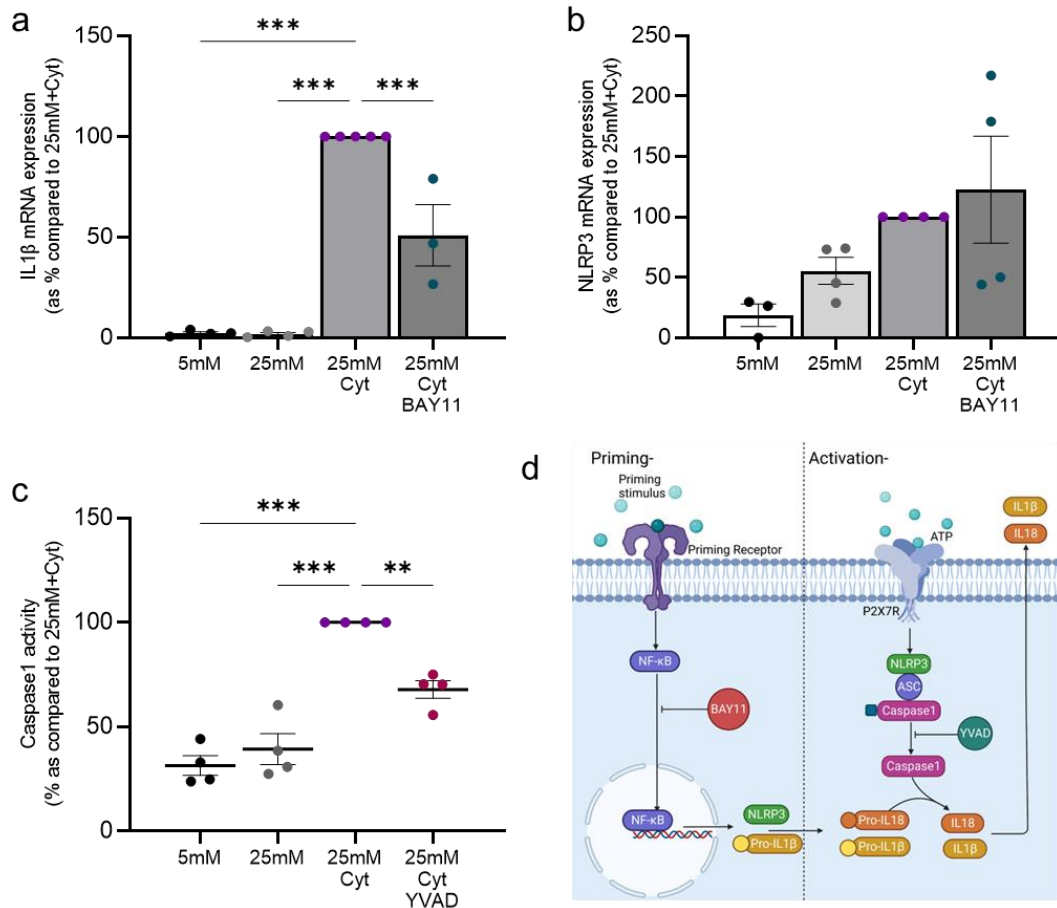


Figure 5.5. The NLRP3 inflammasome is primed and activated by IL1 β and TNF α in 25mmol/L glucose in primary human proximal tubule cells. RPTECs were treated with 5mmol/L or 25mmol/L glucose +/- IL1 β (10ng/mL) and TNF α (10ng/mL; Cyt) +/- BAY11 7082 (5 μ M) +/- YVAD CMK (10 μ M) for 48 hours. Use of RT-qPCR evaluated changes in mRNA expression normalised against housekeeping gene GAPDH (a & b) whilst a caspase glo-1 assay (c) assessed caspase 1 activity. A schematic shows the molecular mechanisms of inflammasome priming and activation (d). n=3-5. Significance is displayed as ** P <0.01 and *** P <0.001.

5.3.4. Hemichannel blocker Tonabersat blocks an NFκB-mediated increase in NLRP3 inflammasome priming and activation in treated RPTECs.

Whilst evidence links Cx43 hemichannel activity to NLRP3 priming and hemichannel-mediated ATP release to NLRP3 activation across multiple conditions of chronic inflammation (Huang *et al.*, 2019; Tonkin *et al.*, 2018; Cea *et al.*, 2023; Mugisho *et al.*, 2018a), this relationship has not been determined for the diseased kidney. Having established priming and activation in my *in vitro* model of diabetic nephropathy, I pre-incubated treated RPTECs with hemichannel blocker Tonabersat (50μM) to establish a role for Cx43 hemichannels in mediating this response (Figure 5.6; Figure 5.7c).

Blocking Cx43 hemichannel activity inhibits priming of the NLRP3 inflammasome in IL1β, TNFα and 25mmol/L glucose treated RPTECs, as evidenced by a significant reduction in IL1β (57±5.3%, $P<0.001$; Figure 5.6a) and NLRP3 (51±8.4%, $P<0.01$; Figure 5.6b) mRNA expression (2.3±0.69%, $P<0.001$ and 19±9.4%, $P<0.001$ as compared to 25mmol/L Cyt respectively).

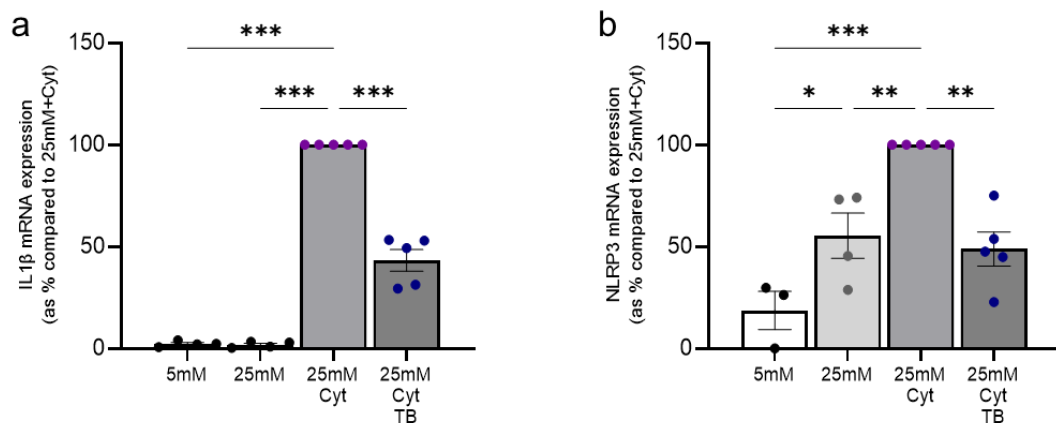


Figure 5.6. Priming of the NLRP3 inflammasome lies downstream of Cx43 hemichannel activity in IL1β, TNFα and 25mmol/L glucose treated RPTECs, effects negated following pre-incubation with Tonabersat. RPTECs were treated with 5mmol/L or 25mmol/L glucose +/- IL1β (10ng/mL) and TNFα (10ng/mL; Cyt) +/- Tonabersat (TB; 50μM). Use of RT-qPCR evaluated changes in mRNA expression of IL1β (a) and NLRP3 (b), normalised against housekeeping gene GAPDH. n=3-5. Significance is displayed as * $P<0.05$, ** $P<0.01$, *** $P<0.001$.

Upregulation of inflammasome components during the priming phase is followed by caspase 1-mediated cleavage and release of pro-inflammatory IL1β by 96.3±0.58%

($P<0.001$) in IL1 β , TNF α and 25mmol/L glucose treated RPTECs (Figure 5.7b). This response is significantly impaired when Cx43 hemichannels are blocked by Tonabersat, with caspase 1 activity (Figure 5.7a) and IL1 β release (Figure 5.7b) reduced by $27\pm5.1\%$ ($P<0.05$) and $18\pm5.3\%$ ($P<0.001$) respectively. Together these results suggest that Cx43 hemichannel activity is directly linked to inflammasome priming (Figure 5.6a) and activation (Figure 5.7c) in IL1 β , TNF α and 25mmol/L glucose treated RPTECs.

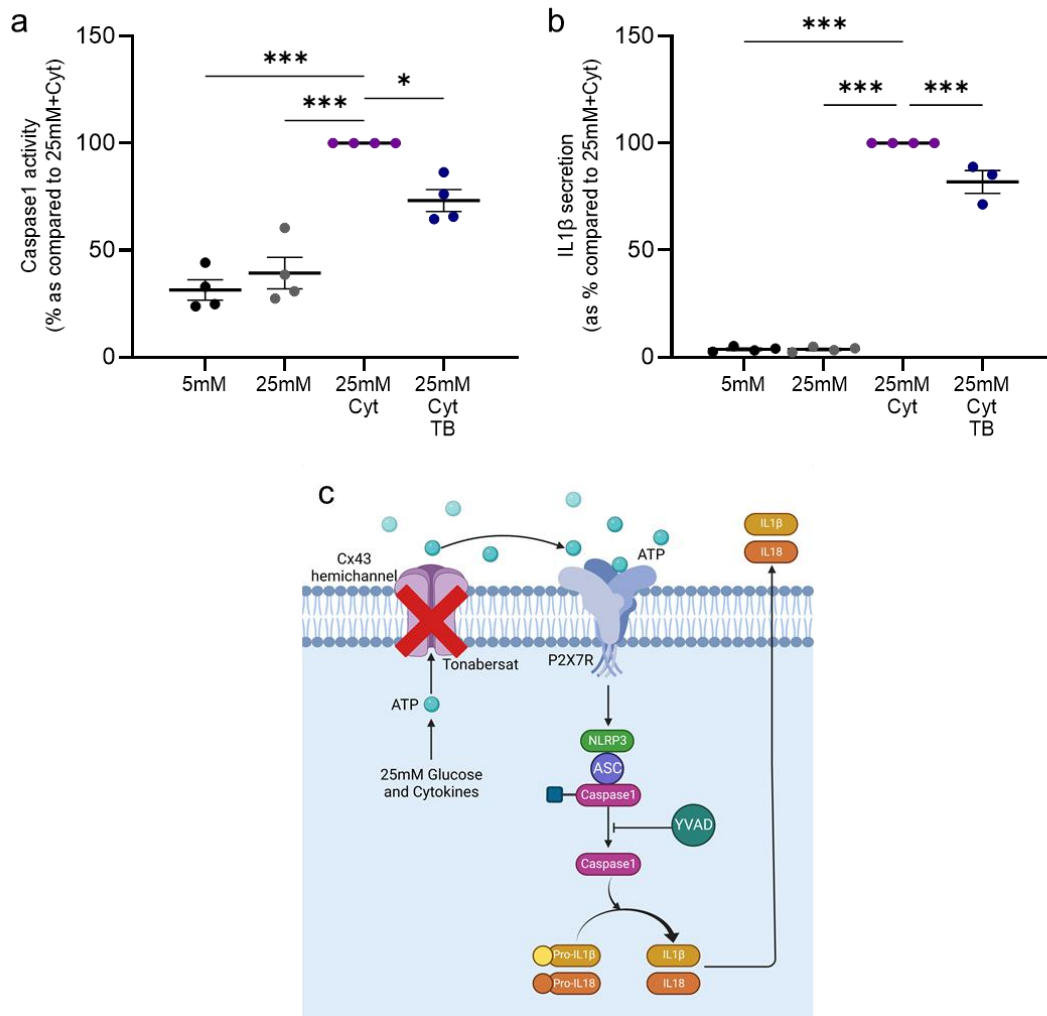


Figure 5.7. Pro-inflammatory cytokines IL1 β , TNF α and 25mmol/L glucose activate the NLRP3 inflammasome via increased Cx43 hemichannel activity, effects reduced when RPTECs are pre-incubated with Tonabersat. RPTECs were treated with 5mmol/L or 25mmol/L glucose +/- IL1 β (10ng/mL) and TNF α (10ng/mL; Cyt) +/- Tonabersat (TB; 50 μ M) for 48 hours. Use of a caspase glo-1 assay (c) assessed caspase 1 activity whilst an ELISA assessed changes in IL1 β secretion. A schematic shows the proposed molecular mechanisms behind the Cx43 hemichannel-mediated NLRP3 inflammasome activation (c). $n=3-5$. Significance is displayed as $*P<0.05$ and $***P<0.001$.

5.3.5. Alterations in calcium and inhibition of non-canonical signalling intermediaries reduced Cx43 hemichannel associated inflammasome activation.

Previous experiments identified that Cx43 hemichannel activity is reduced in response to decreased levels of intracellular Ca^{2+} (Chapter 4, Figure 4.8) and P38/ERK inhibition (Chapter 4, Figure 4.10 and 4.11). Furthermore, in figures 5.6 and 5.7, I demonstrate a link between Cx43 hemichannel activity and NLRP3 activation. Consequently, here I assess the impact of a decrease in intracellular Ca^{2+} and P38/ERK inhibition events on inflammasome priming and activation.

RPTECs were treated with $\text{IL1}\beta$, $\text{TNF}\alpha$ and 25mmol/L glucose +/- either the calcium chelator BAPTA (5 μM), +/- ERK inhibitor PD98059 (50 μM) +/- P38 inhibitor SB203580 (10 μM) and inflammasome activity was assessed via caspase 1 activity. Chelation of calcium with BAPTA successfully reduced caspase 1 activity from $69\pm4.7\%$ by $43\pm9.9\%$ ($P<0.01$; Figure 5.8a) in treated RPTECs whilst treatment of proximal tubule cells with inhibitors to either ERK (Figure 5.8b) or P38 (Figure 5.8c) prior to $\text{IL1}\beta$, $\text{TNF}\alpha$ and 25mmol/L glucose treatment significantly reduced caspase 1 activity by $27\pm8.5\%$ ($P<0.05$) and $30\pm5.2\%$ ($P<0.01$) respectively.

These findings demonstrate that reduced Cx43 hemichannel activity through blocking known gating stimuli and cell signalling pathways is also linked to decreased inflammasome activation.

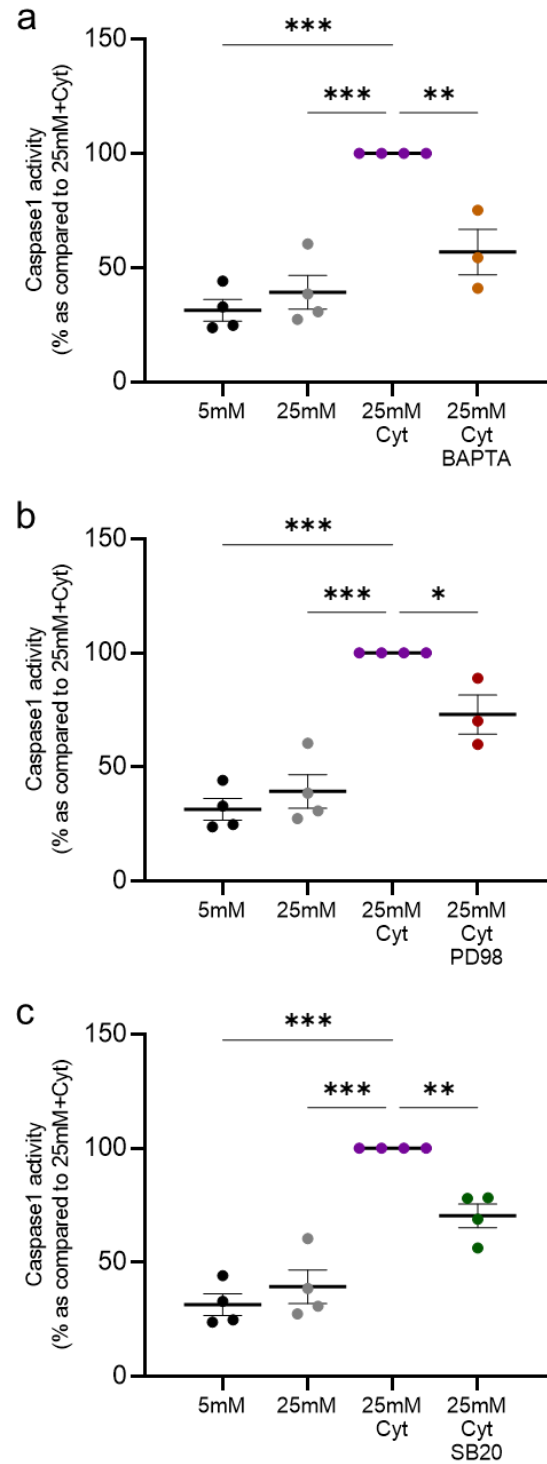


Figure 5.8. Pro-inflammatory cytokines IL1 β , TNF α and 25mmol/L glucose activate the NLRP3 inflammasome via increased Cx43 hemichannel activity, effects blocked when RPTEC Ca²⁺ gating, ERK and P38 signalling are inhibited. RPTECs were treated with 5mmol/L or 25mmol/L glucose +/- IL1 β (10ng/mL) and TNF α (10ng/mL; Cyt) +/- either BAPTA (5 μ M), PD98059 (PD98; 50 μ M) or SB203580 (SB20; 10 μ M) for 48 hours. A caspase glo-1 assay (a-c) assessed caspase 1 activity. n=3-5. Significance is displayed as * P <0.05, ** P <0.01 and *** P <0.001.

5.3.6. Aberrant Cx43 hemichannel activity is linked to an increase in Cx43 expression, a mechanism blocked through inhibition of transcription factor NFκB.

Priming of the NLRP3 inflammasome, e.g., increased IL1β transcription, is NFκB dependent. Studies by Alonso *et al.*, determined that NFκB can bind to the Cx43 promoter and increase Cx43 transcription (Alonso *et al.*, 2010; Xu *et al.*, 2015). Furthermore, recent studies in retinal pigment epithelial cells determined that NLRP3 priming is linked to increased Cx43 expression, an event dependent upon increased NFκB activation. Having previously established that Cx43 hemichannel-mediated ATP release primes and activates the NLRP3 inflammasome in RPTEC cells, initial studies assessed the implication of blocking NFκB activity on Cx43 expression,

RPTECs were treated with IL1β, TNFα and 25mmol/L glucose +/- preincubation with either BAY11 7082 (5μM) or Tonabersat (50μM) for 48 hours. qRT-PCR determined that Cx43 mRNA expression was upregulated in IL1β, TNFα and 25mmol/L glucose treated cells by 54±6.4% ($P<0.001$), a response which was significantly reduced by 29±3.4% ($P<0.05$; Figure 5.9a) when cells were pre-incubated with NFκB inhibitor BAY11 7082. These data suggest that NFκB-mediated priming of the NLRP3 inflammasome is indirectly linked to an increase in Cx43 expression. Consequently, I further assessed if NFκB inhibition and the reduction in Cx43 mRNA, directly correlated to reduced Cx43 hemichannel activity. Pre-incubation with BAY11 7082 negated a IL1β, TNFα and 25mmol/L glucose-induced increase in carboxyfluorescein dye uptake (61±3.2%, $P<0.001$; Figure 5.9c&d) and ATP release (54±6.4%, $P<0.001$; Figure 5.9e) as compared to control by 55±5.9% ($P<0.001$) and 95.6±2.8% ($P<0.001$) respectively.

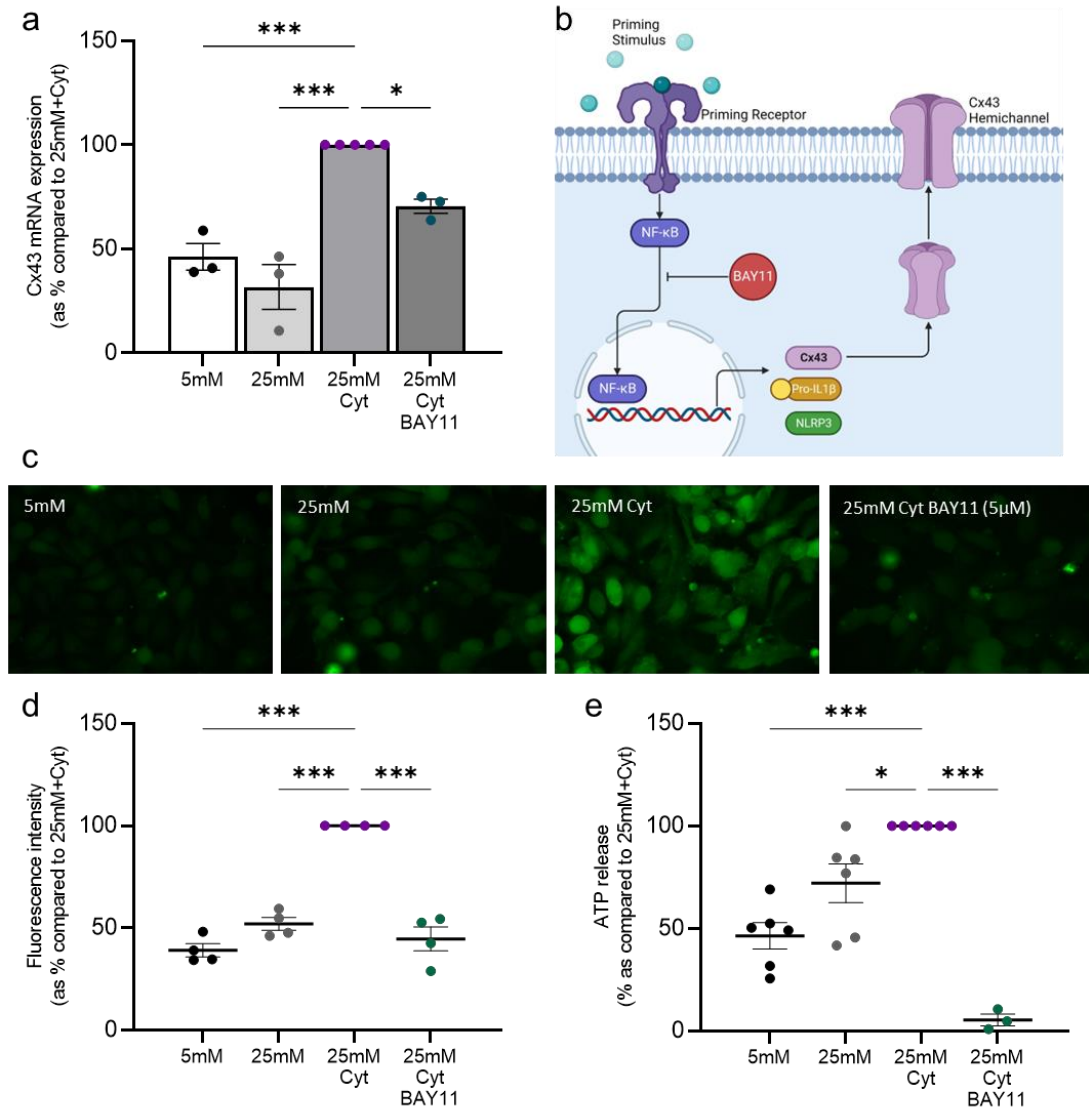


Figure 5.9. Blocking NFκB-mediated priming of the inflammasome reduces Cx43 expression and hemichannel activity. RPTECs were treated with 5mmol/L or 25mmol/L glucose +/- IL1β (10ng/mL) and TNFα (10ng/mL; Cyt) +/- BAY11 7082 (5μM) for 48 hours. Use of RT-qPCR evaluated changes in Cx43 mRNA expression in response to inhibition of NFκB, when normalised against housekeeping gene GAPDH (a) with a schematic of the potential mechanism shown (b). Carboxyfluorescein dye uptake studies determined change in hemichannel number at the cell surface (c) which was quantified using Fiji software (d). An ATPlite luminescence assay measured cellular release of ATP into the supernatant (e). n=3-6. Significance is displayed as * $P<0.05$, *** $P<0.001$.

I have previously observed that aberrant Cx43 hemichannel activity is linked to downstream changes in NLRP3 priming (NFkB-mediated) and activation. Since NFkB indirectly regulates Cx43 expression (binds to Cx43 promoter (Alonso *et al.*, 2010)) and ultimately hemichannel activity (Figure 5.9), inhibition of Cx43 hemichannel activity may not only decrease inflammasome priming and activation but may also indirectly feed-forward to reduce further downstream changes in Cx43 expression and function at both the transcript and protein level.

RPTECs pre-treated with Tonabersat prior to treatment with IL1 β and TNF α under conditions of 25mmol/L glucose exhibit a 43 \pm 4.3% (P <0.001) reduction in Cx43 mRNA (Figure 5.10a) and 34 \pm 6.4% (P <0.01) reduction in Cx43 protein expression (Figure 5.10b).

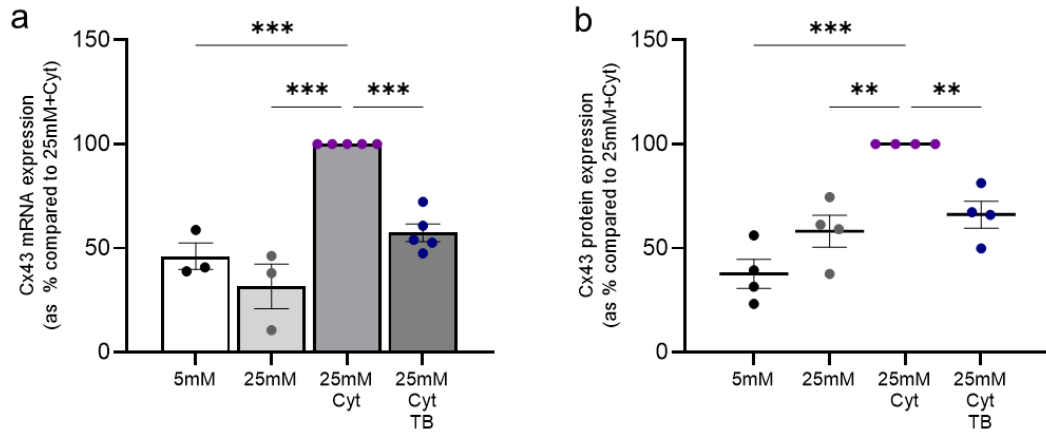


Figure 5.10. Tonabersat negates a proinflammatory cytokine and 25mmol/L glucose-induced increase in Cx43 expression. RPTECs were treated with 5mmol/L or 25mmol/L glucose +/- IL1 β (10ng/mL) and TNF α (10ng/mL; Cyt) +/- Tonabersat (TB; 50 μ M) for 48 hours. Use of RT-qPCR evaluated changes in Cx43 mRNA expression normalised against housekeeping gene GAPDH (a) whilst western blotting (b) assessed altered Cx43 protein expression. Results were normalised against expression of housekeeping protein, α -Tubulin as a loading control. n=3-5. Significance is displayed as ** P <0.01 and *** P <0.001.

5.3.7. Blocking inflammasome activation reduces Cx43 expression and hemichannel activity.

Inflammasome activation leads to caspase 1-mediated cleavage of pro-inflammatory cytokines including IL1 β , which are then released into the extracellular space. Thus far I have demonstrated that Cx43 hemichannel activity is increased following treatment in the presence of IL1 β , TNF α and high glucose. In addition, Cx43 hemichannel activity evokes priming and activation of the NLRP3 inflammasome, resulting in increased release of IL1 β . Therefore, it is possible that in addition to an NF κ B-mediated increase in Cx43 expression during the priming stage, the release of IL1 β and other cytokines following inflammasome activation could further increase Cx43 hemichannel activity.

To investigate the effect of inflammasome activation on Cx43 hemichannel activity, RPTECs were treated with IL1 β , TNF α and 25mmol/L glucose for 48 hours +/- caspase 1 inhibitor YVAD CMK (10 μ M) ahead of evaluating changes in Cx43 expression, hemichannel-mediated dye uptake and ATP release.

In IL1 β , TNF α and 25mmol/L glucose treated RPTECs, pre-incubation with YVAD CMK decreased Cx43 mRNA (Figure 5.11a) and protein expression (Figure 5.11b) by 29 \pm 5.0% (P <0.01) and 34 \pm 9.1% (P <0.05) respectively. This reduction in expression in response to caspase 1 inhibition was paralleled by reduced Cx43 hemichannel activity. YVAD CMK effectively negated a 25mmol/L + cytokine-induced increase in both carboxyfluorescein dye uptake (37 \pm 2.7%, P <0.001; Figure 5.11c-d) and hemichannel-mediated ATP release (32 \pm 8.7%, P <0.05; Figure 5.11e) suggesting that NLRP3 inflammasome activation further exacerbates the effects of Cx43 hemichannel activity through increased Cx43 expression and hemichannel-mediated ATP release.

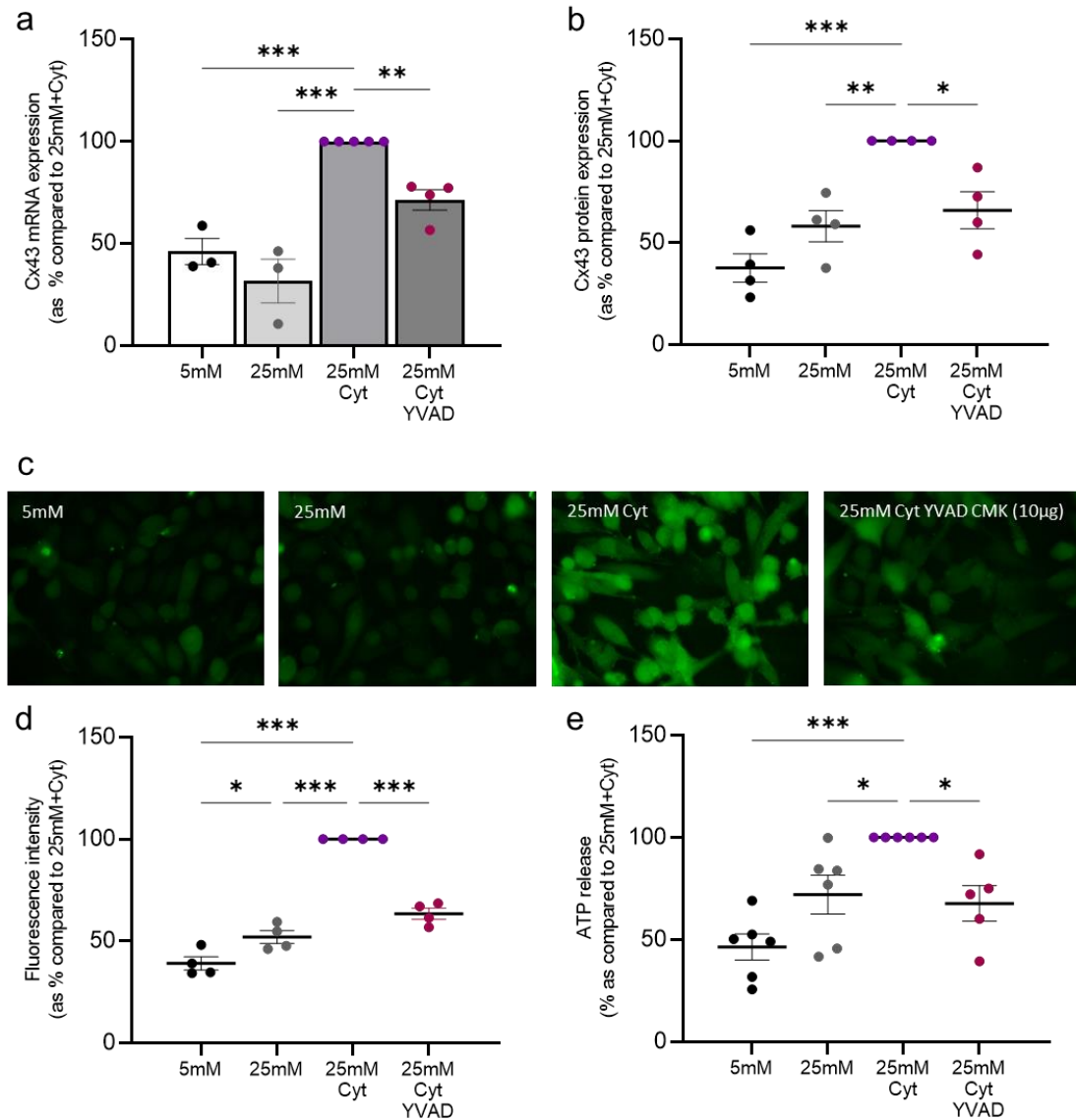


Figure 5.11. Blocking caspase 1 activity reduces pro-inflammatory cytokine-induced increases in Cx43 expression and hemichannel activity. RPTECs were treated with 5mmol/L or 25mmol/L glucose +/- IL1 β (10ng/mL) and TNF α (10ng/mL; Cyt) +/- YVAD CMK (10 μ M) for 48 hours. Use of RT-qPCR evaluated changes in Cx43 mRNA expression normalised against housekeeping gene GAPDH (a) whilst western blotting (b) assessed altered Cx43 protein expression. Results were normalised against expression of housekeeping protein, α -Tubulin as a loading control. Carboxyfluorescein dye uptake studies determined change in hemichannel number at the cell surface (c) which was quantified using Fiji software (d). An ATPlite luminescence assay measured cellular release of ATP into the supernatant (e). n=3-6. Significance is displayed as * P <0.05, ** P <0.01, *** P <0.001.

5.3.8. Tubule Cx43 deletion in the mouse UUO model ameliorates an increase in tubule injury, inflammation and fibrosis.

In this chapter I show for the first time that deletion of tubule Cx43 from the diseased kidney, is paralleled by a reduction in the expression of NLRP3 and associated proteins. Through *in vitro* analysis, I report that this protection is likely a consequence of diminished Cx43 hemichannel activity, an event which sits upstream of NLRP3 priming, activation and downstream inflammation. The implications of blocking these processes *in vivo*, were further assessed using the tubule specific UUO-Cx43^{-/-} knockout mouse model. All *in vivo* work was carried out by collaborators at INSERM.

Masson's trichrome and Sirius red staining of renal tissue showed a significant increase in tubular dilation (2.5 ± 0.27 , $P < 0.001$; Figure 5.12a&b) and tubulointerstitial fibrosis (0.62 ± 0.11 , $P < 0.01$; Figure 5.12a&c) 10 days post UUO as compared to WT healthy controls (0 ± 0 and 0.12 ± 0.021 respectively). In Cx43^{-/-} mice, the effects on tubular dilation (1.6 ± 0.15 , $P < 0.01$) and tubulointerstitial fibrosis (0.24 ± 0.067 , $P < 0.01$) were significantly reduced following UUO, further supporting a role for Cx43 as a driver of renal injury.

Inflammation and fibrosis are the two main pathologies implicated in late-stage kidney disease (Gusev *et al.*, 2021), with macrophages and fibroblasts being the major immune cell types responsible for driving injury and subsequent disease progression (An *et al.*, 2023). In the UUO-Cx43^{-/-} mouse model, F4/80⁺ macrophage infiltration (4.3 ± 0.87 , $P < 0.01$; Figure 5.12a&d) and FSP1⁺ fibroblast staining (245 ± 18 , $P < 0.001$; Figure 5.12a&e) were significantly increased in the interstitium 10 days post UUO, as compared to WT healthy controls (0 ± 0 and 21 ± 2.2 respectively). Again, deletion of tubule Cx43 was protective in the face of UUO renal injury, significantly reducing macrophage infiltration (2.0 ± 0.12 , $P < 0.05$) and fibroblast number (109 ± 11 , $P < 0.0001$) back towards control. Using immunohistochemical staining, the UUO-Cx43^{-/-} mouse model demonstrates that Cx43 deletion in the renal tubules significantly ameliorates inflammation and fibrosis following renal injury.

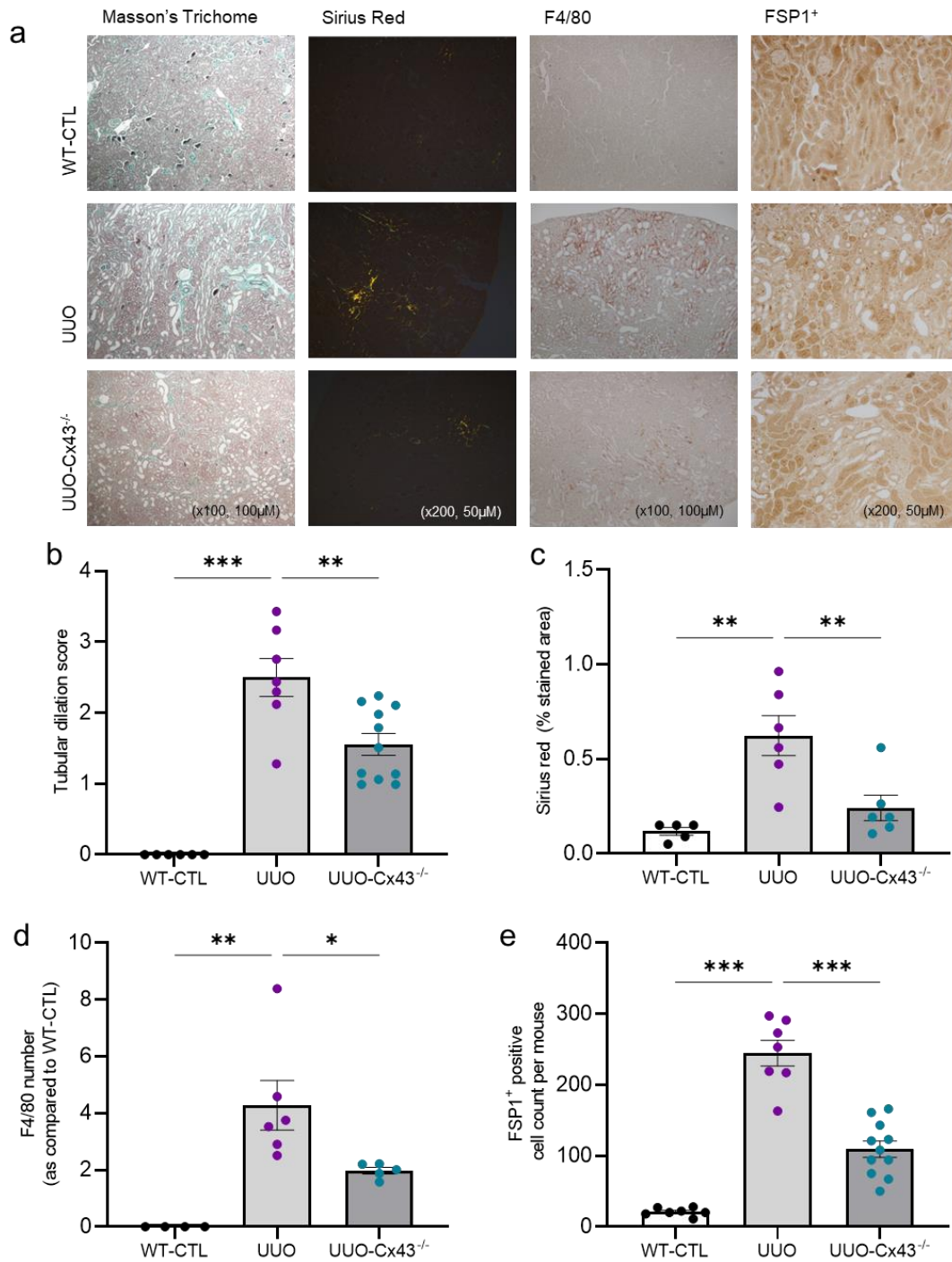


Figure 5.12. Tubule-specific Cx43 knockout reduces markers of kidney injury in a mouse model of tubulointerstitial fibrosis. Kidneys were harvested from wild type control (WT-CTL) mice, mice that had undergone unilateral ureteral obstruction (UUO) and UUO mice with a tubule Cx43 deletion (UUO-Cx43^{-/-}). Animal work was carried out by collaborators at INSERM. Representative images (a) and quantification illustrate Masson's Trichrome staining (tubular dilation score; b), Sirius Red staining (interstitial fibrosis; c), F4/80 cell number (macrophage abundance; d) and FSP1⁺ cell count (fibroblast number; e). All groups are n=5-12 unless specified, analysed using ANOVA and Tukey post-test. **P*<0.05, ***P*< 0.01 and ****P*< 0.001.

To build upon these findings, changes in mRNA expression of inflammatory markers were explored to identify potential mechanisms through which increased Cx43 hemichannel activity and inflammasome activation in RPTECs translates to increased inflammation, fibrosis, and immune cell number in injured UUO mice. Downstream of IL1 β and IL18 release, IL6 is a proinflammatory cytokine involved in macrophage activation and essential for the inflammatory acute phase response induced by tissue damage (Yang *et al.*, 2020a). In the mouse UUO model, IL6 mRNA expression (Figure 5.13a) is upregulated in injury (97 ± 14 , $P<0.001$) as compared to control (1.0 ± 0.3), changes negated in mice with a tubule specific Cx43 deletion (38 ± 5.0 , $P<0.01$). Whilst IL6 could contribute to the macrophage population through promotion of monocyte to macrophage differentiation (Yang *et al.*, 2020a), chemokine MCP1 (Figure 5.13b) can also increase macrophage number through regulation of macrophage migration and infiltration (Du *et al.*, 2021). Deletion of tubule Cx43 (99 ± 13 , $P<0.01$) reduces a UUO-induced increase in MCP1 mRNA expression (151 ± 11 , $P<0.001$), as compared to WT, healthy control (0.71 ± 0.037). A key biomarker of inflammation in kidney injury, neutrophil gelatinase-associated lipocalin (N-GAL) production is stimulated by release of pro-inflammatory cytokines (Seibert *et al.*, 2018). In Cx43^{-/-} mice, N-GAL expression (Figure 5.13c) is reduced following UUO (199 ± 26 , $P<0.05$) as compared to WT UUO (280 ± 18), where expression was significantly increased as compared to WT healthy control (1.5 ± 0.16 , $P<0.001$). In combination, these results show that Cx43 deletion protects against an increase in inflammation and cytokine/chemokine expression in an *in vivo* model of diabetic nephropathy.

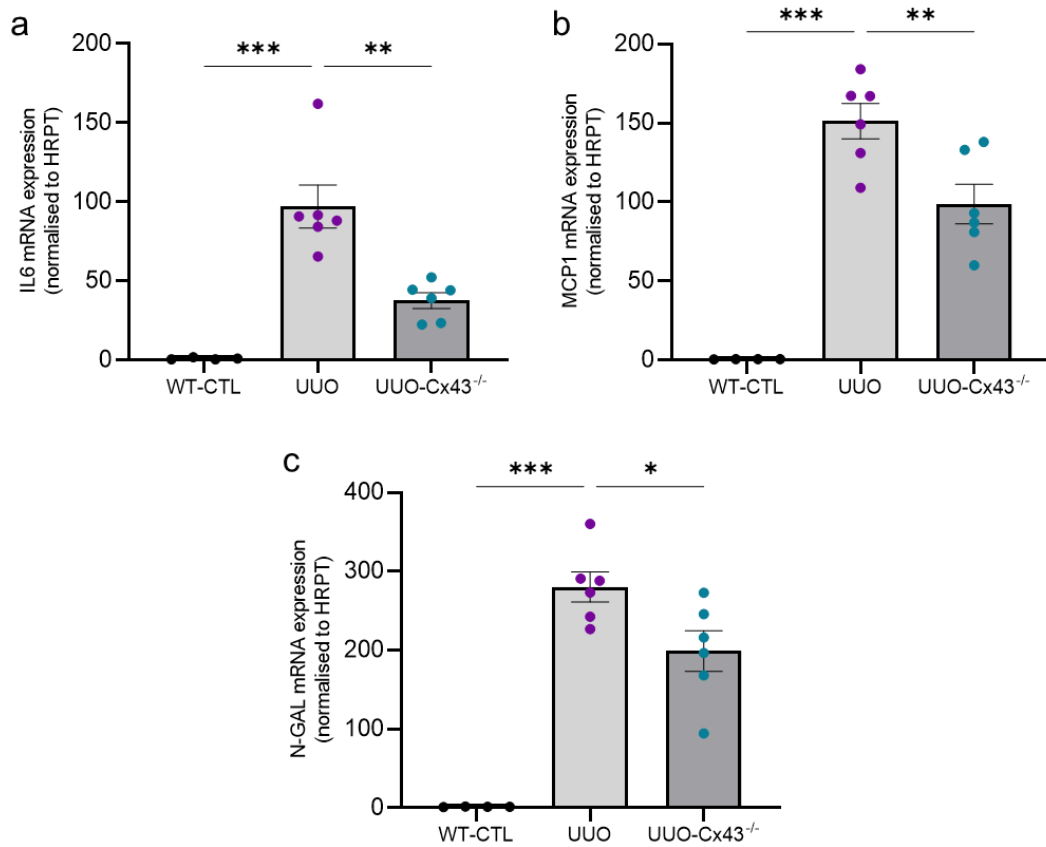


Figure 5.13. Tubule-specific Cx43 knockout reduces markers of inflammation in a mouse model of renal injury. Kidneys were harvested from wild type control (WT-CTL) mice, mice that had undergone unilateral ureteral obstruction (UUO) and UUO mice with a tubule Cx43 deletion (UUO-Cx43^{-/-}). Use of RT-qPCR evaluated changes in mRNA expression of IL6 (a), MCP1 (b) and N-GAL (c) normalised against housekeeping gene GAPDH. n=3-6. * $P < 0.05$, ** $P < 0.01$ and *** $P < 0.001$.

5.3.9. Tonabersat negates an increase in pro-inflammatory markers associated with diabetic nephropathy in an *in vitro* model of diabetic kidney disease.

Data from the UUO-Cx43^{-/-} mouse model has established a role for Cx43 in mediating upregulated inflammasome activation, pro-inflammatory cytokine/chemokine expression and immune cell infiltration resulting in inflammation and fibrosis. As with the NLRP3 data presented in Figure 4, we do not know if Cx43 mediates these changes via altered gap junction communication or an increase in Cx43 hemichannel activity. To establish whether the increase in cytokine and chemokine expression is Cx43 hemichannel-mediated I treated RPTECs with IL1 β , TNF α and 25mmol/L glucose +/- Tonabersat (50 μ M) and assessed mRNA expression of proinflammatory cytokines and chemokines.

Following IL1 β , TNF α and 25mmol/L glucose treatment, a significant increase in mRNA expression of both TNF α (84 \pm 7.0%, P <0.001; Figure 5.14a) and IL6 (95.1 \pm 2.9%, P <0.001; Figure 5.14b) as compared to control was observed. Tonabersat significantly reduced changes in expression of IL6 (49 \pm 3.7%, P <0.001) but not TNF α .

Data showing diminished number of F4/80 and FSP1⁺ cells in tubules from Cx43^{-/-} UUO mice suggests a reduction in expression of immune cell chemoattractants and activators, ultimately impacting on paracrine-mediated signaling between the different cell types known to promote TIF. Consequently, I explored the effect of blocking Cx43 hemichannel activity on the expression of G-CSF and MCP1, as important mediators of macrophage infiltration and activation. Tonabersat significantly reduced an inflammation-mediated increase in G-CSF (99.985 \pm 0.0085%, P <0.001; Figure 5.14c) and MCP1 (90 \pm 3.7%, P <0.001; Figure 5.14d) by 52 \pm 7.9% (P <0.001) and 44 \pm 7.8% (P <0.001) respectively, implicating hemichannel-mediated ATP release as a key mediator of macrophage infiltration. Similar to IL1 β , interleukin 1-alpha (IL1 α) mediates inflammation through binding to IL1-R following injury. Expression of IL1 α is significantly upregulated (97.1 \pm 1.8%, P <0.001; Figure 5.14e) following IL1 β , TNF α and 25mmol/L glucose stimulation, changes that were reduced by treatment with Tonabersat (61 \pm 5.5%, P <0.001). Together these data demonstrate a clear role for Cx43 hemichannel-mediated ATP release in the upregulation of pro-inflammatory cytokines and chemokines, which likely drive infiltration of immune cells, inflammation and fibrosis, as seen in the UUO mouse model of CKD.

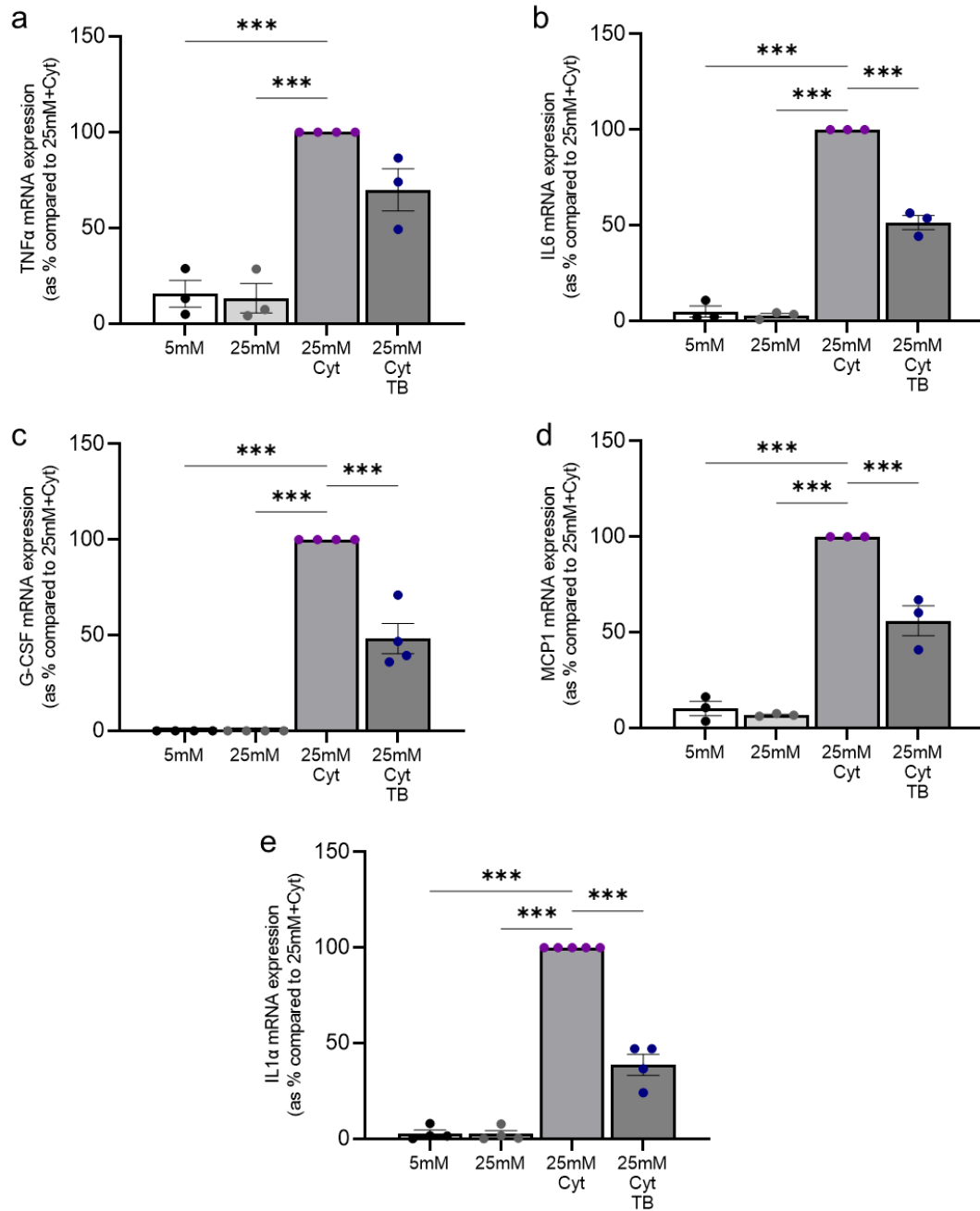


Figure 5.14. Tonabersat blocks a pro-inflammatory cytokine and high glucose-mediated increase in the expression of pro-inflammatory markers. RPTECs were treated with 5mmol/L or 25mmol/L glucose +/- IL1 β (10ng/mL) and TNF α (10ng/mL; Cyt) +/- Tonabersat (TB; 50 μ M) for 48 hours. Use of RT-qPCR evaluated changes in mRNA expression of TNF α (a), IL6 (b), G-CSF (c), MCP1 (d) and IL1 α (e), normalised against housekeeping gene GAPDH. n=3-6. Significance is displayed as *** P <0.001.

5.3.10. Blocking inflammasome activation prevents downstream changes in EMT and fibrosis marker expression.

Results from the UUO-Cx43^{-/-} mouse model showed that Cx43 tubule deletion protected against an increase in fibroblast number and tubule fibrosis. This is corroborated by previous experiments in RPTEC and HK-2 proximal tubule cells showing that Tonabersat protects against an upregulation of proteins associated with EMT and fibrosis (Chapter 4, Figure 4.6, 4.7 and 4.9). Research in other models of chronic inflammation demonstrate a link between NLRP3 inflammasome activation, a complex regulated by Cx43 hemichannel activity in renal cells, and pEMT (Song *et al.*, 2018; Alyaseer *et al.*, 2020), a process also shown to be blocked following Cx43 hemichannel inhibition. Since fibrosis is a consequence of chronic inflammation and lies downstream of p-EMT (Lovisa *et al.*, 2015; Grande *et al.*, 2015; Masola *et al.*, 2019), I aimed to determine the role of the inflammasome in mediating changes in the expression of N-cadherin and fibronectin, proteins associated with EMT and fibrosis respectively, in my *in vitro* model.

During pEMT, proximal tubule epithelial cells undergo a phenotypic switch from classic epithelial to a more fibrotic mesenchymal state. A marker of this process is N-cadherin, which is upregulated to compensate for a loss of E-cadherin. Transcriptomic analysis shows a significant increase ($P < 0.001$) in N-cadherin mRNA expression (Figure 5.15a) in people with chronic kidney disease as compared to healthy volunteers. Blocking inflammasome activity using caspase 1 inhibitor YVAD CMK reduced an IL1 β , TNF α and 25mmol/L glucose-mediated increase ($68 \pm 2.5\%$, $P < 0.001$) in the expression of N-cadherin by $29 \pm 11\%$ ($P < 0.05$), linking inflammasome activity to the onset of pEMT (Figure 5.15b).

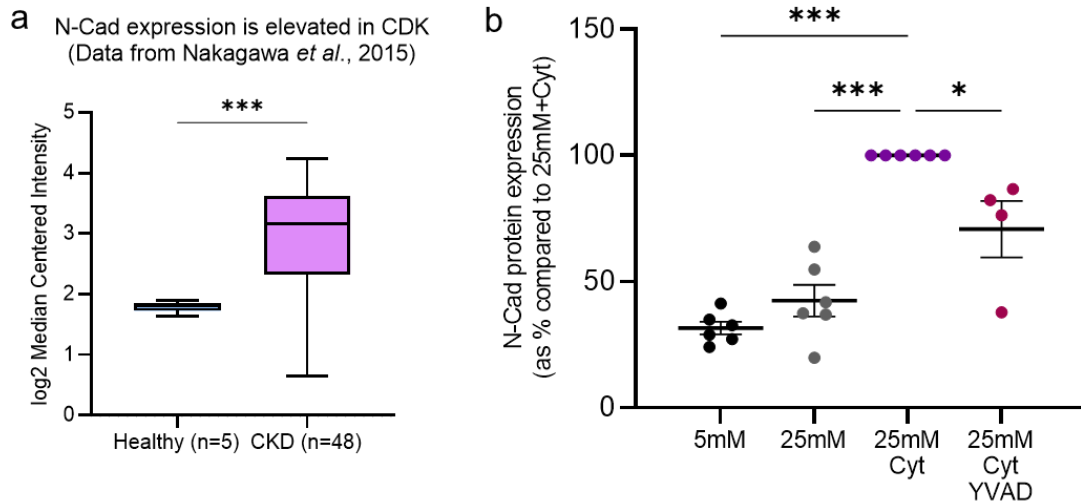


Figure 5.15. N-cadherin is elevated in human chronic kidney disease and reduced by caspase 1 inhibition. Transcriptomic analysis was performed on Nephroseq publicly available data from Nakagawa *et al.*, 2015 (a) comparing mRNA expression in the tubules of kidney biopsies from healthy donors and donors with chronic kidney disease. n is specified where appropriate. An unpaired t-test with Welch's correction analysis (a) was used for statistical analysis. RTECs were treated with 5mmol/L or 25mmol/L glucose +/- IL1 β (10ng/mL) and TNF α (10ng/mL; Cyt) +/- YVAD CMK (YVAD; 10 μ M) for 48 hours. Western blotting (b) assessed altered N-cadherin (N-Cad) protein expression. Results were normalised against expression of housekeeping protein, α -Tubulin as a loading control. n=4-6. Significance is displayed as * P <0.05 and *** P <0.001.

Downstream to inflammation and pEMT, tubulointerstitial fibrosis is the final common pathology of chronic kidney disease and causes irreversible damage to the proximal tubule. A key marker of fibrosis, fibronectin is significantly upregulated in people with diabetic nephropathy (P <0.001; Figure 5.16a) and chronic kidney disease (P <0.05; Figure 5.16c) as compared to healthy controls, and correlates with declining GFR, a marker of kidney function (P <0.001; Figure 5.16b). Caspase 1 inhibition significantly negates an IL1 β , TNF α and 25mmol/L glucose-mediated increase ($45 \pm 6.4\%$, P <0.001) in the expression of fibronectin by $28 \pm 2.9\%$ (P <0.001), demonstrating a role for the NLRP3 inflammasome in downstream fibrosis (Figure 5.16d). Collectively these data suggest that targeting aberrant Cx43 hemichannel activity can suppress the NLRP3 inflammasome and downstream changes associated with ECM remodelling and pEMT.

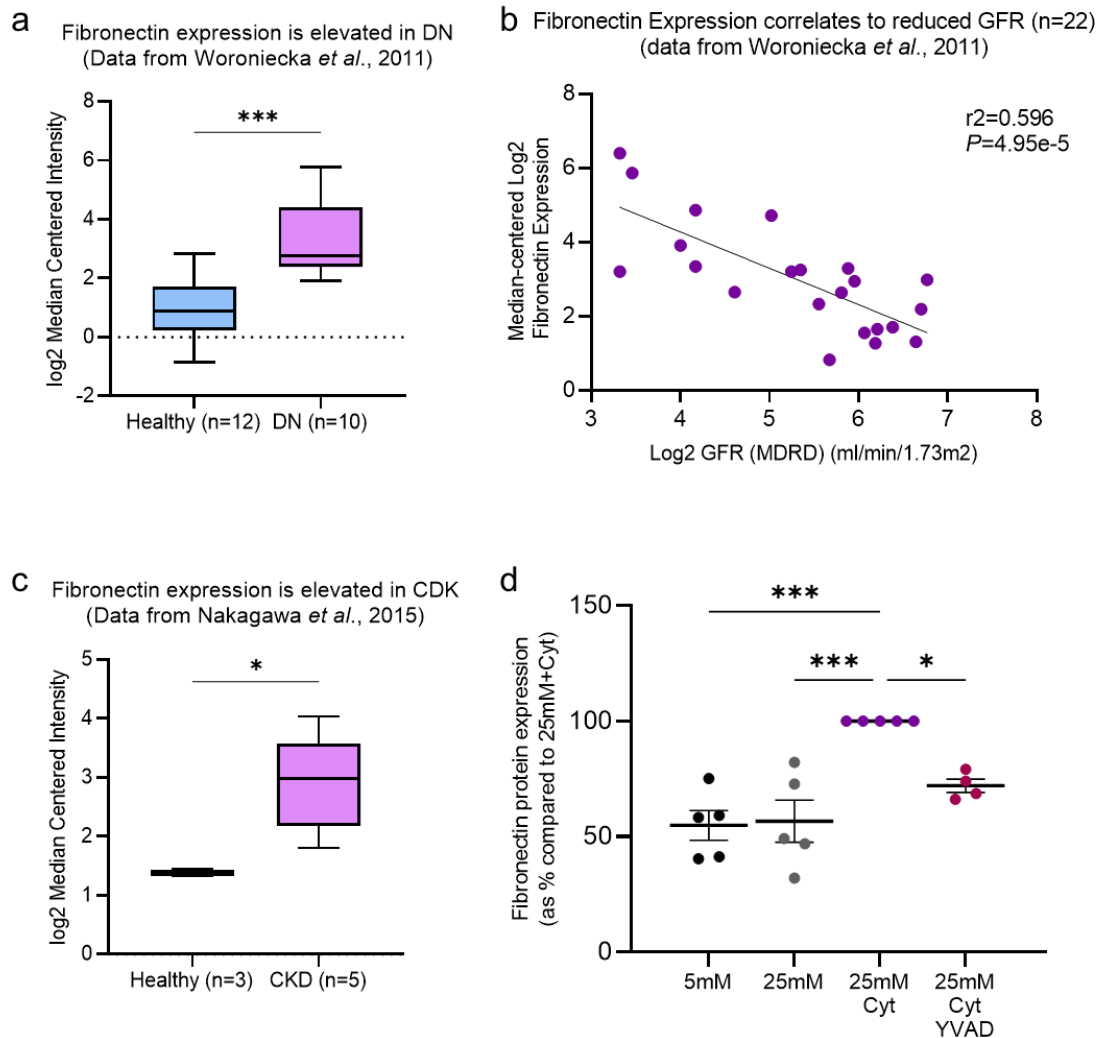


Figure 5.16. Fibronectin is elevated in human diabetic nephropathy and chronic kidney disease, correlating to measures of reduced renal function. Transcriptomic analysis was performed on Nephroseq publicly available data from Nakagawa *et al.*, 2015 (a) and Woroniecka *et al.*, 2011 (b) comparing mRNA expression in the tubules of kidney biopsies from healthy donors and donors with diabetic nephropathy or chronic kidney disease. *n* is specified where appropriate. An unpaired t-test with Welch's correction analysis (a) and simple linear regression (b) were used for statistical analysis. RPTECs were treated with 5mmol/L or 25mmol/L glucose +/- IL1 β (10ng/mL) and TNF α (10ng/mL; Cyt) +/- YVAD CMK (YVAD; 10 μ M) for 48 hours. Western blotting (c) assessed altered fibronectin protein expression. Results were normalised against expression of housekeeping protein, α -Tubulin as a loading control. *n*=4-6. Significance is displayed as **P*<0.05, and ****P*<0.001.

5.4. Discussion-

The NLRP3 inflammasome is an immune complex implicated in the pathogenesis of an array of chronic inflammatory diseases, including microvascular complications of diabetes such as diabetic retinopathy and diabetic nephropathy. Whilst studies in diabetic nephropathy show the protective effects of blocking inflammasome activation, the mechanisms behind its dysregulation in disease are yet to be established. Composed of two stages, I show an increase in markers of both NLRP3 priming and activation in human diabetic nephropathy and chronic kidney disease, paralleled by a decline in kidney function, corroborating findings in studies by Vilaysane *et al.*, and affirming its role in human disease (Vilaysane *et al.*, 2010). Similar findings were also shown in UUO-treated mice and IL1 β , TNF α and high glucose treated primary RPTECs, which further validated their physiological relevance as models of diabetic nephropathy.

Blocking activation of the inflammasome in primary RPTECs, reduced expression of EMT and fibrosis markers, N-cadherin and fibronectin, and supported earlier studies where NLRP3 knockdown prevented reduced changes indicative of EMT in high glucose treated clonal HK-2 cells (Song *et al.*, 2018). These changes were shown to be a result of inhibition of phosphorylation of cell signalling cascades SMAD 3, p38 MAPK and ERK1/2. The authors speculated that p38 and ERK signalling may play a role in high glucose-induced NLRP3 inflammasome activation (Song *et al.*, 2018), a suggestion supported by data from this thesis that demonstrates reduced caspase 1 activity following p38 and ERK inhibition. In addition to reduced EMT-like changes, blocking inflammasome activation in STZ-treated mice negated an increase in the expression of fibrosis markers including fibronectin (Song *et al.*, 2018), findings I recapitulate in my RPTEC model of diabetic nephropathy.

The NLRP3 inflammasome plays an essential role in the pathogenesis of numerous chronic inflammatory diseases (Seok *et al.*, 2021), justifying the growth of interest in using NLRP3 as a viable therapeutic target in multiple disease presentations. However, due to the complexity of the inflammasome, and the many components necessary for its priming and activation, there are numerous routes to intervention that include: transcription factors (NF κ B), inflammasome components (NLRP3, ASC, caspase 1), and downstream inflammasome mediators (IL1 β , IL6 and TNF α). Inhibitors of NLRP3 have attracted a lot of attention and whilst there are not any clinically available, there are several ongoing trials designed to determine a therapeutically viable option (Figure 5.17).

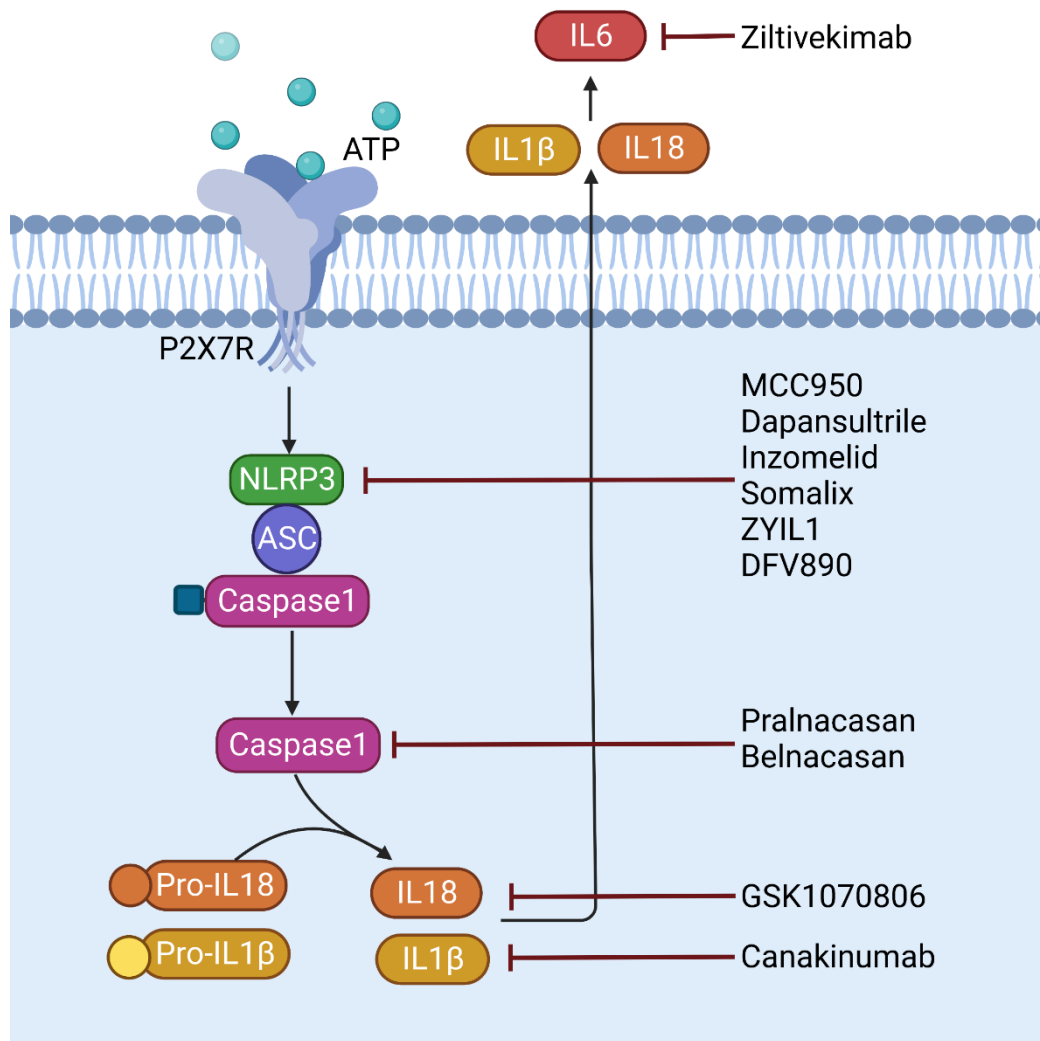


Figure 5.17. Schematic demonstrating some of the therapeutic compounds that have been/are in clinical trial targeting components of the inflammasome. Complications such as lack of effect, side effects and liver toxicity have thus far prevented approval for a drug targeting the inflammasome. Therefore, targeting upstream to reduce activation of the inflammasome represents an alternative that carries reduced risk of side effects linked with innate immune response suppression.

The first of many NLRP3 inhibitors, MCC950 was originally developed by Pfizer and reached phase II clinical trials targeting rheumatoid arthritis. Despite being the most potent and well characterised NLRP3 inhibitor, the trial was discontinued because of what is believed to be elevated levels of liver enzymes indicating liver toxicity (Chen *et al.*, 2021). Dapansultrile (OLT1177), which inhibits the ATPase activity of NLRP3 preventing its association with ASC, was the first NLRP3 inhibitor to complete phase I clinical trials in 2012, where it was well tolerated in healthy human volunteers (Marchetti *et al.*, 2018). Since then, it has reached phase II clinical trials treating the Covid-19-induced cytokine storm (Clinical Trial identifier: NCT04540120, Olatec

Therapeutics, 2022) and cardiovascular disease (Clinical Trial identifier: NCT03534297) and completed phase II clinical trials for osteoarthritis (Clinical Trial identifier: NCT02104050) and acute gouty arthritis (Clinical Trial identifier: 2016-000943-14 and NCT05658575; Klück *et al.*, 2020), but results are yet to be released. In addition, the pharmaceutical company Inflazone Ltd (Roche) developed oral NLRP3 inhibitors Inzomelid (Clinical Trials Identifier: NCT04086602) and Somalix which have thus far completed clinical trials for treatment of Cryopyrin-associated periodic syndrome (CAPS) and cardiovascular disease respectively (Nature, 2020). Also targeting CAPS syndrome, NLRP3 inhibitor ZYIL1 (Clinical Trials Identifier: NCT04731324) completed phase I clinical trials in healthy individuals and has progressed onto phase II (Clinical Trials Arena, 2021). Having currently completed phase I and II clinical trials for multiple inflammatory diseases (CDFV890D12201, NCT04382053, CDFV890B12201, CDFV890A12201, NCT04382053), DfV890 (previously referred to as IFM-2427) is a systemic NLRP3 antagonist, yet to be approved.

In addition to directly targeting NLRP3, other components of the inflammasome have also been identified as worthwhile targets, including caspase 1. Reversible inhibitors Pralnacasan (VX-740) and Belnacasan (VX-765) reached phase II clinical trials and showed efficacy for treatment of rheumatoid and osteoarthritis but were terminated due to liver toxicity (Dhani *et al.*, 2021). Caspase 1 cleavage is also essential for activation of other inflammasomes and so the lack of specificity when targeting caspase 1 also increases risk of severe infection (Chen *et al.*, 2021). Whilst these trials initially provided hope for a novel therapeutic to target chronic inflammation as a result of NLRP3 inflammasome activity, results have been met with concerns regarding inhibition of both sterile inflammation and the innate immune response, where activation of the NLRP3 inflammasome plays a pivotal role in defence against pathogens.

Drugs blocking IL1 β , a pro-inflammatory product of inflammasome activation have also reached clinical trial. Unfortunately, despite their success *in vitro*, trials in T1DM (NCT00947427) and diabetic retinopathy (NCT01589029) utilising the recombinant human monoclonal antibody Canakinumab (ACZ885, Novartis) yielded disappointing results. The ineffectiveness of these drugs could be due to alternative inflammasome pathways including IL18 release (Hirooka and Nozaki, 2021) and pyroptosis (Lin *et al.*, 2020) remaining active. The phase III CANTOS trial also utilised Canakinumab to target inflammation in atherosclerotic disease. The study demonstrated that treatment was partially protective against cardiovascular events. A sub-study looking at patients

who additionally presented with chronic kidney disease, due to the prominence of the cardiac-renal axis, showed that Canakinumab was also associated with reduced major vascular events in this sub-set of patients. However, despite the selective effectiveness of Canakinumab, the drug also showed increased rates of fatal infection and sepsis as a result of a dampened inflammatory response in the CANTOS trial for cardiovascular disease (Ridker *et al.*, 2017). Results also showed that raised IL18 and IL6 were associated with a significant residual inflammatory risk, despite effectively blocking IL1 β release (Ridker *et al.*, 2020), highlighting the requirement to target multiple pathways to achieve efficacy. One such drug is the IL18 antibody GSK1070806. Developed by GlaxoSmithKline, GSK1070806 completed phase I clinical trial (Clinical Trials Identifier: NCT01035645) and is currently undergoing phase I/II clinical trial for treatment of cardiovascular disease (Clinical Trials Identifier: NCT03681067). Following promising results in the phase II RESCUE trial (Ridker, 2021), IL6 inhibitor Ziltivekimab has entered a phase III ZEUS clinical trial in people with cardiovascular disease, chronic kidney disease and inflammation (Clinical Trials Identifier: NCT05021835). Whilst Canakinumab may be more effective when used in combination with these other drugs to target multiple inflammatory pathways, this raises new concerns regarding potential side effects, harmful drug interactions and liver toxicity (Sriutta *et al.*, 2018).

Acknowledging that interference to the innate immune response to microbial challenge represents a potential hurdle in targeting the NLRP3 and its downstream products directly, focusing upstream of the inflammasome represents a promising opportunity to dampen sterile inflammation whilst leaving the inflammasome open to microbial activation. One such target is the P2X7 receptor, which when stimulated in response to ATP triggers inflammasome activation. Attempts to date at blocking the P2X7 receptor have proven unsuccessful, producing variable pharmacodynamic responses, likely a result of genetic variability in the human P2X7 receptor gene (McHugh *et al.*, 2012; Burnstock and Knight, 2018). In other chronic inflammatory diseases, increased Cx43 has been linked to an increase in inflammasome activity, with findings in diabetic retinopathy showing that Cx43 hemichannel activity lies upstream of inflammasome activity, where aberrant ATP release activates P2X7 receptors driving NLRP3 activation (Mugisho *et al.*, 2018). Crucially, studies have shown that targeting Cx43 protects against inflammasome activation and negates the occurrence of downstream damage. Whilst increased Cx43 hemichannel activity (Price *et al.*, 2020) and NLRP3 expression (Cheng *et al.*, 2021) have both independently been demonstrated in diabetic nephropathy, a link between the two is yet to be established.

Data from our UUO-Cx43^{-/-} tubule knockout mouse model demonstrates a clear role for Cx43 in mediating inflammasome activation, with tubule-specific knockout of Cx43 reducing inflammasome activation and protecting against kidney injury. This aligns with findings in a mouse model of lipopolysaccharide-initiated acute renal injury, where peritoneal macrophages displayed elevated Cx43 and inflammasome activation. Heterozygous mouse models with genetically reduced Cx43 expression (Cx43^{+/-}) had significantly reduced inflammasome activation as compared to WT (Cx43^{+/+}) as shown by lower levels of blood IL1 β and renal expression of NLRP3. Ultimately reduced Cx43-mediated inflammasome activity culminated in reduced blood urea nitrogen (BUN), proteinuria and renal pathological changes (Huang *et al.*, 2019). Human RPTEC cells treated with IL1 β , TNF α and 25mmol/L glucose showed reduced inflammasome priming and activation following incubation with Cx43 hemichannel blocker Tonabersat, supporting the notion that hemichannel-mediated ATP release is responsible for this effect. As a DAMP, it is possible that ATP released from hemichannels activates cell surface receptors such as TLR4 to induce inflammasome priming whilst simultaneously triggering P2X7R-mediated inflammasome activation, a hypothesis outlined in figure 5.18. On the other hand, increased release of inflammatory cytokines including IL1 β and TNF α following activation may also mediate increased priming through IL1-R and TNFR stimulation and downstream NF κ B activation. Further experiments could determine the initiating signal/signals involved in inflammasome priming. Similarly in an *in vitro* model of diabetic retinopathy, use of hemichannel blocker Tonabersat negated an IL1 β , TNF α and 25mmol/L glucose-mediated increase in NLRP3 inflammasome activation (Figure 5.18) and downstream upregulation of pro-inflammatory cytokines IL1 β , IL6 and VEGF (Lyon *et al.*, 2021a). As well as a good safety profile evidenced in phase II clinical trials for migraine prophylaxis (Goadsby *et al.*, 2009), these findings highlight Tonabersat as a promising potential therapeutic to target Cx43 in diabetic nephropathy and retinopathy.

In addition to these novel findings, I show for the first time in an *in vitro* model of diabetic nephropathy both priming and activation of the inflammasome also contribute to increased hemichannel activity, indicating the presence of a vicious perpetual cycle of inflammation driven by a feed forward loop between Cx43 hemichannel activity and inflammasome activity (Figure 5.18). Data in the RPTEC model of diabetic nephropathy shows that blocking inflammasome priming through inhibition of NF κ B prevents inflammation-mediated upregulation of Cx43 expression and hemichannel ATP release. In other models of disease, when activated NF κ B binds to the Cx43 promoter its expression is upregulated (Alonso *et al.*, 2010), a likely mechanism

through which NLRP3 priming increases Cx43 expression after NFκB activation (Figure 5.18).

Furthermore, findings from TNFα treated bronchial epithelial cells demonstrated interesting interactions between NFκB activation and Wnt signalling (Jang *et al.*, 2017). Initially data showed that TNFα-induced Wnt signalling, resulting in increased expression of fibrotic markers, as well as NFκB and subsequent expression of pro-inflammatory cytokines. Use of an NFκB inhibitor was shown to not only block NFκB-mediated transcription, but also Wnt signalling. Moreover, use of β-catenin siRNA to block Wnt signalling also reduced NFκB activation and subsequent increased cytokine expression. This data provides evidence of a link between inflammation and fibrosis that may also be relevant in diabetic nephropathy (Jang *et al.*, 2017). Whilst further experiments were needed to confirm Wnt signalling in IL1β, TNFα and 25mmol/L glucose treated cells, altered expression associated with EMT and upregulation of Wnt signalling products fibronectin and collagen I, when combined with findings in bronchial epithelial cells, would suggest the possibility that one way in which the inflammasome is contributing to fibrosis is through increased Wnt signalling (Figure 5.18).

In addition to priming, activation was also shown to be a mediator of increased Cx43 hemichannel activity. Potential mechanisms behind this effect include the subsequent release of pro-inflammatory cytokines, e.g., IL1β and TNFα, which I have previously shown to lead to increased Cx43 expression, potentially through their ability to directly prime the NLRP3 and indirectly increase expression, and hemichannel activity (Chapter 4). Key to gating of Cx43 hemichannels and to inflammasome activation is an increase in intracellular Ca²⁺. Here, I propose that another method through which inflammasome activation contributes to increased hemichannel activity is through a P2X7R-mediated influx of Ca²⁺ ions resulting in the opening of Cx43 hemichannels (Figure 5.18). Additionally, with data in a model of diabetic retinopathy demonstrating that inflammasome activity activates non-canonical signalling molecules P38 and ERK (Song *et al.*, 2018), and having elucidated a role for these signalling pathways in increased Cx43 hemichannel activity in this RPTEC model of diabetic nephropathy (Chapter 4), it is also probable that the inflammasome upregulates Cx43 hemichannel activity through activation of P38 and ERK signalling pathways (Figure 5.18). Together, inflammasome-mediated upregulation of Cx43 hemichannel activity lends to the formation of a perpetual cycle of inflammation, driving chronic injury in diabetic nephropathy, as illustrated in figure 19. Experiments with Tonabersat demonstrates that blocking one step of this cycle, and beneficially targeting upstream of the

inflammasome leaving it open for microbial defence, blocks the feedforward loop, preventing downstream inflammation and fibrosis.

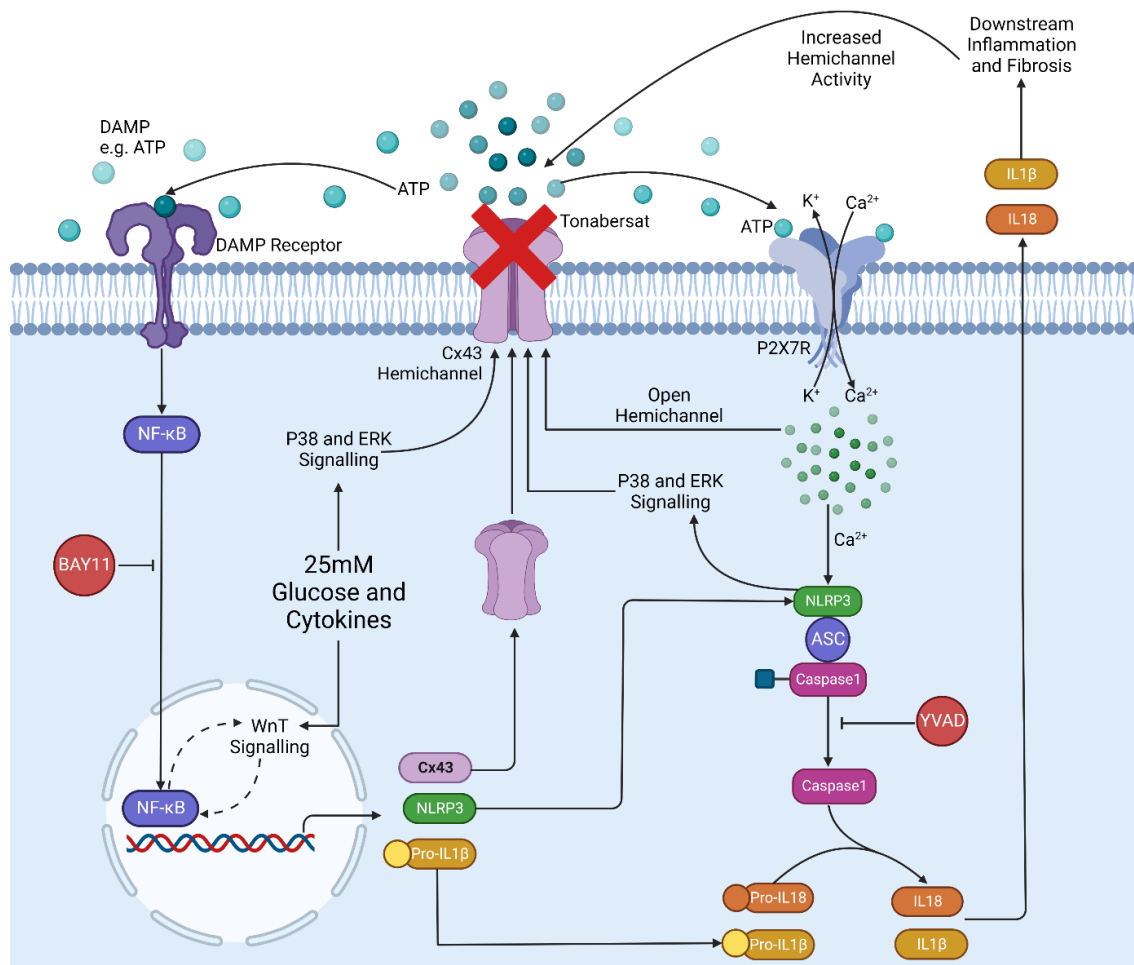


Figure 5.18. A schematic outlining the proposed mechanisms through which Cx43 hemichannel activity and NLRP3 inflammasome activation exacerbate each other resulting in downstream inflammation and fibrosis, characteristic of diabetic nephropathy.

Inflammasome activation leads to downstream loss of kidney structure (Ding *et al.*, 2018; Zhang *et al.*, 2019), fibrosis (Wu *et al.*, 2018; Song *et al.*, 2018) and recruitment of immune cells such as macrophages (Hou *et al.*, 2021; Kim *et al.*, 2015). In the UO-Cx43^{-/-} model, data demonstrate that Cx43 deletion successfully blocks these downstream effects of inflammasome activation *in vivo*, protecting against kidney injury and highlighting the therapeutic potential of Cx43 as a therapeutic target for diabetic nephropathy. Specifically, a reduction in several pro-inflammatory cytokines and chemokines are observed, changes replicated in an *in vitro* model of diabetic nephropathy and negated using hemichannel blocker Tonabersat. A reduction in

MCP1 and G-CSF was determined, translating to reduced macrophage infiltration in the UUO-Cx43^{-/-} mouse model, demonstrating that the effects shown *in vitro* are relevant to disease protection *in vivo*. Of the immune cells involved in diabetic and chronic kidney disease, macrophages are the primary cell type infiltrating the kidney and play a pivotal role in disease. Interestingly, in addition to proximal tubule epithelial cells used here, macrophages stimulated with LPS also show a Cx43-mediated increase in NLRP3 inflammasome activity (Huang *et al.*, 2019), indicating that the protective effects of Tonabersat may extend to multiple cell types involved in the progression of diabetic nephropathy. Combined with data showing a Tonabersat and inflammasome-mediated decrease in markers of EMT and fibrosis, these findings provide evidence for the protective effects of blocking Cx43 on inflammation and fibrosis downstream of inflammasome activation.

In conclusion, data from *in vitro* and *in vivo* models of diabetic nephropathy demonstrate a role for the NLRP3 inflammasome in mediating downstream inflammation and fibrosis associated with loss of renal function. Late-stage diabetic nephropathy includes proximal tubule inflammation, where increased damage positively correlates with disease progression (Takaori *et al.*, 2016). Despite this, effective treatment of renal inflammation represents an unmet clinical need. Whilst early stages of diabetic nephropathy are managed via control of blood glucose and pressure, (Selby and Taal, 2020) many people still progress to late-stage disease despite good glycaemic control, where treatment options are limited to dialysis and transplant, negatively impacting quality of life (Selby and Taal, 2020). Targeting the NLRP3 inflammasome has shown potential in treating several chronic inflammatory diseases however, side effects and increased risk of infection limit the effectiveness of directly targeting the NLRP3 inflammasome (Niu *et al.*, 2019). Therefore, focussing upstream to block Cx43 hemichannel-mediated inflammasome activation might represent a more effective therapeutic avenue in treating late stage kidney disease, with promising results thus far.

6.0. Discussion.

Diabetic nephropathy is the most frequent cause of chronic kidney disease and the largest contributor to end stage renal disease (Byrne *et al.*, 2018; Koye *et al.*, 2017). In addition to kidney-specific risks associated with chronic kidney disease, development of renal complications is also linked to an increased risk of developing other secondary complications, particularly cardiovascular complications, which accounts for the majority of diabetes associated mortality (Wetmore *et al.*, 2019). As GFR declines, glucose regulation becomes increasingly challenging and individuals with an eGFR between 15-30mL/min have a 14 times greater risk of cardiovascular complications and increased risk of early mortality (Cabrera *et al.*, 2020). Consequently, therapies for diabetic nephropathy are essential. Current treatments focus on control of blood glucose and blood pressure, however many individuals progress to late-stage kidney disease despite good glycaemic control, and there is an urgent need for novel therapies to target these late stages of disease to reduce risks of not only severe renal complications, but also exacerbated risk of other secondary complications. In this PhD, I aimed to elucidate the role of Cx43 hemichannels in mediating tubulointerstitial inflammation and fibrosis in response to elevated levels of inflammatory cytokines and glucose. Importantly, these observations informed studies which assessed the ability of the hemichannel blocker Tonabersat in blocking connexin hemichannel activity to observe associated downstream effects and assess the potential of this drug as a novel intervention for late stage diabetic nephropathy.

Work from the group has previously determined the effect of pro-fibrotic cytokine TGF β 1 on altered Cx43 hemichannel-mediated ATP release (Price *et al.*, 2020; Potter *et al.*, 2021a; Squires *et al.*, 2021; Williams *et al.*, 2022). Elevated in diabetic nephropathy, TGF β 1 is linked to increased blood glucose and associated with tubulointerstitial fibrosis. In this project, I examined the role of elevated systemic pro-inflammatory cytokines IL1 β , IL18 and TNF α , often present in individuals with diabetes despite good glycaemic control and implicated as an initiating factor of secondary complications of diabetes. Acting through multiple pathways, these cytokines amplify inflammation in disease, which precedes establishment of fibrosis in DN. The effects of inflammatory cytokines with and without high glucose were initially characterised in PTECs to develop a physiologically relevant *in vitro* model of tubule injury in diabetic nephropathy. Optimised cytokine treatment was consistent with treatments used previously to model diabetic retinopathy (Mugisho *et al.* 2018), another microvascular complication of diabetes with similar pathological mechanisms. Treatment of PTECs

with high (25mmol/L) glucose in combination with proinflammatory cytokines IL1 β (10ng/mL) and TNF α (10ng/mL)-induced changes in protein expression indicative of increased inflammation, ECM deposition and pEMT, changes consistent with proximal tubule injury in diabetic nephropathy.

Elevated in biopsy samples from individuals with diabetes and in mouse models of kidney injury, Cx43 expression was increased in high glucose and cytokine treated PTECs, changes paralleled by increased hemichannel-mediated ATP release. These findings were also demonstrated in TGF β 1 treated PTECs (Price *et al.*, 2020; Squires *et al.*, 2021) and high glucose and cytokine treated ARPE cells (Mugisho *et al.*, 2018a). Additionally, altered Cx43 expression and ATP release is observed in models of acute kidney injury (Huang *et al.*, 2019) and chronic inflammatory conditions including diabetes-induced skeletal muscle myopathy (Cea *et al.*, 2023), wound healing (Zhang *et al.*, 2021a), temporal lobe epilepsy (Guo *et al.*, 2022) and neuropathic pain following peripheral nerve injury (Tonkin *et al.*, 2018). Whilst each of these conditions exhibit subtle differences in the mechanism of action, a common theme centres on the fact that altered Cx43 expression/hemichannel activity is linked with increased NLRP3 inflammasome activity, highlighting a key mechanism through which Cx43-mediated ATP release contributes to inflammation.

Upregulated in diabetic nephropathy (Shen *et al.*, 2022), the NLRP3 inflammasome is a major inflammatory complex characterised by NF κ B-mediated priming of inflammasome components, and P2X7R-NLRP3-caspase 1-mediated activation of IL1 β and IL18 maturation and secretion. A previous study demonstrated that exposure of mouse peritoneal macrophages to LPS and ATP increased NLRP3 inflammasome activity, an upregulation that was dampened in heterogenous Cx43^{+/-} macrophages or those treated with Cx43 siRNA (Huang *et al.*, 2019). More recently, a study investigating the mechanisms by which bioactive glass promotes wound healing determined that bioglass down-regulated Cx43 expression, reduced pyroptosis and release of reactive oxygen species in endothelial cells taken from skin tissues of the wound edges of mice following surgery (Zhang *et al.*, 2021a). Pyroptosis is initiated by inflammasome activation and formation of GSDMD pores and as such this study also investigated changes in protein expression of inflammasome components NLRP3, pro-caspase 1, cleaved caspase 1, GSDMD, cleaved GSDMD, IL1 β and IL18. Expression of all candidate proteins were upregulated in an *in vivo* mouse model of wound healing 7 days post-surgery, changes significantly negated following bio-glass treatments, demonstrating its protective effects post-injury. Supporting the notion that these effects are Cx43-mediated, use of a Cx43 activator (GAP134) in wounded mice increased

Cx43 and ROS levels, reducing overall wound healing. Moreover, treatment with Cx43 inhibitor (GAP26) reduced expression of Cx43, pyroptosis markers and ROS levels resulting in dense granulation and capillary formation to aid more complete wound healing (Zhang *et al.*, 2021a). Whilst this demonstrates a link between Cx43 and NLRP3 inflammasome activation, the mechanism through which Cx43 mediates this effect, whether it be hemichannel or gap junction dependant, is yet to be established.

Studies in other models have elucidated a hemichannel-specific role for Cx43 in activating the inflammasome. In a mouse model of temporal lobe epilepsy, treatment with small molecule Cx43 hemichannel blocker D4 (5-10 mg/kg) negated a pilocarpine-induced increase in mRNA expression of NLRP3 in the hippocampus following x1 and x3 doses at 5 hours, 1 day, and 2 days (Guo *et al.*, 2022). In skeletal muscle myopathy, another secondary complication of diabetes, Cx43 hemichannel activity was increased in skeletal myofibers of streptozotocin-induced diabetic mice as compared to control. These results were paralleled *in vitro* by an increase in NLRP3 activity in high glucose treated murine myofibers, which when blocked by hemichannel blocker Boldine further support the link between increased hemichannel activity to inflammation (Cea *et al.*, 2023). Moreover, in a mouse model of chronic constriction injury, Cx43 hemichannel blockade via Peptide5 negated an injury-induced increase in expression of NLRP3, ASC and caspase 1 in the ipsilateral spinal cord (Tonkin *et al.*, 2018).

Similar findings have been observed in models of diabetic retinopathy in which inflammasome activation is regulated through Cx43 hemichannel-mediated ATP release in *in vitro* (Mugisho *et al.*, 2018a; Lyon *et al.*, 2021a), *in vivo* (Mat Nor *et al.*, 2020) and *ex vivo* (Louie *et al.*, 2021) models of disease. Until now, a link between connexin 43 hemichannel activity and inflammasome priming/activation has not been established in the diseased kidney. In this project, a Cx43 hemichannel dependant increase in both inflammasome priming and activation was observed, events which were shown to drive a further increase in Cx43 hemichannel activity. These findings allude to the presence of a positive feedforward cycle driving the chronic inflammation which contributes to the pathogenesis of diabetic nephropathy. Having previously shown beneficial effects in models of retinopathy (Mat Nor *et al.*, 2020; Lyon *et al.*, 2021a; Louie *et al.*, 2021), Tonabersat effectively blocked Cx43 hemichannel-mediated dye uptake and ATP release, resulting in reduced inflammasome priming and activation. Further to this, altered expression of downstream markers of pEMT and fibrosis were also ameliorated. These findings highlight the beneficial effects of targeting inflammation in a model of advanced renal injury.

Use of SGLT2 inhibitors has been the biggest recent breakthrough in treating diabetic nephropathy. Originally used as a glucose lowering drug, SGLT2i's have since been shown to have direct beneficial effects on both renal (Neal *et al.*, 2017) and cardiovascular complications (Zinman *et al.*, 2015; Wiviott *et al.*, 2019; Cannon *et al.*, 2020). The mechanisms through which SGLT2i's mediate these additional effects are still being explored. Although a game changer, SGLT2i's do have limitations which prevent them from being a viable treatment for all. Dapagliflozin is the first, and only, SGLT2i to be approved for use in chronic kidney disease and can be prescribed to individuals with a GFR between 25-75ml/min (National Institute for Health and Care Excellence (NICE), 2022). Therefore, in addition to people with T1DM who are excluded due to the risks associated with the drug's glucose lowering effects (National Institute for Health and Care Excellence (NICE), 2022), those with a GFR below 25ml/min still have a lack of available treatment options. With DN being the leading cause of ERSD and the general population living longer, urgent therapeutic approaches are required. Novel Cx43 hemichannel blockers may represent one such approach.

The connexin 43 hemichannel blocker Tonabersat is currently undergoing phase 2b clinical trial for treatment of diabetic retinopathy (ClinicalTrials.gov Identifier: NCT05727891). Diabetic nephropathy and diabetic retinopathy have similar underlying characteristics including epithelial cell dysfunction, immune cell infiltration, extracellular matrix deposition and NLRP3 inflammasome activation. Therefore, use of Tonabersat could also be protective in DN. My data demonstrates that Tonabersat can successfully block Cx43 hemichannel opening and ATP release in a model of kidney disease, subsequently reducing downstream inflammation associated with NLRP3 inflammasome priming and activation. Interestingly, current phase 2b clinical trial aims for Tonabersat in diabetic retinopathy have been amended to include the effect on biomarkers of renal function (Clinical Trials Identifier: NCT05727891). In addition to their use in individuals unsuitable for SGLT2i use, future studies could investigate the effects of using SGLT2i's and Cx43 hemichannel blockers in combination, to potentially generate greater levels of protection across several comorbidities.

Data presented in this thesis offers compelling evidence to support a role for Cx43 in driving changes commonly associated with inflammation in proximal tubule epithelial cells though hemichannel-mediated ATP release, and subsequent inflammasome activation. However, tubulointerstitial fibrosis is contributed to by the activation of multiple different cell types both in and around the tubules (Lin *et al.*, 2022; Xie *et al.*, 2021; Li *et al.*, 2019). Therefore, understanding how Cx43 hemichannels may evoke

paracrine-mediated signalling is important in successfully targeting the activation of key effector cells e.g., macrophages and fibroblasts. In a heterozygous Cx43 knockout (Abed *et al.*, 2014) and homozygous tubule specific Cx43 knockout (Chapter 5) UUO mouse model of advanced tubulointerstitial injury, partial and full tubule Cx43 knockdown reduced macrophage (F4/80) and fibroblast (FSP1⁺) accumulation respectively. In support of these observations, our previous findings determined that conditioned media transfer (CMT) from kidney tubule cells triggers activation of renal medullary fibroblasts and increased extracellular matrix deposition, a response significantly reduced in the presence of Tonabersat (Williams *et al.*, 2022). Interestingly however, CMT from high glucose/TGF- β 1 activated fibroblasts, failed to evoke significant changes in tubule cell phenotype. Furthermore, in addition to the irrefutable role of Cx43 in driving heterotypic myofibroblast activation, promoting the fibrotic state, *in vivo* work in chapter 5 highlights a clear link between altered Cx43 tubule cell expression and macrophage recruitment, the main immune cell type contributing to inflammation in DN. Recent studies by Xu *et al.*, have identified that increased renal tubule Cx43 expression in UUO mice is paralleled by increased macrophage infiltration, a high percentage of which had undergone pyroptosis. Nevertheless, in the absence of the authors employing a specific hemichannel blocker for their *in vivo* work, further studies are now needed to evaluate the precise mechanisms that underpin the effect of PTEC Cx43 hemichannel activity on the recruitment and activation of macrophages (Xu *et al.*, 2022). Future experiments in which conditioned media from high glucose and cytokine treated RPTECs is applied to healthy human monocyte derived macrophages as a form of indirect cell culture will assess the effect of paracrine-mediated signalling on macrophage motility, polarity, NLRP3 inflammasome activity and expression profile. Use of Tonabersat will elucidate the contribution of Cx43 hemichannel activity to these effects when applied to RPTECs, macrophages or both.

In summary, I present data that links aberrant Cx43-hemichannel-mediated ATP release to increased NLRP3 inflammasome priming and activation, resulting in secretion of pro-inflammatory cytokines and chemokines which drive recruitment and activation of F4/80⁺ macrophages and FSP1⁺ fibroblasts (Figure 6.1). Moreover, I demonstrate that inflammasome priming and activation contribute to a perpetual cycle of inflammation through increasing Cx43 expression and hemichannel activity. Importantly, experiments utilising Tonabersat establish that blocking Cx43 hemichannel activity protects against these effects, and downstream altered expression associated with pEMT and fibrosis, changes characteristic of late stage

tubulointerstitial inflammation in DN. These findings highlight the potential of targeting Cx43 hemichannels to dampen tubular inflammation and fibrosis in diabetic nephropathy. Whilst the work shows that targeting Cx43 hemichannels prevents the severity of tubulointerstitial fibrosis that develops in the UUO mice, future studies are now required to determine the efficacy of Peptide5 and other Cx43 hemichannel blockers in other models of CKD notably those in which kidney function can be assessed.

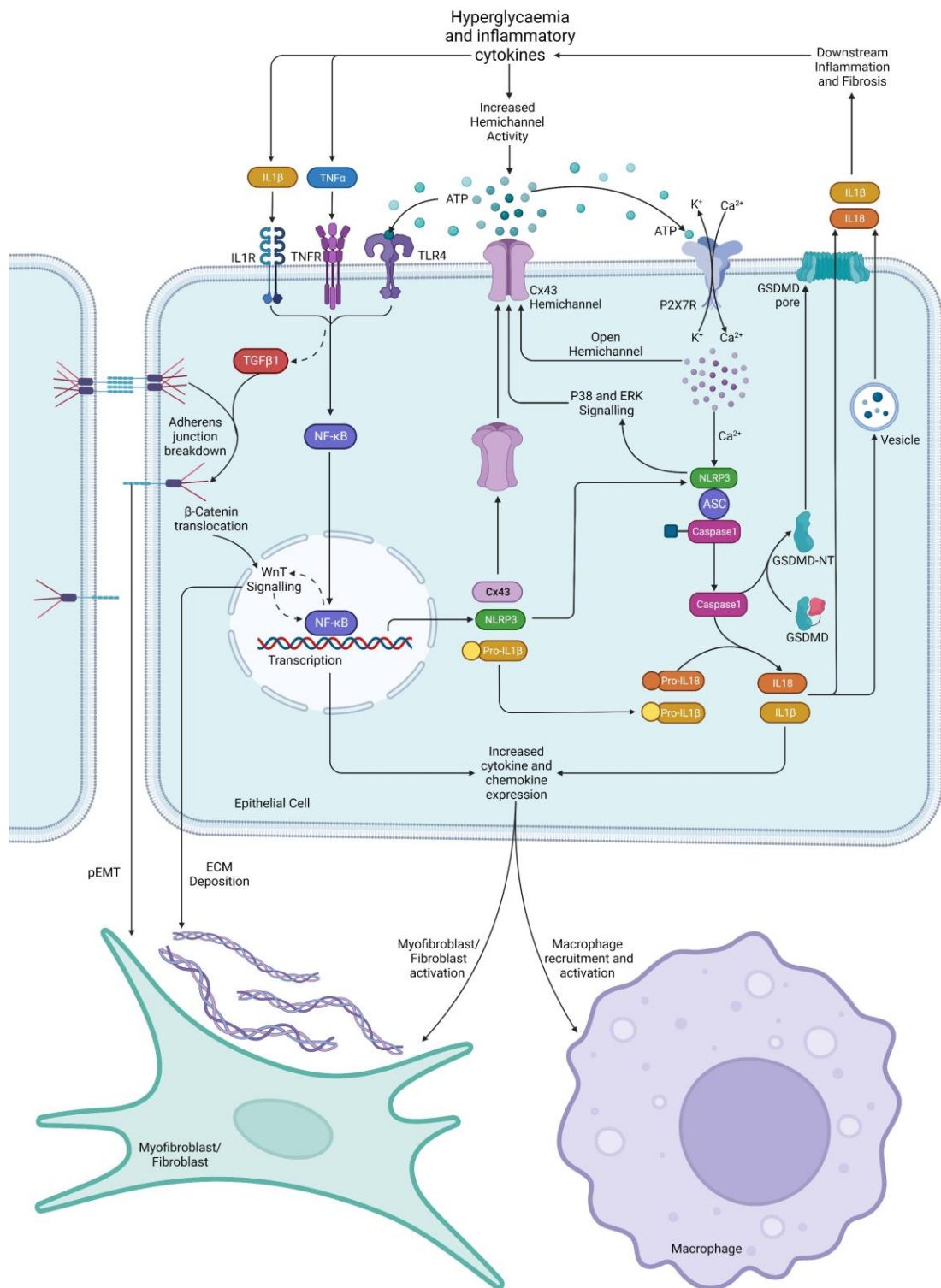


Figure 6.12. Schematic illustrating the proposed mechanisms through which Cx43 hemichannel activity contributes to tubulointerstitial inflammation and fibrosis. High glucose and inflammatory cytokines drive increased inflammasome priming and activation, pEMT, extracellular matrix deposition and cytokine/chemokine release via increased Cx43 hemichannel-mediated ATP release in proximal tubule epithelial cells, leading to recruitment and activation of macrophage and fibroblast cells. Created in Biorender.

Future experiments could be performed to determine whether changes in Cx43 hemichannels are paralleled by a breakdown in gap junction formation, an expected change following loss of adherens junctions to maintain close cell contact and integrity. This project utilised the UUO mouse model of advanced tubulointerstitial injury. Whilst the model is not one of diabetes, it does represent the pathology of late-stage kidney disease regardless of the cause of onset (Martínez-Klimova *et al.*, 2019), allowing us to determine the effect of Cx43 on chronic kidney disease. Future experiments using a model of diabetes such as the streptozotocin-induced diabetic mice or the db/db mice could be carried out to support current findings, albeit the streptozotocin mouse model is more akin to early stage injury with damage originating in response to STZ-mediated destruction of pancreatic beta cells (Giralt-López *et al.*, 2020). Similarly, whilst our *in vitro* model recapitulates glycaemic injury, repeating experiments at basal (5mmol/L) glucose would allow the effect of Cx43 on other causes of chronic kidney disease to be elucidated. Moreover, in clinical practise, Tonabersat would likely be used after onset of disease, especially given the fact that hemichannels tend to fully open only in the face of injury. Therefore, future experiments in which Tonabersat is applied post treatment of high glucose and inflammatory cytokines, would help to further evaluate the extent of the benefits of blocking Cx43 hemichannels in the context of established injury.

7.0. References

- Abed, A., Toubas, J., Kavvadas, P., Authier, F., Cathelin, D., Alfieri, C., Boffa, J. J., Dussaule, J. C., Chatziantoniou, C. and ChadjiChristos, C. E. (2014) 'Targeting connexin 43 protects against the progression of experimental chronic kidney disease in mice', *Kidney International*, 86(4), pp. 768–779. doi: 10.1038/ki.2014.108.
- Abudara, V., Bechberger, J., Freitas-Andrade, M., De Bock, M., Wang, N., Bultynck, G., Naus, C. C., Leybaert, L. and Giaume, C. (2014) 'The connexin43 mimetic peptide Gap19 inhibits hemichannels without altering gap junctional communication in astrocytes', *Frontiers in Cellular Neuroscience*, 8(OCT), p. 306. doi: 10.3389/FNCEL.2014.00306/BIBTEX.
- Abu-Saleh, N., Yaseen, H., Kinaneh, S., Khamaisi, M. and Abassi, Z. (2021) 'Combination of hyperglycaemia and hyperlipidaemia induces endothelial dysfunction: Role of the endothelin and nitric oxide systems', *Journal of Cellular and Molecular Medicine*, 25(4), pp. 1884–1895. doi: 10.1111/JCMM.15787.
- Adhikary, L., Chow, F., Nikolic-Paterson, D. J., Stambe, C., Dowling, J., Atkins, R. C. and Tesch, G. H. (2004) 'Abnormal p38 mitogen-activated protein kinase signalling in human and experimental diabetic nephropathy', *Diabetologia*, 47(7), pp. 1210–1222. doi: 10.1007/S00125-004-1437-0/FIGURES/6.
- Agashe, S. and Petak, S. (2018) 'Cardiac Autonomic Neuropathy in Diabetes Mellitus', *Methodist DeBakey Cardiovascular Journal*, 14(4), p. 251. doi: 10.14797/MDCJ-14-4-251.
- Ahmed, B., Sultana, R. and Greene, M. W. (2021) 'Adipose tissue and insulin resistance in obese', *Biomedicine & Pharmacotherapy*, 137, p. 111315. doi: 10.1016/J.BIOPHA.2021.111315.
- Alberts, B., Johnson, A., Lewis, J., Raff, M., Roberts, K. and Walter, P. (2002) *Molecular Biology of the Cell*. 4th edn. New York: Garland Science. Available at: <https://www.ncbi.nlm.nih.gov/books/NBK21054/>.
- Albino, A. H., Zambom, F. F. F., Foresto-Neto, O., Oliveira, K. C., Ávila, V. F., Arias, S. C. A., Seguro, A. C., Malheiros, D. M. A. C., Camara, N. O. S., Fujihara, C. K. and Zatz, R. (2021) 'Renal Inflammation and Innate Immune Activation Underlie the Transition From Gentamicin-Induced Acute Kidney Injury to Renal Fibrosis', *Frontiers in Physiology*, 12, p. 1021. doi: 10.3389/FPHYS.2021.606392/BIBTEX.

- Alessi, D. R., Cuenda, A., Cohen, P., Dudley, D. T. and Saltiel, A. R. (1995) 'PD 098059 is a specific inhibitor of the activation of mitogen-activated protein kinase kinase in vitro and in vivo', *The Journal of biological chemistry*, 270(46), pp. 27489–27494. doi: 10.1074/JBC.270.46.27489.
- Alhajj, M. and Farhana, A. (2022) 'Enzyme Linked Immunosorbent Assay', *StatPearls*. Available at: <https://www.ncbi.nlm.nih.gov/books/NBK555922/>.
- Allison, S. J. (2019) 'A signature of inflammatory proteins associated with ESRD in diabetes', *Nature Reviews Nephrology*, 15(7), pp. 387. doi: 10.1038/s41581-019-0157-0.
- Alonso, F., Krattinger, N., Mazzolai, L., Simon, A., Waeber, G., Meda, P. and Haefliger, J. A. (2010) 'An angiotensin II- and NF-kappaB-dependent mechanism increases connexin 43 in murine arteries targeted by renin-dependent hypertension', *Cardiovascular research*, 87(1), pp. 166–176. doi: 10.1093/CVR/CVQ031.
- Al-Qabbaa, S. M., Qaboli, S. I., Alshammari, T. K., Alamin, M. A., Alrajeh, H. M., Almuthnabi, L. A., Alotaibi, R. R., Alonazi, A. S., Bin Dayel, A. F., Alrasheed, Nawal M. and Alrasheed, Nouf M. (2023) 'Sitagliptin Mitigates Diabetic Nephropathy in a Rat Model of Streptozotocin-Induced Type 2 Diabetes: Possible Role of PTP1B/JAK-STAT Pathway', *International journal of molecular sciences*, 24(7). doi: 10.3390/IJMS24076532/S1.
- Alyaseer, A. A. A., de Lima, M. H. S. and Braga, T. T. (2020) 'The Role of NLRP3 Inflammasome Activation in the Epithelial to Mesenchymal Transition Process During the Fibrosis', *Frontiers in Immunology*, 11, p. 883. doi: 10.3389/FIMMU.2020.00883.
- An, C., Jiao, B., Du, H., Tran, M., Song, B., Wang, P., Zhou, D. and Wang, Y. (2023) 'Jumonji domain-containing protein-3 (JMJD3) promotes myeloid fibroblast activation and macrophage polarization in kidney fibrosis', *British Journal of Pharmacology*. doi: 10.1111/BPH.16096.
- Anthony, C. C., Robbins, D. J., Ahmed, Y. and Lee, E. (2020) 'Nuclear Regulation of Wnt/ β -Catenin Signaling: It's a Complex Situation', *Genes*, 11(8), pp. 1–11. doi: 10.3390/GENES11080886.
- Antonetti, D. A., Silva, P. S. and Stitt, A. W. (2021) 'Current understanding of the molecular and cellular pathology of diabetic retinopathy', *Nature Reviews Endocrinology*, 17(4), pp. 195–206. doi: 10.1038/s41574-020-00451-4.

- Armstrong, D. G., Lavery, L. A., Vela, S. A., Quebedeaux, T. L. and Fleischli, J. G. (1998) 'Choosing a Practical Screening Instrument to Identify Patients at Risk for Diabetic Foot Ulceration', *Archives of Internal Medicine*, 158(3), pp. 289–292. doi: 10.1001/ARCHINTE.158.3.289.
- Arrigo, A., Aragona, E. and Bandello, F. (2022) 'VEGF-targeting drugs for the treatment of retinal neovascularization in diabetic retinopathy', *Annals of medicine*, 54(1), pp. 1089–1111. doi: 10.1080/07853890.2022.2064541.
- Aryal, D., Jackson, K. E., Aryal, D. and Jackson, K. E. (2020) 'Association of Acid-Base Balance in the Renal Proximal Tubule and Blood Pressure Alterations: Potential Role of Local Mediators', *Journal of Biosciences and Medicines*, 8(4), pp. 26–44. doi: 10.4236/JBM.2020.84003.
- Awad, A. S., You, H., Gao, T., Cooper, T. K., Nedospasov, S. A., Vacher, J., Wilkinson, P. F., Farrell, F. X. and Reeves, W. B. (2015) 'Macrophage-derived tumor necrosis factor- α mediates diabetic renal injury', *Kidney International*, 88, pp. 722–733. doi: 10.1038/ki.2015.162.
- Babelova, A., Moreth, K., Tsalastra-Greul, W., Zeng-Brouwers, J., Eickelberg, O., Young, M. F., Brucker, P., Pfeilschifter, J., Schaefer, R. M., Gröne, H. J. and Schaefer, L. (2009) 'Biglycan, a danger signal that activates the NLRP3 inflammasome via toll-like and P2X receptors', *Journal of Biological Chemistry*, 284(36), pp. 24035–24048. doi: 10.1074/jbc.M109.014266.
- Baekkeskov, S., Aanstoot, H. J., Christgai, S., Reetz, A., Solimena, M., Cascalho, M., Folli, F., Richter-Olesen, H. and Camilli, P. De (1990) 'Identification of the 64K autoantigen in insulin-dependent diabetes as the GABA-synthesizing enzyme glutamic acid decarboxylase', *Nature*, 347(6289), pp. 151–156. doi: 10.1038/347151A0.
- Bass, J. J., Wilkinson, D. J., Rankin, D., Phillips, B. E., Szewczyk, N. J., Smith, K. and Atherton, P. J. (2017) 'An overview of technical considerations for Western blotting applications to physiological research', *Scandinavian journal of medicine & science in sports*, 27(1), pp. 4–25. doi: 10.1111/SMS.12702.
- Basu, M., Pandit, K., Banerjee, M., Mondal, S. A., Mukhopadhyay, P. and Ghosh, S. (2020) 'Profile of Auto-antibodies (Disease Related and Other) in Children with Type 1 Diabetes', *Indian Journal of Endocrinology and Metabolism*, 24(3), p. 256. doi: 10.4103/IJEM.IJEM_63_20.

Bauernfeind, F. G., Horvath, G., Stutz, A., Alnemri, E. S., MacDonald, K., Speert, D., Fernandes-Alnemri, T., Wu, J., Monks, B. G., Fitzgerald, K. A., Hornung, V. and Latz, E. (2009) 'Cutting Edge: NF- κ B Activating Pattern Recognition and Cytokine Receptors License NLRP3 Inflammasome Activation by Regulating NLRP3 Expression', *The Journal of Immunology*, 183(2), pp. 787–791. doi: 10.4049/JIMMUNOL.0901363.

Baum, P., Toyka, K. V., Blüher, M., Kosacka, J. and Nowicki, M. (2021) 'Inflammatory Mechanisms in the Pathophysiology of Diabetic Peripheral Neuropathy (DN)—New Aspects', *International Journal of Molecular Sciences*, 22(19), p. 10835. doi: 10.3390/IJMS221910835.

Beagley, J., Guariguata, L., Weil, C. and Motala, A. A. (2014) 'Global estimates of undiagnosed diabetes in adults', *Diabetes Research and Clinical Practice*, 103(2), pp. 150–160. doi: 10.1016/J.DIABRES.2013.11.001.

Becker, D. L., Thrasivoulou, C. and Phillips, A. R. J. (2012) 'Connexins in wound healing; Perspectives in diabetic patients', *Biochimica et Biophysica Acta - Biomembranes*, 1818(8), pp. 2068–2075. doi: 10.1016/j.bbamem.2011.11.017.

Bello, A. K., Levin, A., Lunney, M., Osman, M. A., Ye, F., Ashuntantang, G. E., Bellorin-Font, E., Benganem Gharbi, M., Davison, S. N., Ghnaimat, M., Harden, P., Htay, H., Jha, V., Kalantar-Zadeh, K., Kerr, P. G., Klarenbach, S., Kovesdy, C. P., Luyckx, V. A., Neuen, B. L., *et al.* (2019) 'Status of care for end stage kidney disease in countries and regions worldwide: international cross sectional survey', *BMJ*, p. l5873. doi: 10.1136/bmj.l5873.

Bellou, V., Belbasis, L., Tzoulaki, I. and Evangelou, E. (2018) 'Risk factors for type 2 diabetes mellitus: An exposure-wide umbrella review of meta-analyses', *PLOS ONE*, 13(3), p. e0194127. doi: 10.1371/JOURNAL.PONE.0194127.

Bengal, E., Aviram, S. and Hayek, T. (2020) 'p38 MAPK in Glucose Metabolism of Skeletal Muscle: Beneficial or Harmful?', *International Journal of Molecular Sciences*, 21(18), pp. 1–17. doi: 10.3390/IJMS21186480.

Birnbaum, Y., Bajaj, M., Yang, H. C. and Ye, Y. (2018) 'Combined SGLT2 and DPP4 Inhibition Reduces the Activation of the Nlrp3/ASC Inflammasome and Attenuates the Development of Diabetic Nephropathy in Mice with Type 2 Diabetes', *Cardiovascular Drugs and Therapy*, 32(2), pp. 135–145. doi: 10.1007/s10557-018-6778-x.

- Blevins, H. M., Xu, Y., Biby, S. and Zhang, S. (2022) 'The NLRP3 Inflammasome Pathway: A Review of Mechanisms and Inhibitors for the Treatment of Inflammatory Diseases', *Frontiers in aging neuroscience*, 14. doi: 10.3389/FNAGI.2022.879021.
- Boutens, L., Hooiveld, G. J., Dhingra, S., Cramer, R. A., Netea, M. G. and Stienstra, R. (2018) 'Unique metabolic activation of adipose tissue macrophages in obesity promotes inflammatory responses', *Diabetologia*, 61(4), pp. 942–953. doi: 10.1007/S00125-017-4526-6/FIGURES/6.
- Bradford, M. M. (1976) 'A rapid and sensitive method for the quantitation of microgram quantities of protein utilizing the principle of protein-dye binding', *Analytical Biochemistry*, 72(1–2), pp. 248–254. doi: 10.1016/0003-2697(76)90527-3.
- Braga, T. T., Forni, M. F., Correa-Costa, M., Ramos, R. N., Barbuto, J. A., Branco, P., Castoldi, A., Hiyane, M. I., Davanzo, M. R., Latz, E., Franklin, B. S., Kowaltowski, A. J. and Camara, N. O. S. (2017) 'Soluble Uric Acid Activates the NLRP3 Inflammasome', *Scientific Reports*, 7. doi: 10.1038/SREP39884.
- Brucklacher-Waldert, V. (2018) *Application Note: ATPlite assay performance in human primary cells*, *Drug Target Review*. Cambridge. Available at: <https://www.drugtargetreview.com/whitepaper/33324/application-note-atplite-assay-performance-in-human-primary-cells/>.
- Budd, M. A., Monajemi, M., Colpitts, S. J., Crome, S. Q., Verchere, C. B. and Levings, M. K. (2021) 'Interactions between islets and regulatory immune cells in health and type 1 diabetes', *Diabetologia*, 64(11), pp. 2378–2388. doi: 10.1007/S00125-021-05565-6.
- Burhans, M. S., Hagman, D. K., Kuzma, J. N., Schmidt, K. A. and Kratz, M. (2018) 'Contribution of adipose tissue inflammation to the development of type 2 diabetes mellitus', *Comprehensive Physiology*, 9(1), p. 1. doi: 10.1002/CPHY.C170040.
- Burns, W. C. and Thomas, M. C. (2010) 'The molecular mediators of type 2 epithelial to mesenchymal transition (EMT) and their role in renal pathophysiology', *Expert Reviews in Molecular Medicine*, 12, p. e17. doi: 10.1017/S1462399410001481.
- Burnstock, G. and Knight, G. E. (2018) 'The potential of P2X7 receptors as a therapeutic target, including inflammation and tumour progression', *Purinergic signalling*, 14(1). doi: 10.1007/S11302-017-9593-0.
- Butera, J. A., Larsen, B. D., Herman, J. K., Kerns, E., Di, L., Alimardanov, A., Swillo, R. E., Morgan, G. A., Liu, K., Wang, Q., Rossman, E. I., Unwalla, R., McDonald, L.,

- Huselton, C. and Petersen, J. S. (2009) 'Discovery of (2S,4R)-1-(2-aminoacetyl)-4-benzamidopyrrolidine-2-carboxylic acid hydrochloride (GAP-134) 13, an orally active small molecule gap-junction modifier for the treatment of atrial fibrillation', *Journal of Medicinal Chemistry*, 52(4), pp. 908–911. doi: 10.1021/JM801558D/SUPPL_FILE/JM801558D_SI_001.PDF.
- Byrne, C., Caskey, F., Castledine, C., Dawnay, A., Ford, D., Fraser, S., Lambie, M., Maxwell, H., Steenkamp, R., Wilkie, M. and Williams, A. (2018) 'UK Renal Registry: 20th Annual Report of the Renal Association.', *Nephron*, 139, pp. 24–35.
- Cabrera, C. S., Lee, A. S., Olsson, M., Schnecke, V., Westman, K., Lind, M., Greasley, P. J. and Skrtic, S. (2020) 'Impact of CKD Progression on Cardiovascular Disease Risk in a Contemporary UK Cohort of Individuals With Diabetes', *Kidney International Reports*, 5(10), p. 1651. doi: 10.1016/J.EKIR.2020.07.029.
- Calle, P. and Hotter, G. (2020) 'Macrophage Phenotype and Fibrosis in Diabetic Nephropathy', *International Journal of Molecular Sciences*, 21(8), p. 2806. doi: 10.3390/IJMS21082806.
- Cannon, C. P., Pratley, R., Dagogo-Jack, S., Mancuso, J., Huyck, S., Masiukiewicz, U., Charbonnel, B., Frederich, R., Gallo, S., Cosentino, F., Shih, W. J., Gantz, I., Terra, S. G., Cherney, D. Z. I. and McGuire, D. K. (2020) 'Cardiovascular Outcomes with Ertugliflozin in Type 2 Diabetes', *The New England journal of medicine*, 383(15), pp. 1425–1435. doi: 10.1056/NEJMOA2004967.
- Cao, H., Wang, C., Chen, X., Hou, J., Xiang, Z., Shen, Y. and Han, X. (2018) 'Inhibition of Wnt/ β -catenin signaling suppresses myofibroblast differentiation of lung resident mesenchymal stem cells and pulmonary fibrosis', *Scientific Reports*, 8(1), pp. 1–14. doi: 10.1038/s41598-018-28968-9.
- Cassel, S. L. and Sutterwala, F. S. (2010) 'Sterile inflammatory responses mediated by the NLRP3 inflammasome', *European Journal of Immunology*, 40(3), pp. 607–611. doi: 10.1002/EJI.200940207.
- Catalán, V., Gómez-Ambrosi, J., Rodríguez, A., Ramírez, B., Rotellar, F., Valentí, V., Silva, C., Gil, M. J., Salvador, J. and Frühbeck, G. (2011) 'Increased circulating and visceral adipose tissue expression levels of YKL-40 in obesity-associated type 2 diabetes are related to inflammation: impact of conventional weight loss and gastric bypass', *The Journal of clinical endocrinology and metabolism*, 96(1), pp. 200–209. doi: 10.1210/JC.2010-0994.

Cea, L. A., Vásquez, W., Hernández-Salinas, R., Vielma, A. Z., Castillo-Ruiz, M., Velarde, V., Salgado, M. and Sáez, J. C. (2023) 'Skeletal Muscle Atrophy Induced by Diabetes Is Mediated by Non-Selective Channels and Prevented by Boldine', *Biomolecules*, 13(4). doi: 10.3390/BIOM13040708/S1.

Centers for Disease Control and Prevention (CDC; 2020) *National Diabetes Statistics Report*. Available at: <https://www.cdc.gov/diabetes/pdfs/data/statistics/national-diabetes-statistics-report.pdf>.

Chakravarthy, A., Khan, L., Bensler, N. P., Bose, P. and De Carvalho, D. D. (2018) 'TGF- β -associated extracellular matrix genes link cancer-associated fibroblasts to immune evasion and immunotherapy failure', *Nature Communications*, 9(1), pp. 1–10. doi: 10.1038/s41467-018-06654-8.

Chatterjee, S. and Tao, J. Q. (2019) 'Reactive Oxygen Species activate the NLRP3 Inflammasome in a model of lung transplant', *The FASEB Journal*, 33(S1), pp. 549.2-549.2. doi: 10.1096/FASEBJ.2019.33.1_SUPPLEMENT.549.2.

Che, D., Zhou, T., Lan, Y., Xie, J., Gong, H., Li, C., Feng, J., Hong, H., Qi, W., Ma, C., Wu, Q., Yang, X. and Gao, G. (2016) 'High glucose-induced epithelial-mesenchymal transition contributes to the upregulation of fibrogenic factors in retinal pigment epithelial cells', *International Journal of Molecular Medicine*, 38(6), pp. 1815–1822. doi: 10.3892/IJMM.2016.2768/HTML.

Chen, B., Yang, L., Chen, J., Chen, Y., Zhang, L., Wang, L., Li, X., Li, Y. and Yu, H. (2019) 'Inhibition of Connexin43 hemichannels with Gap19 protects cerebral ischemia/reperfusion injury via the JAK2/STAT3 pathway in mice', *Brain Research Bulletin*, 146, pp. 124–135. doi: 10.1016/j.brainresbull.2018.12.009.

Chen, Q. L., Yin, H. R., He, Q. Y. and Wang, Y. (2021) 'Targeting the NLRP3 inflammasome as new therapeutic avenue for inflammatory bowel disease', *Biomedicine & Pharmacotherapy*, 138, p. 111442. doi: 10.1016/J.BIOPHA.2021.111442.

Chen, Y. ling, Qiao, Y. chao, Xu, Y., Ling, W., Pan, Y. hong, Huang, Y. cheng, Geng, L. jun, Zhao, H. lu and Zhang, X. xi (2017) 'Serum TNF- α concentrations in type 2 diabetes mellitus patients and diabetic nephropathy patients: A systematic review and meta-analysis', *Immunology letters*, 186, pp. 52–58. doi: 10.1016/J.IMLET.2017.04.003.

- Chen, Y. S., Green, C. R., Teague, R., Perrett, J., Danesh-Meyer, H. V., Toth, I. and Rupenthal, I. D. (2015) 'Intravitreal injection of lipoamino acid-modified connexin43 mimetic peptide enhances neuroprotection after retinal ischemia', *Drug Delivery and Translational Research*, 5(5), pp. 480–488. doi: 10.1007/s13346-015-0249-8.
- Chen, Y., Wang, L., Zhang, L., Chen, B., Yang, L., Li, X., Li, Y. and Yu, H. (2018) 'Inhibition of Connexin 43 Hemichannels Alleviates Cerebral Ischemia/Reperfusion Injury via the TLR4 Signaling Pathway', *Frontiers in Cellular Neuroscience*, 12. doi: 10.3389/FNCEL.2018.00372.
- Cheng, D., Liang, R., Huang, B., Hou, J., Yin, J., Zhao, T., Zhou, L., Wu, R., Qian, Y. and Wang, F. (2021) 'Tumor necrosis factor- α blockade ameliorates diabetic nephropathy in rats', *Clinical Kidney Journal*, 14(1), pp. 301–308. doi: 10.1093/CKJ/SFZ137.
- Chin, H. M., Lai, D. K. and Falchook, G. S. (2019) 'Extracellular Signal-Regulated Kinase (ERK) Inhibitors in Oncology Clinical Trials', *Journal of Immunotherapy and Precision Oncology*, 2(1), pp. 10–16. doi: 10.4103/JIPO.JIPO_17_18.
- Chiu, P. F., Su, S. L., Tsai, C. C., Wu, C. L., Kuo, C. L., Kor, C. T., Chang, C. C. and Liu, C. S. (2018) 'Cyclophilin A and CD147 associate with progression of diabetic nephropathy', *Free radical research*, 52(11–12), pp. 1456–1463. doi: 10.1080/10715762.2018.1523545.
- Choi, C., Saha, A., An, S., Cho, Y. K., Kim, H., Noh, M. and Lee, Y. H. (2022) 'Macrophage-Specific Connexin 43 Knockout Protects Mice from Obesity-Induced Inflammation and Metabolic Dysfunction', *Frontiers in Cell and Developmental Biology*, 10, p. 1309. doi: 10.3389/FCELL.2022.925971/BIBTEX.
- Chomarat, P., Banchereau, J., Davoust, J. and Palucka, A. K. (2000) 'IL-6 switches the differentiation of monocytes from dendritic cells to macrophages', *Nature Immunology*, 1(6), pp. 510–514. doi: 10.1038/82763.
- Christie, M. R. (2016) 'Delving Into the Type 1 Diabetic Islet: Evidence That B-Cell Infiltration of Islets Is Linked to Local Hyperimmunity and Accelerated Progression to Disease', *Diabetes*, 65(5), pp. 1146–1148. doi: 10.2337/DBI16-0008.
- Chung, H., Jung, H., Jho, E. hoon, Multhaupt, H. A. B., Couchman, J. R. and Oh, E. S. (2018) 'Keratinocytes negatively regulate the N-cadherin levels of melanoma cells via contact-mediated calcium regulation', *Biochemical and biophysical research communications*, 503(2), pp. 615–620. doi: 10.1016/J.BBRC.2018.06.050.

Cliff, C. L., Williams, B. M., Chadjichristos, C. E., Mouritzen, U., Squires, P. E. and Hills, C. E. (2022) 'Connexin 43: A Target for the Treatment of Inflammation in Secondary Complications of the Kidney and Eye in Diabetes', *International Journal of Molecular Sciences*, 23(2), p. 600. doi: 10.3390/IJMS23020600.

Clinical Trials Arena (no date) *Zydus to commence Phase IIa CAPS trial of drug in Australia*. Available at: <https://www.clinicaltrialsarena.com/news/zydus-caps-trial-australia/>.

Cogliati, B., Vinken, M., Silva, T. C., Araújo, C. M. M., Aloia, T. P. A., Chaible, L. M., Mori, C. M. C. and Dagli, M. L. Z. (2015) 'Connexin 43 deficiency accelerates skin wound healing and extracellular matrix remodeling in mice', *Journal of Dermatological Science*, 79(1), pp. 50–56. doi: 10.1016/j.jdermsci.2015.03.019.

Coppolino, G., Leporini, C., Rivoli, L., Ursini, F., di Paola, E. D., Cernaro, V., Arturi, F., Bolignano, D., Russo, E., De Sarro, G. and Andreucci, M. (2018) 'Exploring the effects of DPP-4 inhibitors on the kidney from the bench to clinical trials', *Pharmacological research*, 129, pp. 274–294. doi: 10.1016/J.PHRS.2017.12.001.

Coutinho, F. P., Green, C. R., Acosta, M. L. and Rupenthal, I. D. (2020) 'Xentry-Gap19 inhibits Connexin43 hemichannel opening especially during hypoxic injury', *Drug Delivery and Translational Research*, 10(3), pp. 751–765. doi: 10.1007/S13346-020-00763-Y/FIGURES/11.

Crespo Yanguas, S., da Silva, T., Pereira, I., Willebrords, J., Maes, M., Sayuri Nogueira, M., Alves de Castro, I., Leclercq, I., Romualdo, G., Barbisan, L., Leybaert, L., Cogliati, B. and Vinken, M. (2018) 'TAT-Gap19 and Carbenoxolone Alleviate Liver Fibrosis in Mice', *International Journal of Molecular Sciences*, 19(3), p. 817. doi: 10.3390/ijms19030817.

Cruz-Solbes, A. S. and Youker, K. (2017) 'Epithelial to mesenchymal transition (EMT) and endothelial to mesenchymal transition (EndMT): Role and implications in kidney fibrosis', in *Results and Problems in Cell Differentiation*. Springer Verlag, pp. 345–372. doi: 10.1007/978-3-319-51436-9_13.

Cuollo, L., Antonangeli, F., Santoni, A. and Soriani, A. (2020) 'The Senescence-Associated Secretory Phenotype (SASP) in the Challenging Future of Cancer Therapy and Age-Related Diseases', *Biology*, 9(12), p. 485. doi: 10.3390/BIOLOGY9120485.

Dalui, S., Chakraverty, R., Yasmin, N., Pattanaik, S., Pandit, K. and Chatterjee, S. (2021) 'Effects of DPP4 inhibitors on renal outcomes in diabetes mellitus: A systematic

review and meta-analysis', *Indian Journal of Endocrinology and Metabolism*, 25(4), pp. 283–292. doi: 10.4103/IJEM.IJEM_237_21.

Danek, P., Kardosova, M., Janeckova, L., Karkoulia, E., Vanickova, K., Fabisik, M., Lozano-Asencio, C., Benoukraf, T., Tirado-Magallanes, R., Zhou, Q., Burocchiova, M., Rahmatova, S., Pytlik, R., Brdicka, T., Tenen, D. G., Korinek, V. and Alberich-Jorda, M. (2020) ' β -Catenin–TCF/LEF signaling promotes steady-state and emergency granulopoiesis via G-CSF receptor upregulation', *Blood*, 136(22), pp. 2574–2587. doi: 10.1182/BLOOD.2019004664.

Danesh-Meyer, H. V., Kerr, N. M., Zhang, J., Eady, E. K., O'Carroll, S. J., Nicholson, L. F. B., Johnson, C. S. and Green, C. R. (2012) 'Connexin43 mimetic peptide reduces vascular leak and retinal ganglion cell death following retinal ischaemia', *Brain*, 135(2), pp. 506–520. doi: 10.1093/brain/awr338.

Davidson, E. P., Coppey, L. J., Dake, B. and Yorek, M. A. (2011) 'Treatment of Streptozotocin-Induced Diabetic Rats with Alogliptin: Effect on Vascular and Neural Complications', *Experimental Diabetes Research*, 2011. doi: 10.1155/2011/810469.

Davidson, J. O., Drury, P. P., Green, C. R., Nicholson, L. F., Bennet, L. and Gunn, A. J. (2014) 'Connexin Hemichannel Blockade Is Neuroprotective after Asphyxia in Preterm Fetal Sheep', *PLoS ONE*, 9(5), p. e96558. doi: 10.1371/journal.pone.0096558.

De Vries, A. P. J., Ruggenenti, P., Ruan, X. Z., Praga, M., Cruzado, J. M., Bajema, I. M., D'Agati, V. D., Lamb, H. J., Barlovic, D. P., Hojs, R., Abbate, M., Rodriguez, R., Mogensen, C. E. and Porrini, E. (2014) 'Fatty kidney: emerging role of ectopic lipid in obesity-related renal disease', *The lancet. Diabetes & endocrinology*, 2(5), pp. 417–426. doi: 10.1016/S2213-8587(14)70065-8.

Deacon, C. F. (2020) 'Dipeptidyl peptidase 4 inhibitors in the treatment of type 2 diabetes mellitus', *Nature Reviews Endocrinology*, 16(11), pp. 642–653. doi: 10.1038/s41574-020-0399-8.

Delvaeye, T., De Smet, M. A. J., Verwaerde, S., Decrock, E., Czekaj, A., Vandenbroucke, R. E., Lemeire, K., Gonçalves, A., Declercq, W., Vandenabeele, P., Krysko, D. V. and Leybaert, L. (2019) 'Blocking connexin43 hemichannels protects mice against tumour necrosis factor-induced inflammatory shock', *Scientific Reports*, 9(1), pp. 1–12. doi: 10.1038/s41598-019-52900-4.

Desjardins-Park, H. E., Foster, D. S. and Longaker, M. T. (2018) 'Fibroblasts and wound healing: An update', *Regenerative Medicine*, 13(5), pp. 491–495. doi: 10.2217/RME-2018-0073/ASSET/IMAGES/LARGE/FIGURE1.JPEG.

Dhani, S., Zhao, Y. and Zhivotovsky, B. (2021) 'A long way to go: caspase inhibitors in clinical use', *Cell Death & Disease*, 12(10), p. 949. doi: 10.1038/s41419-021-04240-3.

Dhimolea, E. (2010) 'Canakinumab', *mAbs*, 2(1), p. 3. doi: 10.4161/MABS.2.1.10328. Cotrina, M. L., Lin, J. H. C., Alves-Rodrigues, A., Liu, S., Li, J., Azmi-Ghadimi, H., Kang, J., Naus, C. C. G. and Nedergaard, M. (1998) 'Connexins regulate calcium signaling by controlling ATP release', *Proceedings of the National Academy of Sciences of the United States of America*, 95(26), p. 15735. doi: 10.1073/PNAS.95.26.15735.

Dilworth, L., Facey, A. and Omoruyi, F. (2021) 'Diabetes Mellitus and Its Metabolic Complications: The Role of Adipose Tissues', *International Journal of Molecular Sciences*, 22(14), p. 7644. doi: 10.3390/IJMS22147644.

Dinarello, C. A. (2018) 'Overview of the IL-1 family in innate inflammation and acquired immunity', *Immunological reviews*, 281(1), p. 8. doi: 10.1111/IMR.12621.

Ding, H., Li, J., Li, Y., Yang, M., Nie, S., Zhou, M., Zhou, Z., Yang, X., Liu, Y. and Hou, F. F. (2021) 'MicroRNA-10 negatively regulates inflammation in diabetic kidney via targeting activation of the NLRP3 inflammasome', *Molecular Therapy*, 29(7), pp. 2308–2320. doi: 10.1016/J.YMTHE.2021.03.012.

Ding, S., Xu, S., Ma, Y., Liu, G., Jang, H. and Fang, J. (2019) 'Modulatory Mechanisms of the NLRP3 Inflammasomes in Diabetes', *Biomolecules*, 9(12). doi: 10.3390/BIOM9120850.

Ding, T., Wang, S., Zhang, X., Zai, W., Fan, J., Chen, W., Bian, Q., Luan, J., Shen, Y., Zhang, Y., Ju, D. and Mei, X. (2018) 'Kidney protection effects of dihydroquercetin on diabetic nephropathy through suppressing ROS and NLRP3 inflammasome', *Phytomedicine: international journal of phytotherapy and phytopharmacology*, 41, pp. 45–53. doi: 10.1016/J.PHYMED.2018.01.026.

Dong, Y., Wu, Z., He, M., Chen, Yuhan, Chen, Yixing, Shen, X., Zhao, X., Zhang, L., Yuan, B. and Zeng, Z. (2018) 'ADAM9 mediates the interleukin-6-induced Epithelial–Mesenchymal transition and metastasis through ROS production in hepatoma cells', *Cancer Letters*, 421, pp. 1–14. doi: 10.1016/J.CANLET.2018.02.010.

Dosch, M., Zindel, J., Jebbawi, F., Melin, N., Sanchez-Taltavull, D., Stroka, D., Candinas, D. and Beldi, G. (2019) 'Connexin-43-dependent ATP release mediates macrophage activation during sepsis', *eLife*, 8. doi: 10.7554/ELIFE.42670.

Downs, K. P., Nguyen, H., Dorfleutner, A. and Stehlik, C. (2020) 'An overview of the non-canonical inflammasome', *Molecular aspects of medicine*, 76. doi: 10.1016/J.MAM.2020.100924.

Du, Q., Fu, Y. xue, Shu, A. mei, Lv, X., Chen, Y. ping, Gao, Y. yan, Chen, J., Wang, W., Lv, G. hong, Lu, J. fu and Xu, H. qin (2021) 'Loganin alleviates macrophage infiltration and activation by inhibiting the MCP-1/CCR2 axis in diabetic nephropathy', *Life Sciences*, 272, p. 118808. doi: 10.1016/J.LFS.2020.118808.

Elbadawy, H. M., Mirabelli, P., Xeroudaki, M., Parekh, M., Bertolin, M., Breda, C., Cagini, C., Ponzin, D., Lagali, N. and Ferrari, S. (2016) 'Effect of connexin 43 inhibition by the mimetic peptide Gap27 on corneal wound healing, inflammation and neovascularization', *British Journal of Pharmacology*, 173(19), pp. 2880–2893. doi: 10.1111/bph.13568.

El-Dawla, N. M. Q., Sallam, A. A. M., El-Hefnawy, M. H. and El-Mesallamy, H. O. (2019) 'E-cadherin and periostin in early detection and progression of diabetic nephropathy: epithelial-to-mesenchymal transition', *Clinical and Experimental Nephrology*, 23(8), pp. 1050–1057. doi: 10.1007/S10157-019-01744-3/FIGURES/3.

Engstrøm, T., Nepper-Christensen, L., Helqvist, S., Kløvgaard, L., Holmvang, L., Jørgensen, E., Pedersen, F., Saunamaki, K., Tilsted, H. H., Steensberg, A., Fabricius, S., Mouritzen, U., Vejstrup, N., Ahtarovski, K. A., Göransson, C., Bertelsen, L., Kyhl, K., Olivecrona, G., Kelbæk, H., *et al.* (2018) 'Danegaptide for primary percutaneous coronary intervention in acute myocardial infarction patients: a phase 2 randomised clinical trial', *Heart (British Cardiac Society)*, 104(19), pp. 1593–1599. doi: 10.1136/HEARTJNL-2017-312774.

Esposito, K., Nappo, F., Marfella, R., Giugliano, G., Giugliano, F., Ciotola, M., Quagliaro, L., Ceriello, A. and Giugliano, D. (2002) 'Inflammatory Cytokine Concentrations Are Acutely Increased by Hyperglycemia in Humans', *Circulation*, 106(16), pp. 2067–2072. doi: 10.1161/01.CIR.0000034509.14906.AE.

Evangelista, L. S., Cho, W. K. and Kim, Y. (2018) 'Obesity and chronic kidney disease: A population-based study among South Koreans', *PLOS ONE*, 13(2), pp. e0193559. doi: 10.1371/JOURNAL.PONE.0193559.

Evans, J. R., Michelessi, M. and Virgili, G. (2014) 'Laser photocoagulation for proliferative diabetic retinopathy', *The Cochrane Database of Systematic Reviews*, 2014(11). doi: 10.1002/14651858.CD011234.PUB2.

Everett, L. A. and Paulus, Y. M. (2021) 'Laser Therapy in the Treatment of Diabetic Retinopathy and Diabetic Macular Edema', *Current diabetes reports*, 21(9). doi: 10.1007/S11892-021-01403-6.

Fallon, C., Jones, E., Oliver, N., Reddy, M. and Avari, P. (2022) 'The impact of socio-economic deprivation on access to diabetes technology in adults with type 1 diabetes', *Diabetic medicine: a journal of the British Diabetic Association*, 39(10). doi: 10.1111/DME.14906.

Faniku, C., O'Shaughnessy, E., Lorraine, C., Johnstone, S. R., Graham, A., Greenhough, S. and Martin, P. E. M. (2018) 'The Connexin Mimetic Peptide Gap27 and Cx43-Knockdown Reveal Differential Roles for Connexin43 in Wound Closure Events in Skin Model Systems', *International Journal of Molecular Sciences*, 19(2), p. 604. doi: 10.3390/IJMS19020604.

Feldman, E. L., Callaghan, B. C., Pop-Busui, R., Zochodne, D. W., Wright, D. E., Bennett, D. L., Bril, V., Russell, J. W. and Viswanathan, V. (2019) 'Diabetic neuropathy', *Nature Reviews Disease Primers*, 5(1), pp. 1–18. doi: 10.1038/s41572-019-0092-1.

Feng, B., Chen, S., Gordon, A. D. and Chakrabarti, S. (2017) 'miR-146a mediates inflammatory changes and fibrosis in the heart in diabetes', *Journal of Molecular and Cellular Cardiology*, 105, pp. 70–76. doi: 10.1016/J.YJMCC.2017.03.002.

Feng, H., Zhu, X., Tang, Y., Fu, S., Kong, B. and Liu, X. (2021) 'Astragaloside IV ameliorates diabetic nephropathy in db/db mice by inhibiting NLRP3 inflammasome-mediated inflammation', *International Journal of Molecular Medicine*, 48(2), pp. 1–12. doi: 10.3892/IJMM.2021.4996/HTML.

Feoktistova, M., Geserick, P. and Leverkus, M. (2016) 'Crystal violet assay for determining viability of cultured cells', *Cold Spring Harbor Protocols*, 2016(4), pp. 343–346. doi: 10.1101/pdb.prot087379.

Fernández-Juárez, G., Villacorta Perez, J., Luño Fernández, J. L., Martinez-Martinez, E., Cachafeiro, V., Barrio Lucia, V., Tato Ribera, A. M., Mendez Abreu, A., Cordon, A., Oliva Dominguez, J. A. and Praga Terente, M. (2017) 'High levels of circulating TNFR1

increase the risk of all-cause mortality and progression of renal disease in type 2 diabetic nephropathy', *Nephrology*, 22(5), pp. 354–360. doi: 10.1111/nep.12781.

Foresto-Neto, O., Ávila, V. F., Arias, S. C. A., Zambom, F. F. F., Rempel, L. C. T., Faustino, V. D., Machado, F. G., Malheiros, D. M. A. C., Abensur, H., Camara, N. O. S., Zatz, R. and Fujihara, C. K. (2018) 'NLRP3 inflammasome inhibition ameliorates tubulointerstitial injury in the remnant kidney model', *Laboratory Investigation*, 98(6), pp. 773–782. doi: 10.1038/s41374-018-0029-4.

Foretz, M., Guigas, B. and Viollet, B. (2019) 'Understanding the glucoregulatory mechanisms of metformin in type 2 diabetes mellitus', *Nature Reviews Endocrinology*, 15(10), pp. 569–589. doi: 10.1038/s41574-019-0242-2.

Forrester, J. V., Kuffova, L. and Delibegovic, M. (2020) 'The Role of Inflammation in Diabetic Retinopathy', *Frontiers in Immunology*, 11, p. 2644. doi: 10.3389/FIMMU.2020.583687/BIBTEX.

Fox, C. S., Matsushita, K., Woodward, M., Bilo, H. J. G., Chalmers, J., Lambers Heerspink, H. J., Lee, B. J., Perkins, R. M., Rossing, P., Sairenchi, T., Tonelli, M., Vassalotti, J. A., Yamagishi, K., Coresh, J., De Jong, P. E., Wen, C. P. and Nelson, R. G. (2012) 'Associations of kidney disease measures with mortality and end-stage renal disease in individuals with and without diabetes: a meta-analysis', *Lancet*, 380(9854), pp. 1662–1673. doi: 10.1016/S0140-6736(12)61350-6.

Frantz, C., Stewart, K. M. and Weaver, V. M. (2010) 'The extracellular matrix at a glance', *Journal of Cell Science. The Company of Biologists Ltd*, pp. 4195–4200. doi: 10.1242/jcs.023820.

Furman, D., Campisi, J., Verdin, E., Carrera-Bastos, P., Targ, S., Franceschi, C., Ferrucci, L., Gilroy, D. W., Fasano, A., Miller, G. W., Miller, A. H., Mantovani, A., Weyand, C. M., Barzilai, N., Goronzy, J. J., Rando, T. A., Effros, R. B., Lucia, A., Kleinstreuer, N., *et al.* (2019) 'Chronic inflammation in the etiology of disease across the life span', *Nature Medicine*, 25(12), pp. 1822–1832. doi: 10.1038/s41591-019-0675-0.

Fusco, R., Siracusa, R., Genovese, T., Cuzzocrea, S. and Paola, R. Di (2020) 'Focus on the Role of NLRP3 Inflammasome in Diseases', *International Journal of Molecular Sciences*, 21(12), p. 4223. doi: 10.3390/IJMS21124223.

- Gaidt, M. M., Ebert, T. S., Cooper, M. A. and Graf, T. (2016) 'Human Monocytes Engage an Alternative Inflammasome Pathway', *Immunity*, 44, pp. 833–846. doi: 10.1016/j.immuni.2016.01.012.
- Ge, K., Wang, Y., Li, P., Li, M., Zhang, W., Dan, H., Hu, X., Zhou, J., Yang, Q., Wang, J. and Song, Z. (2022) 'Down-expression of the NLRP3 inflammasome delays the progression of diabetic retinopathy', *Microvascular research*, 139. doi: 10.1016/J.MVR.2021.104265.
- Geraghty, R. J., Capes-Davis, A., Davis, J. M., Downward, J., Freshney, R. I., Knezevic, I., Lovell-Badge, R., Masters, J. R. W., Meredith, J., Stacey, G. N., Thraves, P. and Vias, M. (2014) 'Guidelines for the use of cell lines in biomedical research', *British Journal of Cancer*, 111(6), pp. 1021–1046. doi: 10.1038/bjc.2014.166.
- Ghatnekar, G. S., O'Quinn, M. P., Jourdan, L. J., Gurjarpadhye, A. A., Draughn, R. L. and Gourdie, R. G. (2009) 'Connexin43 carboxyl-terminal peptides reduce scar progenitor and promote regenerative healing following skin wounding', *Regenerative Medicine*, 4(2), pp. 205–223. doi: 10.2217/17460751.4.2.205.
- Ghigliotti, G., Barisione, C., Garibaldi, S., Fabbi, P., Brunelli, C., Spallarossa, P., Altieri, P., Rosa, G., Spinella, G., Palombo, D., Arsenescu, R. and Arsenescu, V. (2014) 'Adipose tissue immune response: novel triggers and consequences for chronic inflammatory conditions', *Inflammation*, 37(4), pp. 1337–1353. doi: 10.1007/S10753-014-9914-1.
- Giannopoulos, S. and Armstrong, E. J. (2020) 'Diabetes mellitus: an important risk factor for peripheral vascular disease', *Expert Review of Cardiovascular Therapy*, 18(3), pp. 131–137. doi: 10.1080/14779072.2020.1736562.
- Giralt-López, A., Den Bosch, M. M. Van, Vergara, A., García-Carro, C., Seron, D., Jacobs-Cachá, C. and Soler, M. J. (2020) 'Revisiting Experimental Models of Diabetic Nephropathy', *International Journal of Molecular Sciences*, 21(10), p. 3587. doi: 10.3390/IJMS21103587.
- Goadsby, P. J., Ferrari, M. D., Csanyi, A., Olesen, J. and Mills, J. G. (2009) 'Randomized, double-blind, placebo-controlled, proof-of-concept study of the cortical spreading depression inhibiting agent tonabersat in migraine prophylaxis', *Cephalalgia: an international journal of headache*, 29(7), pp. 742–750. doi: 10.1111/J.1468-2982.2008.01804.X.

Gong, Z., Pan, J., Shen, Q., Li, M. and Peng, Y. (2018) 'Mitochondrial dysfunction induces NLRP3 inflammasome activation during cerebral ischemia/reperfusion injury', *Journal of Neuroinflammation*, 15(1), pp. 1–17. doi: 10.1186/S12974-018-1282-6/FIGURES/9.

Gonzalez, J. P., Ramachandran, J., Xie, L.-H., Contreras, J. E. and Fraidenraich, D. (2015) 'Selective Connexin43 Inhibition Prevents Isoproterenol-Induced Arrhythmias and Lethality in Muscular Dystrophy Mice', *Scientific Reports*, 5(1), p. 13490. doi: 10.1038/srep13490.

González-Casanova, J., Schmachtenberg, O., Martínez, A. D., Sanchez, H. A., Harcha, P. A. and Rojas-Gomez, D. (2021) 'An update on connexin gap junction and hemichannels in diabetic retinopathy', *International Journal of Molecular Sciences*, pp. 1–19. doi: 10.3390/ijms22063194.

González-Pérez, A., Saez, M., Vizcaya, D., Lind, M. and Garcia Rodriguez, L. (2021) 'Incidence and risk factors for mortality and end-stage renal disease in people with type 2 diabetes and diabetic kidney disease: a population-based cohort study in the UK', *BMJ Open Diabetes Research and Care*, 9(1), p. e002146. doi: 10.1136/BMJDRC-2021-002146.

Grande, M. T., Sánchez-Laorden, B., López-Blau, C., De Frutos, C. A., Boutet, A., Arévalo, M., Rowe, R. G., Weiss, S. J., López-Novoa, J. M. and Nieto, M. A. (2015) 'Snail1-induced partial epithelial-to-mesenchymal transition drives renal fibrosis in mice and can be targeted to reverse established disease', *Nature medicine*, 21(9), pp. 989–997. doi: 10.1038/NM.3901.

Green, C. R., Mat Nor, M. N., Mugisho, O. O., Rupenthal, I. D., Squirrell, D. M. and Acosta, M. L. (2019) 'Connexin hemichannel block shuts down inflammation in an animal model of chronic diabetic retinopathy to improve structural and functional outcomes', *Investigative ophthalmology and visual science*, 60(9), p. 2784. Available at: <https://iovs.arvojournals.org/article.aspx?articleid=2742820>.

Grek, C. L., Montgomery, J., Sharma, M., Ravi, A., Rajkumar, J. S., Moyer, K. E., Gourdie, R. G. and Ghatnekar, G. S. (2017) 'A Multicenter Randomized Controlled Trial Evaluating a Cx43-Mimetic Peptide in Cutaneous Scarring', *Journal of Investigative Dermatology*, 137(3), pp. 620–630. doi: 10.1016/j.jid.2016.11.006.

Grek, C. L., Prasad, G. M., Viswanathan, V., Armstrong, D. G., Gourdie, R. G. and Ghatnekar, G. S. (2015) 'Topical administration of a connexin43-based peptide augments healing of chronic neuropathic diabetic foot ulcers: A multicenter,

randomized trial', *Wound Repair and Regeneration*, 23(2), pp. 203–212. doi: 10.1111/wrr.12275.

Grönholm, T., Zhong, J. C., Palojoki, E., Eriksson, A., Bäcklund, T., Vuolteenaho, O., Finckenberg, P., Laine, M., Mervaala, E. and Tikkanen, I. (2005) 'Vasopeptidase inhibition has beneficial cardiac effects in spontaneously diabetic Goto–Kakizaki rats', *European Journal of Pharmacology*, 519(3), pp. 267–276. doi: 10.1016/J.EJPHAR.2005.07.015.

Güemes, M., Rahman, S. A. and Hussain, K. (2016) 'What is a normal blood glucose?', *Archives of Disease in Childhood*, 101(6), pp. 569–574. doi: 10.1136/ARCHDISCHILD-2015-308336.

Guey, B., Bodnar, M., Manié, S. N., Tardivel, A. and Petrilli, V. (2014) 'Caspase-1 autoproteolysis is differentially required for NLRP1b and NLRP3 inflammasome function', *Proceedings of the National Academy of Sciences of the United States of America*, 111(48), pp. 17254–17259. doi: 10.1073/PNAS.1415756111/SUPPL_FILE/PNAS.201415756SI.PDF.

Guo, A., Zhang, H., Li, H., Chiu, A., García-Rodríguez, C., Lagos, C. F., Sáez, J. C. and Lau, C. G. (2022) 'Inhibition of connexin hemichannels alleviates neuroinflammation and hyperexcitability in temporal lobe epilepsy', *Proceedings of the National Academy of Sciences of the United States of America*, 119(45), p. e2213162119. doi: 10.1073/PNAS.2213162119/SUPPL_FILE/PNAS.2213162119.SAPP.PDF.

Guo, C. X., Nor, M. N. M., Danesh-Meyer, H. V., Vessey, K. A., Fletcher, E. L., O'Carroll, S. J., Acosta, M. L. and Green, C. R. (2016) 'Connexin43 mimetic peptide improves retinal function and reduces inflammation in a light-damaged albino rat model', *Investigative Ophthalmology and Visual Science*, 57(10), pp. 3961–3973. doi: 10.1167/iov.15-16643.

Guo, X., Li, H., Xu, H., Woo, S., Dong, H., Lu, F., Lange, A. J. and Wu, C. (2012) 'Glycolysis in the control of blood glucose homeostasis', *Acta Pharmaceutica Sinica B*, 2(4), pp. 358–367. doi: 10.1016/J.APSB.2012.06.002.

Gusev, E., Solomatina, L., Zhuravleva, Y. and Sarapultsev, A. (2021) 'The Pathogenesis of End-Stage Renal Disease from the Standpoint of the Theory of General Pathological Processes of Inflammation', *International Journal of Molecular Sciences*, 22(21), pp. 11453. doi: 10.3390/IJMS222111453.

- Haeusler, R. A., McGraw, T. E. and Accili, D. (2017) 'Biochemical and cellular properties of insulin receptor signalling', *Nature Reviews Molecular Cell Biology*, 19(1), pp. 31–44. doi: 10.1038/nrm.2017.89.
- Harding, J. L., Pavkov, M. E., Magliano, D. J., Shaw, J. E. and Gregg, E. W. (2019) 'Global trends in diabetes complications: a review of current evidence', *Diabetologia*, 62(1), pp. 3–16. doi: 10.1007/S00125-018-4711-2/TABLES/5.
- Hartsock, A. and Nelson, W. J. (2008) 'Adherens and tight junctions: Structure, function and connections to the actin cytoskeleton', *Biochimica et Biophysica Acta (BBA) - Biomembranes*, 1778(3), pp. 660–669. doi: 10.1016/J.BBAMEM.2007.07.012.
- Hawat, G., Hélie, P. and Baroudi, G. (2012) 'Single intravenous low-dose injections of connexin 43 mimetic peptides protect ischemic heart in vivo against myocardial infarction', *Journal of Molecular and Cellular Cardiology*, 53(4), pp. 559–566. doi: 10.1016/j.yjmcc.2012.07.008.
- Hawkes, C. J., Schloot, N. C., Marks, J., Willemen, S. J. M., Drijfhout, J. W., Mayer, E. K., Christie, M. R. and Roep, B. O. (2000) 'T-cell lines reactive to an immunodominant epitope of the tyrosine phosphatase-like autoantigen IA-2 in type 1 diabetes.', *Diabetes*, 49(3), pp. 356–366. doi: 10.2337/DIABETES.49.3.356.
- Heneka, M. T., Kummer, M. P., Stutz, A., Delekate, A., Schwartz, S., Vieira-Saecker, A., Griep, A., Axt, D., Remus, A., Tzeng, T. C., Gelpi, E., Halle, A., Korte, M., Latz, E. and Golenbock, D. T. (2013) 'NLRP3 is activated in Alzheimer's disease and contributes to pathology in APP/PS1 mice', *Nature*, 493(7434), p. 674. doi: 10.1038/NATURE11729.
- Hicks, C. W., Selvarajah, S., Mathioudakis, N., Sherman, R. E., Hines, K. F., Black, J. H. and Abularrage, C. J. (2016) 'Burden of Infected Diabetic Foot Ulcers on Hospital Admissions and Costs', *Annals of vascular surgery*, 33, pp. 149–158. doi: 10.1016/J.AVSG.2015.11.025.
- Hills, C. E., Siamantouras, E., Smith, S. W., Cockwell, P., Liu, K. K. and Squires, P. E. (2012) 'TGFβ modulates cell-to-cell communication in early epithelial-to-mesenchymal transition', *Diabetologia*, 55(3), pp. 812–824. doi: 10.1007/S00125-011-2409-9/FIGURES/10.
- Hills, C., Price, G. W., Wall, M. J., Kaufmann, T. J., Chi-Wai Tang, S., Yiu, W. H. and Squires, P. E. (2018) 'Transforming Growth Factor Beta 1 Drives a Switch in Connexin

Mediated Cell-to-Cell Communication in Tubular Cells of the Diabetic Kidney', *Cellular Physiology and Biochemistry*, 45(6), pp. 2369–2388. doi: 10.1159/000488185.

Hirooka, Y. and Nozaki, Y. (2021) 'Interleukin-18 in Inflammatory Kidney Disease', *Frontiers in Medicine*, 8, p. 193. doi: 10.3389/FMED.2021.639103/BIBTEX.

Hoffman, R. P., Dye, A. S., Huang, H. and Bauer, J. A. (2016) 'Glycemic variability predicts inflammation in adolescents with type 1 diabetes', *Journal of Pediatric Endocrinology and Metabolism*, 29(10), pp. 1129–1133. doi: 10.1515/JPEM-2016-0139/MACHINEREADABLECITATION/RIS.

Hofherr, A., Williams, J., Gan, L. M., Söderberg, M., Hansen, P. B. L. and Woollard, K. J. (2022) 'Targeting inflammation for the treatment of Diabetic Kidney Disease: a five-compartment mechanistic model', *BMC Nephrology*, 23(1), pp. 1–17. doi: 10.1186/S12882-022-02794-8.

Hotamisligil, G. S., Shargill, N. S. and Spiegelman, B. M. (1993) 'Adipose expression of tumor necrosis factor- α : direct role in obesity-linked insulin resistance', *Science*, 259(5091), pp. 87–91. doi: 10.1126/SCIENCE.7678183.

Hou, Y., Wang, Q., Han, B., Chen, Y., Qiao, X. and Wang, L. (2021) 'CD36 promotes NLRP3 inflammasome activation via the mtROS pathway in renal tubular epithelial cells of diabetic kidneys', *Cell Death & Disease*, 12(6), pp. 1–16. doi: 10.1038/s41419-021-03813-6.

Hsu, W. C., Lin, C. S., Chen, J. F. and Chang, C. M. (2022) 'The Effects of Dipeptidyl Peptidase 4 Inhibitors on Renal Function in Patients with Type 2 Diabetes Mellitus', *Journal of clinical medicine*, 11(9). doi: 10.3390/JCM11092653.

Huang, X., Pan, Q., Mao, Z., Wang, P., Zhang, R., Ma, X., Chen, J. and You, H. (2018) 'Kaempferol inhibits interleukin-1 β stimulated matrix metalloproteinases by suppressing the MAPK-associated ERK and P38 signaling pathways', *Molecular Medicine Reports*, 18(3), pp. 2697–2704. doi: 10.3892/MMR.2018.9280/HTML.

Huang, Yanru, Mao, Z., Zhang, Z., Obata, F., Yang, X., Zhang, X., Huang, Yong, Mitsui, T., Fan, J., Takeda, M. and Yao, J. (2019) 'Connexin43 Contributes to Inflammasome Activation and Lipopolysaccharide-Initiated Acute Renal Injury via Modulation of Intracellular Oxidative Status', *Antioxidants & redox signaling*, 31(16), pp. 1194–1212. doi: 10.1089/ARS.2018.7636.

Huang, Z. and Xu, A. (2021) 'Adipose Extracellular Vesicles in Intercellular and Inter-Organ Crosstalk in Metabolic Health and Diseases', *Frontiers in Immunology*, 12, p. 463. doi: 10.3389/FIMMU.2021.608680/BIBTEX.

Hull, C., Dekeryte, R., Buchanan, H., Kamli-Salino, S., Robertson, A., Delibegovic, M. and Platt, B. (2020) 'NLRP3 inflammasome inhibition with MCC950 improves insulin sensitivity and inflammation in a mouse model of frontotemporal dementia', *Neuropharmacology*, 180, p. 108305. doi: 10.1016/j.neuropharm.2020.108305.

IDF Diabetes Atlas 10th edition (2021). Available at: www.diabetesatlas.org.

Ikram, K., Carrillo Vico, A., Cruz-Chamorro, I., Khutami, C., Adi Sumiwi, S., Kusaira Khairul Ikram, N. and Muchtaridi, M. (2022) 'The Effects of Antioxidants from Natural Products on Obesity, Dyslipidemia, Diabetes and Their Molecular Signaling Mechanism', *International Journal of Molecular Sciences*, 23(4), p. 2056. doi: 10.3390/IJMS23042056.

Insel, R. A., Dunne, J. L., Atkinson, M. A., Chiang, J. L., Dabelea, D., Gottlieb, P. A., Greenbaum, C. J., Herold, K. C., Krischer, J. P., Lernmark, A., Ratner, R. E., Rewers, M. J., Schatz, D. A., Skyler, J. S., Sosenko, J. M. and Ziegler, A. G. (2015) 'Staging presymptomatic type 1 diabetes: a scientific statement of JDRF, the Endocrine Society, and the American Diabetes Association', *Diabetes care*, 38(10), pp. 1964–1974. doi: 10.2337/DC15-1419.

Ismail-Beigi, F., Craven, T., Banerji, M. A., Basile, J., Calles, J., Cohen, R. M., Cuddihy, R., Cushman, W. C., Genuth, S., Grimm, R. H., Hamilton, B. P., Hoogwerf, B., Karl, D., Katz, L., Krikorian, A., O'Connor, P., Pop-Busui, R., Schubart, U., Simmons, D., *et al.* (2010) 'Effect of intensive treatment of hyperglycaemia on microvascular outcomes in type 2 diabetes: an analysis of the ACCORD randomised trial', *Lancet*, 376(9739), pp. 419–430. doi: 10.1016/S0140-6736(10)60576-4.

Iwano, M., Plieth, D., Danoff, T. M., Xue, C., Okada, H. and Neilson, E. G. (2002) 'Evidence that fibroblasts derive from epithelium during tissue fibrosis', *The Journal of clinical investigation*, 110(3), pp. 341–350. doi: 10.1172/JCI15518.

Ixcamey, M. and Palma, C. (2021) 'Diabetic macular edema', *Disease-a-Month*, 67(5), p. 101138. doi: 10.1016/J.DISAMONTH.2021.101138. Raghavan, S., Vassy, J. L., Ho, Y. L., Song, R. J., Gagnon, D. R., Cho, K., Wilson, P. W. F. and Phillips, L. S. (2019) 'Diabetes Mellitus–Related All-Cause and Cardiovascular Mortality in a National Cohort of Adults', *Journal of the American Heart Association*, 8(4). doi: 10.1161/JAHA.118.011295.

- Iyyathurai, J., Wang, N., D'hondt, C., Jiang, J. X., Leybaert, L. and Bultynck, G. (2018) 'The SH3-binding domain of Cx43 participates in loop/tail interactions critical for Cx43-hemichannel activity', *Cellular and Molecular Life Sciences*, 75(11), pp. 2059–2073. doi: 10.1007/s00018-017-2722-7.
- Jahng, J. W. S., Song, E. and Sweeney, G. (2016) 'Crosstalk between the heart and peripheral organs in heart failure', *Experimental & molecular medicine*, 48(3). doi: 10.1038/EMM.2016.20.
- Jämsen, E., Pajarinen, J., Kouri, V. P., Rahikkala, A., Goodman, S. B., Manninen, M., Nordström, D. C., Eklund, K. K. and Nurmi, K. (2020) 'Tumor necrosis factor primes and metal particles activate the NLRP3 inflammasome in human primary macrophages', *Acta Biomaterialia*, 108, pp. 347–357. doi: 10.1016/J.ACTBIO.2020.03.017.
- Jang, J., Jung, Y., Chae, S., Chung, S. I., Kim, S. M. and Yoon, Y. (2017) 'WNT/ β -catenin pathway modulates the TNF- α -induced inflammatory response in bronchial epithelial cells', *Biochemical and biophysical research communications*, 484(2), pp. 442–449. doi: 10.1016/J.BBRC.2017.01.156.
- Jankowski, J., Perry, H. M., Medina, C. B., Huang, L., Yao, J., Bajwa, A., Lorenz, U. M., Rosin, D. L., Ravichandran, K. S., Isakson, B. E. and Okusa, M. D. (2018) 'Epithelial and Endothelial Pannexin1 Channels Mediate AKI', *Journal of the American Society of Nephrology*, 29(7), pp. 1887–1899. doi: 10.1681/ASN.2017121306.
- Jeng, C. J., Hsieh, Y. T., Yang, C. M., Yang, C. H., Lin, C. L. and Wang, I. J. (2016) 'Diabetic Retinopathy in Patients with Diabetic Nephropathy: Development and Progression', *PLOS ONE*, 11(8), p. e0161897. doi: 10.1371/JOURNAL.PONE.0161897.
- Jiang, J., Hoagland, D., Palatinus, J. A., He, H., Iyyathurai, J., Jourdan, L. J., Bultynck, G., Wang, Z., Zhang, Z., Schey, K., Poelzing, S., McGowan, F. X. and Gourdie, R. G. (2019) 'Interaction of α Carboxyl Terminus 1 Peptide With the Connexin 43 Carboxyl Terminus Preserves Left Ventricular Function After Ischemia-Reperfusion Injury', *Journal of the American Heart Association*, 8(16). doi: 10.1161/JAHA.119.012385.
- Jin, R., Zhao, A., Han, S., Zhang, D., Sun, H., Li, M., Su, D. and Liang, X. (2021) 'The interaction of S100A16 and GRP78 activates endoplasmic reticulum stress-mediated through the IRE1 α /XBP1 pathway in renal tubulointerstitial fibrosis', *Cell Death & Disease*, 12(10), pp. 1–9. doi: 10.1038/s41419-021-04249-8.

- Jo, D. H., Yun, J. H., Cho, C. S., Kim, Jin Hyoun, Kim, Jeong Hun and Cho, C. H. (2019) 'Interaction between microglia and retinal pigment epithelial cells determines the integrity of outer blood-retinal barrier in diabetic retinopathy', *Glia*, 67(2), pp. 321–331. doi: 10.1002/GLIA.23542.
- Johnson, J. A., Majumdar, S. R., Simpson, S. H. and Toth, E. L. (2002) 'Decreased Mortality Associated With the Use of Metformin Compared With Sulfonylurea Monotherapy in Type 2 Diabetes', *Diabetes Care*, 25(12), pp. 2244–2248. doi: 10.2337/DIACARE.25.12.2244.
- Ju, W., Nair, V., Smith, S., Zhu, L., Shedden, K., Song, P. X. K., Mariani, L. H., Eichinger, F. H., Berthier, C. C., Randolph, A., Lai, J. Y. C., Zhou, Y., Hawkins, J. J., Bitzer, M., Sampson, M. G., Their, M., Solier, C., Duran-Pacheco, G. C., Duchateau-Nguyen, G., *et al.* (2015) 'Tissue transcriptome-driven identification of epidermal growth factor as a chronic kidney disease biomarker', *Science translational medicine*, 7(316). doi: 10.1126/SCITRANSLMED.AAC7071.
- Kane, J. P., Pullinger, C. R., Goldfine, I. D. and Malloy, M. J. (2021) 'Dyslipidemia and diabetes mellitus: Role of lipoprotein species and interrelated pathways of lipid metabolism in diabetes mellitus', *Current Opinion in Pharmacology*, 61, pp. 21–27. doi: 10.1016/J.COPH.2021.08.013.
- Kaneko, N., Kurata, M., Yamamoto, T., Morikawa, S. and Masumoto, J. (2019) 'The role of interleukin-1 in general pathology', *Inflammation and Regeneration*, 39(1), pp. 1–16. doi: 10.1186/S41232-019-0101-5.
- Kang, H. M., Ahn, S. H., Choi, P., Ko, Y. A., Han, S. H., Chinga, F., Park, A. S. D., Tao, J., Sharma, K., Pullman, J., Bottinger, E. P., Goldberg, I. J. and Susztak, K. (2015) 'Defective fatty acid oxidation in renal tubular epithelial cells has a key role in kidney fibrosis development', *Nature medicine*, 21(1), pp. 37–46. doi: 10.1038/NM.3762.
- Kang, S., Tanaka, T., Inoue, H., Ono, C., Hashimoto, S., Kioi, Y., Matsumoto, H., Matsuura, H., Matsubara, T., Shimizu, K., Ogura, H., Matsuura, Y. and Kishimoto, T. (2020) 'IL-6 trans-signaling induces plasminogen activator inhibitor-1 from vascular endothelial cells in cytokine release syndrome', *Proceedings of the National Academy of Sciences of the United States of America*, 117(36), pp. 22351–22356. doi: 10.1073/PNAS.2010229117/SUPPL_FILE/PNAS.2010229117.SAPP.PDF.
- Kaur, J. and Seaquist, E. R. (2022) 'Hypoglycaemia in type 1 diabetes mellitus: risks and practical prevention strategies', *Nature Reviews Endocrinology*, 19(3), pp. 177–186. doi: 10.1038/s41574-022-00762-8.

- Kavvadas, P., Abed, A., Poulain, C., Authier, F., Labéjof, L. P., Calmont, A., Afieri, C., Prakoura, N., Dussaule, J. C., Chatziantoniou, C. and Chadjichristos, C. E. (2017) 'Decreased expression of connexin 43 blunts the progression of experimental GN', *Journal of the American Society of Nephrology*, 28(10), pp. 2915–2930. doi: 10.1681/ASN.2016111211.
- Kawano, A., Kadomatsu, R., Ono, M., Kojima, S., Tsukimoto, M. and Sakamoto, H. (2015) 'Autocrine Regulation of UVA-Induced IL-6 Production via Release of ATP and Activation of P2Y Receptors', *PLOS ONE*, 10(6), p. e0127919. doi: 10.1371/JOURNAL.PONE.0127919.
- Kaze, A. D., Santhanam, P., Musani, S. K., Ahima, R. and Echouffo-Tcheugui, J. B. (2021) 'Metabolic dyslipidemia and cardiovascular outcomes in type 2 diabetes mellitus: Findings from the look ahead study', *Journal of the American Heart Association*, 10(7), p. 16947. doi: 10.1161/JAHA.120.016947.
- Kelley, N., Jeltema, D., Duan, Y. and He, Y. (2019) 'The NLRP3 Inflammasome: An Overview of Mechanisms of Activation and Regulation', *International Journal of Molecular Sciences*, 20(13). doi: 10.3390/IJMS20133328.
- Kelly, K. J. and Dominguez, J. H. (2010) 'Rapid Progression of Diabetic Nephropathy Is Linked to Inflammation and Episodes of Acute Renal Failure', *American Journal of Nephrology*, 32(5), pp. 469–475. doi: 10.1159/000320749.
- Khadilkar, A. and Oza, C. (2022) 'Glycaemic Control in Youth and Young Adults: Challenges and Solutions', *Diabetes, Metabolic Syndrome and Obesity: Targets and Therapy*, 15, p. 121. doi: 10.2147/DMSO.S304347.
- Khanna, D., Khanna, S., Khanna, P., Kahar, P. and Patel, B. M. (2022) 'Obesity: A Chronic Low-Grade Inflammation and Its Markers', *Cureus*, 14(2). doi: 10.7759/CUREUS.22711.
- Kim, D., Mouritzen, U., Larsen, B. D. and Roy, S. (2018) 'Inhibition of Cx43 gap junction uncoupling prevents high glucose-induced apoptosis and reduces excess cell monolayer permeability in retinal vascular endothelial cells', *Experimental Eye Research*, 173, pp. 85–90. doi: 10.1016/j.exer.2018.05.003.
- Kim, H. S., Kim, H. J., Lee, M. R. and Han, I. (2021) 'EMMPRIN expression is associated with metastatic progression in osteosarcoma', *BMC Cancer*, 21(1), pp. 1–12. doi: 10.1186/S12885-021-08774-9/FIGURES/6.

- Kim, S. M., Lee, S. H., Kim, Y. G., Kim, S. Y., Seo, J. W., Choi, Y. W., Kim, D. J., Jeong, K. H., Lee, T. W., Ihm, C. G., Won, K. Y. and Moon, J. Y. (2015) 'Hyperuricemia-induced NLRP3 activation of macrophages contributes to the progression of diabetic nephropathy', *American journal of physiology. Renal physiology*, 308(9), pp. F993–F1003. doi: 10.1152/AJPRENAL.00637.2014.
- Kim, S. Y. and Nair, M. G. (2019) 'Macrophages in wound healing: activation and plasticity', *Immunology and Cell Biology*, 97(3), pp. 258–267. doi: 10.1111/IMCB.12236.
- Kim, Y., Griffin, J. M., Nor, M. N. M., Zhang, J., Freestone, P. S., Danesh-Meyer, H. V., Rupenthal, I. D., Acosta, M., Nicholson, L. F. B., O'Carroll, S. J. and Green, C. R. (2017) 'Tonabersat Prevents Inflammatory Damage in the Central Nervous System by Blocking Connexin43 Hemichannels', *Neurotherapeutics*, 14(4), pp. 1148–1165. doi: 10.1007/s13311-017-0536-9.
- King, D. R., Sedovy, M. W., Leng, X., Xue, J., Lamouille, S., Koval, M., Isakson, B. E. and Johnstone, S. R. (2021) 'Mechanisms of Connexin Regulating Peptides', *International Journal of Molecular Sciences*, 22(19), p. 10186. doi: 10.3390/IJMS221910186.
- Klessens, C. Q. F., Zandbergen, M., Wolterbeek, R., Bruijn, J. A., Rabelink, T. J., Bajema, I. M. and Ijpelaar, D. H. T. (2017) 'Macrophages in diabetic nephropathy in patients with type 2 diabetes', *Nephrology Dialysis Transplantation*, 32(8), pp. 1322–1329. doi: 10.1093/ndt/gfw260.
- Klück, V., Jansen, T. L. T. A., Janssen, M., Comarniceanu, A., Efdé, M., Tengesdal, I. W., Schraa, K., Cleophas, M. C. P., Scribner, C. L., Skouras, D. B., Marchetti, C., Dinarello, C. A. and Joosten, L. A. B. (2020) 'Dapansutrile, an oral selective NLRP3 inflammasome inhibitor, for treatment of gout flares: an open-label, dose-adaptive, proof-of-concept, phase 2a trial', *The Lancet Rheumatology*, 2(5), pp. e270–e280. doi: 10.1016/S2665-9913(20)30065-5.
- Koleva-Georgieva, D. N., Sivkova, N. P. and Terzieva, D. (2011) 'Serum inflammatory cytokines IL-1beta, IL-6, TNF-alpha and VEGF have influence on the development of diabetic retinopathy.', *Folia medica*, 53(2), pp. 44–50. doi: 10.2478/v10153-010-0036-8.
- Komala, M. G., Gross, S., Zaky, A., Pollock, C. and Panchapakesan, U. (2015) 'Linagliptin Limits High Glucose Induced Conversion of Latent to Active TGFβ through

Interaction with CIM6PR and Limits Renal Tubulointerstitial Fibronectin', *PLoS ONE*, 10(10). doi: 10.1371/JOURNAL.PONE.0141143.

Kormann, R., Kavvas, P., Placier, S., Vandermeersch, S., Dorison, A., Dussaule, J.-C., Chadji-christos, C. E., Prakoura, N. and Chatziantoniou, C. (2020) 'Periostin Promotes Cell Proliferation and Macrophage Polarization to Drive Repair after AKI', *Journal of the American Society of Nephrology*, 31(1), pp. 85–100. doi: 10.1681/ASN.2019020113.

Koye, D. N., Shaw, J. E., Reid, C. M., Atkins, R. C., Reutens, A. T. and Magliano, D. J. (2017) 'Incidence of chronic kidney disease among people with diabetes: a systematic review of observational studies', *Diabetic medicine: a journal of the British Diabetic Association*, 34(7), pp. 887–901. doi: 10.1111/DME.13324.

Krebs, J. (2018) 'Membrane Dynamics and Calcium Signaling', *Advances in Experimental Medicine and Biology*. doi: 10.1007/978-3-319-55858-5

Kuo, C., Green, C. R., Rupenthal, I. D. and Mugisho, O. O. (2020) 'Connexin43 hemichannel block protects against retinal pigment epithelial cell barrier breakdown', *Acta Diabetologica*, 57(1), pp. 13–22. doi: 10.1007/s00592-019-01352-3.

Kurtzeborn, K., Kwon, H. N. and Kuure, S. (2019) 'MAPK/ERK Signaling in Regulation of Renal Differentiation', *International Journal of Molecular Sciences*, 20(7), p. 1779. doi: 10.3390/IJMS20071779.

Kwon, S., Kim, Y. C., Park, J. Y., Lee, J., An, J. N., Kim, C. T., Oh, S., Park, S., Kim, D. K., Oh, Y. K., Kim, Y. S., Lim, C. S. and Lee, J. P. (2020) 'The Long-term Effects of Metformin on Patients With Type 2 Diabetic Kidney Disease', *Diabetes Care*, 43(5), pp. 948–955. doi: 10.2337/DC19-0936.

Laakso, M. and Kuusisto, J. (2014) 'Insulin resistance and hyperglycaemia in cardiovascular disease development', *Nature Reviews Endocrinology*, 10(5), pp. 293–302. doi: 10.1038/nrendo.2014.29.

Lali, F. V., Hunt, A. E., Turner, S. J. and Foxwell, B. M. J. (2000) 'The pyridinyl imidazole inhibitor SB203580 blocks phosphoinositide-dependent protein kinase activity, protein kinase B phosphorylation, and retinoblastoma hyperphosphorylation in interleukin-2-stimulated T cells independently of p38 mitogen-activated protein kinase', *The Journal of biological chemistry*, 275(10), pp. 7395–7402. doi: 10.1074/JBC.275.10.7395.

- Lam, S., Van Der Geest, R. N., Verhagen, N. A. M., Daha, M. R. and Van Kooten, C. (2004) 'Secretion of collagen type IV by human renal fibroblasts is increased by high glucose via a TGF- β -independent pathway', *Nephrol Dial Transplant*, 19, pp. 1694–1701. doi: 10.1093/ndt/gfh235.
- Lampe, P. D. and Laird, D. W. (2022) 'Recent advances in connexin gap junction biology', *Faculty Reviews*, 11(14). doi: 10.12703/R/11-14.
- Land, W. G. (2015) 'The Role of Damage-Associated Molecular Patterns in Human Diseases: Part I - Promoting inflammation and immunity', *Sultan Qaboos University Medical Journal*, 15(1), p. e9. Available at: /pmc/articles/PMC4318613/.
- László, Z. I., Bercsényi, K., Mayer, M., Lefkovics, K., Szabó, G., Katona, I. and Lele, Z. (2020) 'N-cadherin (Cdh2) Maintains Migration and Postmitotic Survival of Cortical Interneuron Precursors in a Cell-Type-Specific Manner', *Cerebral Cortex*, 30(3), pp. 1318–1329. doi: 10.1093/CERCOR/BHZ168.
- Laurent, G., Leong-Poi, H., Mangat, I., Moe, G. W., Hu, X., So, P. P. S., Tarulli, E., Ramadeen, A., Rossman, E. I., Hennen, J. K. and Dorian, P. (2009) 'Effects of chronic gap junction conduction-enhancing antiarrhythmic peptide gap-134 administration on experimental atrial fibrillation in dogs', *Circulation: Arrhythmia and Electrophysiology*, 2(2), pp. 171–178. doi: 10.1161/CIRCEP.108.790212.
- Lawson, C. A., Seidu, S., Zaccardi, F., McCann, G., Kadam, U. T., Davies, M. J., Lam, C. S., Heerspink, H. L. and Khunti, K. (2021) 'Outcome trends in people with heart failure, type 2 diabetes mellitus and chronic kidney disease in the UK over twenty years: Clinical Practice Research Datalink cohort study', *EClinicalMedicine*, 32, p. 100739. doi: 10.1016/j.eclinm.2021.100739.
- Lebleu, V. S., Taduri, G., O'Connell, J., Teng, Y., Cooke, V. G., Woda, C., Sugimoto, H. and Kalluri, R. (2013) 'Origin and function of myofibroblasts in kidney fibrosis', *Nature Medicine*, 19(8), pp. 1047–1053. doi: 10.1038/nm.3218.
- Lee, S., Huen, S., Nishio, H., Nishio, S., Lee, H. K., Choi, B. S., Ruhrberg, C. and Cantley, L. G. (2011) 'Distinct macrophage phenotypes contribute to kidney injury and repair', *Journal of the American Society of Nephrology : JASN*, 22(2), pp. 317–326. doi: 10.1681/ASN.2009060615.
- Leithe, E., Mesnil, M. and Aasen, T. (2018) 'The connexin 43 C-terminus: A tail of many tales', *Biochimica et biophysica acta. Biomembranes*, 1860(1), pp. 48–64. doi: 10.1016/J.BBAMEM.2017.05.008.

Leslie, R. D., Palmer, J., Schloot, N. C. and Lernmark, A. (2016) 'Diabetes at the crossroads: relevance of disease classification to pathophysiology and treatment', *Diabetologia*, 59(1), pp. 13–20. doi: 10.1007/S00125-015-3789-Z.

Leu, S.-Y., Tsang, Y.-L., Ho, L.-C., Yang, C.-C., Shao, A.-N., Chang, C.-Y., Lin, H.-K., Tsai, P.-J., Sung, J.-M. and Tsai, Y.-S. (2023) 'NLRP3 inflammasome activation, metabolic danger signals, and protein binding partners', *Journal of Endocrinology*, 257(2). doi: 10.1530/JOE-22-0184.

Li, H., Jeong, J. H., Kwon, S. W., Lee, S. K., Lee, H. J. and Ryu, J. H. (2020a) 'Z-Ajoene Inhibits Growth of Colon Cancer by Promotion of CK1 α Dependent β -Catenin Phosphorylation', *Molecules*, 25(3). doi: 10.3390/MOLECULES25030703.

Li, J., Liu, H., Takagi, S., Nitta, K., Kitada, M., Srivastava, S. P., Takagaki, Y., Kanasaki, K. and Koya, D. (2020b) 'Renal protective effects of empagliflozin via inhibition of EMT and aberrant glycolysis in proximal tubules', *JCI Insight*, 5(6). doi: 10.1172/JCI.INSIGHT.129034.

Li, M., Wang, T., Tian, H., Wei, G., Zhao, L. and Shi, Y. (2019a) 'Macrophage-derived exosomes accelerate wound healing through their anti-inflammation effects in a diabetic rat model', *Artificial Cells, Nanomedicine and Biotechnology*, 47(1), pp. 3793–3803. doi: 10.1080/21691401.2019.1669617/SUPPL_FILE/IANB_A_1669617_SM0135.JPG.

Li, W., Bao, G., Chen, W., Qiang, X., Zhu, S., Wang, S., He, M., Ma, G., Ochani, M., Al-Abed, Y., Yang, H., Tracey, K. J., Wang, P., D'Angelo, J. and Wang, H. (2018) 'Connexin 43 Hemichannel as a Novel Mediator of Sterile and Infectious Inflammatory Diseases', *Scientific Reports*, 8(1), p. 166. doi: 10.1038/s41598-017-18452-1.

Li, X., Zhao, H., Tan, X., Kostrzewa, R. M., Du, G., Chen, Y., Zhu, J., Miao, Z., Yu, H., Kong, J. and Xu, X. (2015) 'Inhibition of connexin43 improves functional recovery after ischemic brain injury in neonatal rats', *Glia*, 63(9), pp. 1553–1567. doi: 10.1002/glia.22826.

Li, Y., Huang, H., Liu, B., Zhang, Y., Pan, X., Yu, X. Y., Shen, Z. and Song, Y. H. (2021) 'Inflammasomes as therapeutic targets in human diseases', *Signal Transduction and Targeted Therapy*, 6(1), pp. 1–14. doi: 10.1038/s41392-021-00650-Z.

Li, Z. L., Lv, L. L., Tang, T. T., Wang, B., Feng, Y., Zhou, L. T., Cao, J. Y., Tang, R. N., Wu, M., Liu, H., Crowley, S. D. and Liu, B. C. (2019b) 'HIF-1 α inducing exosomal

microRNA-23a expression mediates the cross-talk between tubular epithelial cells and macrophages in tubulointerstitial inflammation', *Kidney International*, 95(2), pp. 388–404. doi: 10.1016/J.KINT.2018.09.013.

Li, Z., Yuan, W. and Lin, Z. (2020c) 'Functional roles in cell signaling of adaptor protein TRADD from a structural perspective', *Computational and Structural Biotechnology Journal*, 18, pp. 2867–2876. doi: 10.1016/J.CSBJ.2020.10.008.

Liao, M., Wang, X., Yu, J., Meng, X., Liu, Y., Dong, X., Li, J., Brant, R., Huang, B. and Yan, H. (2020) 'Characteristics and outcomes of vitrectomy for proliferative diabetic retinopathy in young versus senior patients', *BMC Ophthalmology*, 20(1), pp. 1–8. doi: 10.1186/S12886-020-01688-3/FIGURES/3.

Licor (2020) Which Western Blot Transfer Method Should You Use? Available from https://www.licor.com/bio/guide/westerns/transfer_options

Lin, J., Cheng, A., Cheng, K., Deng, Q., Zhang, S., Lan, Z., Wang, W. and Chen, J. (2020) 'New Insights into the Mechanisms of Pyroptosis and Implications for Diabetic Kidney Disease', *International Journal of Molecular Sciences*, 21(19), pp. 1–23. doi: 10.3390/IJMS21197057.

Lin, Z., Chen, A., Cui, H., Shang, R., Su, T., Li, X., Wang, K., Yang, J., Gao, K., Lv, J., Shen, J., Wang, S., Qi, Y., Guo, M. and Zhu, Y. (2022) 'Renal tubular epithelial cell necroptosis promotes tubulointerstitial fibrosis in patients with chronic kidney disease', *The FASEB Journal*, 36(12), p. e22625. doi: 10.1096/FJ.202200706RR.

Liu, B. C., Tang, T. T., Lv, L. L. and Lan, H. Y. (2018) 'Renal tubule injury: a driving force toward chronic kidney disease', *Kidney international*, 93(3), pp. 568–579. doi: 10.1016/J.KINT.2017.09.033.

Liu, H., Lessieur, E. M., Saadane, A., Lindstrom, S. I., Taylor, P. R. and Kern, T. S. (2019a) 'Neutrophil elastase contributes to the pathological vascular permeability characteristic of diabetic retinopathy', *Diabetologia*, 62(12), pp. 2365–2374. doi: 10.1007/S00125-019-04998-4/FIGURES/6.

Liu, L., Wu, N., Wang, Y., Zhang, X., Xia, B., Tang, J., Cai, J., Zhao, Z., Liao, Q. and Wang, J. (2019b) 'TRPM7 promotes the epithelial-mesenchymal transition in ovarian cancer through the calcium-related PI3K / AKT oncogenic signaling', *Journal of Experimental and Clinical Cancer Research*, 38(1), pp. 1–15. doi: 10.1186/S13046-019-1061-Y/FIGURES/7.

- Liu, T., Zhang, L., Joo, D. and Sun, S. C. (2017) 'NF- κ B signaling in inflammation', *Signal Transduction and Targeted Therapy*, 2(1), pp. 1–9. doi: 10.1038/sigtrans.2017.23.
- Liu, W., Zhang, D., Li, X., Zheng, L., Cui, C., Cui, Y., Sun, J., Xie, J. and Zhou, X. (2019c) 'TGF- β 1 facilitates cell–cell communication in osteocytes via connexin43- and pannexin1-dependent gap junctions', *Cell Death Discovery*, 5(1), pp. 1–14. doi: 10.1038/s41420-019-0221-3.
- Liu, X. (2008) 'Inflammatory cytokines augments TGF- β 1-induced epithelial-mesenchymal transition in A549 cells by up-regulating T β R-I', *Cell Motility and the Cytoskeleton*, 65(12), pp. 935–944. doi: 10.1002/CM.20315.
- Loh, C. Y., Chai, J. Y., Tang, T. F., Wong, W. F., Sethi, G., Shanmugam, M. K., Chong, P. P. and Looi, C. Y. (2019) 'The E-Cadherin and N-Cadherin Switch in Epithelial-to-Mesenchymal Transition: Signaling, Therapeutic Implications, and Challenges', *Cells*, 8(10). doi: 10.3390/CELLS8101118.
- Lopez, W., Ramachandran, J., Alsamarah, A., Luo, Y., Harris, A. L. and Contreras, J. E. (2016) 'Mechanism of gating by calcium in connexin hemichannels', *Proceedings of the National Academy of Sciences of the United States of America*, 113(49), pp. E7986–E7995. doi: 10.1073/PNAS.1609378113.
- Louie, H. H., Shome, A., Kuo, C. Y., Rupenthal, I. D., Green, C. R. and Mugisho, O. O. (2021) 'Connexin43 hemichannel block inhibits NLRP3 inflammasome activation in a human retinal explant model of diabetic retinopathy', *Experimental Eye Research*, 202. doi: 10.1016/j.exer.2020.108384.
- Lovisa, S., LeBleu, V. S., Tampe, B., Sugimoto, H., Vadrnagara, K., Carstens, J. L., Wu, C. C., Hagos, Y., Burckhardt, B. C., Pentcheva-Hoang, T., Nischal, H., Allison, J. P., Zeisberg, M. and Kalluri, R. (2015) 'Epithelial-to-mesenchymal transition induces cell cycle arrest and parenchymal damage in renal fibrosis', *Nature medicine*, 21(9), pp. 998–1009. doi: 10.1038/NM.3902.
- Lynch, S. K., Lee, K., Chen, Z., Folk, J. C., Schmidt-Erfurth, U., Gerendas, B. S., Wahle, A., Wykoff, C. C. and Abramoff, M. D. (2019) 'Intravitreal Fluocinolone Acetonide May Decelerate Diabetic Retinal Neurodegeneration', *Investigative Ophthalmology & Visual Science*, 60(6), pp. 2134–2139. doi: 10.1167/IOVS.18-24643.
- Lyon, H., Shome, A., Rupenthal, I. D., Green, C. R. and Mugisho, O. O. (2021a) 'Tonabersat inhibits connexin43 hemichannel opening and inflammasome activation in

an in vitro retinal epithelial cell model of diabetic retinopathy', *International Journal of Molecular Sciences*, 22(1), pp. 1–12. doi: 10.3390/ijms22010298.

Lyon, H., Yin, N., Rupenthal, I. D., Green, C. R., Odunayo, | and Mugisho, O. (2021b) 'Blocking connexin43 hemichannels prevents TGF- β 2 upregulation and epithelial–mesenchymal transition in retinal pigment epithelial cells', *Cell Biology International*. doi: 10.1002/CBIN.11718.

Ma, J. W., Ji, D. D., Li, Q. Q., Zhang, T. and Luo, L. (2020) 'Inhibition of connexin 43 attenuates oxidative stress and apoptosis in human umbilical vein endothelial cells', *BMC Pulmonary Medicine*, 20(1), pp. 1–10. doi: 10.1186/S12890-019-1036-Y/FIGURES/5.

Maatouk, L., Yi, C., Carrillo-de Sauvage, M.-A., Compagnion, A.-C., Hunot, S., Ezan, P., Hirsch, E. C., Koulakoff, A., Pfrieder, F. W., Tronche, F., Leybaert, L., Giaume, C. and Vyas, S. (2019) 'Glucocorticoid receptor in astrocytes regulates midbrain dopamine neurodegeneration through connexin hemichannel activity', *Cell Death & Differentiation*, 26(3), pp. 580–596. doi: 10.1038/s41418-018-0150-3.

Maeda, S., Hsu, L. C., Liu, H., Bankston, L. A., Iimura, M., Kagnoff, M. F., Eckmann, L. and Karin, M. (2005) 'Nod2 mutation in Crohn's disease potentiates NF-kappaB activity and IL-1beta processing', *Science*, 307(5710), pp. 734–738. doi: 10.1126/SCIENCE.1103685.

Maes, M., Crespo Yanguas, S., Willebrords, J., Weemhoff, J. L., da Silva, T. C., Decrock, E., Lebofsky, M., Pereira, I. V. A., Leybaert, L., Farhood, A., Jaeschke, H., Cogliati, B. and Vinken, M. (2017) 'Connexin hemichannel inhibition reduces acetaminophen-induced liver injury in mice', *Toxicology Letters*, 278, pp. 30–37. doi: 10.1016/J.TOXLET.2017.07.007.

Marchetti, C., Swartzwelter, B., Gamboni, F., Neff, C. P., Richter, K., Azam, T., Carta, S., Tengesdal, I., Nemkov, T., D'Alessandro, A., Henry, C., Jones, G. S., Goodrich, S. A., St. Laurent, J. P., Jones, T. M., Scribner, C. L., Barrow, R. B., Altman, R. D., Skouras, D. B., *et al.* (2018) 'OLT1177, a β -sulfonyl nitrile compound, safe in humans, inhibits the NLRP3 inflammasome and reverses the metabolic cost of inflammation', *Proceedings of the National Academy of Sciences of the United States of America*, 115(7), pp. E1530–E1539. doi: 10.1073/PNAS.1716095115.

Martínez-Klimova, E., Aparicio-Trejo, O. E., Tapia, E. and Pedraza-Chaverri, J. (2019) 'Unilateral Ureteral Obstruction as a Model to Investigate Fibrosis-Attenuating Treatments', *Biomolecules*, 9(4). doi: 10.3390/BIOM9040141.

- Marx, N., Davies, M. J., Grant, P. J., Mathieu, C., Petrie, J. R., Cosentino, F. and Buse, J. B. (2021) 'Guideline recommendations and the positioning of newer drugs in type 2 diabetes care', *The Lancet Diabetes & Endocrinology*, 9(1), pp. 46–52. doi: 10.1016/S2213-8587(20)30343-0.
- Masola, V., Carraro, A., Granata, S., Signorini, L., Bellin, G., Violi, P., Lupo, A., Tedeschi, U., Onisto, M., Gambaro, G. and Zaza, G. (2019) 'In vitro effects of interleukin (IL)-1 beta inhibition on the epithelial-to-mesenchymal transition (EMT) of renal tubular and hepatic stellate cells', *J Transl Med*, 17, pp. 12. doi: 10.1186/s12967-019-1770-1.
- Mat Nor, M. N., Rupenthal, I. D., Green, C. R. and Acosta, M. L. (2020) 'Connexin Hemichannel Block Using Orally Delivered Tonabersat Improves Outcomes in Animal Models of Retinal Disease', *Neurotherapeutics*, 17(1), pp. 371–387. doi: 10.1007/s13311-019-00786-5.
- Mathebula, S. D. (2018) 'Biochemical changes in diabetic retinopathy triggered by hyperglycaemia: A review', *African Vision and Eye Health*, 77(1). doi: 10.4102/AVEH.V77I1.439.
- Mathew, J., Mohan, M. and Menon, A. (2019) 'Multiple Cranial Neuropathies in a Patient with Diabetes Mellitus', *Annals of Indian Academy of Neurology*, 22(3), p. 353. doi: 10.4103/AIAN.AIAN_402_18.
- McCormick, J. A. and Ellison, D. H. (2015) 'Distal convoluted tubule', *Comprehensive Physiology*, 5(1), pp. 45–98. doi: 10.1002/CPHY.C140002.
- McGuire, D. K., Shih, W. J., Cosentino, F., Charbonnel, B., Cherney, D. Z. I., Dagogo-Jack, S., Pratley, R., Greenberg, M., Wang, S., Huyck, S., Gantz, I., Terra, S. G., Masiukiewicz, U. and Cannon, C. P. (2021) 'Association of SGLT2 Inhibitors With Cardiovascular and Kidney Outcomes in Patients With Type 2 Diabetes: A Meta-analysis', *JAMA Cardiology*, 6(2), pp. 148–158. doi: 10.1001/JAMACARDIO.2020.4511.
- McHugh, S. M., Roman, S., Davis, B., Koch, A., Pickett, A. M., Richardson, J. C., Miller, S. R., Wetten, S., Cox, C. J., Karpe, F., Todd, J. A. and Bullmore, E. T. (2012) 'Effects of genetic variation in the P2RX7 gene on pharmacodynamics of a P2X7 receptor antagonist: a prospective genotyping approach', *British Journal of Clinical Pharmacology*, 74(2), p. 376. doi: 10.1111/J.1365-2125.2012.04200.X.

- McLaughlin, K. A., Richardson, C. C., Ravishankar, A., Brigatti, C., Liberati, D., Lampasona, V., Piemonti, L., Morgan, D., Feltbower, R. G. and Christie, M. R. (2016) 'Identification of Tetraspanin-7 as a Target of Autoantibodies in Type 1 Diabetes', *Diabetes*, 65(6), pp. 1690–1698.
- McLaughlin, K. A., Tombs, M. A. and Christie, M. R. (2020) 'Autoimmunity to tetraspanin-7 in type 1 diabetes', *Medical Microbiology and Immunology*, 209(4), pp. 437–445. doi: 10.1007/S00430-020-00674-2/FIGURES/2.
- McLaughlin, T., Deng, A., Gonzales, O., Aillaud, M., Yee, G., Lamendola, C., Abbasi, F., Connolly, A. J., Sherman, A., Cushman, S. W., Reaven, G. and Tsao, P. S. (2008) 'Insulin resistance is associated with a modest increase in inflammation in subcutaneous adipose tissue of moderately obese women', *Diabetologia*, 51(12), pp. 2303–2308. doi: 10.1007/S00125-008-1148-Z.
- Mencher, S. R., Frank, G. and Fishbein, J. (2019) 'Diabetic Ketoacidosis at Onset of Type 1 Diabetes: Rates and Risk Factors Today to 15 Years Ago', *Global Pediatric Health*, 6. doi: 10.1177/2333794X19870394.
- Milner, M. T., Maddugoda, M., Götz, J., Burgener, S. S. and Schroder, K. (2021) 'The NLRP3 inflammasome triggers sterile neuroinflammation and Alzheimer's disease', *Current Opinion in Immunology*, 68, pp. 116–124. doi: 10.1016/J.COI.2020.10.011.
- Miloudi, K., Oubaha, M., Ménard, C., Dejda, A., Guber, V., Cagnone, G., Wilson, A. M., Tétreault, N., Mawambo, G., Binet, F., Chidiac, R., Delisle, C., Buscarlet, M., Cerani, A., Crespo-Garcia, S., Bentley, K., Rezende, F., Joyal, J. S., Mallette, F. A., *et al.* (2019) 'NOTCH1 signaling induces pathological vascular permeability in diabetic retinopathy', *Proceedings of the National Academy of Sciences of the United States of America*, 116(10), pp. 4538–4547. doi: 10.1073/PNAS.1814711116/SUPPL_FILE/PNAS.1814711116.SAPP.PDF.
- Mobasser, M., Shirmohammadi, M., Amiri, T., Vahed, N., Fard, H. H. and Ghofazadeh, M. (2020) 'Prevalence and incidence of type 1 diabetes in the world: a systematic review and meta-analysis', *Health Promotion Perspectives*, 10(2), p. 98. doi: 10.34172/HPP.2020.18.
- Moeller, M. J., Kramann, R., Lammers, T., Hoppe, B., Latz, E., Ludwig-Portugall, I., Boor, P., Floege, J., Kurts, C., Weiskirchen, R. and Ostendorf, T. (2022) 'New Aspects of Kidney Fibrosis—From Mechanisms of Injury to Modulation of Disease', *Frontiers in Medicine*, 8, p. 2978. doi: 10.3389/FMED.2021.814497/BIBTEX.

- Montero, D., Diaz-Canestro, C., Oberholzer, L. and Lundby, C. (2019) 'The role of blood volume in cardiac dysfunction and reduced exercise tolerance in patients with diabetes', *The Lancet Diabetes & Endocrinology*, 7(10), pp. 807–816. doi: 10.1016/S2213-8587(19)30119-6.
- Montgomery, J., Ghatnekar, G. S., Grek, C. L., Moyer, K. E. and Gourdie, R. G. (2018) 'Connexin 43-based therapeutics for dermal wound healing', *International Journal of Molecular Sciences*, p. 1778. doi: 10.3390/ijms19061778.
- Montgomery, J., Richardson, W. J., Marsh, S., Rhett, J. M., Bustos, F., Degen, K., Ghatnekar, G. S., Grek, C. L., Jourdan, L. J., Holmes, J. W. and Gourdie, R. G. (2021) 'The connexin 43 carboxyl terminal mimetic peptide α CT1 prompts differentiation of a collagen scar matrix in humans resembling unwounded skin', *FASEB Journal*, 35(8). doi: 10.1096/FJ.202001881R.
- Moore, K., Bryant, Z. J., Ghatnekar, G., Singh, U. P., Gourdie, R. G. and Potts, J. D. (2013) 'A synthetic connexin 43 mimetic peptide augments corneal wound healing', *Experimental Eye Research*, 115, pp. 178–188. doi: 10.1016/j.exer.2013.07.001.
- Mótyán, J. A., Tóth, F. and Tózsér, J. (2013) 'Research Applications of Proteolytic Enzymes in Molecular Biology', *Biomolecules*, 3(4), p. 923. doi: 10.3390/BIOM3040923.
- Mrozik, K. M., Blaschuk, O. W., Cheong, C. M., Zannettino, A. C. W. and Vandyke, K. (2018) 'N-cadherin in cancer metastasis, its emerging role in haematological malignancies and potential as a therapeutic target in cancer', *BMC cancer*, 18(1). doi: 10.1186/S12885-018-4845-0.
- Mugisho, O. O., Green, C. R., Kho, D. T., Zhang, J., Graham, E. S., Acosta, M. L. and Rupenthal, I. D. (2018a) 'The inflammasome pathway is amplified and perpetuated in an autocrine manner through connexin43 hemichannel mediated ATP release', *Biochimica et Biophysica Acta - General Subjects*, 1862(3), pp. 385–393. doi: 10.1016/j.bbagen.2017.11.015.
- Mugisho, O. O., Green, C. R., Squirrel, D. M., Bould, S., Danesh-Meyer, H. V., Zhang, J., Acosta, M. L. and Rupenthal, I. D. (2019) 'Connexin43 hemichannel block protects against the development of diabetic retinopathy signs in a mouse model of the disease', *Journal of molecular medicine*, 97(2), pp. 215–229. doi: 10.1007/S00109-018-1727-5.

- Mugisho, O. O., Rupenthal, I. D., Squirrell, D. M., Bould, S. J., Danesh-Meyer, H. V., Zhang, J., Green, C. R. and Acosta, M. L. (2018b) 'Intravitreal pro-inflammatory cytokines in non-obese diabetic mice: Modelling signs of diabetic retinopathy', *PLoS ONE*, 13(8). doi: 10.1371/JOURNAL.PONE.0202156.
- Mukhtar, A., Khan, M. S., Junejo, M., Ishaq, M. and Akbar, B. (2016) 'Effect of pan retinal photocoagulation on central macular thickness and visual acuity in proliferative diabetic retinopathy', *Pakistan Journal of Medical Sciences*, 32(1), p. 221. doi: 10.12669/PJMS.321.8758.
- Münger, K., Werness, B. A., Dyson, N., Phelps, W. C., Harlow, E. and Howley, P. M. (1989) 'Complex formation of human papillomavirus E7 proteins with the retinoblastoma tumor suppressor gene product.', *The EMBO Journal*, 8(13), pp. 4099–4105. doi: 10.1002/j.1460-2075.1989.tb08594.x.
- Muroi, M. and Tanamoto, K. (2008) 'TRAF6 distinctively mediates MyD88- and IRAK-1-induced activation of NF-kappaB', *Journal of leukocyte biology*, 83(3), pp. 702–707. doi: 10.1189/JLB.0907629.
- Muskiet, M. H. A., Tonneijck, L., Smits, M. M., Kramer, M. H. H., Margriet Ouwens, D., Hartmann, B., Holst, J. J., Touw, D. J., Jan Danser, A. H., Joles, J. A. and van Raalte, D. H. (2020) 'Effects of DPP-4 Inhibitor Linagliptin Versus Sulfonylurea Glimepiride as Add-on to Metformin on Renal Physiology in Overweight Patients With Type 2 Diabetes (RENALIS): A Randomized, Double-Blind Trial', *Diabetes care*, 43(11), pp. 2889–2893. doi: 10.2337/DC20-0902.
- Nadasdy, T., Laszik, Z., Blick, K. E., Johnson, D. L. and Silva, F. G. (1994) 'Tubular atrophy in the end-stage kidney: a lectin and immunohistochemical study', *Human pathology*, 25(1), pp. 22–28. doi: 10.1016/0046-8177(94)90166-X.
- Nakagawa, S., Nishihara, K., Miyata, H., Shinke, H., Tomita, E., Kajiwara, M., Matsubara, T., Iehara, N., Igarashi, Y., Yamada, H., Fukatsu, A., Yanagita, M., Matsubara, K. and Masuda, S. (2015) 'Molecular Markers of Tubulointerstitial Fibrosis and Tubular Cell Damage in Patients with Chronic Kidney Disease', *PloS one*, 10(8). doi: 10.1371/JOURNAL.PONE.0136994.
- Nalewajska, M., Opara-Bajerowicz, M., Safranow, K., Pawlik, A., Ciechanowski, K., Kwiatkowski, S. and Kwiatkowska, E. (2022) 'The Effects of EMMPRIN/CD147 on Late Function and Histopathological Lesions of the Renal Graft', *Biology*, 11(2). doi: 10.3390/BIOLOGY11020232.

Narahari, A. K., Kreutzberger, A. J. B., Gaete, P. S., Chiu, Y. H., Leonhardt, S. A., Medina, C. B., Jin, X., Oleniacz, P. W., Kiessling, V., Barrett, P. Q., Ravichandran, K. S., Yeager, M., Contreras, J. E., Tamm, L. K. and Bayliss, D. A. (2021) 'Atp and large signaling metabolites flux through caspase-activated pannexin 1 channels', *eLife*, 10, pp. 1–21. doi: 10.7554/ELIFE.64787.

National Institute for Health and Care Excellence (NICE; 2022) *Dapagliflozin for treating chronic kidney disease*. Available at: www.nice.org.uk/guidance/ta775.

Neal, B., Perkovic, V., Mahaffey, K. W., de Zeeuw, D., Fulcher, G., Erondur, N., Shaw, W., Law, G., Desai, M. and Matthews, D. R. (2017) 'Canagliflozin and Cardiovascular and Renal Events in Type 2 Diabetes', *New England Journal of Medicine*, 377(7), pp. 644–657. doi: 10.1056/NEJMOA1611925/SUPPL_FILE/NEJMOA1611925_DISCLOSURES.PDF.

Netea, M. G., Kullberg, B. J., Verschueren, I. and Van Der Meer, J. W. M. (2000) 'Interleukin-18 induces production of proinflammatory cytokines in mice: no intermediate role for the cytokines of the tumor necrosis factor family and interleukin-1 β ', *European Journal of Immunology*, 30. doi: 10.1002/1521-4141.

Newman, D. K. (2010) 'Surgical management of the late complications of proliferative diabetic retinopathy', *Eye*, 24(3), pp. 441–449. doi: 10.1038/eye.2009.325.

Nieto-Vazquez, I., Fernández-Veledo, S., Krämer, D. K., Vila-Bedmar, R., Garcia-Guerra, L. and Lorenzo, M. (2008) 'Insulin resistance associated to obesity: The link TNF- α ', *Archives of Physiology and Biochemistry*, 114(3), pp. 183–194. doi: 10.1080/13813450802181047.

Niewczas, M. A., Pavkov, M. E., Skupien, J., Smiles, A., Md Dom, Z. I., Wilson, J. M., Park, J., Nair, V., Schlafly, A., Saulnier, P. J., Satake, E., Simeone, C. A., Shah, H., Qiu, C., Looker, H. C., Fiorina, P., Ware, C. F., Sun, J. K., Doria, A., *et al.* (2019) 'A signature of circulating inflammatory proteins and development of end-stage renal disease in diabetes', *Nature medicine*, 25(5), pp. 805–813. doi: 10.1038/S41591-019-0415-5.

Nikzad, S., Baradaran-Ghahfarokhi, M. and Nasri, P. (2014) 'Dose-response modeling using MTT assay: a short review', *Life Science Journal*, 11(9s), pp. 1097–1135. doi: 10.15171/lrj.2014.04.

Niu, J., Wu, S., Chen, M., Xu, K., Guo, Q., Lu, A., Zhao, L., Sun, B. and Meng, G. (2019) 'Hyperactivation of the NLRP3 inflammasome protects mice against influenza A

virus infection via IL-1 β mediated neutrophil recruitment', *Cytokine*, 120, pp. 115–124. doi: 10.1016/J.CYTO.2019.04.019.

Norris, J. M., Johnson, R. K. and Stene, L. C. (2020) 'Type 1 diabetes—early life origins and changing epidemiology', *The Lancet Diabetes & Endocrinology*, 8(3), pp. 226–238. doi: 10.1016/S2213-8587(19)30412-7.

O'Brien, M., Moehring, D., Muñoz-Planillo, R., Núñez, G., Callaway, J., Ting, J., Scurria, M., Ugo, T., Bernad, L., Cali, J. and Lazar, D. (2017) 'A bioluminescent caspase-1 activity assay rapidly monitors inflammasome activation in cells', *Journal of Immunological Methods*, 447, pp. 1–13. doi: 10.1016/J.JIM.2017.03.004.

O'Carroll, S. J., Gorrie, C. A., Velamoor, S., Green, C. R. and Nicholson, L. F. B. (2013) 'Connexin43 mimetic peptide is neuroprotective and improves function following spinal cord injury', *Neuroscience Research*, 75(3), pp. 256–267. doi: 10.1016/j.neures.2013.01.004.

O'Quinn, M. P., Palatinus, J. A., Harris, B. S., Hewett, K. W. and Gourdie, R. G. (2011) 'A peptide mimetic of the connexin43 carboxyl terminus reduces gap junction remodeling and induced arrhythmia following ventricular injury', *Circulation Research*, 108(6), pp. 704–715. doi: 10.1161/CIRCRESAHA.110.235747.

Obert, E., Strauss, R., Brandon, C., Grek, C., Ghatnekar, G., Gourdie, R. and Rohrer, B. (2017) 'Targeting the tight junction protein, zonula occludens-1, with the connexin43 mimetic peptide, α CT1, reduces VEGF-dependent RPE pathophysiology', *Journal of Molecular Medicine*, 95(5), pp. 535–552. doi: 10.1007/s00109-017-1506-8.

Ohkuma, T., Komorita, Y., Peters, S. A. E. and Woodward, M. (2019) 'Diabetes as a risk factor for heart failure in women and men: a systematic review and meta-analysis of 47 cohorts including 12 million individuals', *Diabetologia*, 62(9), pp. 1550–1560. doi: 10.1007/S00125-019-4926-X/FIGURES/4.

Olatec Therapeutics (2022) *Current Clinical Trials for OLT1177 Dapansutride*. Available at: <http://www.olatec.com/patients.html>.

Oraby, M. A., El-Yamany, M. F., Safar, M. M., Assaf, N. and Ghoneim, H. A. (2019) 'Amelioration of Early Markers of Diabetic Nephropathy by Linagliptin in Fructose-Streptozotocin-Induced Type 2 Diabetic Rats', *Nephron*, 141(4), pp. 273–286. doi: 10.1159/000495517.

Orellana, J. A., Shoji, K. F., Abudara, V., Ezan, P., Amigou, E., Sáez, P. J., Jiang, J. X., Naus, C. C., Sáez, J. C. and Giaume, C. (2011) 'Amyloid β -Induced Death in

Neurons Involves Glial and Neuronal Hemichannels', *Journal of Neuroscience*, 31(13), pp. 4962–4977. doi: 10.1523/JNEUROSCI.6417-10.2011.

Ouyang, H., Du, A., Zhou, L., Zhang, T., Lu, B., Wang, Z. and Ji, L. (2022) 'Chlorogenic acid improves diabetic retinopathy by alleviating blood-retinal-barrier dysfunction via inducing Nrf2 activation', *Phytotherapy Research*, 36(3), pp. 1386–1401. doi: 10.1002/PTR.7401.

Pan, X., Pei, J., Wang, A., Shuai, W., Feng, L., Bu, F., Zhu, Y., Zhang, L., Wang, G. and Ouyang, L. (2022) 'Development of small molecule extracellular signal-regulated kinases (ERKs) inhibitors for cancer therapy', *Acta Pharmaceutica Sinica B*, 12(5), pp. 2171–2192. doi: 10.1016/J.APSB.2021.12.022.

Pandey, S., Maharana, J., Li, X. X., Woodruff, T. M. and Shukla, A. K. (2020) 'Emerging Insights into the Structure and Function of Complement C5a Receptors', *Trends in Biochemical Sciences*, 45(8), pp. 693–705. doi: 10.1016/J.TIBS.2020.04.004.

Paolisso, P., Bergamaschi, L., Santulli, G., Gallinoro, E., Cesaro, A., Gragnano, F., Sardu, C., Mileva, N., Foà, A., Armillotta, M., Sansonetti, A., Amicone, S., Impellizzeri, A., Casella, G., Mauro, C., Vassilev, D., Marfella, R., Calabrò, P., Barbato, E., *et al.* (2022) 'Infarct size, inflammatory burden, and admission hyperglycemia in diabetic patients with acute myocardial infarction treated with SGLT2-inhibitors: a multicenter international registry', *Cardiovascular Diabetology*, 21(1), pp. 1–12. doi: 10.1186/S12933-022-01506-8/FIGURES/4.

Paolisso, P., Foà, A., Bergamaschi, L., Donati, F., Fabrizio, M., Chiti, C., Angeli, F., Toniolo, S., Stefanizzi, A., Armillotta, M., Rucci, P., Iannopolo, G., Casella, G., Marrozzini, C., Galiè, N. and Pizzi, C. (2021) 'Hyperglycemia, inflammatory response and infarct size in obstructive acute myocardial infarction and MINOCA', *Cardiovascular Diabetology*, 20(1), pp. 1–11. doi: 10.1186/S12933-021-01222-9/FIGURES/2.

Papachristoforou, E., Lambadiari, V., Maratou, E. and Makrilakis, K. (2020) 'Association of Glycemic Indices (Hyperglycemia, Glucose Variability, and Hypoglycemia) with Oxidative Stress and Diabetic Complications', *Journal of Diabetes Research*. doi: 10.1155/2020/7489795.

Paschou, S. A., Papadopoulou-Marketou, N., Chrousos, G. P. and Kanaka-Gantenbein, C. (2018) 'On type 1 diabetes mellitus pathogenesis', *Endocrine Connections*, 7(1), p. R38. doi: 10.1530/EC-17-0347.

- Patel, S., Srivastava, S., Singh, M. R. and Singh, D. (2019) 'Mechanistic insight into diabetic wounds: Pathogenesis, molecular targets and treatment strategies to pace wound healing', *Biomedicine & Pharmacotherapy*, 112, p. 108615. doi: 10.1016/J.BIOPHA.2019.108615.
- Pathak, V., Pathak, N. M., O'Neill, C. L., Guduric-Fuchs, J. and Medina, R. J. (2019) 'Therapies for Type 1 Diabetes: Current Scenario and Future Perspectives', *Clinical Medicine Insights: Endocrinology and Diabetes*, 12. doi: 10.1177/1179551419844521/ASSET/IMAGES/LARGE/10.1177_1179551419844521-FIG3.JPEG.
- Pedroza, A. R., Martinez, A., Wauquier, F., Lee, D.-Y., Gorin, Y. and Ford, B. M. (2019) 'Calcium-dependent dual oxidase 2 is a novel source of reactive oxygen species implicated in glomerular mesangial cell fibrotic response to angiotensin II', *The FASEB Journal*, 33(S1), pp. 567.13-567.13. doi: 10.1096/FASEBJ.2019.33.1_SUPPLEMENT.567.13.
- Pegg, D. E. (2015) 'Principles of cryopreservation', *Methods in molecular biology*, 1257, pp. 3–19. doi: 10.1007/978-1-4939-2193-5_1.
- Peng, B., Xu, C., Wang, S., Zhang, Y. and Li, W. (2022) 'The Role of Connexin Hemichannels in Inflammatory Diseases', *Biology*, 11(2). doi: 10.3390/BIOLOGY11020237.
- Peng, Q., Wu, W., Wu, K. Y., Cao, B., Qiang, C., Li, K., Sacks, S. H. and Zhou, W. (2019) 'The C5a/C5aR1 axis promotes progression of renal tubulointerstitial fibrosis in a mouse model of renal ischemia/reperfusion injury', *Kidney international*, 96(1), pp. 117–128. doi: 10.1016/J.KINT.2019.01.039.
- Pérez-Morales, R. E., del Pino, M. D., Valdivielso, J. M., Ortiz, A., Mora-Fernández, C. and Navarro-González, J. F. (2019) 'Inflammation in Diabetic Kidney Disease', *Nephron*, 143(1), pp. 12–16. doi: 10.1159/000493278.
- Perlman, A. S., Chevalier, J. M., Wilkinson, P., Liu, H., Parker, T., Levine, D. M., Sloan, B. J., Gong, A., Sherman, R. and Farrell, F. X. (2015) 'Serum Inflammatory and Immune Mediators Are Elevated in Early Stage Diabetic Nephropathy', *Annals of Clinical & Laboratory Science*, 25(3), pp. 256–263.
- Petersen, M. C. and Shulman, G. I. (2018) 'Mechanisms of Insulin Action and Insulin Resistance', *Physiological Reviews*, 98(4), p. 2133. doi: 10.1152/PHYSREV.00063.2017.

- Pitere, R. R., van Heerden, M. B., Pepper, M. S. and Ambele, M. A. (2022) 'Slc7a8 Deletion Is Protective against Diet-Induced Obesity and Attenuates Lipid Accumulation in Multiple Organs', *Biology*, 11(2), pp. 311. doi: 10.3390/BIOLOGY11020311.
- Pop-Busui, R., Lu, J., Lopes, N., Jones, T. L. Z., Detre, K. M., Rankin, S., *et al.* (2009) 'Prevalence of diabetic peripheral neuropathy and relation to glycemic control therapies at baseline in the BARI 2D cohort', *Journal of the peripheral nervous system : JPNS*, 14(1), pp. 1–13. doi: 10.1111/J.1529-8027.2009.00200.X.
- Portou, M. J., Yu, R., Baker, D., Xu, S., Abraham, D. and Tsui, J. (2020) 'Hyperglycaemia and Ischaemia Impair Wound Healing via Toll-like Receptor 4 Pathway Activation in vitro and in an Experimental Murine Model', *European Journal of Vascular and Endovascular Surgery*, 59(1), pp. 117–127. doi: 10.1016/J.EJVS.2019.06.018.
- Potter, J. A., Price, G. W., Cliff, C. L., Green, C. R., Squires, P. E. and Hills, C. E. (2021a) 'Collagen I modifies connexin-43 hemichannel activity via integrin $\alpha 2\beta 1$ binding in TGF β 1-evoked renal tubular epithelial cells', *International Journal of Molecular Sciences*, 22(7), p. 3644. doi: 10.3390/ijms22073644.
- Potter, J. A., Price, G. W., Cliff, C. L., Williams, B. M., Hills, C. E. and Squires, P. E. (2021b) 'Carboxyfluorescein Dye Uptake to Measure Connexin-mediated Hemichannel Activity in Cultured Cells', *Bio-protocol*, 11(3). doi: 10.21769/BIOPROTOCOL.3901.
- Price, G. W., Chadjichristos, C. E., Kavvadas, P., Tang, S. C. W., Yiu, W. H., Green, C. R., Potter, J. A., Siamantouras, E., Squires, P. E. and Hills, C. E. (2020) 'Blocking Connexin-43 mediated hemichannel activity protects against early tubular injury in experimental chronic kidney disease', *Cell Communication and Signaling*, 18(1), pp. 1–17. doi: 10.1186/s12964-020-00558-1.
- Qi, R. and Yang, C. (2018) 'Renal tubular epithelial cells: the neglected mediator of tubulointerstitial fibrosis after injury', *Cell Death and Disease. Nature Publishing Group*, pp. 1–11. doi: 10.1038/s41419-018-1157-x.
- Ram, C., Jha, A. K., Ghosh, A., Gairola, S., Syed, A. M., Murty, U. S., Naidu, V. G. M. and Sahu, B. D. (2020) 'Targeting NLRP3 inflammasome as a promising approach for treatment of diabetic nephropathy: Preclinical evidences with therapeutic approaches', *European Journal of Pharmacology*, 885, p. 173503. doi: 10.1016/J.EJPHAR.2020.173503.

Rathcke, C. N., Johansen, J. S. and Vestergaard, H. (2006) 'YKL-40, a biomarker of inflammation, is elevated in patients with type 2 diabetes and is related to insulin resistance', *Inflammation research: official journal of the European Histamine Research Society*, 55(2), pp. 53–59. doi: 10.1007/S00011-005-0010-8.

Rathcke, C. N., Persson, F., Tarnow, L., Rossing, P. and Vestergaard, H. (2009) 'YKL-40, a Marker of Inflammation and Endothelial Dysfunction, Is Elevated in Patients With Type 1 Diabetes and Increases With Levels of Albuminuria', *Diabetes Care*, 32(2), pp. 323. doi: 10.2337/DC08-1144.

Rayego-Mateos, S., Morgado-Pascual, J. L., Opazo-Ríos, L., Guerrero-Hue, M., García-Caballero, C., Vázquez-Carballo, C., Mas, S., Sanz, A. B., Herencia, C., Mezzano, S., Gómez-Guerrero, C., Moreno, J. A. and Egido, J. (2020) 'Pathogenic Pathways and Therapeutic Approaches Targeting Inflammation in Diabetic Nephropathy', *International Journal of Molecular Sciences*, 21(11), pp. 3798. doi: 10.3390/IJMS21113798.

Reinehr, T. (2005) 'Clinical presentation of type 2 diabetes mellitus in children and adolescents', *International Journal of Obesity*, 29(2), pp. S105–S110. doi: 10.1038/sj.ijo.0803065.

Richardson, C. C., Dromey, J. A., McLaughlin, K. A., Morgan, D., Jonathan Bodansky, H., Feltbower, R. G., Barnett, A. H., Gill, G. V., Bain, S. C. and Christie, M. R. (2013) 'High frequency of autoantibodies in patients with long duration type 1 diabetes', *Diabetologia*, 56(11), pp. 2538–2540. doi: 10.1007/S00125-013-3017-7/TABLES/1.

Ridker, P. M. (2021) 'From RESCUE to ZEUS: will interleukin-6 inhibition with ziltivekimab prove effective for cardiovascular event reduction?', *Cardiovascular Research*, 117(11), pp. e138–e140. doi: 10.1093/cvr/cvab231.

Ridker, P. M., Everett, B. M., Thuren, T., MacFadyen, J. G., Chang, W. H., Ballantyne, C., Fonseca, F., Nicolau, J., Koenig, W., Anker, S. D., Kastelein, J. J. P., Cornel, J. H., Pais, P., Pella, D., Genest, J., Cifkova, R., Lorenzatti, A., Forster, T., Kobalava, Z., *et al.* (2017) 'Antiinflammatory Therapy with Canakinumab for Atherosclerotic Disease', *The New England journal of medicine*, 377(12), pp. 1119–1131. doi: 10.1056/NEJMOA1707914.

Ridker, P. M., MacFadyen, J. G., Thuren, T. and Libby, P. (2020) 'Residual inflammatory risk associated with interleukin-18 and interleukin-6 after successful interleukin-1 β inhibition with canakinumab: further rationale for the development of

targeted anti-cytokine therapies for the treatment of atherothrombosis', *European heart journal*, 41(23), pp. 2153–2163. doi: 10.1093/EURHEARTJ/EHZ542.

Rockey, D. C., Bell, P. D. and Hill, J. A. (2015) 'Fibrosis — A Common Pathway to Organ Injury and Failure', *New England Journal of Medicine*, 372(12), pp. 1138–1149. doi: 10.1056/nejmra1300575.

Rodjakovic, D., Salm, L. and Beldi, G. (2021) 'Function of Connexin-43 in Macrophages', *International Journal of Molecular Sciences*, 22(3), p. 1412. doi: 10.3390/ijms22031412.

Rohm, T. V., Meier, D. T., Olefsky, J. M. and Donath, M. Y. (2022) 'Inflammation in obesity, diabetes, and related disorders', *Immunity*, 55(1), pp. 31–55. doi: 10.1016/J.IMMUNI.2021.12.013.

Romacho, T., Elsen, M., Röhrborn, D. and Eckel, J. (2014) 'Adipose tissue and its role in organ crosstalk', *Acta Physiologica*, 210(4), pp. 733–753. doi: 10.1111/APHA.12246.

Røndbjerg, A. K., Omerovic, E. and Vestergaard, H. (2011) 'YKL-40 levels are independently associated with albuminuria in type 2 diabetes', *Cardiovascular Diabetology*, 10(1), pp. 1–6. doi: 10.1186/1475-2840-10-54/FIGURES/2.

Rossman, E. I., Liu, K., Morgan, G. A., Swillo, R. E., Krueger, J. A., Gardell, S. J., Butera, J., Gruver, M., Kantrowitz, J., Feldman, H. S., Petersen, J. S., Haugan, K. and Hennan, J. K. (2009) 'The Gap Junction Modifier, GAP-134 [(2S,4R)-1-(2-Aminoacetyl)-4-benzamido-pyrrolidine-2-carboxylic Acid], Improves Conduction and Reduces Atrial Fibrillation/Flutter in the Canine Sterile Pericarditis Model', *Journal of Pharmacology and Experimental Therapeutics*, 329(3), pp. 1127–1133. doi: 10.1124/JPET.108.150102.

Ryan, M. J., Johnson, G., Kirk, J., Fuerstenberg, S. M., Zager, R. A. and Torok-Storb, B. (1994) 'HK-2: An immortalized proximal tubule epithelial cell line from normal adult human kidney', *Kidney International*, 45(1), pp. 48–57. doi: 10.1038/ki.1994.6.

Sáez, J. C. and Green, C. (2018) 'Involvement of connexin hemichannels in the inflammatory response of chronic diseases', *International Journal of Molecular Sciences*. MDPI AG. doi: 10.3390/ijms19092469.

Sánchez-Sánchez, A. M., Turos-Cabal, M., Puente-Moncada, N., Herrera, F., Rodríguez, C. and Martín, V. (2022) 'Calcium acts as a central player in melatonin antitumor activity in sarcoma cells', *Cellular Oncology*, 45(3), pp. 415–428. doi: 10.1007/S13402-022-00674-9/FIGURES/7.

Sandall, C. F., Ziehr, B. K. and MacDonald, J. A. (2020) 'ATP-Binding and Hydrolysis in Inflammasome Activation', *Molecules*, 25(19), p. 4572. doi: 10.3390/MOLECULES25194572.

Sattar, N., Lee, M. M. Y., Kristensen, S. L., Branch, K. R. H., Del Prato, S., Khurmi, N. S., Lam, C. S. P., Lopes, R. D., McMurray, J. J. V., Pratley, R. E., Rosenstock, J. and Gerstein, H. C. (2021) 'Cardiovascular, mortality, and kidney outcomes with GLP-1 receptor agonists in patients with type 2 diabetes: a systematic review and meta-analysis of randomised trials', *The Lancet Diabetes & Endocrinology*, 9(10), pp. 653–662. doi: 10.1016/S2213-8587(21)00203-5.

Scheffner, M., Werness, B. A., Huibregtse, J. M., Levine, A. J. and Howley, P. M. (1990) 'The E6 oncoprotein encoded by human papillomavirus types 16 and 18 promotes the degradation of p53', *Cell*, 63(6), pp. 1129–1136. doi: 10.1016/0092-8674(90)90409-8.

Schmid, H., Boucherot, A., Yasuda, Y., Henger, A., Brunner, B., Eichinger, F., Nitsche, A., Kiss, E., Bleich, M., Gröne, H.-J., Nelson, P. J., Schlöndorff, D., Cohen, C. D. and Kretzler, M. (2006) 'Modular Activation of Nuclear Factor- κ B Transcriptional Programs in Human Diabetic Nephropathy', *Diabetes*, 55(11), pp. 2993–3003. doi: 10.2337/db06-0477.

Schwarznau, A., Hanson, M. S., Sperger, J. M., Schram, B. R., Danobeitia, J. S., Greenwood, K. K., Vijayan, A. and Fernandez, L. A. (2009) 'IL-1 β receptor blockade protects islets against pro-inflammatory cytokine induced necrosis and apoptosis', *Journal of Cellular Physiology*, 220(2), pp. 341–347. doi: 10.1002/JCP.21770.

Scott, R. P. and Quaggin, S. E. (2015) 'Formation and Maintenance of a Functional Glomerulus', *Kidney Development, Disease, Repair and Regeneration*, pp. 103–119. doi: 10.1016/B978-0-12-800102-8.00010-2.

Seibert, F. S., Sitz, M., Passfall, J., Haesner, M., Laschinski, P., Buhl, M., Bauer, F., Babel, N., Pagonas, N. and Westhoff, T. H. (2018) 'Prognostic Value of Urinary Calprotectin, NGAL and KIM-1 in Chronic Kidney Disease', *Kidney and Blood Pressure Research*, 43(4), pp. 1255–1262. doi: 10.1159/000492407.

Selby, N. M. and Taal, M. W. (2020) 'An updated overview of diabetic nephropathy: Diagnosis, prognosis, treatment goals and latest guidelines', *Diabetes, Obesity and Metabolism*, 22(S1), pp. 3–15. doi: 10.1111/DOM.14007.

Sen, B., Xie, Z., Howard, S., Styner, M., van Wijnen, A. J., Uzer, G. and Rubin, J. (2022) 'Mechanically Induced Nuclear Shuttling of β -Catenin Requires Co-transfer of Actin', *Stem Cells*, 40(4), pp. 423–434. doi: 10.1093/STMCLS/SXAC006.

Senn, J. J., Klover, P. J., Nowak, I. A., Zimmers, T. A., Koniaris, L. G., Furlanetto, R. W. and Mooney, R. A. (2003) 'Suppressor of cytokine signaling-3 (SOCS-3), a potential mediator of interleukin-6-dependent insulin resistance in hepatocytes', *Journal of Biological Chemistry*, 278(16), pp. 13740–13746. doi: 10.1074/JBC.M210689200.

Seok, J. K., Kang, H. C., Cho, Y. Y., Lee, H. S. and Lee, J. Y. (2021) 'Therapeutic regulation of the NLRP3 inflammasome in chronic inflammatory diseases', *Archives of Pharmacal Research*, 44(1), pp. 16–35. doi: 10.1007/S12272-021-01307-9.

Shah, K. and Maghsoudlou, P. (2016) 'Enzyme-linked immunosorbent assay (ELISA): The basics', *British Journal of Hospital Medicine*, 77(7), pp. C98–C101. doi: 10.12968/HMED.2016.77.7.C98/ASSET/IMAGES/LARGE/HMED.2016.77.7.C98_T02.JPEG.

Sharma, A., Choi, J. S. Y., Stefanovic, N., Al-Sharea, A., Simpson, D. S., Mukhamedova, N., Jandeleit-Dahm, K., Murphy, A. J., Sviridov, D., Vince, J. E., Ritchie, R. H. and de Haan, J. B. (2021) 'Specific NLRP3 Inhibition Protects Against Diabetes-Associated Atherosclerosis', *Diabetes*, 70(3), pp. 772–787. doi: 10.2337/DB20-0357.

Sharma, D., Gondaliya, P., Tiwari, V. and Kalia, K. (2019) 'Kaempferol attenuates diabetic nephropathy by inhibiting RhoA/Rho-kinase mediated inflammatory signalling', *Biomedicine and Pharmacotherapy*, 109, pp. 1610–1619. doi: 10.1016/j.biopha.2018.10.195.

Sharma, K., Jin, Y., Guo, J. and Ziyadeh, F. N. (1996) 'Neutralization of TGF-beta by anti-TGF-beta antibody attenuates kidney hypertrophy and the enhanced extracellular matrix gene expression in STZ-induced diabetic mice', *Diabetes*, 45(4), pp. 522–530. doi: 10.2337/DIAB.45.4.522.

Shen, J., Dai, Z., Li, Y., Zhu, H. and Zhao, L. (2022) 'TLR9 regulates NLRP3 inflammasome activation via the NF- κ B signaling pathway in diabetic nephropathy', *Diabetology & Metabolic Syndrome*, 14(1), pp. 1–12. doi: 10.1186/S13098-021-00780-Y.

- Sheng, L. and Zhuang, S. (2020) 'New Insights Into the Role and Mechanism of Partial Epithelial-Mesenchymal Transition in Kidney Fibrosis', *Frontiers in Physiology*, 11, p. 1190. doi: 10.3389/FPHYS.2020.569322/BIBTEX.
- Shi, W., Meng, Z. and Luo, J. (2022) 'Connexin 43 (Cx43) regulates high-glucose-induced retinal endothelial cell angiogenesis and retinal neovascularization', *Frontiers in Endocrinology*, 13, p. 1730. doi: 10.3389/FENDO.2022.909207/BIBTEX.
- Shimada, K., Crother, T. R., Karlin, J., Dagvadorj, J., Chiba, N., Chen, S., Ramanujan, V. K., Wolf, A. J., Vergnes, L., Ojcius, D. M., Rentsendorj, A., Vargas, M., Guerrero, C., Wang, Y., Fitzgerald, K. A., Underhill, D. M., Town, T. and Arditi, M. (2012) 'Oxidized mitochondrial DNA activates the NLRP3 inflammasome during apoptosis', *Immunity*, 36(3), pp. 401–414. doi: 10.1016/J.IMMUNI.2012.01.009.
- Shimizu, H., Sakimoto, T. and Yamagami, S. (2019) 'Pro-inflammatory role of NLRP3 inflammasome in experimental sterile corneal inflammation', *Scientific Reports*, 9(1), pp. 1–11. doi: 10.1038/s41598-019-46116-9.
- Shintani-Ishida, K., Uemura, K. and Yoshida, K. (2007) 'Hemichannels in cardiomyocytes open transiently during ischemia and contribute to reperfusion injury following brief ischemia', *American Journal of Physiology-Heart and Circulatory Physiology*, 293(3), pp. H1714–H1720. doi: 10.1152/ajpheart.00022.2007.
- Shirakawa, J., De Jesus, D. F. and Kulkarni, R. N. (2017) 'Exploring inter-organ crosstalk to uncover mechanisms that regulate β -cell function and mass', *European journal of clinical nutrition*, 71(7), pp. 896–903. doi: 10.1038/EJCN.2017.13.
- Simon, Á., Magyar, C., Héja, L. and Kardos, J. (2020) 'Peptide Binding Sites of Connexin Proteins', *Chemistry*, 2(3), pp. 662–673. doi: 10.3390/CHEMISTRY2030042.
- Singh, N., Siddarth, M., Ghosh, R., Tripathi, A. and Banerjee, B. (2019) 'Heptachlor-induced epithelial to mesenchymal transition in HK-2 cells mediated via TGF- β 1/Smad signalling', *Human & Experimental Toxicology*, 38(5), pp. 567-577 doi: 10.1177/0960327119828136.
- Singh, R. K., Diwan, M., Dastidar, S. G. and Najmi, A. K. (2018) 'Differential effect of p38 and MK2 kinase inhibitors on the inflammatory and toxicity biomarkers in vitro', *Human and Experimental Toxicology*, 37(5), pp. 521–531. doi: 10.1177/0960327117715901/ASSET/IMAGES/LARGE/10.1177_0960327117715901-FIG2.JPEG.

- Skyschally, A., Walter, B., Schultz Hansen, R. and Heusch, G. (2013) 'The antiarrhythmic dipeptide ZP1609 (danegaptide) when given at reperfusion reduces myocardial infarct size in pigs', *Naunyn-Schmiedeberg's Archives of Pharmacology*, 386(5), pp. 383–391. doi: 10.1007/S00210-013-0840-9/FIGURES/2.
- Sloan, G., Selvarajah, D. and Tesfaye, S. (2021) 'Pathogenesis, diagnosis and clinical management of diabetic sensorimotor peripheral neuropathy', *Nature Reviews Endocrinology*, 17(7), pp. 400–420. doi: 10.1038/s41574-021-00496-z.
- Soehnlein, O. and Libby, P. (2021) 'Targeting inflammation in atherosclerosis — from experimental insights to the clinic', *Nature Reviews Drug Discovery*, 20(8), pp. 589–610. doi: 10.1038/s41573-021-00198-1.
- Sommerfeld, O., Medyukhina, A., Neugebauer, S., Ghait, M., Ulferts, S., Lupp, A., König, R., Wetzker, R., Schulz, S., Figge, M. T., Bauer, M. and Press, A. T. (2021) 'Targeting Complement C5a Receptor 1 for the Treatment of Immunosuppression in Sepsis', *Molecular Therapy*, 29(1), pp. 338–346. doi: 10.1016/J.YMTHE.2020.09.008.
- Song, N., Liu, Z. S., Xue, W., Bai, Z. F., Wang, Q. Y., Dai, J., Liu, X., Huang, Y. J., Cai, H., Zhan, X. Y., Han, Q. Y., Wang, H., Chen, Y., Li, H. Y., Li, A. L., Zhang, X. M., Zhou, T. and Li, T. (2017) 'NLRP3 Phosphorylation Is an Essential Priming Event for Inflammasome Activation', *Molecular cell*, 68(1), pp. 185-197.e6. doi: 10.1016/J.MOLCEL.2017.08.017.
- Song, W., Wei, L., Du, Y., Wang, Y. and Jiang, S. (2018) 'Protective effect of ginsenoside metabolite compound K against diabetic nephropathy by inhibiting NLRP3 inflammasome activation and NF- κ B/p38 signaling pathway in high-fat diet/streptozotocin-induced diabetic mice', *International Immunopharmacology*, 63, pp. 227–238. doi: 10.1016/j.intimp.2018.07.027.
- Soriano, R. M., Penfold, D. and Leslie, S. W. (2022) 'Anatomy, Abdomen and Pelvis: Kidneys', *StatPearls*. Available at: <https://www.ncbi.nlm.nih.gov/books/NBK482385/>.
- Squires, P. E., Price, G. W., Mouritzen, U., Potter, J. A., Williams, B. M. and Hills, C. E. (2021) 'Danegaptide Prevents TGF β 1-Induced Damage in Human Proximal Tubule Epithelial Cells of the Kidney', *International journal of molecular sciences*, 22(6), p. 2809. doi: 10.3390/ijms22062809.
- Stern, J. H., Rutkowski, J. M. and Scherer, P. E. (2016) 'Adiponectin, Leptin, and Fatty Acids in the Maintenance of Metabolic Homeostasis through Adipose Tissue Crosstalk', *Cell metabolism*, 23(5), pp. 770–784. doi: 10.1016/J.CMET.2016.04.011.

- Stone, R. C., Pastar, I., Ojeh, N., Chen, V., Liu, S., Garzon, K. I. and Tomic-Canic, M. (2016) 'Epithelial-mesenchymal transition in tissue repair and fibrosis', *Cell and Tissue Research. Springer Verlag*, pp. 495–506. doi: 10.1007/s00441-016-2464-0.
- Su, H., Lei, C. T. and Zhang, C. (2017) 'Interleukin-6 signaling pathway and its role in kidney disease: An update', *Frontiers in Immunology*. doi: 10.3389/FIMMU.2017.00405/FULL.
- Sun, A. L., Deng, J. T., Guan, G. J., Chen, S. H., Liu, Y. T., Cheng, J., Li, Z. W., Zhuang, X. H., Sun, F. D. and Deng, H. P. (2012) 'Dipeptidyl peptidase-IV is a potential molecular biomarker in diabetic kidney disease', *Diabetes & vascular disease research*, 9(4), pp. 301–308. doi: 10.1177/1479164111434318.
- Sun, Y. B. Y., Qu, X., Caruana, G. and Li, J. (2016) 'The origin of renal fibroblasts/myofibroblasts and the signals that trigger fibrosis', *Differentiation*, 92(3), pp. 102–107. doi: 10.1016/J.DIFF.2016.05.008.
- Sun, Z., Gong, W., Zhang, Y. and Jia, Z. (2020) 'Physiological and Pathological Roles of Mammalian NEK7', *Frontiers in Physiology*, 11, p. 606996. doi: 10.3389/FPHYS.2020.606996.
- Swanson, K. V., Deng, M. and Ting, J. P. Y. (2019) 'The NLRP3 inflammasome: molecular activation and regulation to therapeutics', *Nature Reviews Immunology*, pp. 477–489. doi: 10.1038/s41577-019-0165-0.
- Switching off chronic inflammation* (2020) *Nature*. Available at: <https://www.nature.com/articles/d42473-019-00438-4>.
- Tacheau, C., Fontaine, J., Loy, J., Mauviel, A. and Verrecchia, F. (2008) 'TGF- β induces connexin43 gene expression in normal murine mammary gland epithelial cells via activation of p38 and PI3K/AKT signaling pathways', *Journal of Cellular Physiology*, 217(3), pp. 759–768. doi: 10.1002/JCP.21551.
- Takahashi, M. (2019) 'Cell-Specific Roles of NLRP3 Inflammasome in Myocardial Infarction', *Journal of Cardiovascular Pharmacology*, 74(3), pp. 188–193. doi: 10.1097/FJC.0000000000000709.
- Takaori, K., Nakamura, J., Yamamoto, S., Nakata, H., Sato, Y., Takase, M., Nameta, M., Yamamoto, T., Economides, A. N., Kohno, K., Haga, H., Sharma, K. and Yanagita, M. (2016) 'Severity and frequency of proximal tubule injury determines renal prognosis', *Journal of the American Society of Nephrology*, 27(8), pp. 2393–2406. doi: 10.1681/ASN.2015060647/-/DCSUPPLEMENTAL.

- Tarzemany, R., Jiang, G., Jiang, J. X., Larjava, H. and Häkkinen, L. (2017) 'Connexin 43 Hemichannels Regulate the Expression of Wound Healing-Associated Genes in Human Gingival Fibroblasts', *Scientific Reports*, 7(1), pp. 1–15. doi: 10.1038/s41598-017-12672-1.
- Thorens, B. (2015) 'GLUT2, glucose sensing and glucose homeostasis', *Diabetologia*, 58(2), pp. 221–232. doi: 10.1007/S00125-014-3451-1.
- Tian, X., Liu, Z., Niu, B., Zhang, J., Tan, T. K., Lee, S. R., Zhao, Y., Harris, D. C. H. and Zheng, G. (2011) 'E-Cadherin/ β -catenin complex and the epithelial barrier', *Journal of Biomedicine and Biotechnology*. doi: 10.1155/2011/567305.
- Tien, T., Muto, T., Zhang, J., Sohn, E. H., Mullins, R. F. and Roy, S. (2016) 'Association of reduced Connexin 43 expression with retinal vascular lesions in human diabetic retinopathy', *Experimental Eye Research*, 146, pp. 103–106. doi: 10.1016/j.exer.2015.12.011.
- Tittarelli, A. (2021) 'Connexin channels modulation in pathophysiology and treatment of immune and inflammatory disorders', *Biochimica et Biophysica Acta (BBA) - Molecular Basis of Disease*, 1867(12), p. 166258. doi: 10.1016/J.BBADIS.2021.166258.
- Tonkin, R. S., Bowles, C., Perera, C. J., Keating, B. A., Makker, P. G. S., Duffy, S. S., Lees, J. G., Tran, C., Don, A. S., Fath, T., Liu, L., O'Carroll, S. J., Nicholson, L. F. B., Green, C. R., Gorrie, C. and Moalem-Taylor, G. (2018) 'Attenuation of mechanical pain hypersensitivity by treatment with Peptide5, a connexin-43 mimetic peptide, involves inhibition of NLRP3 inflammasome in nerve-injured mice', *Experimental Neurology*, 300, pp. 1–12. doi: 10.1016/J.EXPNEUROL.2017.10.016.
- Tsuchida, S., Arai, Y., Kishida, T., Takahashi, K. A., Honjo, K., Terauchi, R., Inoue, H., Oda, R., Mazda, O. and Kubo, T. (2013) 'Silencing the expression of connexin 43 decreases inflammation and joint destruction in experimental arthritis', *Journal of Orthopaedic Research*, 31(4), pp. 525–530. doi: 10.1002/jor.22263.
- Tsuchiya, K. (2020) 'Inflammasome-associated cell death: Pyroptosis, apoptosis, and physiological implications', *Microbiology and Immunology*, 64(4), pp. 252–269. doi: 10.1111/1348-0421.12771.
- Tuleta, I. and Frangogiannis, N. G. (2021) 'Fibrosis of the diabetic heart: Clinical significance, molecular mechanisms, and therapeutic opportunities', *Advanced Drug Delivery Reviews*, 176, p. 113904. doi: 10.1016/J.ADDR.2021.113904.

- Tuttle, K. R., Alicic, R. Z., Duru, O. K., Jones, C. R., Daratha, K. B., Nicholas, S. B., McPherson, S. M., Neumiller, J. J., Bell, D. S., Mangione, C. M. and Norris, K. C. (2019) 'Clinical Characteristics of and Risk Factors for Chronic Kidney Disease Among Adults and Children: An Analysis of the CURE-CKD Registry', *JAMA Network Open*, 2(12), pp. e1918169–e1918169. doi: 10.1001/JAMANETWORKOPEN.2019.18169.
- Van Campenhout, R., Gomes, A. R., De Groof, T. W. M., Muyldermans, S., Devoogdt, N. and Vinken, M. (2021) 'Mechanisms underlying connexin hemichannel activation in disease', *International Journal of Molecular Sciences*, p. 3503. doi: 10.3390/ijms22073503.
- Van Loo, G. and Bertrand, M. J. M. (2022) 'Death by TNF: a road to inflammation', *Nature Reviews Immunology*, 23(5), pp. 289–303. doi: 10.1038/s41577-022-00792-3.
- Vega-Avila, E. and Pugsley, M. K. (2011) 'An overview of colorimetric assay methods used to assess survival or proliferation of mammalian cells', *Proceedings of the Western Pharmacology Society*, 54, pp. 10–14.
- Verrotti, A., Prezioso, G., Scattoni, R. and Chiarelli, F. (2014) 'Autonomic Neuropathy in Diabetes Mellitus', *Frontiers in Endocrinology*, 5. doi: 10.3389/FENDO.2014.00205.
- Vilaysane, A., Chun, J., Seamone, M. E., Wang, W., Chin, R., Hirota, S., Li, Y., Clark, S. A., Tschopp, J., Trpkov, K., Hemmelgarn, B. R., Beck, P. L. and Muruve, D. A. (2010) 'The NLRP3 inflammasome promotes renal inflammation and contributes to CKD', *Journal of the American Society of Nephrology*, 21(10), pp. 1732–1744. doi: 10.1681/ASN.2010020143.
- Wang, D., Wang, H., Gao, H., Zhang, Heng, Zhang, Hua, Wang, Q. and Sun, Z. (2020) 'P2X7 receptor mediates NLRP3 inflammasome activation in depression and diabetes', *Cell and Bioscience*, 10(1), pp. 1–9. doi: 10.1186/S13578-020-00388-1/FIGURES/3.
- Wang, N., De Bock, M., Antoons, G., Gadicherla, A. K., Bol, M., Decrock, E., Evans, W. H., Sipido, K. R., Bukauskas, F. F. and Leybaert, L. (2012) 'Connexin mimetic peptides inhibit Cx43 hemichannel opening triggered by voltage and intracellular Ca²⁺ elevation', *Basic Research in Cardiology*, 107(6), p. 17. doi: 10.1007/S00395-012-0304-2/FIGURES/8.
- Wang, N., De Vuyst, E., Ponsaerts, R., Boengler, K., Palacios-Prado, N., Wauman, J., Lai, C. P., De Bock, M., Decrock, E., Bol, M., Vinken, M., Rogiers, V., Tavernier, J., Evans, W. H., Naus, C. C., Bukauskas, F. F., Sipido, K. R., Heusch, G., Schulz, R., *et al.* (2013) 'Selective inhibition of Cx43 hemichannels by Gap19 and its impact on

myocardial ischemia/reperfusion injury', *Basic Research in Cardiology*, 108(1), pp. 1–16. doi: 10.1007/S00395-012-0309-X/FIGURES/6.

Wang, Q. and Liu, S. (2021) 'Analysis of Hemichannels and Gap Junctions: Application and Extension of the Passive Transmembrane Ion Transport Model', *Frontiers in Cellular Neuroscience*, 15, p. 56. doi: 10.3389/FNCEL.2021.596953/BIBTEX.

Wang, Q., Zhou, C., Zhang, D., Zou, J., Liu, W., Cai, L., Cui, Y., Lai, W. and Xie, J. (2019) 'The involvement of the ERK-MAPK pathway in TGF- β 1-mediated connexin43-gap junction formation in chondrocytes', *Connect Tissue Res*, 60(5), pp. 477-486. doi: 10.1080/03008207.2019.1593394.

Wang, Y., Yu, Y., Yu, W., Bian, X. and Gong, L. (2022) 'IL-35 inhibits cell pyroptosis and attenuates cell injury in TNF- α -induced bronchial epithelial cells via p38 MAPK signaling pathway', *Bioengineered*, 13(1), p. 1758. doi: 10.1080/21655979.2021.2022266.

Warner, A., Clements, D. K., Parikh, S., Evans, W. H. and DeHaan, R. L. (1995) 'Specific motifs in the external loops of connexin proteins can determine gap junction formation between chick heart myocytes.', *The Journal of Physiology*, 488(3), pp. 721–728. doi: 10.1113/JPHYSIOL.1995.SP021003.

Wei, Z. and Liu, H. T. (2002) 'MAPK signal pathways in the regulation of cell proliferation in mammalian cells', *Cell Research*, 12(1), pp. 9–18. doi: 10.1038/sj.cr.7290105.

Wenzlau, J. M., Juhl, K., Yu, L., Moua, O., Sarkar, S. A., Gottlieb, P., Rewers, M., Eisenbarth, G. S., Jensen, J., Davidson, H. W. and Hutton, J. C. (2007) 'The cation efflux transporter ZnT8 (Slc30A8) is a major autoantigen in human type 1 diabetes', *Proceedings of the National Academy of Sciences of the United States of America*, 104(43), pp. 17040–17045. doi: 10.1073/PNAS.0705894104/SUPPL_FILE/05894FIG10.PDF.

Western Blotting Principles and Methods (2014). GE Healthcare.

Wetmore, J. B., Li, S., Ton, T. G. N., Peng, Y., Hansen, M. K., Neslusan, C., Riley, R., Liu, J. and Gilbertson, D. T. (2019) 'Association of diabetes-related kidney disease with cardiovascular and non-cardiovascular outcomes: A retrospective cohort study', *BMC Endocrine Disorders*, 19(1), pp. 1–11. doi: 10.1186/S12902-019-0417-9/FIGURES/3.

Wheelock, M. J., Shintani, Y., Maeda, M., Fukumoto, Y. and Johnson, K. R. (2008) 'Cadherin switching', *Journal of cell science*, 121(6), pp. 727–735. doi: 10.1242/JCS.000455.

Wilkinson, H. N. and Hardman, M. J. (2020) 'Wound healing: cellular mechanisms and pathological outcomes: Cellular Mechanisms of Wound Repair', *Open Biology*, 10(9). doi: 10.1098/RSOB.200223/.

Willebrords, J., Cogliati, B., Pereira, I. V. A., da Silva, T. C., Crespo Yanguas, S., Maes, M., Govoni, V. M., Lima, A., Felisbino, D. A., Decrock, E., Nogueira, M. S., de Castro, I. A., Leclercq, I., Leybaert, L., Rodrigues, R. M. and Vinken, M. (2017) 'Inhibition of connexin hemichannels alleviates non-alcoholic steatohepatitis in mice', *Scientific Reports*, 7(1), p. 8268. doi: 10.1038/s41598-017-08583-w.

Williams, B. M., Cliff, C. L., Demirel, I., Squires, P. E. and Hills, C. E. (2022) 'Blocking connexin 43 hemichannel-mediated ATP release reduces communication within and between tubular epithelial cells and medullary fibroblasts in a model of diabetic nephropathy', *Diabetic medicine: a journal of the British Diabetic Association*, 39(12). doi: 10.1111/DME.14963.

Williams, B. M., Cliff, C. L., Lee, K., Squires, P. E. and Hills, C. E. (2022) 'The Role of the NLRP3 Inflammasome in Mediating Glomerular and Tubular Injury in Diabetic Nephropathy', *Frontiers in Physiology*, 13. doi: 10.3389/FPHYS.2022.907504.

Wiviott, S. D., Raz, I., Bonaca, M. P., Mosenzon, O., Kato, E. T., Cahn, A., Silverman, M. G., Zelniker, T. A., Kuder, J. F., Murphy, S. A., Bhatt, D. L., Leiter, L. A., McGuire, D. K., Wilding, J. P. H., Ruff, C. T., Gause-Nilsson, I. A. M., Fredriksson, M., Johansson, P. A., Langkilde, A.-M., *et al.* (2019) 'Dapagliflozin and Cardiovascular Outcomes in Type 2 Diabetes', *The New England journal of medicine*, 380(4), pp. 347–357. doi: 10.1056/NEJMOA1812389.

Wong, M. L. and Medrano, J. F. (2018) 'Real-time PCR for mRNA quantitation', *BioTechniques*, 39(1), pp. 75–85. doi: 10.2144/05391RV01/ASSET/IMAGES/LARGE/TABLE2.JPEG.

Wong, P., Laxton, V., Srivastava, S., Fiona Chan, Y. W. and Tse, G. (2017) 'The role of gap junctions in inflammatory and neoplastic disorders (Review)', *International Journal of Molecular Medicine*, 39(3), pp. 498–506. doi: 10.3892/IJMM.2017.2859/HTML.

World Health Organisation (2019) *Classification of diabetes mellitus 2019*. Available at: <http://apps.who.int/bookorders>. (Accessed: 1 June 2023).

Woroniecka, K. I., Park, A. S. D., Mohtat, D., Thomas, D. B., Pullman, J. M. and Susztak, K. (2011) 'Transcriptome Analysis of Human Diabetic Kidney Disease', *Diabetes*, 60(9), pp. 2354–2369. doi: 10.2337/db10-1181.

Worthen, C. A., Cui, Y., Orringer, J. S., Johnson, T. M., Voorhees, J. J. and Fisher, G. J. (2020) 'CD26 Identifies a Subpopulation of Fibroblasts that Produce the Majority of Collagen during Wound Healing in Human Skin', *Journal of Investigative Dermatology*, 140(12), pp. 2515-2524.e3. doi: 10.1016/J.JID.2020.04.010.

Xie, T., Xia, Z., Wang, W., Zhou, X. and Xu, C. (2021) 'BMPER Ameliorates Renal Fibrosis by Inhibiting Tubular Dedifferentiation and Fibroblast Activation', *Frontiers in Cell and Developmental Biology*, 9, p. 77. doi: 10.3389/FCELL.2021.608396/BIBTEX.

Xin, R., Sun, X., Wang, Z., Yuan, W., Jiang, W., Wang, L., Xiang, Y., Zhang, H., Li, X., Hou, Y., Sun, W. and Du, P. (2018) 'Apocynin inhibited NLRP3/XIAP signalling to alleviate renal fibrotic injury in rat diabetic nephropathy', *Biomedicine & Pharmacotherapy*, 106, pp. 1325–1331. doi: 10.1016/J.BIOPHA.2018.07.036.

Xing, J., Wang, Hongji, Chen, L., Wang, Hanxi, Huang, H., Huang, J. and Xu, C. (2022) 'Blocking Cx43 Alleviates Neuropathic Pain in Rats with CCI Via P2X4 and P38/ERK-P65 Pathway', *SSRN Electronic Journal*. doi: 10.2139/SSRN.4207769.

Xing, X., Guo, S., Liu, Y., Kuang, J., Huang, Z., Wang, X. and Lu, Q. (2021) 'Saxagliptin protects against diabetic nephropathy by inhibiting caspase 3/PARP-1-dependent nephrocyte apoptosis', *Experimental and Therapeutic Medicine*, 22(3). doi: 10.3892/ETM.2021.10422.

Xu, H., Wang, M., Li, Y., Shi, M., Wang, Z., Cao, C., Hong, Y., Hu, B., Zhu, H., Zhao, Z., Chu, X., Zhu, Fan, Deng, X., Wu, J., Zhao, F., Guo, J., Wang, Y., Pei, G., Zhu, Fengming, *et al.* (2022) 'Blocking connexin 43 and its promotion of ATP release from renal tubular epithelial cells ameliorates renal fibrosis', *Cell Death & Disease* 2022 13:5, 13(5), pp. 1–15. doi: 10.1038/s41419-022-04910-w.

Xu, L., Sharkey, D. and Cantley, L. G. (2019) 'Tubular GM-CSF Promotes Late MCP-1/CCR2-Mediated Fibrosis and Inflammation after Ischemia/Reperfusion Injury', *Journal of the American Society of Nephrology*, 30(10), pp. 1825–1840. doi: 10.1681/ASN.2019010068.

- Yang, L., Guo, J., Yu, N., Liu, Y., Song, H., Niu, J. and Gu, Y. (2020) 'Tocilizumab mimotope alleviates kidney injury and fibrosis by inhibiting IL-6 signaling and ferroptosis in UUO model', *Life Sciences*, 261, p. 118487. doi: 10.1016/J.LFS.2020.118487.
- Yang, Lei, Zhou, G., Li, M., Li, Y., Yang, Liqing, Fu, Q. and Tian, Y. (2020) 'High Glucose Downregulates Connexin 43 Expression and Its Gap Junction and Hemichannel Function in Osteocyte-like MLO-Y4 Cells Through Activation of the p38MAPK/ERK Signal Pathway', *Diabetes, metabolic syndrome and obesity: targets and therapy*, 13, pp. 545–557. doi: 10.2147/DMSO.S239892.
- Yang, M., Wang, X., Han, Y., Li, C., Wei, L., Yang, J., Chen, W., Zhu, X. and Sun, L. (2021) 'Targeting the NLRP3 Inflammasome in Diabetic Nephropathy', *Current medicinal chemistry*, 28(42), pp. 8810–8824. doi: 10.2174/0929867328666210705153109.
- Yang, Y., Delalio, L., Best, A. K., Macal, E., Milstein, J., Donnelly, I., Miller, A. M., McBride, M., Shu, X., Koval, M., Isakson, B. E. and Johnstone, S. R. (2019) 'Endothelial pannexin 1 channels control inflammation by regulating intracellular calcium', *bioRxiv*, p. 750323. doi: 10.1101/750323.
- Yasuda, F., Mii, A., Morita, M., Aoki, M., Tagawa, M., Aratani, S., Kaneko, T., Sakai, Y. and Shimizu, A. (2018) 'Importance of frequency and morphological characteristics of nodular diabetic glomerulosclerosis in diabetic nephropathy', *Human Pathology*, 75, pp. 95–103. doi: 10.1016/J.HUMPATH.2018.01.019.
- Yasuda, T., Kaneto, H., Katakami, N., Kuroda, A., Matsuoka, T. aki, Yamasaki, Y., Matsuhisa, M. and Shimomura, I. (2011) 'YKL-40, a new biomarker of endothelial dysfunction, is independently associated with albuminuria in type 2 diabetic patients', *Diabetes research and clinical practice*, 91(2). doi: 10.1016/J.DIABRES.2010.11.015.
- Yi, C., Ezan, P., Fernández, P., Schmitt, J., Sáez, J. C., Giaume, C. and Koulakoff, A. (2017) 'Inhibition of glial hemichannels by boldine treatment reduces neuronal suffering in a murine model of Alzheimer's disease', *Glia*, 65(10), pp. 1607–1625. doi: 10.1002/glia.23182.
- Yin, H., Liu, N., Sigdel, K. R. and Duan, L. (2022) 'Role of NLRP3 Inflammasome in Rheumatoid Arthritis', *Frontiers in immunology*, 13. doi: 10.3389/FIMMU.2022.931690.
- Ying, W., Wollam, J., Ofrecio, J. M., Bandyopadhyay, G., El Ouarrat, D., Lee, Y. S., Oh, D. Y., Li, P., Osborn, O. and Olefsky, J. M. (2017) 'Adipose tissue B2 cells

promote insulin resistance through leukotriene LTB₄/LTB₄R1 signaling', *The Journal of clinical investigation*, 127(3), pp. 1019–1030. doi: 10.1172/JCI90350.

Yorston, D., Wickham, L., Benson, S., Bunce, C., Sheard, R. and Charteris, D. (2008) 'Predictive clinical features and outcomes of vitrectomy for proliferative diabetic retinopathy', *British Journal of Ophthalmology*, 92(3), pp. 365–368. doi: 10.1136/BJO.2007.124495.

Yu, H., Cao, X., Li, W., Liu, P., Zhao, Y., Song, L., Chen, J., Chen, B., Yu, W. and Xu, Y. (2020) 'Targeting connexin 43 provides anti-inflammatory effects after intracerebral hemorrhage injury by regulating YAP signaling', *Journal of Neuroinflammation*, 17(1), p. 322. doi: 10.1186/s12974-020-01978-z.

Yue, J. and López, J. M. (2020) 'Understanding MAPK Signaling Pathways in Apoptosis', *International Journal of Molecular Sciences*, 21(7). doi: 10.3390/IJMS21072346.

Yun, J. H. (2021) 'Interleukin-1 β induces pericyte apoptosis via the NF- κ B pathway in diabetic retinopathy', *Biochemical and Biophysical Research Communications*, 546, pp. 46–53. doi: 10.1016/J.BBRC.2021.01.108.

Zacchia, M., Capolongo, G., Rinaldi, L. and Capasso, G. (2018) 'The importance of the thick ascending limb of Henle's loop in renal physiology and pathophysiology', *International journal of nephrology and renovascular disease*, 11, pp. 81–92. doi: 10.2147/IJNRD.S154000.

Zeng, L. F., Xiao, Y. and Sun, L. (2019) 'A Glimpse of the Mechanisms Related to Renal Fibrosis in Diabetic Nephropathy', *Advances in Experimental Medicine and Biology*, 1165, pp. 49–79. doi: 10.1007/978-981-13-8871-2_4.

Zha, Q. B., Wei, H. X., Li, C. G., Liang, Y. D., Xu, L. H., Bai, W. J., Pan, H., He, X. H. and Ouyang, D. Y. (2016) 'ATP-induced inflammasome activation and pyroptosis is regulated by AMP-activated protein kinase in macrophages', *Frontiers in Immunology*, 7, p. 597. doi: 10.3389/FIMMU.2016.00597/FULL.

Zhang, H. and Wang, Z. (2020) 'Effect and Regulation of the NLRP3 Inflammasome During Renal Fibrosis', *Frontiers in Cell and Developmental Biology*, 7, p. 379. doi: 10.3389/FCELL.2019.00379/BIBTEX.

Zhang, J., Wang, Y., Li, L., Zhang, R., Guo, R., Li, H., Han, Q., Teng, G. and Liu, F. (2018) 'Diabetic retinopathy may predict the renal outcomes of patients with diabetic

nephropathy', <https://doi.org/10.1080/0886022X.2018.1456453>, 40(1), pp. 243–251. doi: 10.1080/0886022X.2018.1456453.

Zhang, K., Chai, B., Ji, H., Chen, liuqing, Ma, Y., Zhu, L., Xu, J., Wu, Y., Lan, Y., Li, H., Feng, Z., Xiao, J., Zhang, H. and Xu, K. (2021a) 'Bioglass promotes wound healing by inhibiting endothelial cell pyroptosis through regulation of the connexin 43/reactive oxygen species (ROS) signaling pathway', *Laboratory Investigation* 2021, pp. 1–12. doi: 10.1038/s41374-021-00675-6.

Zhang, K., Yang, W., Dai, H. and Deng, Z. (2020) 'Cardiovascular risk following metformin treatment in patients with type 2 diabetes mellitus: Results from meta-analysis', *Diabetes Research and Clinical Practice*, 160, p. 108001. doi: 10.1016/J.DIABRES.2020.108001.

Zhang, T., Wang, Y., Xia, Q., Tu, Z., Sun, J., Jing, Q., Chen, P. and Zhao, X. (2021b) 'Propofol Mediated Protection of the Brain From Ischemia/Reperfusion Injury Through the Regulation of Microglial Connexin 43', *Frontiers in Cell and Developmental Biology*, 9, p. 1104. doi: 10.3389/FCELL.2021.637233/BIBTEX.

Zhang, W., Liu, Y. and Zhang, H. (2021c) 'Extracellular matrix: an important regulator of cell functions and skeletal muscle development', *Cell & Bioscience*, 11(1), pp. 1–13. doi: 10.1186/S13578-021-00579-4.

Zhao, L., Zou, Y. and Liu, F. (2020) 'Transforming Growth Factor-Beta1 in Diabetic Kidney Disease', *Frontiers in Cell and Developmental Biology*, 8, p. 187. doi: 10.3389/FCELL.2020.00187.

Zhao, T., Su, Z., Li, Y., Zhang, X. and You, Q. (2020) 'Chitinase-3 like-protein-1 function and its role in diseases', *Signal Transduction and Targeted Therapy*, 5(1). doi: 10.1038/S41392-020-00303-7.

Zheng, L. W., Wang, W. C., Mao, X. Z., Luo, Y. H., Tong, Z. Y. and Li, D. (2020) 'TNF- α regulates the early development of avascular necrosis of the femoral head by mediating osteoblast autophagy and apoptosis via the p38 MAPK/NF- κ B signaling pathway', *Cell Biology International*, 44(9), pp. 1881–1889. doi: 10.1002/CBIN.11394.

Zheng, Z. and Zheng, F. (2016) 'Immune Cells and Inflammation in Diabetic Nephropathy', *Journal of Diabetes Research*. doi: 10.1155/2016/1841690.

Zhou, D., Fu, H., Zhang, L., Zhang, K., Min, Y., Xiao, L., Lin, L., Bastacky, S. I. and Liu, Y. (2017) 'Tubule-Derived Wnts Are Required for Fibroblast Activation and Kidney

Fibrosis', *Journal of the American Society of Nephrology: JASN*, 28(8), pp. 2322–2336. doi: 10.1681/ASN.2016080902.

Zhou, K. Q., Green, C. R., Bennet, L., Gunn, A. J. and Davidson, J. O. (2019) 'The Role of Connexin and Pannexin Channels in Perinatal Brain Injury and Inflammation', *Frontiers in Physiology*, 10. doi: 10.3389/fphys.2019.00141.

Zhou, R., Tardivel, A., Thorens, B., Choi, I. and Tschopp, J. (2010) 'Thioredoxin-interacting protein links oxidative stress to inflammasome activation', *Nature immunology*, 11(2), pp. 136–140. doi: 10.1038/NI.1831.

Zhou, Y., Ma, X.-Y., Han, J.-Y., Yang, M., Lv, C., Shao, Y., Wang, Y.-L., Kang, J.-Y. and Wang, Q.-Y. (2021a) 'Metformin regulates inflammation and fibrosis in diabetic kidney disease through TNC/TLR4/NF- κ B/miR-155-5p inflammatory loop', *World Journal of Diabetes*, 12(1), p. 19. doi: 10.4239/WJD.V12.I1.19.

Zhou, Yao, Gao, L., Xia, P., Zhao, J., Li, W., Zhou, Yufeng, Wei, Q., Wu, Qijing, Wu, Qi, Sun, D. and Gao, K. (2021b) 'Glycyrrhetic Acid Protects Renal Tubular Cells against Oxidative Injury via Reciprocal Regulation of JNK-Connexin 43-Thioredoxin 1 Signaling', *Frontiers in Pharmacology*, 12, p. 19. doi: 10.3389/FPHAR.2021.619567.

Zhu, Q. and Scherer, P. E. (2018) 'Immunologic and endocrine functions of adipose tissue: implications for kidney disease', *Nature reviews. Nephrology*, 14(2), pp. 105–120. doi: 10.1038/NRNEPH.2017.157.

Zhu, Y., Chen, X., Lu, Y., Fan, S., Yang, Y., Chen, Q., Huang, Q., Xia, L., Wei, Y., Zheng, J. and Liu, X. (2021) 'Diphenyleneiodonium enhances P2X7 dependent non-opsonized phagocytosis and suppresses inflammasome activation via blocking CX43-mediated ATP leakage', *Pharmacological Research*, 166, p. 105470. doi: 10.1016/J.PHRS.2021.105470.

Zinman, B., Wanner, C., Lachin, J. M., Fitchett, D., Bluhmki, E., Hantel, S., Mattheus, M., Devins, T., Johansen, O. E., Woerle, H. J., Broedl, U. C. and Inzucchi, S. E. (2015) 'Empagliflozin, Cardiovascular Outcomes, and Mortality in Type 2 Diabetes', *The New England journal of medicine*, 373(22), pp. 17–18. doi: 10.1056/NEJMOA1504720.